

1991

Transition metal complexes of a novel tetradentate phosphine and of a new diphosphine ether

Mark R. Mason
Iowa State University

Follow this and additional works at: <https://lib.dr.iastate.edu/rtd>

 Part of the [Inorganic Chemistry Commons](#)

Recommended Citation

Mason, Mark R., "Transition metal complexes of a novel tetradentate phosphine and of a new diphosphine ether" (1991). *Retrospective Theses and Dissertations*. 9554.
<https://lib.dr.iastate.edu/rtd/9554>

This Dissertation is brought to you for free and open access by the Iowa State University Capstones, Theses and Dissertations at Iowa State University Digital Repository. It has been accepted for inclusion in Retrospective Theses and Dissertations by an authorized administrator of Iowa State University Digital Repository. For more information, please contact digirep@iastate.edu.

INFORMATION TO USERS

This manuscript has been reproduced from the microfilm master. UMI films the text directly from the original or copy submitted. Thus, some thesis and dissertation copies are in typewriter face, while others may be from any type of computer printer.

The quality of this reproduction is dependent upon the quality of the copy submitted. Broken or indistinct print, colored or poor quality illustrations and photographs, print bleedthrough, substandard margins, and improper alignment can adversely affect reproduction.

In the unlikely event that the author did not send UMI a complete manuscript and there are missing pages, these will be noted. Also, if unauthorized copyright material had to be removed, a note will indicate the deletion.

Oversize materials (e.g., maps, drawings, charts) are reproduced by sectioning the original, beginning at the upper left-hand corner and continuing from left to right in equal sections with small overlaps. Each original is also photographed in one exposure and is included in reduced form at the back of the book.

Photographs included in the original manuscript have been reproduced xerographically in this copy. Higher quality 6" x 9" black and white photographic prints are available for any photographs or illustrations appearing in this copy for an additional charge. Contact UMI directly to order.

U·M·I

University Microfilms International
A Bell & Howell Information Company
300 North Zeeb Road, Ann Arbor, MI 48106-1346 USA
313/761-4700 800/521-0600



Order Number 9126222

**Transition metal complexes of a novel tetradentate phosphine
and of a new diphosphine ether**

Mason, Mark Richard, Ph.D.

Iowa State University, 1991

U·M·I

300 N. Zeeb Rd.
Ann Arbor, MI 48106

**Transition metal complexes of a novel tetradentate
phosphine and of a new diphosphine ether**

by

Mark R. Mason

**A Dissertation Submitted to the
Graduate Faculty in Partial Fulfillment of the
Requirements for the Degree of
DOCTOR OF PHILOSOPHY**

**Department: Chemistry
Major: Inorganic Chemistry**

Approved:

Signature was redacted for privacy.

In Charge of Major Work

Signature was redacted for privacy.

For the Major Department

Signature was redacted for privacy.

For the Graduate College

**Iowa State University
Ames, Iowa**

1991

TABLE OF CONTENTS

	<u>Page</u>
DEDICATION	v
PREFACE	1
SECTION I. GENERAL INTRODUCTION	2
INTRODUCTION	3
MULTITERTIARY PHOSPHINES	7
PHOSPHINE ETHERS	22
STATEMENT OF RESEARCH PROJECT	35
REFERENCES	39
SECTION II. COORDINATION CHEMISTRY OF A NEW TETRATERTIARY PHOSPHINE LIGAND	48
ABSTRACT	49
INTRODUCTION	51
EXPERIMENTAL SECTION	54
RESULTS AND DISCUSSION	73
ACKNOWLEDGMENTS	105
REFERENCES	106
SUPPLEMENTARY MATERIAL	112
SECTION III. BIDENTATE AND TRIDENTATE COORDINATION MODES OF A NOVEL BICYCLIC DITERTIARY PHOSPHINE ETHER	130
ABSTRACT	131
INTRODUCTION	132

EXPERIMENTAL SECTION	135
RESULTS AND DISCUSSION	151
ACKNOWLEDGMENTS	173
REFERENCES	174
SUPPLEMENTARY MATERIAL	178
SECTION IV. UNAMBIGUOUS DEMONSTRATION OF VACANT SITE INVERSION IN A <i>cis</i> -P ₂ M(CO) ₃ INTERMEDIATE	211
ABSTRACT	212
COMMUNICATION	213
ACKNOWLEDGMENTS	218
REFERENCES	219
SECTION V. LIGAND SUBSTITUTION REACTIONS IN GROUP VI METAL CARBONYL COMPLEXES OF A NOVEL BICYCLIC DITERTIARY PHOSPHINE ETHER	221
ABSTRACT	222
INTRODUCTION	223
EXPERIMENTAL SECTION	226
RESULTS AND DISCUSSION	237
ACKNOWLEDGMENTS	254
REFERENCES	255
SECTION VI. FLUORIDE-ASSISTED REDUCTION OF PALLADIUM(II) PHOSPHINE COMPLEXES	259
ABSTRACT	260

COMMUNICATION	261
ACKNOWLEDGMENTS	264
REFERENCES	265
SECTION VII. A NEW REDOX REACTION INVOLVING FLUORIDE AND PHOSPHINE COMPLEXES OF GROUP X METALS. CRYSTAL AND MOLECULAR STRUCTURE OF Pd(dppp) ₂ .	267
ABSTRACT	268
INTRODUCTION	269
EXPERIMENTAL SECTION	271
RESULTS AND DISCUSSION	286
ACKNOWLEDGMENTS	302
REFERENCES	303
SUPPLEMENTARY MATERIAL	308
GENERAL SUMMARY	325
ACKNOWLEDGMENTS	327

DEDICATION

To my wife and family for their constant love and encouragement

PREFACE

This dissertation consists of seven sections. The first section is a review of the pertinent literature on which this thesis is based. At the end of the first section is a Statement of Research Project which outlines the goals of the research described herein. Each of the remaining six sections represents research as it was submitted for journal publication. Literature citations, tables, and figures pertain only to the section in which they are included. Section II involved the reinvestigation and continuation of a project initiated by Dr. Colleen M. Duff, and as such, a brief description of her contribution is included in the Acknowledgments portion of that section. Likewise, all other contributions to the work presented herein are similarly acknowledged.

SECTION I. GENERAL INTRODUCTION

INTRODUCTION

Phosphines have constituted one of the most extensively investigated classes of ligands in transition metal chemistry. Their use in a variety of homogeneous transition metal catalyzed applications of industrial significance, such as hydroformylation, hydrogenation, olefin isomerization, olefin oligomerization and olefin hydrocyanation (a phosphite is used in the Du Pont adiponitrile process), attest to their importance in the field of organometallic chemistry.¹

Multidentate phosphines, in particular, have several distinct advantages which account for their increasing use. Careful adjustments to steric, electronic, and structural features in multidentate phosphines can be used to control the coordination number, stereochemistry, and basicity at a metal center. In comparison to their monodentate counterparts, chelation of multidentate phosphines has been found to add increased stability to transition metal complexes. The chelate ring size is also of great importance and may drastically alter the reactivity of a given complex. For example, the bidentate ligand dppe prefers to bridge two metal centers rather than chelate to one metal. Hence "A-frame" bimetallic complexes comprise a large portion of the chemistry of this ligand. As a second example, the rates of rhodium-catalyzed hydrogenation and hydroformylation have also been shown to be highly dependent on chelate ring size.²

Multidentate phosphines may also possess other donor atoms including N, As, Sb, O, S, and Se. Incorporation of these donor atoms into phosphine ligands has been achieved using a variety of functional groups such as amines,³ thioethers,^{3e,f} ethers, esters,⁴ phosphine oxides, phosphine sulfides,^{5, 6} and phosphine selenides.⁶ Mixed donor ligands which contain phosphine groups, as well as weak donor atoms such as N, O, S, or Se, have been labeled "hemilabile".⁷ The phosphine groups provide a strong

anchor to the metal complex but the weak donors are readily displaced by other substrates, thus providing accessible coordination sites on the metal. Coordinative unsaturation is a known prerequisite for a catalytic transition metal catalyzed system.⁸

Numerous review articles pertaining to phosphine transition metal complexes have appeared in the literature over the past twenty years. Early reviews by McAuliffe detailed the chemistry of bidentate and tetradentate phosphines including some mixed donor ligands.⁹ Meek published¹⁰ a less extensive review of phosphine transition metal chemistry in 1978. A legendary review addressing steric factors in phosphine complexes was published¹¹ by Tolman in 1977. The coverage in this review included cone angles, chelate ring effects, ³¹P NMR spectroscopy and some X-ray crystallographic data. Garrou has presented two reviews recently; the first detailing P-C bond cleavage in homogeneous systems¹² and the second discussing the utility of ³¹P NMR spectroscopy in the study of transition metal phosphine complexes.¹³ An extensive compilation of relevant ³¹P NMR spectroscopic data and references has also been included in a recent text edited by Quin and Verkade.¹⁴ An excellent review of transition metal catalyzed asymmetric synthesis, including a discussion of approximately thirty chiral bidentate phosphines, has also been published.¹⁵ The most recent review was put forth by McAuliffe in 1987.¹⁶ Included in his discussion are common synthetic routes used in the preparation of phosphines as well as recent advances in the chemistry of macrocyclic phosphine ligands.

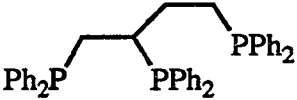
Although the number of review articles relevant to this topic is large (above is only a partial listing), several recent developments in the area of multidentate phosphines have not been covered. Additionally, the topic of mixed donor ligands has received little attention in review articles and the author is aware of no review articles concerning phosphine ether ligands. This general survey will thus be divided into two parts. The

first will cover tertiary phosphines with a denticity of three or greater, concentrating on important contributions over the past fifteen years. The works of McAuliffe and Kagan together reference an incomplete list of approximately ninety different bidentate phosphines. Hence, bidentate phosphines, as well as macrocyclic ligands, will not be included in this discussion. The second part of this general survey will focus on the important aspects of phosphine ether coordination to transition metals. Following this general survey will be a brief statement addressing the purpose for the research presented in the remainder of this thesis.

Table 1. Compilation of tritertiary phosphine ligands

Tritertiary Phosphines		Substituents	References
	<u>Type I</u>		
CH ₃ C(CH ₂ PR ₂) ₃	1	R = Me	17 - 20
	2	Et	21
	3	Ph	21 - 24
HC(PR ₂) ₃	4	R = Me	25
	5	Ph	26 - 38
CH ₃ Si(PR ₂) ₃	6	R = <i>n</i> -Bu	39, 40
	7	Et	40
	8	Pr	40
CH ₃ Si(CH ₂ CH ₂ PPh ₂) ₃	9		41

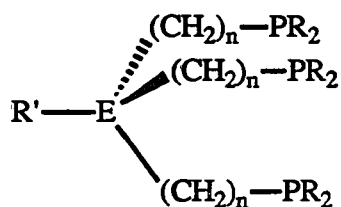
Table 1. Continued

Tertiary Phosphines		Substituents	References
$\text{RP}(\text{CH}_2\text{CH}_2\text{PR}'_2)_2$	10	R = Ph, R' = Ph	42, 43
	11	R = Ph, R' = Me	43, 44
	12	R = Me, R' = Ph	44
	13	R = Me, R' = Me	43, 44
	14	R = R' = CH_2CMe_3	45
$\text{RP}(\text{CH}_2\text{CH}_2\text{CH}_2\text{PR}'_2)_2$	15	R = Ph, R' = Ph	46, 47
	16	R = Ph, R' = Cy	47
	17	R = Me, R' = Me	48
	18	R = Me, R' = Et	48
	19	R = <i>t</i> -Bu, R' = Me	48
$\text{Me}_2\text{P}(\text{CH}_2)_2\text{P}(\text{Ph})(\text{CH}_2)_2\text{PPh}_2$	20		43, 49
$\text{Ph}_2\text{P}(\text{CH}_2)_3\text{P}(\text{Ph})(\text{CH}_2)_2\text{PPh}_2$	21		50
$\text{PhP}(\text{o-C}_6\text{H}_4\text{PPh}_2)_2$	22		51
	23		52, 53

MULTITERTIARY PHOSPHINES

Tertiary Phosphines

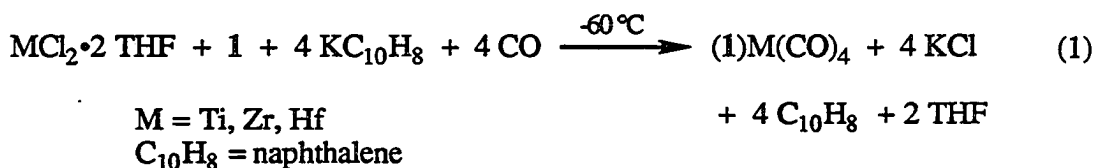
Tertiary phosphines can readily be divided into two types as shown in Table 1. Tertiary phosphines of type I are based on the ligands $\text{CH}_3\text{C}(\text{CH}_2\text{PR}_2)_3$ synthesized²¹ by Hewertson and Watson in 1962. These tripodal ligands all possess essentially C_{3v} symmetry, but differ in the identity of the bridgehead atom (Si, C), the number of methylene groups between the bridgehead atom and phosphorus ($n = 0, 1, 2$), and the identity of the alkyl or aryl substituent on phosphorus. These differences account for the wide range of chemistry observed for these ligands.



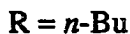
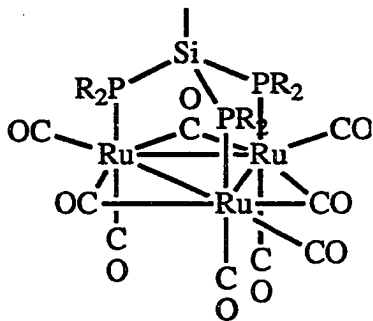
Type I

Recently, Ellis has used $\text{CH}_3\text{C}(\text{CH}_2\text{PMe}_2)_3$ (**1**) to stabilize phosphine analogues of the unknown compounds $\text{M}(\text{CO})_7$ where $\text{M} = \text{Zr}, \text{Ti}, \text{or Hf}$. The zirconium complex $(\eta^3\text{-1})\text{Zr}(\text{CO})_4$ represents only the fourth example of a Zr^0 carbonyl complex and the first to be characterized by X-ray crystallography.¹⁸ Its synthesis is shown in reaction 1. The titanium analogue $(\eta^3\text{-1})\text{Ti}(\text{CO})_4$ was synthesized^{19, 20} by the reaction of **1** with $(\text{dmpe})\text{Ti}(\text{CO})_5$. This complex is thermally stable up to 150°C and represents one of the most thermally stable Ti^0 carbonyl phosphine complexes known. The stability of these seven coordinate complexes is attributable to the chelating nature and the basicity of the

tertiary phosphine ligand. The less basic phenyl substituted phosphines $\text{CH}_3\text{C}(\text{CH}_2\text{PPh}_2)_3$ and $\text{PhP}(\text{CH}_2\text{CH}_2\text{PPh}_2)_2$, as well as the non-chelating but highly basic PMe_3 , do not react with $(\text{dmpe})\text{Ti}(\text{CO})_4$ to form complexes of this kind.



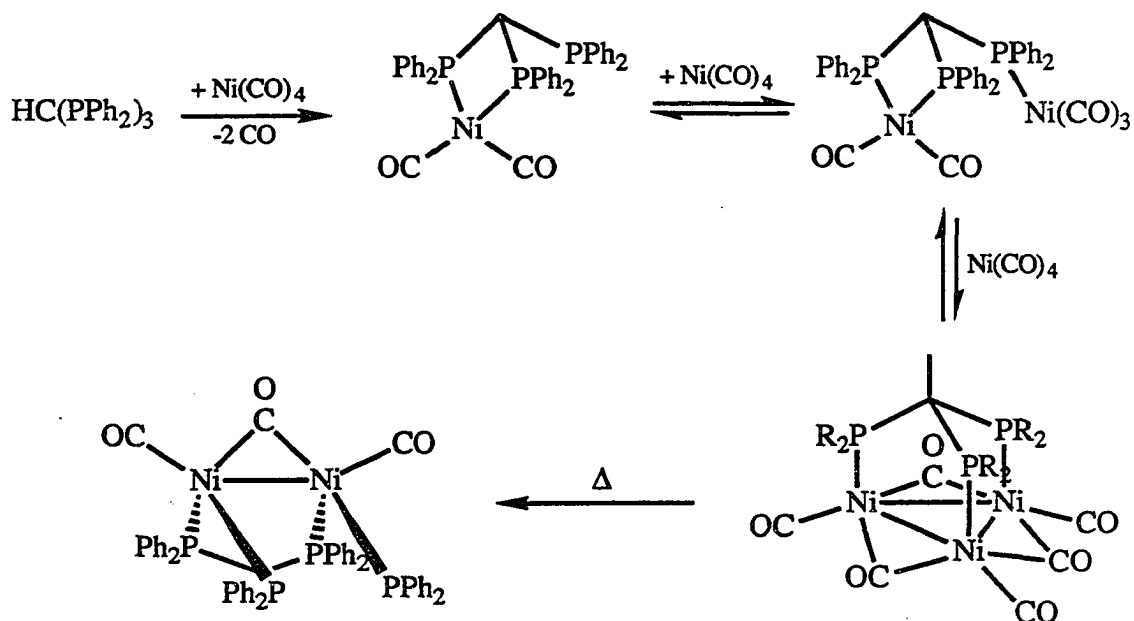
The first tripodal tertiary phosphine of type I where $n = 0$ was synthesized²⁶ in 1970, but the transition metal chemistry of this group of ligands did not begin to flourish until 1978 when de Boer et al. reported³⁹ that $\text{CH}_3\text{Si}(\text{P}n\text{-Bu}_2)_3$ (**6**) can face-cap a tetrahedral cluster of metals as verified by X-ray crystallography for $\text{Ru}_3(\text{CO})_9(\mu_3\text{-}\eta^3\text{-6})$.



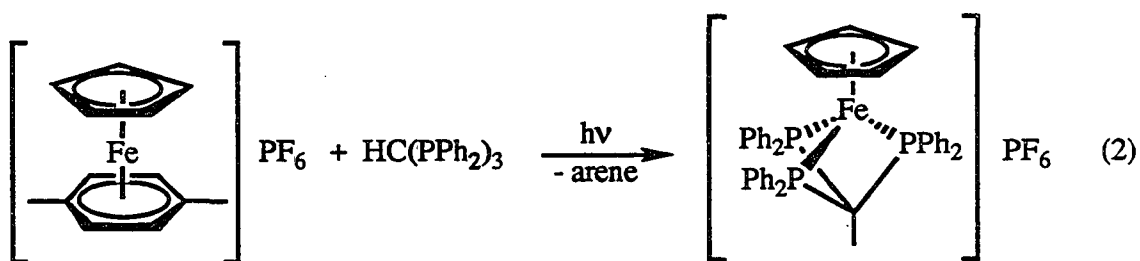
Other examples of face-capped clusters with these tripodal ligands quickly followed and crystal structures were reported for $(\eta^6\text{-toluene})\text{Co}_4(\text{CO})_6[\mu_3\text{-}\eta^3\text{-}\{(\text{Ph}_2\text{P})_3\text{CH}\}]$,²⁷ $\text{Ir}_4(\text{CO})_9[\mu_3\text{-}\eta^3\text{-}\{(\text{Ph}_2\text{P})_3\text{CH}\}]$,²⁸ and $\text{Co}_4(\text{CO})_9[\mu_3\text{-}\eta^3\text{-}\{(\text{Ph}_2\text{P})_3\text{CH}\}]$.²⁹ The tripodal ligand $\text{HC}(\text{PPh}_2)_3$ was also found to act as a template³⁰ with the sequential incorporation

of three equivalents of $\text{Ni}(\text{CO})_4$ to form the face-capped cluster $\text{Ni}_3(\text{CO})_6[\mu_3\text{-}\eta^3\text{-}\{(\text{Ph}_2\text{P})_3\text{CH}\}]$ as shown in Scheme I. These face-capped clusters exhibit much improved thermal stability with a decreasing tendency for cluster fragmentation. This is an important discovery since fragmentation has severely hindered attempts to use small metal clusters in homogeneous metal-catalyzed applications. The tripodal ligands in these cluster systems, however, are not completely inert to thermal decomposition. Extended heating of the trinuclear nickel cluster in Scheme I results in P-C bond cleavage with the formation of the bimetallic complex $\text{Ni}_2(\mu\text{-dppm})_2(\mu\text{-CO})(\text{CO})_2$.³³ Similarly, extended heating of $\text{Ru}_3(\text{CO})_9[\mu_3\text{-}\eta^3\text{-}\{(\text{Ph}_2\text{P})_3\text{CH}\}]$ in THF results in the *ortho*-metallation of one phenyl substituent by the phosphorus atom of a neighboring phosphine group with concomitant loss of benzene.³²

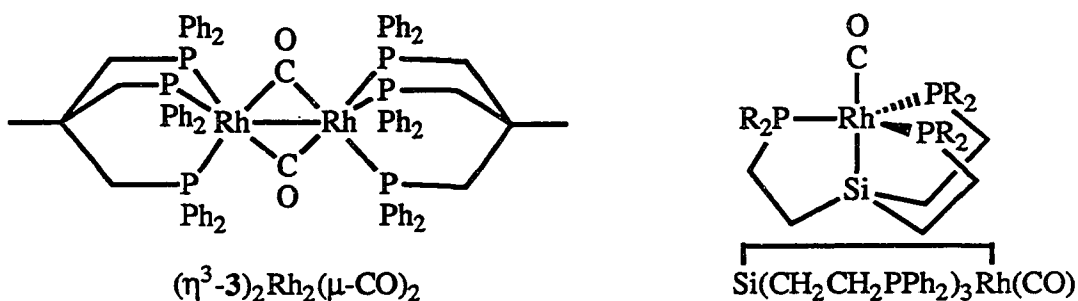
Scheme I



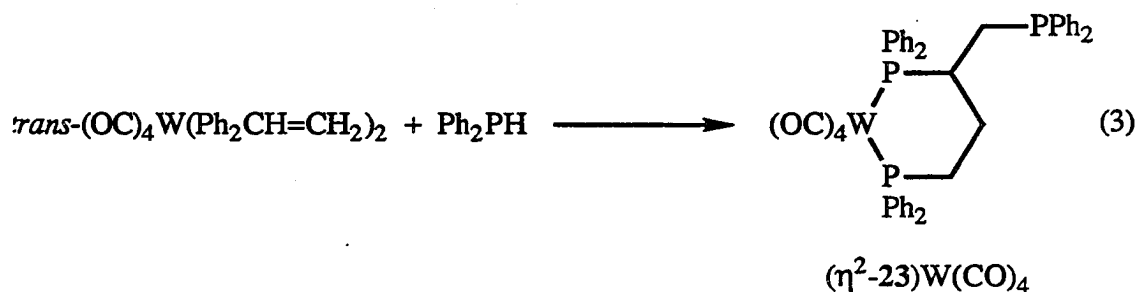
The tripodal tritertiary phosphines where $n = 0$ exhibit other coordination modes in addition to face-capping small clusters. Mague et al. have reported³⁷ the preparation of $\{\text{HC}(\text{PPh}_2)_3\}\text{Fe}(\text{CO})_4$ and $\{\text{HC}(\text{PPh}_2)_3\}\text{Mo}(\text{CO})_4$ where $\text{HC}(\text{PPh}_2)_3$ coordinates in η^1 and η^2 modes respectively. Selegue et al. reported³⁸ the first example of $\text{HC}(\text{PPh}_2)_3$ acting as a tridentate ligand to one metal atom as verified by X-ray crystallography for $[\text{CpFe}(\eta^3\text{-(Ph}_2\text{P)}_3\text{CH)}]\text{PF}_6$. This coordination mode is expected to be unfavorable due to the formation of highly strained four-membered chelate rings. The synthesis of this complex is shown in reaction 2.



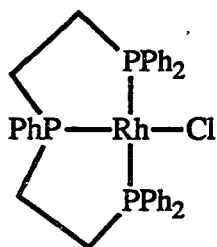
Other interesting chemistry of the tripodal tritertiary phosphines of type I includes the synthesis of the carbonyl bridged rhodium dimer $(\eta^3\text{-3})_2(\mu\text{-CO})_2\text{Rh}_2$ while trying to synthesize a face-capped tetranuclear cluster,²³ the formation of a novel "atrane" structure, and the metal-promoted formation of the non-symmetrical tripodal ligand 23.



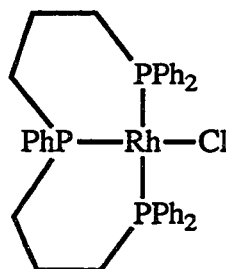
The "atrane" complex was reported⁴¹ by Hendriksen et al. as part of an investigation of the series of ligands $\text{Me}_x\text{Si}(\text{CH}_2\text{CH}_2\text{PPh}_2)_{4-x}$ for the rhodium-catalyzed hydroformylation of 1-butene to pentanal. For $x = 1$, the catalyst became deactivated with the formation of a bright yellow solid. This complex was characterized as $\text{Si}(\text{CH}_2\text{CH}_2\text{PPh}_2)_3\text{Rh}(\text{CO})$ by X-ray crystallography, apparently resulting from Si-C bond cleavage under the reaction conditions. Ligand **23** was formed⁵² by the addition of diphenylphosphine to bis(diphenylvinylphosphine)tetracarbonyl tungsten as shown in reaction 3. Heating the complex $(\eta^2\text{-23})\text{W}(\text{CO})_4$ results in the loss of CO and the formation of $(\eta^3\text{-23})\text{W}(\text{CO})_3$.⁵³



The tritertiary phosphines of type II are all open-chain analogues of $\text{PhP}(\text{CH}_2\text{CH}_2\text{PPh}_2)_2$ and $\text{PhP}(o\text{-C}_6\text{H}_4\text{PPh}_2)_2$. These ligands can triligate to a metal atom in several geometries. However, P-M-P angles in five-membered chelate rings are typically about 83° . In square planar or *mer*-octahedral complexes with ligands of type II and $n = 2$, the presence of two fused five-membered chelate rings introduces some strain to the complex. Meek has shown⁴⁶ by X-ray crystallographic analysis of $\text{PhP}(\text{CH}_2\text{CH}_2\text{PPh}_2)_2\text{RhCl}$ that this ring strain can be removed by incorporating additional methylene groups into the ligand backbone such that $n = 3$.



$$\text{Ph}_2\text{P-Rh-PPh}_2 \cong 166^\circ$$



$$\text{Ph}_2\text{P-Rh-PPh}_2 = 171^\circ$$

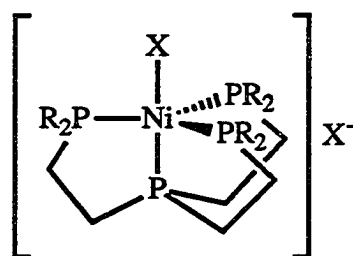
Tetratertiary Phosphines

As shown in Table 2, there are three types of tetratertiary phosphine ligands; tetrapodic, tripodic, and open-chain. The tetrapodic ligands are exemplified by $\text{Si}(\text{CH}_2\text{CH}_2\text{PPh}_2)_4$ ⁴¹ and $\text{C}(\text{CH}_2\text{PPh}_2)_4$.⁵⁴ These ligands are incapable of coordinating all four phosphine groups to a single metal atom and have not been extensively studied.

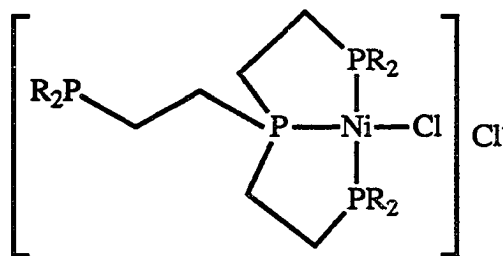
The tripodic tetratertiary phosphines are similar to the tritertiary phosphines of type I where the bridgehead atom is phosphorus. This class of ligands can accommodate metals of trigonal bipyramidal, square pyramidal, square planar, and octahedral geometries. Which geometry is favored is dependent on the metal, the number of methylene groups between the phosphorus donors, and the substituents on phosphorus. For example, King et al.⁴⁵ have shown that $\text{P}(\text{CH}_2\text{CH}_2\text{PR}_2)_3$ forms trigonal bipyramidal five-coordinate nickel(II) complexes for $\text{R} = \text{Me}$ and Ph . For the bulky neopentyl group, however, a square planar complex is formed and one terminal phosphine group remains uncoordinated. The formation of a trigonal bipyramidal nickel complex is sterically prevented by the six bulky neopentyl groups of the terminal phosphine groups.

Table 2. Compilation of tetratertiary phosphine ligands

Tetratertiary Phosphines		Substituents	References
$C(CH_2PPh_2)_4$	24		54
$Si(CH_2CH_2PPh_2)_4$	25		41
$P(o-C_6H_4PPh_2)_3$	26		51
$P(CH_2CH_2PR_2)_3$	27	R = Ph	55 - 64
	28	Me	44
	29	$CH_2C(CH_3)_3$	45
$P(CH_2CH_2CH_2PR_2)_3$	30	R = Me	48, 65 - 68
	31	Et	48
$\{R_2P(CH_2)_2P(R')\}_2(CH_2)_n$	32	n = 3, R = Ph, R' = Ph	50
	33	n = 2, R = Ph, R' = Ph	55, 69 - 71
	34	n = 2, R = Me, R' = Ph	44
	35	n = 1, R = Ph, R' = Ph	73
	36	n = 1, R = Et, R' = Ph	72 - 74
$\{R_2P(CH_2)_3P(R)\}_2CH_2$	37	R = <i>i</i> -Pr	75
$\{R_2PCH_2P(R)\}_2(CH_2)_n$	38	n = 1, R = <i>i</i> -Pr	75
	39	n = 2, R = <i>i</i> -Pr	75
	40	n = 3, R = <i>i</i> -Pr	75
	41	n = 6, R = <i>i</i> -Pr	75
	42	n = 10, R = <i>i</i> -Pr	75

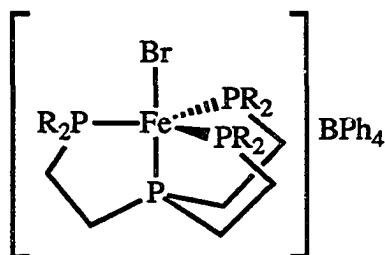


R = Me, Ph; X = Cl, Br, I

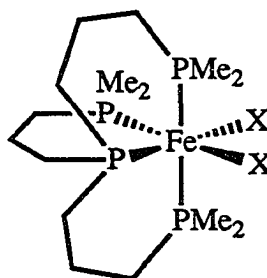


R = CH₂C(CH₃)₃

The dependence of the metal geometry on the chelate ring size has been demonstrated by Sacconi and Dahlenburg. Sacconi et al. have shown⁵⁶ that the geometry for [FeBr{(Ph₂PCH₂CH₂)₃P}]BPh₄ is a trigonal bipyramid. The adoption of this geometry reflects the increased strain introduced by two or more fused five-membered chelate rings if an octahedral geometry were adopted. This strain is minimized in a trigonal bipyramidal geometry. In contrast, the longer chain phosphine P(CH₂CH₂CH₂PMe₂)₃ forms octahedral complexes with FeX₂ (X = Cl, Br, I).⁶⁵ This ligand has a larger bite angle and can readily accommodate an octahedral geometry without suffering from ring strain.



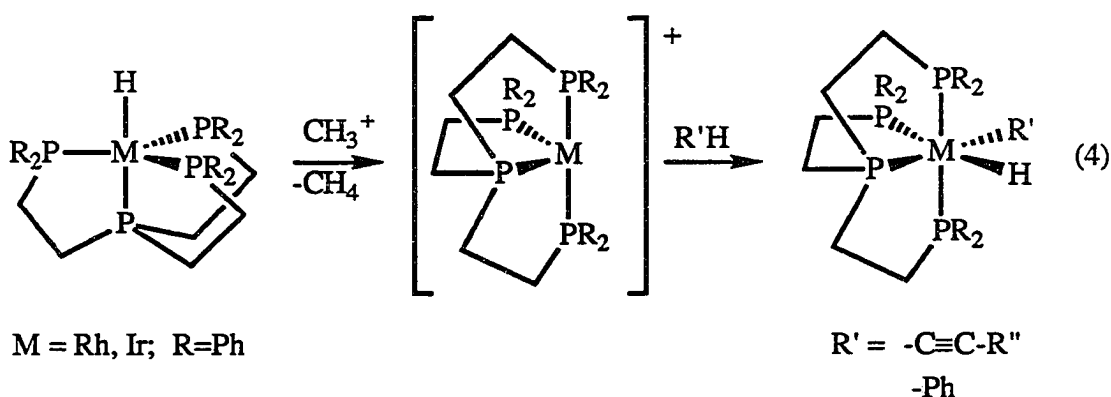
R = Ph



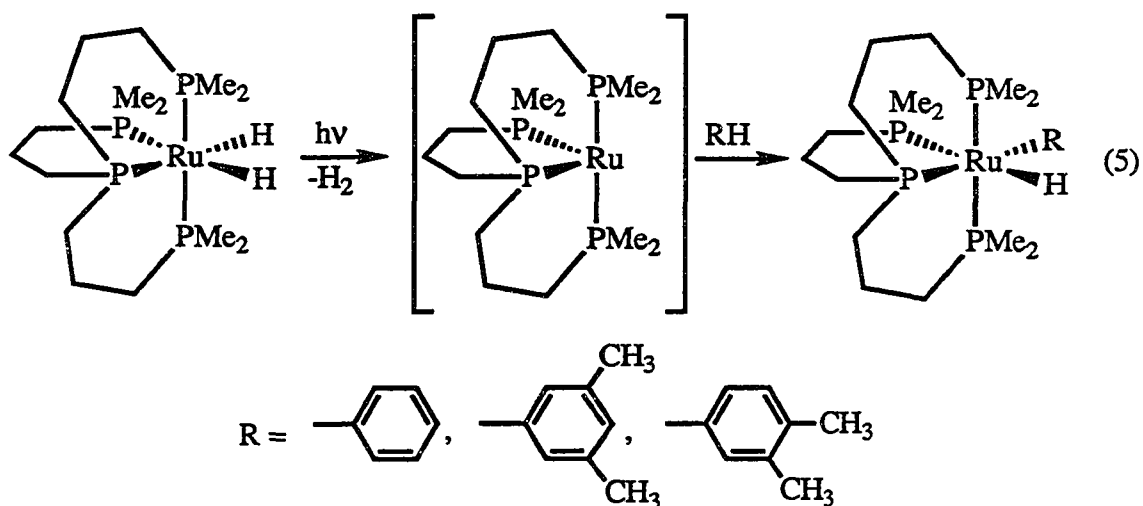
X = Cl, Br, I

Recently, this interconversion between trigonal bipyramidal and octahedral geometries has allowed transition metal complexes of these tetratertiary tripodal ligands

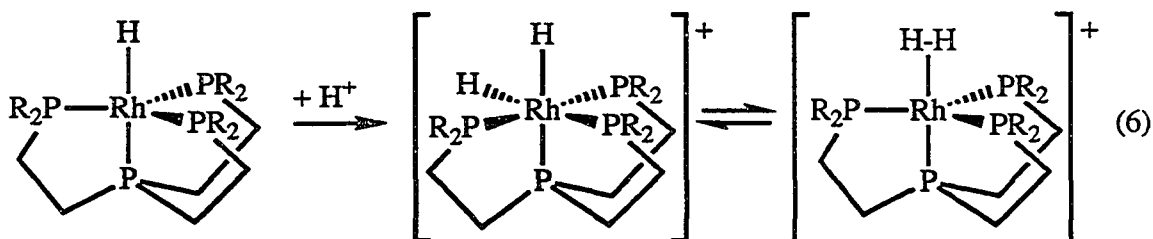
to contribute significantly to the area of C-H bond activation. The trigonal bipyramidal rhodium and iridium monohydride complexes $\{P(CH_2CH_2PPh_2)_3\}MH$ ($M = Rh, Ir$) form highly reactive cationic complexes when the hydride is removed with CH_3^+ . These reactive cationic complexes oxidatively add acetylenes and arenes, including the phenyl substituents on the phosphine ligand, to yield octahedral complexes as shown in reaction 4.⁵⁸⁻⁶⁴ The *ortho*-metallation resulting from oxidative addition of a phosphine phenyl



group is a reversible reaction in the presence of other donors such as carbon monoxide or acetylenes.⁶⁰ Similarly, photolysis of the octahedral ruthenium dihydride complex $\{P(CH_2CH_2CH_2PMe_2)_3\}RuH_2$ results in elimination of H_2 to form a highly reactive intermediate which also oxidatively adds arenes (reaction 5).^{66, 67} Crystal structures have been reported⁶⁸ for several of these oxidative addition products. In addition to this rich C-H bond activation chemistry, Bianchini has also reported⁶⁴ the reversible reaction between a *cis*-dihydride complex, which has been characterized by X-ray crystallography, and an η^2-H_2 complex (reaction 6).



The open-chain tetratertiary phosphines are all analogues of ligand **33** prepared by King et al.⁵⁵ These phosphines can coordinate to one or two metals as bi-, tri-, or tetradentate ligands. These ligands are prepared as a mixture of *meso* and *rac* diastereomers.⁶⁹ The synthesis of metal complexes with this mixture leads to a mixture

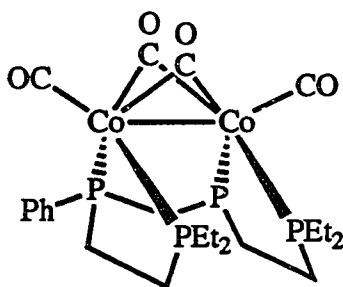


of diastereomeric products which can be differentiated spectroscopically in some cases. In both crystal structures that have been reported for metal complexes of **33**, the ligand is in the *meso* form.^{70, 71}

Stanley et al. have recently reported⁷² the synthesis of the new ligand $\text{Et}_2\text{PCH}_2\text{CH}_2\text{P}(\text{Ph})\text{CH}_2\text{P}(\text{Ph})\text{CH}_2\text{CH}_2\text{PEt}_2$ (**36**) in which only one methylene group

separates the two internal phosphorus donors. This design feature is commonly used to favor a bridged coordination mode as is often found for dppm. Again, this takes advantage of the ring strain that would be induced if dppm were to chelate to one metal. Bimetallic complexes with M-M bonds should readily be obtainable with this ligand. As for the other open-chain tetratertiary phosphines, ligand **36** is formed as a mixture of *meso* and *rac* forms. For **36**, however, these forms are readily separated. Reaction of this mixture with NiCl₂ yields two diastereomers of Ni₂Cl₄(**36**) having different crystal morphologies.⁷³ Both have been characterized by X-ray crystallography. These two complexes can be separated by recrystallization or chromatography. The diastereomerically pure ligand can be freed from the metal by displacement with cyanide.

Reaction of **36** with Co₂(μ-CO)₂(CO)₂(norbornadiene) forms a mixture of diastereomeric Co₂(CO)₄(**36**). Recrystallization yields crystals of the diastereomer containing the *meso* form of the ligand. X-ray crystallography confirmed a ligand-enforced "cradle" geometry with the two internal phosphorus donors spanning the Co-Co bond.⁷⁴ In bimetallic complexes containing two bridging dppm ligands, the



"cradle geometry" of
Co₂(μ-CO)₂(CO)₂(**36**)

phosphines are usually oriented *trans* to one another. Only a few bimetallic dppm complexes which adopt a cisoid or "cradle" geometry have been reported.⁷⁶⁻⁷⁸

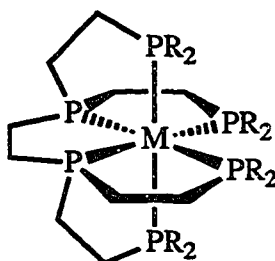
Bimetallic complexes which adopt a "cradle" geometry may exhibit unusual reactivity due to the steric accessibility of the two metal atoms.

Pentatertiary Phosphines

Only one pentatertiary phosphine ligand (**43**) has been synthesized (See Table 3).⁴⁴ No transition metal chemistry has been reported for this ligand, however. A second pentatertiary phosphine ligand (**44**) was obtained⁷⁹ during the photolysis of a hexatertiary phosphine metal complex as will be discussed in the next section. The ligand **44** has not been prepared in its uncoordinated form.

Hexatertiary Phosphines

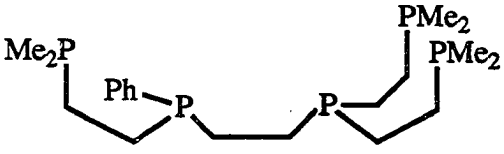
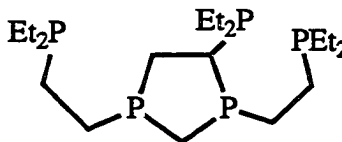
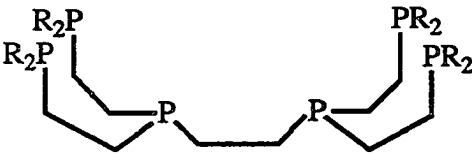
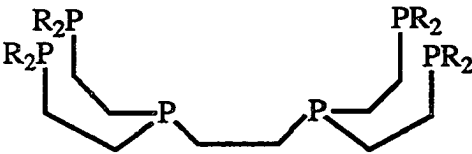
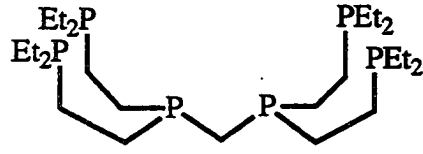
King et al. have synthesized two hexatertiary phosphine ligands, **45**⁴⁴ and **46**.⁸⁰ The framework for these ligands was chosen to favor hexacoordination to one metal making a phosphine analogue of EDTA (ethylenediaminetetraacetic acid). No transition metal chemistry of the methyl derivative **46** has been reported. The phenyl derivative **45** reacts with a variety of metal precursors yielding mixtures of monometallic and bimetallic complexes. These products suffered from poor solubility, hindering



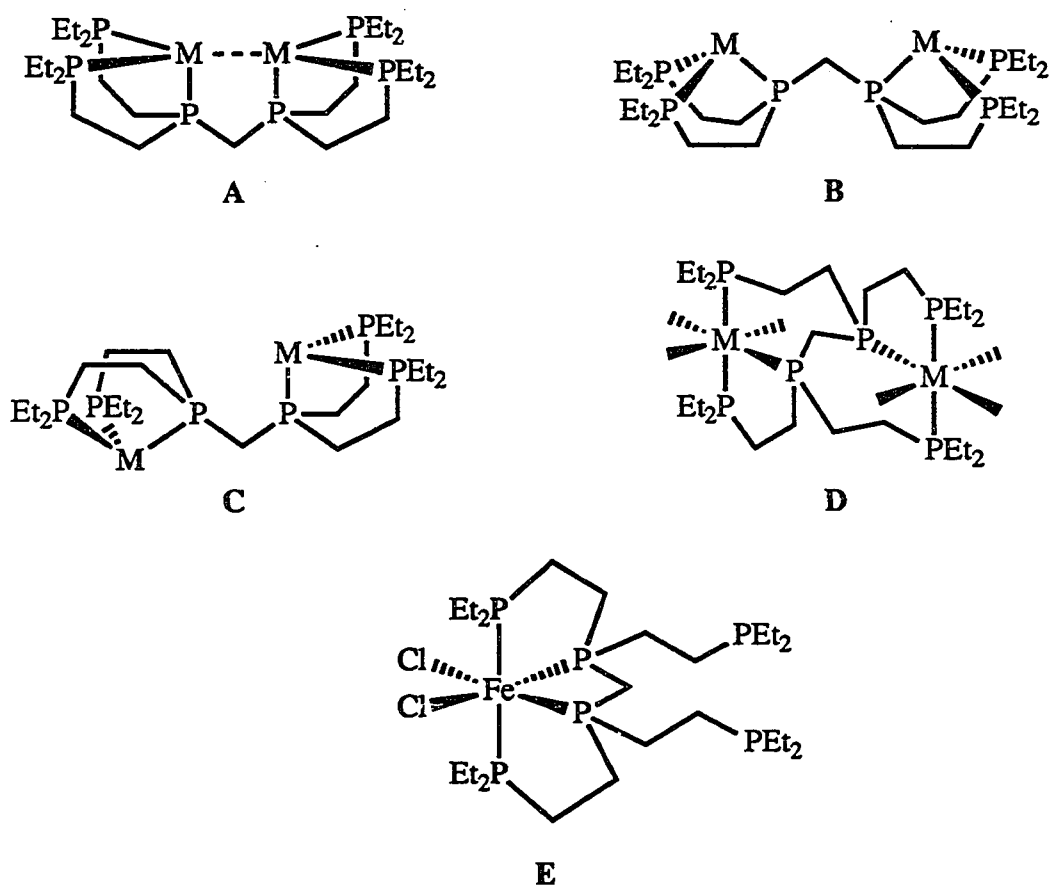
attempts at purification. No monometallic hexacoordinated complexes were obtained. The formation of such a complex is undoubtedly severely restricted by steric interactions

of the eight phenyl substituents as well as the strain that would be inherent in the formation of five fused five-membered chelate rings.

Table 3. Compilation of penta- and hexatertiary phosphines

Ligands	Substituents	References	
<u>Pentatertiary Phosphines</u>			
	43	44	
	44	79	
<u>Hexatertiary Phosphines</u>			
	45	R = Ph	80
	46	R = Me	44
	47		81 - 88

The major contribution to the transition metal chemistry of hexatertiary phosphines has come from the group of G. G. Stanley. Stanley et al. have recently synthesized⁸¹ an analogue of 45 and 46 which incorporates a single methylene bridge between the two internal phosphorus atoms. This feature allows 47 to favor bimetallic complexation with M-M bonded systems. It is hoped that cooperative behavior might be observed in bimetallic complexes with short metal-metal contacts, with potential application in homogeneous transition metal catalyzed systems. Homobimetallic complexes of NiCl₂,^{82, 83} PdCl₂,⁸³ PtCl₂,^{83, 84} CrCl₃,⁸⁵ FeCl₂,⁸⁸ Cr(CO)₃,⁸⁶ Mo(CO)₃,⁸⁶ and W(CO)₃,⁸⁶ as well as heterobimetallic complexes of Ni, Pd and



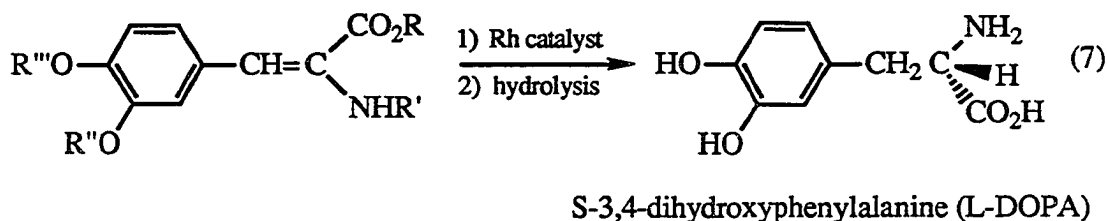
Ni, Co, ⁸⁷ which do not contain M-M bonds, have been synthesized. A novel chiral complex of iron has also been prepared⁸⁸ where **47** chelates to one iron atom as a tetradentate ligand. In addition, spectroscopic data has been reported for $\text{Co}_2(\text{CO})_2(\mathbf{47})$ which presumably has a structure of type A. The various coordination modes observed for this ligand are illustrated on the previous page. In **B** and **C**, both octahedral and square planar geometries have been observed.

Attempts were made to prepare M-M bonded systems from complexes of types **B** and **C** thermally or photochemically.⁷⁹ However, photolysis of $\text{W}_2(\text{CO})_6(\mathbf{47})$ in CH_2Cl_2 yielded the seven coordinate complex $\text{W}_2\text{Cl}_4(\text{CO})_4(\mathbf{47})$. The thermal reaction of **47** and $\text{W}(\text{CO})_6$ yielded the unusual complex $\text{W}_2(\text{CO})_7(\mathbf{44})$. The ligand **47** has lost an $\text{Et}_2\text{PCH}_2\text{CH}_2$ group and a new P-C bond has been formed.

No tertiary phosphine ligands with a denticity greater than six have been reported.

PHOSPHINE ETHERS

Interest in phosphine ether ligands emerged in 1969 with the report of the crystal structure of $\{\text{Me}_2\text{As}(o\text{-C}_6\text{H}_4\text{OCH}_3)\}_2\text{RhCl}_3$, in which an ether oxygen of an arsine ligand is coordinated to rhodium.⁸⁹ Knowles et al.⁹⁰⁻⁹² at Monsanto quickly made use of the related 2-methoxyphenylphosphines PAMP (104), CAMP (105), and DiPAMP (106) in the rhodium-catalyzed asymmetric hydrogenation of N-acylaminocinnamic acids as shown in reaction 7. The synthesis of S-3,4-dihydroxyphenylalanine, or L-DOPA, was achieved with an enantiomeric excess of up to 95%; an important find considering L-DOPA is used in the treatment of Parkinson's disease. This was a major breakthrough which aroused considerable interest in the area of transition metal catalyzed asymmetric transformations as well as phosphine ether ligands.

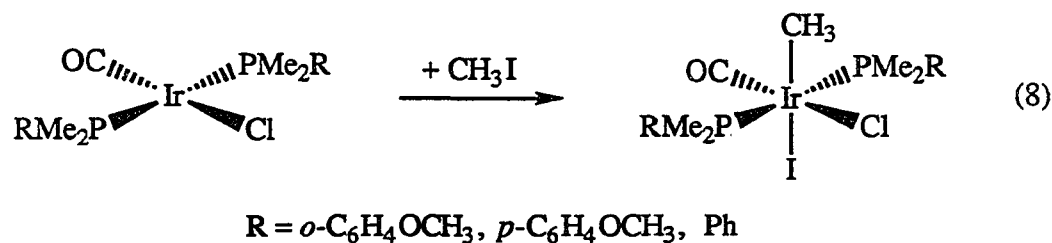


Although some debate continues,¹⁵ many feel that a preferential arrangement of aryl substituents of the ligand around the metal center, and the steric interactions between these aryl groups and the substrate, mediate chiral recognition.⁹² For 104 - 106, weak interactions between the metal and the ether oxygen of the ligand may aid in providing the necessary arrangement of these aryl groups. In support of this proposal, the X-ray structure of $[(\text{DiPAMP})\text{Rh}(\text{COD})]^+$ shows that the methoxy oxygen atoms of DiPAMP

are oriented towards the rhodium atom at nonbonding distances of about 3.7 Å.

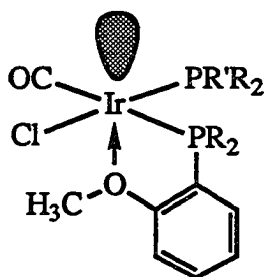
Furthermore, recent NMR spectroscopic data confirms⁹³ coordination of an ether group of DiPAMP to the metal center of an iridium alkyl hydride complex.

Also in the early 1970's, Shaw et al. found^{94, 95} an increase in the rate of oxidative addition of methyl iodide to rhodium(I) and iridium(I) complexes of 2-methoxyphenylphosphines. For reaction 8, the rates of reaction for the ligands Me₂PPh,



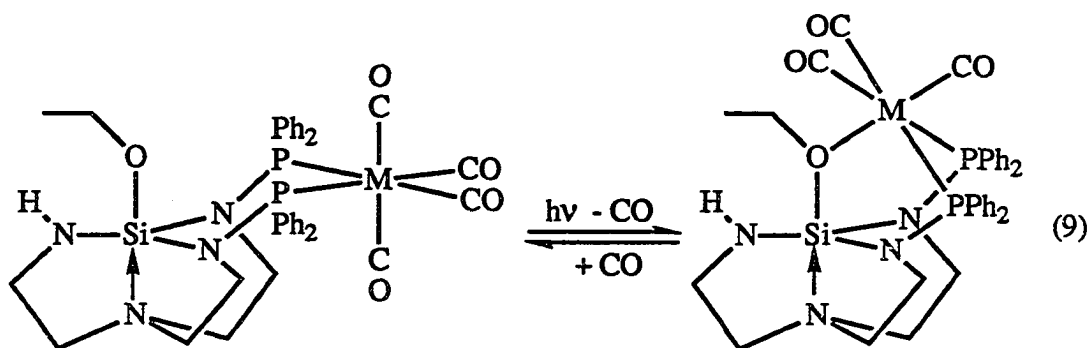
Me₂P(*p*-C₆H₄OCH₃), and Me₂P(*o*-C₆H₄OCH₃) (**102**) were measured to be 4.75 x 10⁻², 6.75 x 10⁻², and 530 x 10⁻² mol⁻¹s⁻¹, respectively. The rate of reaction is approximately 100 times greater for the complex containing ligand **102** than for that containing the electronically very similar Me₂P(*p*-C₆H₄OCH₃). Shaw explained his observations by proposing a weak coordination of the ether oxygen of ligand **102** to the metal as illustrated below. This is the same kind of interaction proposed above in the rhodium-catalyzed asymmetric hydrogenation reactions using ligands **104** - **106**. This additional donor ligand on the metal may increase the basicity at the metal and hence increase the rate of oxidative addition. The rates of oxidative addition reactions are known to increase with increasing electron density on the metal.

Stable Ru(II) complexes containing coordinated ether groups of ligands **102** and **103** were isolated⁹⁶ in 1975. The first X-ray structure for an oxygen coordinated



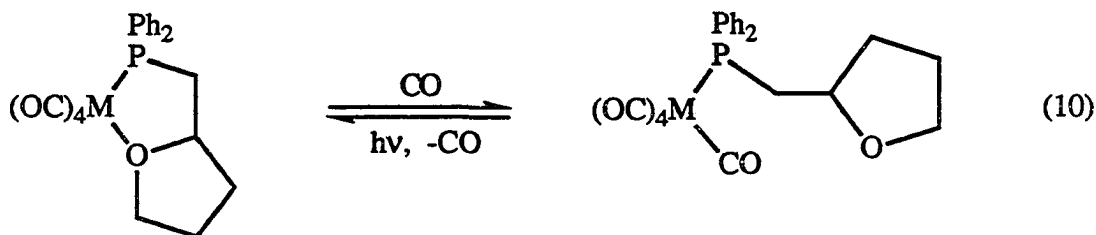
phosphine ether complex was reported⁹⁷ in 1976. Since then the investigation of phosphine ethers has expanded rapidly. Table 4 contains a comprehensive list of phosphine ethers reported in the literature. (This list and the present discussion exclude macrocyclic crown ethers attached to phosphine ligands for the purpose of coordinating alkali metal cations near transition metals. For recent information on this area see reference 98.) Ether coordination for these mixed donor ligands has been observed in complexes of Mo, W, Ru, Co, Rh, and Pt. Ether coordination has been confirmed by X-ray crystallography for $[(\text{Ph}_2\text{PCH}_2\text{CH}_2)_2\text{O}]\text{Rh}(\text{CO})\text{PF}_6$,⁹⁷ $(o\text{-diphenylphosphinoanisole})_2\text{RuCl}_2$,⁷ $(\text{CH}_3\text{OCH}_2\text{CH}_2\text{PPh}_2)_2\text{RuCl}_2$,⁹⁹ $(\text{CH}_3\text{OCH}_2\text{CH}_2\text{PPh}_2)_2\text{Ru}(\text{CO})\text{Cl}_2$,⁹⁹ $[\text{CH}_3\text{OCH}_2\text{CH}_2\text{P}(i\text{-Pr})_2]_2\text{RhCl}$,¹⁰⁰ $[\text{Rh}(\text{TMPP})_2]\text{BF}_4$,¹⁰¹ $(\text{TMPP})\text{Mo}(\text{CO})_3$,¹⁰² and $\text{Rh}_2(\text{O}_2\text{CCH}_3)_3(\text{TMPP})(\text{MeOH})$ ¹⁰³ (TMPP = tris-(2,4,6-trimethoxyphenyl)phosphine, 112).

Ethers are usually poor ligands to low valent mid- to late-group transition metals and should readily be displaced by other donor ligands. The lability of the ether portion of these "hemilabile" phosphine ethers has been demonstrated by substitution with ethylene (Rh),¹⁰⁰ acetylenes (Rh),¹⁰⁰ phosphites (Mo, W),¹⁰⁴ nitriles (Mo,¹⁰² Ru⁷), dimethylsulfide (Pt),^{3f} pyridine (Pt),^{3f} isocyanides (Ru),⁷ and carbon monoxide (Mo,¹⁰⁴ W,^{104, 105} Rh,^{100, 106} Ru,^{7, 96, 99} Pt^{3f}). Some of these substitution reactions



M = Mo, W

are reversible. Two examples of reversible binding of CO under thermal or photolytic conditions are given in reactions 9¹⁰⁷ and 10.¹⁰⁴

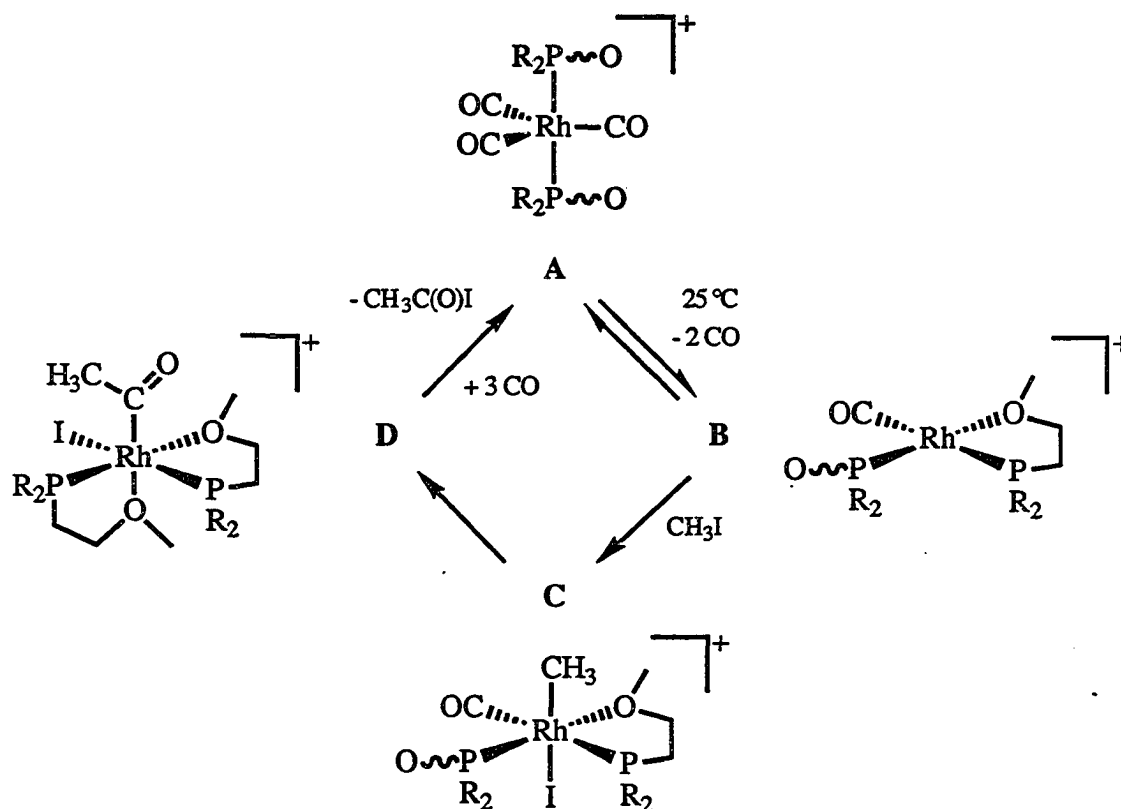


M=Mo, W

Two groups have investigated the potential implications of reversible complex formation with these ligands in transition metal catalyzed systems. Horner et al. have examined¹⁰⁸ the effects of aryl substitution in the ligands 114 - 177 on the rhodium-catalyzed hydrogenation of 1-hexene. Their interest was spurred by the results of asymmetric hydrogenation studies of Knowles mentioned above. Horner concluded from his study that *ortho*-methoxy substitution in the aryl substituents of the phosphine ether ligands favors a *brief coordinative* interaction between the ether oxygen of the ligand and rhodium. This brief interaction stabilizes the configuration of the catalytic intermediate. The role of this rapidly reversing ether coordination has been called the "Scheibenwischer-Effekt" or "Windshield-Wiper Effect".

Recently, Lindner et al. have undertaken^{99, 104, 106, 109-121} a major study of cobalt- and rhodium-catalyzed carbonylations utilizing the ligands **109** - **111** and **178** - **198**. Numerous reports in this series have dealt with the rhodium-catalyzed conversion of methyl iodide to acetic acid, a phosphine ether model for the Monsanto acetic acid synthesis. The Monsanto synthesis¹²² produces acetic acid from methanol and carbon monoxide with the intermediate formation of methyl iodide generated from methanol and HI, which is a cocatalyst in the system. A typical mechanistic scheme accounting for Lindner's observations is shown in Scheme IV. The five-coordinate complexes **A** have been spectroscopically characterized in solution at low temperature, but reversibly form square planar complexes of type **B** at higher temperatures. Complexes of type **B** have been isolated and fully characterized. Intermediates of type **C** have been characterized spectroscopically in some cases, but they readily form the isolable acyl complexes **D**. In the presence of additional CO the acyl complexes reductively eliminate $\text{CH}_3\text{C}(\text{O})\text{I}$ and reform **A**. Subsequent hydrolysis of $\text{CH}_3\text{C}(\text{O})\text{I}$ yields acetic acid. An interesting note in the conversion of **D** to **A** is the dependence of this step on the ligand. Lindner reports^{109, 115, 119} that in the presence of CO reductive elimination of $\text{CH}_3\text{C}(\text{O})\text{I}$ from the acyl complex takes place at 100 °C for ligands **181** and **192**, but takes place at 0 °C for ligand **109**. No rationale for this observed difference was given. Similar to Horner's conclusions for rhodium-catalyzed hydrogenation, Lindner concludes that the reversible phosphine ether coordination plays an important role in these rhodium catalyzed carbonylations by occupying or providing vacant coordination sites on the metal catalyst at various stages of the catalytic pathway. He distinguishes this important contribution of the phosphine ether ligands as the "Auf- und Zuklapp-Mechanismus" or an "Opening and Closing Mechanism".

Scheme IV



In addition to the early work of Shaw and Knowles, and the aforementioned work by Lindner, Dunbar et al. have very recently reported some interesting chemistry of the very bulky phosphine ether **112**. For example, **112** reacts with $(\eta^6\text{-cycloheptatriene})\text{Mo}(\text{CO})_3$ to yield the complex $(\mathbf{112})\text{Mo}(\text{CO})_3$ in which two ether oxygens of the ligand are coordinated to molybdenum.¹⁰² More interesting is the ability of this ligand to form an air-stable monometallic complex of Rh(II). The complex

[Rh(112)₂][BF₄]₂ is the first structurally characterized example of a monomeric cationic rhodium(II) complex.¹⁰¹

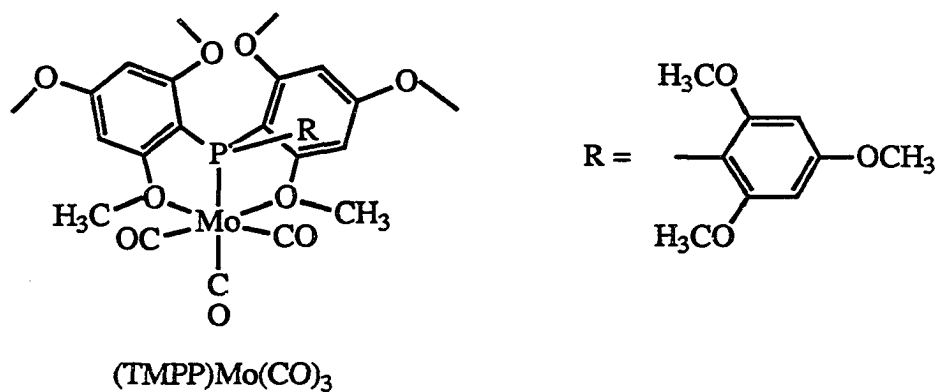


Table 4. Compilation of phosphine ether ligands

Ligands		Substituents	References
	101	R = Me	94, 95
	102	R = Ph	7, 94 - 96
	103		96
	104		90 - 92

Table 4. Continued

Ligands		Substituents	References
<p>CAMP</p>	105		90 - 92
<p>DiPAMP</p>	106		90 - 93
	107		97, 123
	108		124, 125
	109	R = <i>i</i> -Pr	100, 109
	110	Cy	99, 110, 111
	111	Ph	3e, 3f, 109, 99, 112-114
	112		101 - 103

Table 4. Continued

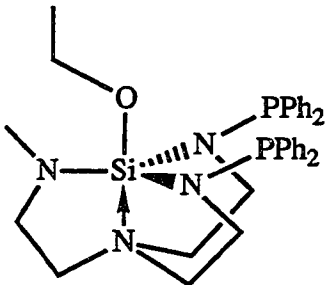
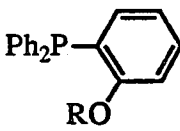
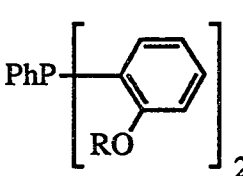
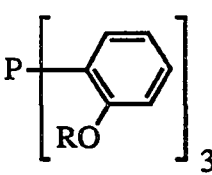
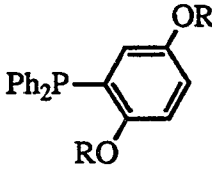
Ligands		Substituents	References
	113		107
	114	R = Et	108
	115	Pr	108
	116	<i>i</i> -Pr	108
	117	<i>t</i> -Bu	108
	118	R = Me	108
	119	Et	108
	120	Pr	108
	121	<i>i</i> -Pr	108
	122	R = Me	108
	123	R = Me	108
	124	Et	108
	125	Pr	108
	126	<i>i</i> -Pr	108
	127	<i>t</i> -Bu	108

Table 4. Continued

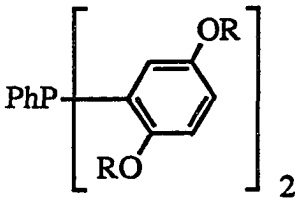
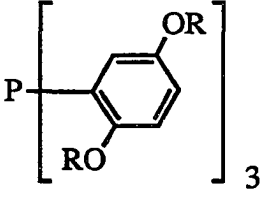
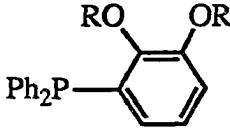
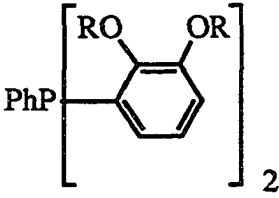
Ligands		Substituents	References
	128	R = Me	108
	129	Et	108
	130	Pr	108
	131	<i>i</i> -Pr	108
	132	<i>t</i> -Bu	108
	133	R = Me	108
	134	R = Me	108
	135	Et	108
	136	Pr	108
	137	<i>i</i> -Pr	108
	138	Bu	108
	139	<i>t</i> -Bu	108
	140	<i>s</i> -Bu	108
	141	R = Me	108
	142	Et	108
	143	Pr	108
	144	<i>i</i> -Pr	108
	145	Bu	108
	146	<i>t</i> -Bu	108
	147	<i>s</i> -Bu	108

Table 4. Continued

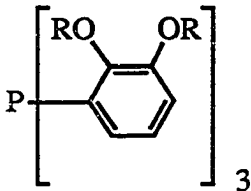
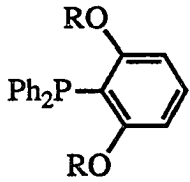
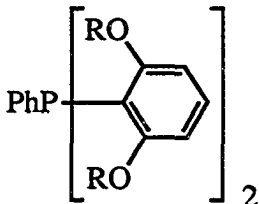
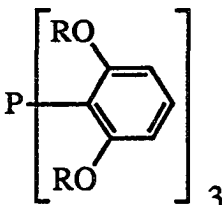
Ligands		Substituents	References
	148	R = Me	108
	149	R = Me	108
	150	Et	108
	151	Pr	108
	152	<i>i</i> -Pr	108
	153	Bu	108
	154	<i>t</i> -Bu	108
	155	<i>s</i> -Bu	108
	156	R = Me	108
	157	Et	108
	158	Pr	108
	159	<i>i</i> -Pr	108
	160	Bu	108
	161	<i>t</i> -Bu	108
	162	<i>s</i> -Bu	108
	163	R = Me	108
	164	Et	108
	165	Pr	108
	166	<i>i</i> -Pr	108
	167	Bu	108
	168	<i>t</i> -Bu	108
	169	<i>s</i> -Bu	108

Table 4. Continued

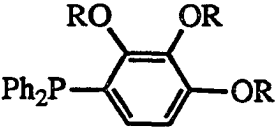
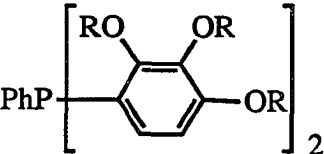
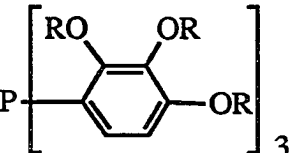
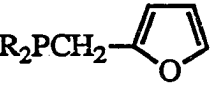
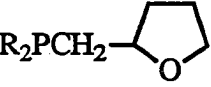
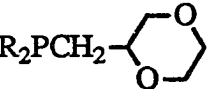
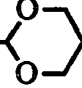
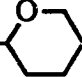
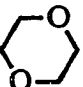
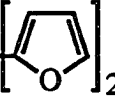
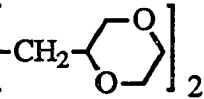
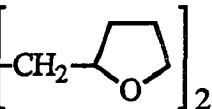
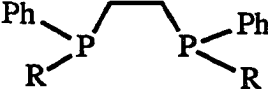
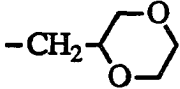
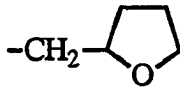
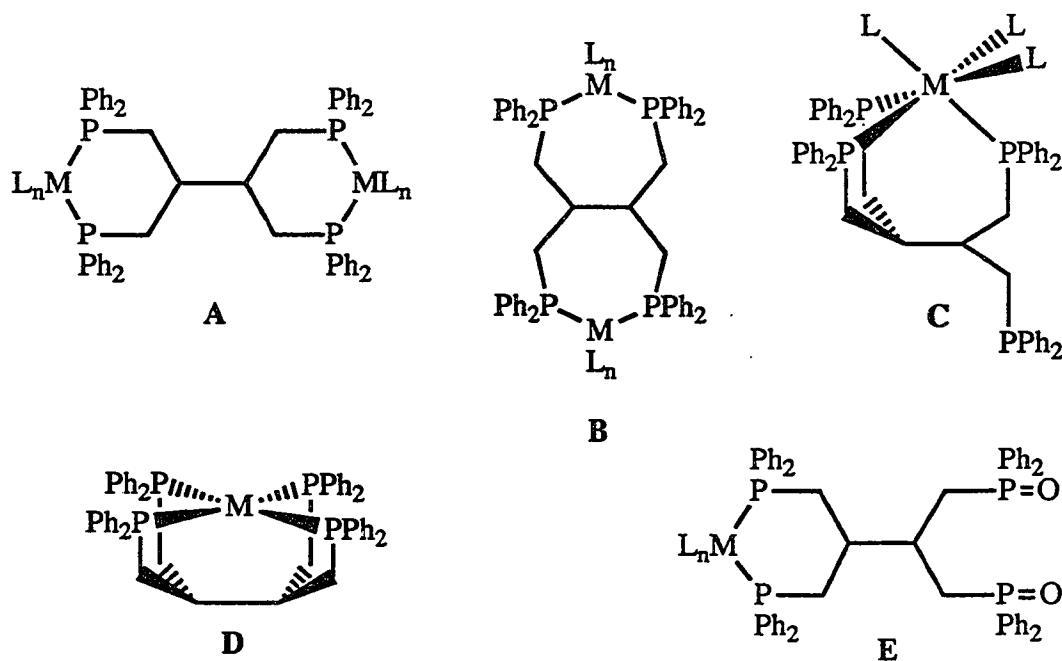
Ligands		Substituents	References
	170	R = Me	108
	171	Et	108
	172	Pr	108
	173	<i>i</i> -Pr	108
	174	R = Me	108
	175	Et	108
	176	Pr	108
	177	R = Me	108
	178	R = Me	12
	179	<i>t</i> -Bu	12
	180	Ph	12
	181	R = Me	115, 116
	182	<i>t</i> -Bu	116
	183	Cy	99, 106, 111
	184	Ph	99, 104, 106 114, 116
	185	R = Cy	117
	186	Ph	117, 118
	187	Mes	117

Table 4. Continued

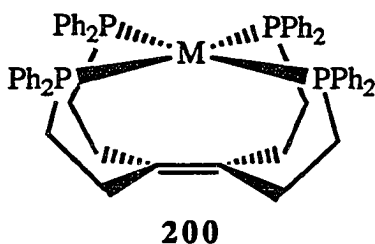
Ligands		Substituents	References
R_2PCH_2- 	188	R = Cy	117
	189	Ph	117
	190	Mes	117
R_2PCH_2- 	191	R = Ph	114
$R(Ph)PCH_2-$ 	192	R = $(CH_2)_3SiMe_3$	119
MeP 	193		116
PhP 	194		120
PhP 	195		104, 116
	196	R = 	120, 121
	197	R = 	120
	198	R = $CH_2CH_2OCH_3$	120

STATEMENT OF RESEARCH PROJECT

Recently, the new tetratertiary phosphine 2,3-bis(diphenylphosphinomethyl)-1,4-bis(diphenylphosphino)-butane (**199**) was synthesized in our group.¹²⁶ This ligand is dissimilar from the previously reported phosphines compiled in Table 2 in that **199** is not tripodic, as are **26** - **31**, and it is not an open-chain ligand like **32** - **42**. Ligand **199** is a tetrapodic ligand, but differs from **24** and **25** since it may potentially tetracoordinate to one metal as shown for **D**. Other coordination modes are also plausible and are illustrated as **A** - **E**. For complexes of type **D**, the unique geometric constraints of the ligand limit metals to square planar or square pyramidal geometries with the sixth coordination site effectively blocked by the ligand backbone. Such a complex may exhibit unusual reactivity since changes in steric and electronic factors can dramatically alter the reactivity patterns of a metal complex as was discussed with numerous examples



in the general survey of multidentate phosphines. No comparable phosphine ligands have been reported, with the exception of ligand **200** which was previously proposed^{9a} by Chiswell as a ligand which may favor the formation of square planar or square pyramidal complexes. The synthesis and chemistry of this ligand has not been reported and merits consideration for future work.



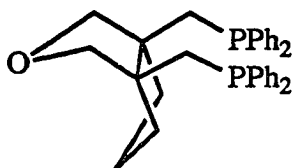
In a previous study of Group X metals,¹²⁶ ligand **199** was shown to form complexes of type A for $ML_n = PdCl_2$ and type E for $ML_n = PdCl_2$ and PdI_2 . No complexes of types B or C were reported. Preliminary evidence was presented for complexes of type D for Ni(II), Pd(II), and Ag(I). There are discrepancies in the spectral data presented for these complexes, however, and I have found the syntheses of these complexes to be irreproducible.

The chemistry of this ligand has now been reinvestigated. The scope of this study has been expanded to include transition metals from Groups VI, VIII, IX, and X, and the emphasis of this study has been aimed at identifying all of the common coordination modes of this ligand so that prior discrepancies can be addressed. Section II of this thesis details these results, including the identification of complexes of types A, C, and E, the possible formation of a complex of type B, and a rationale for the inability of this ligand to form complexes of type D.

In an attempt to prepare $[\text{Pd}(\text{dppp})_2][\text{BF}_4]_2$ as a model for complexes of type **D**, an unprecedented fluoride-induced redox reaction was discovered. In this reaction $\text{Pd}(\text{II})$ phosphine complexes are reduced to $\text{Pd}(0)$ complexes with the concomitant formation of one equivalent of a difluorophosphorane (R_3PF_2). The scope of this new reaction was explored for several aryl phosphine complexes of $\text{Ni}(\text{II})$, $\text{Pd}(\text{II})$, and $\text{Pt}(\text{II})$. The results of this study are presented here in Sections VI and VII.

From the overview of phosphine ether ligands presented earlier, and a brief perusal of Table 4, it is apparent that new variations on this limited class of ligands may be of interest. Of the ninety ligands listed in this table, seventy contain methoxyphenyl substituents on phosphorus. Sixty three of these were utilized in Horner's rhodium-catalyzed hydrogenation study and have not been systematically investigated in other systems. Few of these ligands are capable of ether coordination with the formation of six-membered chelate rings (only ligand **102** has been demonstrated to coordinate with the formation of six-membered chelate rings) and only five ligands (**106**, **107**, **196** - **198**) contain two phosphine groups. Furthermore, these ditertiary phosphine ether ligands are not constrained to a particular geometry upon ether coordination and may accommodate both *fac* and *mer* arrangements of ligands.

The new ditertiary phosphine ether **201** has been synthesized starting from 1,1,2,2-tetrakis(hydroxymethyl)cyclopentane and an investigation of its basic coordination chemistry has been undertaken. (This tetraol framework was chosen since it

**201**

was also being studied¹²⁷ as a precursor for the synthesis of new tetratertiary phosphine analogues to ligand **199** in connection with the chemistry in Section I). This ligand has been found to coordinate to transition metals in either bidentate (P, P') or tridentate (P, P', O) coordination modes as reported in Section III of this dissertation. The lability of the coordinated ether in the tridentate coordination mode of this ligand has been investigated and has yielded interesting results in regard to the stereospecificity of substitution reactions in Group VI metal carbonyl complexes. These results are presented in Sections IV and V.

REFERENCES

1. Parshall, G. W. *Homogeneous Catalysis*; John Wiley & Sons: New York, 1980.
2. Hendriksen, D. E.; Oswald, A. A.; Ansell, G. B.; Leta, S.; Kastrup, R. V. *Organometallics* **1989**, *8*, 1153.
3. For a few examples, see: (a) Sacconi, L.; Bertini, I. *J. Am. Chem. Soc.* **1968**, *90*, 5443. (b) Du Bois, D. L.; Meyers, W. H.; Meek, D. W. *J. Chem. Soc., Dalton Trans.* **1975**, 1011. (c) Lindner, E.; Rauleder, H.; Hiller, W. Z. *Naturforsch.* **1983**, *38b*, 417. (d) Ellermann, J.; Moll, M.; Will, N. *J. Organomet. Chem.* **1989**, *378*, 73. (e) Anderson, G. K.; Kumar, R. *Inorg. Chim. Acta* **1988**, *146*, 89. (f) Anderson, G. K.; Kumar, R. *Inorg. Chem.* **1984**, *23*, 4064. (g) Danopoulos, A. A.; Edwards, P. G.; Parry, J. S.; Willis, A. R. *Polyhedron* **1989**, *8*, 1767. (h) Uriarte, R.; Mazanec, T.J.; Tau, K.D.; Meek, D. W. *Inorg. Chem.* **1980**, *19*, 79.
4. (a) Braunstein, P.; Matt, D.; Nobel, D.; Bouaoud, S. E.; Carluer, B.; Grandjean, D.; Lemoine, P. *J. Chem. Soc., Dalton Trans.* **1986**, 415. (b) Braunstein, P.; Matt, D.; Dusausoy, Y. *Inorg. Chem.* **1983**, *22*, 2043. (c) Braunstein, P.; Matt, D.; Dusausoy, Y.; Fischer, J.; Mitschler, A.; Ricard, L. *J. Am. Chem. Soc.* **1981**, *103*, 5115.
5. Abbassioun, M. S.; Chaloner, P. A.; Hitchcock, P. B.; Claver, C.; Masdeu, A. M.; Ruiz, A.; Saballs, T. *J. Organomet. Chem.* **1991**, *403*, 229.
6. Bond, A. M.; Colton, R.; Panagiotidou, P. *Organometallics* **1988**, *7*, 1767.
7. Jeffrey, J. C.; Rauchfuss, T. B. *Inorg. Chem.* **1979**, *18*, 2658.
8. Collman, J. P. *Acc. Chem. Res.* **1968**, *1*, 136.

9. (a) McAuliffe, C. A.; Levason, W. *Phosphine, Arsine, and Stibine Complexes of the Transition Elements*; Elsevier: New York, 1973; p. 271. (b) Levason, W.; McAuliffe, C. A. *Adv. Inorg. Chem. Radiochem.* **1974**, *14*, 173.
(c) McAuliffe, C. A. *Adv. Inorg. Chem. Radiochem.* **1975**, *17*, 165.
10. Mason, R.; Meek, D. W. *Angew. Chem., Int. Ed. Engl.* **1978**, *17*, 183.
11. Tolman, C. A. *Chem. Rev.* **1977**, *77*, 313.
12. Garrou, P. E. *Chem. Rev.* **1985**, *85*, 171.
13. Garrou, P. E. *Chem. Rev.* **1981**, *81*, 229.
14. *Phosphorus-31 NMR Spectroscopy in Stereochemical Analysis*; Verkade, J. G.; Quin, L. D., Eds.; VCH Publishers: Deerfield Beach, 1987.
15. Kagan, H. B. in *Comprehensive Organometallic Chemistry*; Wilkinson, G.; Stone, F. G. A.; Abel, E. W., Eds.; Pergamon: New York, 1982; vol. 8, p. 463.
16. McAuliffe, C. A. in *Comprehensive Coordination Chemistry*; Wilkinson, G.; Gillard, R. D.; McCleverty, J. A., Eds.; Pergamon: New York, 1987; vol. 2, p. 989.
17. Whitesides, G. M.; Casey, C. P.; Krieger, J. K. *J. Am. Chem. Soc.* **1971**, *93*, 1379.
18. Blackburn, D. W.; Chi, K. M.; Frerichs, S. R.; Tinkham, M. L.; Ellis, J. E. *Angew. Chem., Int. Ed. Engl.* **1988**, *27*, 437.
19. Chi, K. M.; Frerichs, S. R.; Stein, B. K.; Blackburn, D. W.; Ellis, J. E. *J. Am. Chem. Soc.* **1988**, *110*, 163.
20. Ellis, J. E. *Polyhedron* **1989**, *8*, 1611.
21. Hewertson, W.; Watson, H. R. *J. Chem. Soc.* **1962**, 1490.
22. Chatt, J.; Hart, F. A.; Watson, H. R. *J. Chem. Soc.* **1962**, 2537.

23. Allevi, C.; Golding, M.; Heaton, B. T.; Ghilardi, C. A.; Midollini, S.; Orlandini, A. *J. Organomet. Chem.* **1987**, *326*, C19.
24. Cecconi, F.; Ghilardi, C. A.; Midollini, S.; Orlandini, A.; Zanello, P.; Heaton, B. T.; Huang, L.; Iggo, J. A.; Bordoni, S. *J. Organomet. Chem.* **1988**, *353*, C5.
25. Karsch, H. H.; Schubert, U.; Neugebar, D. *Angew. Chem., Int. Ed. Engl.* **1979**, *18*, 484.
26. Issleib, K.; Abicht, H. P. *J. Prakt. Chem.* **1970**, *312*, 456.
27. Bahsoun, A. A.; Osborn, J. A.; Voelker, C.; Bonnet, J. J.; Lavigne, G. *Organometallics* **1982**, *1*, 1114.
28. Clucas, J. A.; Harding, M. M.; Nicholls, B. S.; Smith, A. K. *J. Chem. Soc., Chem. Commun.* **1984**, 319.
29. Darensbourg, D. J.; Zalewski, D. J.; Delord, T. *Organometallics* **1984**, *3*, 1210.
30. Osborn, J. A.; Stanley, G. G. *Angew. Chem., Int. Ed. Engl.* **1980**, *19*, 1025.
31. Osborn, J. A.; Stanley, G. G.; Bird, P. H. *J. Am. Chem. Soc.* **1988**, *110*, 2117.
32. Harding, M. M.; Nicholls, B. S.; Smith, A. K. *J. Organomet. Chem.* **1982**, *226*, C17.
33. Arduini, A. A.; Bahsoun, A. A.; Osborn, J. A.; Voelker, C. *Angew. Chem., Int. Ed. Engl.* **1980**, *19*, 1024.
34. Foster, D. F.; Harrison, J.; Nicholls, B. S.; Smith, A. K. *J. Organomet. Chem.* **1983**, *248*, C29.
35. Lusser, M.; Perringer, P. *J. Organomet. Chem.* **1986**, *301*, 269.
36. Amouri, H. E.; Bahsoun, A. A.; Osborn, J. A.; Youinou, A. T.; Fischer, J. *Polyhedron* **1989**, *8*, 2119.
37. Mague, J. T.; Dessens, S. E. *J. Organomet. Chem.* **1984**, *262*, 347.

38. Goodrich, J. D.; Selegue, J. P. *Organometallics* **1985**, *4*, 798.
39. de Boer, J. J.; van Doorn, J. A.; Masters, C. J. *J. Chem. Soc., Chem. Commun.* **1978**, 1005.
40. Foster, D. F.; Nicholls, B. S.; Smith, A. K. *J. Organomet. Chem.* **1983**, *244*, 159.
41. Hendriksen, D. E.; Oswald, A. A.; Ansell, G. B., Leta, S.; Kastrup, R. V. *Organometallics* **1989**, *8*, 1153.
42. King, R. B.; Kapoor, P. N.; Kapoor, R. N. *Inorg. Chem.* **1971**, *10*, 1841.
43. King, R. B.; Cloyd, J. C. *Inorg. Chem.* **1975**, *14*, 1550.
44. King, R. B.; Cloyd, J. C. *J. Am. Chem. Soc.* **1975**, *97*, 53.
45. King, R. B.; Cloyd, J. C.; Reimann, R. H. *Inorg. Chem.* **1976**, *15*, 449.
46. Napier, T. E. Jr.; Meek, D. W.; Kirchner, R. M.; Ibers, J. A. *J. Am. Chem. Soc.* **1973**, *95*, 4194.
47. Uriarte, R.; Mazanec, T. J.; Tau, K. D.; Meek, D. W. *Inorg. Chem.* **1980**, *19*, 79.
48. Antberg, M.; Prengel, C.; Dahlenburg, L. *Inorg. Chem.* **1984**, *23*, 4170.
49. King, R. B.; Zinich, J. A.; Cloyd, J. C. *Inorg. Chem.* **1975**, *14*, 1554.
50. Du Bois, D. L.; Meyers, W. H.; Meek, D. W. *J. Chem. Soc., Dalton Trans.* **1975**, 1011.
51. Hartley, J. G.; Venanzi, L. M.; Goodall, D. C. *J. Chem. Soc.* **1963**, 3930.
52. Keiter, R. L.; Sun, Y. Y.; Brodack, J. W.; Carey, L. W. *J. Am. Chem. Soc.* **1979**, *101*, 2638.
53. Colquhoun, I. J.; McFarlane, W.; Keiter, R. L. *J. Chem. Soc., Dalton Trans.* **1984**, 455.
54. Ellermann, J.; Dorn, K. *Chem. Ber.* **1966**, *99*, 653.

55. King, R. B.; Kapoor, R. N.; Saran, M. S.; Kapoor, P. N. *Inorg. Chem.* **1971**, *10*, 1851.
56. Sacconi, L.; Di Vaira *Inorg. Chem.* **1978**, *17*, 810.
57. Bruggeller, P. *Inorg. Chim. Acta* **1987**, *129*, L27.
58. Bianchini, C.; Masi, D.; Meli, A.; Peruzzini, M.; Zanobini, F. *J. Am. Chem. Soc.* **1988**, *110*, 6411.
59. Bianchini, C.; Peruzzini, M.; Zanobini, F. *J. Organomet. Chem.* **1987**, *326*, C79.
60. Bianchini, C.; Meli, A.; Peruzzini, M.; Zanobini, F. *J. Chem. Soc., Chem. Commun.* **1987**, 971.
61. Bianchini, C.; Meli, A.; Peruzzini, M.; Francesco, V. *Organometallics* **1990**, *9*, 1146.
62. Bianchini, C.; Meli, A.; Peruzzini, M.; Zanobini, F.; Bruneau, C.; Dixneuf, P. H. *Organometallics* **1990**, *9*, 1155.
63. Bianchini, C.; Meli, A.; Peruzzini, M.; Zanobini, F. *Organometallics* **1990**, *9*, 241.
64. Bianchini, C.; Meli, A.; Peruzzini, M.; Zanobini, F. *J. Am. Chem. Soc.* **1987**, *109*, 5548.
65. Antberg, M.; Dahlenburg, L. *Inorg. Chim. Acta* **1985**, *104*, 51.
66. Antberg, M.; Dahlenburg, L. *Inorg. Chim. Acta* **1986**, *111*, 73.
67. Antberg, M.; Dahlenburg, L.; Frosin, K. M.; Hock, N. *Chem. Ber.* **1988**, *121*, 859.
68. Dahlenburg, L.; Frosin, K. M. *Chem. Ber.* **1988**, *121*, 865.
69. King, R. B.; Heckley, P. R.; Cloyd, J. C. *Z. Naturforsch. B* **1974**, *296*, 574.

70. Ghilardi, C. A.; Midollini, S.; Sacconi, L.; Stoppioni, P. *J. Organomet. Chem.* **1981**, *205*, 193.
71. Ghilardi, C. A.; Bacci, M. *Inorg. Chem.* **1974**, *13*, 2398.
72. Laneman, S. A.; Fronczek, F. R.; Stanley, G. G. *J. Am. Chem. Soc.* **1988**, *110*, 5585.
73. Laneman, S. A.; Fronczek, F. R.; Stanley, G. G. *Inorg. Chem.* **1989**, *28*, 1872.
74. Laneman, S. A.; Fronczek, F. R.; Stanley, G. G. *Inorg. Chem.* **1989**, *28*, 1206.
75. Sommer, H.; Hietkamp, S.; Stelzer, O. *Chem. Ber.* **1984**, *117*, 3414.
76. DeLaet, D. L.; Fanwick, P. F.; Kubiak, C. P. *Organometallics* **1986**, *5*, 1807.
77. Berry, D. H.; Eisenberg, R. *Organometallics* **1987**, *6*, 1796.
78. Cotton, F. A.; Dunbar, K. R.; Verbruggen, M. G. *J. Am. Chem. Soc.* **1987**, *109*, 5498.
79. Saum, S. E.; Fronczek, F. R.; Laneman, S. A.; Stanley, G. G. *Inorg. Chem.* **1989**, *28*, 1878.
80. King, R. B.; Saran, M. S. *Inorg. Chem.* **1971**, *10*, 1861.
81. Askham, F. R.; Stanley, G. G.; Marques, E. C. *J. Am. Chem. Soc.* **1985**, *107*, 7423.
82. Laneman, S. A.; Stanley, G. G. *Inorg. Chem.* **1987**, *26*, 1177.
83. Saum, S. E.; Laneman, S. A.; Stanley, G. G. *Inorg. Chem.* **1990**, *29*, 5065.
84. Saum, S. E.; Stanley, G. G. *Polyhedron* **1987**, *6*, 1803.
85. Askham, F. R.; Maverick, A. W.; Stanley, G. G. *Inorg. Chem.* **1987**, *26*, 3963.
86. Saum, S. E.; Askham, F. R.; Fronczek, F. R.; Stanley, G. G. *Organometallics* **1988**, *7*, 1409.
87. Saum, S. E.; Askham, F. R.; Stanley, G. G. *Polyhedron* **1990**, *9*, 1317.
88. Askham, F. R.; Saum, S. E.; Stanley, G. G. *Organometallics* **1987**, *6*, 1370.

89. Graziani, R.; Bombieri, G.; Volponi, L.; Panattoni, C. *J. Chem. Soc. (A)* **1969**, 1236.
90. Knowles, W. S.; Sabacky, M. J.; Vineyard, B. D. *J. Chem. Soc., Chem. Commun.* **1972**, 10.
91. Vineyard, B. D.; Knowles, W. S.; Sabacky, M. J.; Bachman, G. L.; Weinkauff, D. J. *J. Am. Chem. Soc.* **1977**, *99*, 5946.
92. Knowles, W. S. *Acc. Chem. Res.* **1983**, *16*, 106.
93. (a) Brown, J. M.; Maddox, P. J. *J. Chem. Soc., Chem. Commun.* **1987**, 1276.
(b) Brown, J. M.; Maddox, P. J. *J. Chem. Soc., Chem. Commun.* **1987**, 1278.
94. Miller, E. M.; Shaw, B. L. *J. Chem. Soc., Dalton Trans.* **1974**, 480.
95. Empsall, H. D.; Hyde, E. M.; Jones, C. E.; Shaw, B. L. *J. Chem. Soc., Dalton Trans.* **1974**, 1980.
96. Rauchfuss, T. B.; Patino, F. T.; Roundhill, D. M. *Inorg. Chem.* **1975**, *14*, 652.
97. Alcock, N. W.; Brown, J. M.; Jeffrey, J. C. *J. Chem. Soc., Dalton Trans.* **1976**, 583.
98. (a) Powell, J.; Gregg, M. R.; Kuskis, A.; May, C. J.; Smith, S. J. *Organometallics* **1989**, *8*, 2918. (b) Powell, J.; Kuskis, A.; May, C. J.; Smith, S. J. *Organometallics* **1989**, *8*, 2933.
99. Lindner, E.; Schober, V.; Fawzi, R.; Hiller, W.; Englert, V.; Wegner, P. *Chem. Ber.* **1987**, *120*, 1621.
100. Werner, H.; Hampp, A.; Peters, K.; Peters, E. M.; Walz, L.; von Schnering, H. *G. Z. Naturforsch.* **1990**, *45b*, 1548.
101. Dunbar, K. R.; Haefner, S. C.; Pence, L. E. *J. Am. Chem. Soc.* **1989**, *111*, 5504.

102. Dunbar, K. R.; Haefner, S. C.; Burzynski, D. J. *Organometallics* **1990**, *9*, 1347.
103. Chen, S. J.; Dunbar, K. R. *Inorg. Chem.* **1990**, *29*, 588.
104. Lindner, E.; Mayer, H. A.; Wegner, P. *Chem. Ber.* **1986**, *119*, 2616.
105. Lindner, E.; Meyer, S.; Wegner, P.; Karle, B.; Sickinger, A.; Steger, B. J. *Organomet. Chem.* **1987**, *335*, 59.
106. Lindner, E.; Andres, B. *Chem. Ber.* **1987**, *120*, 761.
107. Gudat, D.; Daniels, L. M.; Verkade, J. G. *Organometallics* **1990**, *9*, 1464.
108. Horner, L.; Simmons, G. Z. *Naturforsch.* **1984**, *39b*, 497.
109. Lindner, E.; Norz, H. *Chem. Ber.* **1990**, *123*, 459.
110. Lindner, E.; Meyer, S. J. *Organomet. Chem.* **1988**, *339*, 193.
111. Lindner, E.; Schober, U.; Stangle, M. J. *Organomet. Chem.* **1987**, *331*, C13.
112. Lindner, E.; Schober, U. *Inorg. Chem.* **1988**, *27*, 212.
113. McCann, G. M.; Carvill, A.; Lindner, E.; Karle, B.; Mayer, H. A. *J. Chem. Soc., Dalton Trans.* **1990**, 3107.
114. Lindner, E.; Speidel, R. Z. *Naturforsch.* **1989**, *44b*, 437.
115. Lindner, E.; Andres, B. *Chem. Ber.* **1988**, *121*, 829.
116. Lindner, E.; Rauleder, H.; Scheytt, C.; Mayer, H. A.; Hiller, W.; Fawzi, R.; Wegner, P. Z. *Naturforsch.* **1984**, *39b*, 632.
117. Lindner, E.; Sickinger, A.; Wegner, P. J. *Organomet. Chem.* **1988**, *349*, 75.
118. Lindner, E.; Sickinger, A.; Wegner, P. J. *Organomet. Chem.* **1986**, *312*, C37.
119. Lindner, E.; Glaser, E. J. *Organomet. Chem.* **1990**, *391*, C37.
120. Lindner, E.; Schober, U.; Glaser, E.; Norz, H.; Wegner, P. Z. *Naturforsch.* **1987**, *42b*, 1527.

121. Lindner, E.; Bader, A.; Braunling, H.; Reinhard, J. *J. Mol. Catal.* **1990**, *57*, 291.
122. Forster, D.; Dekleva, T. W. *J. Chem. Ed.* **1986**, *63*, 204.
123. Greene, P. T.; Sacconi, L. *J. Chem. Soc. (A)* **1970**, 866.
124. Vijay Sen Reddy, V.; Varshney, A.; Gray, G. M. *J. Organomet. Chem.* **1990**, *391*, 259.
125. Vijay Sen Reddy, V.; Whitten, J. E.; Redmill, K. A.; Varshney, A.; Gray, G. M. *J. Organomet. Chem.* **1989**, *372*, 207.
126. Duff, C. M. Ph.D. Dissertation, Iowa State University, 1987.
127. Mason, M. R., unpublished results.

**SECTION II. COORDINATION CHEMISTRY OF A NEW
TETRATERTIARY PHOSPHINE LIGAND**

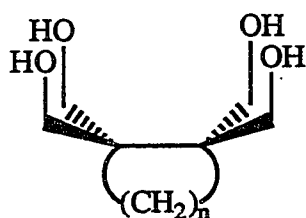
ABSTRACT

The synthesis and characterization of the new tetratertiary phosphine 2,3-bis(diphenyl-phosphinomethyl)-1,4-bis(diphenylphosphino)butane (**5**) is reported. Oxidation of **5** with *t*-BuOOH or S₈ yields the tetraphosphoryl and tetrathiophosphoryl derivatives **6** and **7**, respectively. The molecular structure of **6** was confirmed by X-ray crystallography. Crystals of **6** are triclinic, space group P $\bar{1}$, with unit cell dimensions $a = 11.70(3)$ Å, $b = 21.80(3)$ Å, $c = 9.28(6)$ Å, $\alpha = 94.0(3)^\circ$, $\beta = 102.7(3)^\circ$ and $\gamma = 88.4(2)^\circ$. The structure was refined to $R = 0.065$ and $R_w = 0.053$ for 1207 unique reflections with $I > 2\sigma(I)$. The complexes $[\text{CH}(\text{CH}_2\text{PPh}_2)_2\text{ML}_n]_2$ have been prepared for $\text{ML}_n = \text{PdCl}_2, \text{PdBr}_2, \text{PdI}_2, \text{NiCl}_2, \text{PtCl}_2, \text{Cr}(\text{CO})_4, \text{Mo}(\text{CO})_4, \text{W}(\text{CO})_4, \text{Fe}(\text{CO})_3, \text{Rh}(\text{COD})^+$ and $\text{Rh}(\text{CO})_2^+$, in which **5** coordinates in a bis-bidentate manner to two metals with the formation of six-membered chelate rings. This coordination mode was confirmed by single crystal X-ray diffraction studies on the complexes $[\text{CH}(\text{CH}_2\text{PPh}_2)_2\text{ML}_n]_2$ for $\text{ML}_n = \text{PdCl}_2$ and NiCl_2 . Crystals of $[\text{CH}(\text{CH}_2\text{PPh}_2)_2\text{PdCl}_2]_2$ are monoclinic, space group P2₁/n, with unit cell dimensions $a = 21.798(8)$ Å, $b = 13.927(5)$ Å, $c = 22.802(9)$ Å, and $\beta = 115.81(4)^\circ$. The structure was refined to $R = 0.13$ and $R_w = 0.11$ for 1996 unique reflections with $I > 2\sigma(I)$. Crystals of $[\text{CH}(\text{CH}_2\text{PPh}_2)_2\text{NiCl}_2]_2$ are triclinic, space group P $\bar{1}$, with unit cell dimensions $a = 14.320(5)$ Å, $b = 14.601(2)$ Å, $c = 19.448(15)$ Å, $\alpha = 92.39(2)^\circ$, $\beta = 99.83(4)^\circ$, $\gamma = 99.00(1)^\circ$ and $Z = 4$. The structure was refined to $R = 0.096$ and $R_w = 0.13$ for 5341 unique reflections with $F_o^2 > 3\sigma(F_o^2)$. The monometallic complex $(\text{Ph}_2\text{P}(\text{O})\text{CH}_2)_2\text{CHCH}(\text{CH}_2\text{PPh}_2)_2\text{PdCl}_2$ was also synthesized. Crystals of this complex are orthorhombic, space group Pna2, No. 33, with unit cell dimensions $a = 33.375(5)$ Å, $b = 11.125(2)$ Å, $c = 14.886(3)$ Å, and $Z = 4$. The structure was refined to $R = 0.048$ and $R_w = 0.066$ for 3031 unique reflections with $F_o^2 > 3\sigma(F_o^2)$. The

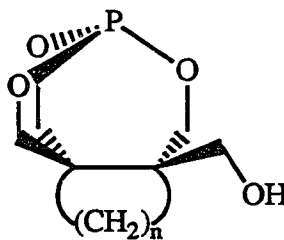
monometallic complexes (**5**-*P,P',P'',P=E*)Mo(CO)₃ were prepared for E = lone pair, O, and S in which **5** exhibits a tridentate (*P,P',P''*) coordination mode. The monometallic complex (**5**)RhCl was also prepared but ³¹P NMR spectroscopy indicates a complicated solution behavior for this complex. Similarly, attempted syntheses of monometallic complexes of Ni(II) and Pd(II) yielded mixtures which also exhibit complex behavior in solution as shown by ³¹P NMR spectroscopy.

INTRODUCTION

Recently, our group has been investigating the coordination chemistry of the main group elements P, As, Si and Ge with the tetraol frameworks **1a-1d**. These investigations have focused on the synthesis and reactivity of the orthoesters of these elements, such as phosphorus in **2a-2d**,¹ as well as the attempted synthesis of novel rectangular pyramidal five-coordinate species. Whereas five-coordinate phosphorus, arsenic, silicon and germanium compounds typically favor a TBP geometry, the

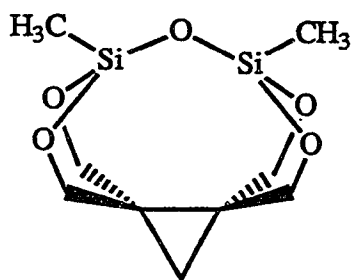


$\frac{n}{}$
1a 0
1b 1
1c 2
1d 3

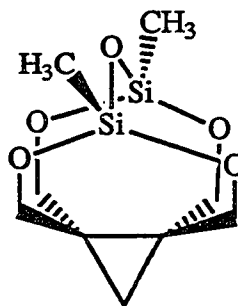


$\frac{n}{}$
2a 0
2b 1
2c 2
2d 3

structural requirements of **1a-1d** are such that five-coordinate tetra-alkoxide species of these elements must exhibit a SP geometry. As a step toward this goal we have recently



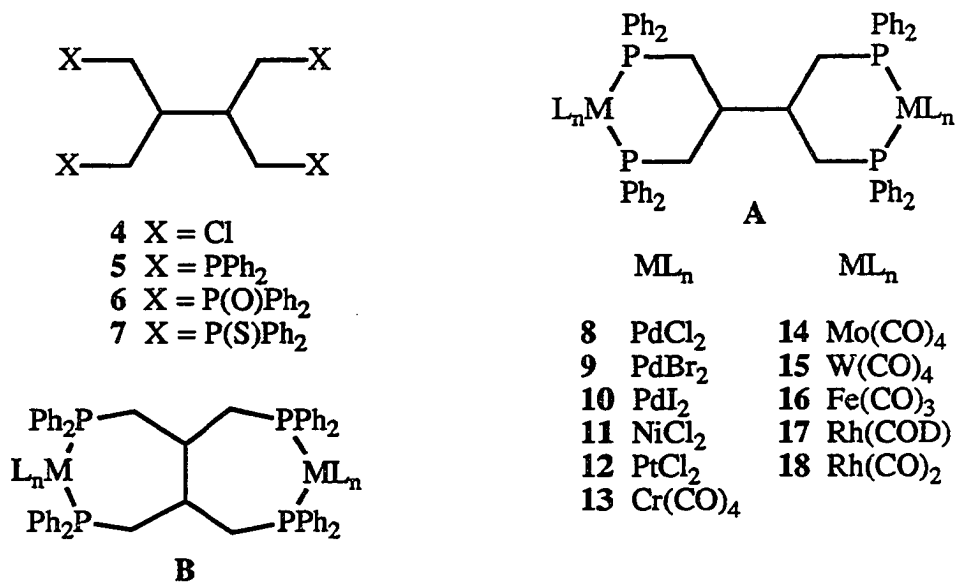
3a



3b

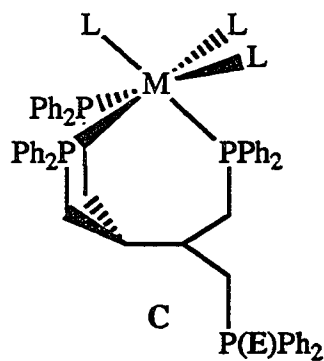
reported the results of deprotonation studies of the pendant alcohol group of **2a-2d**^{1,2} and the structures of the two novel silicon isomers **3a** and **3b**.³

We have now undertaken an elaboration of this project to include the chemistry of the transition metal elements with donor atoms other than oxygen in **1a-1d**. Of interest here is the introduction of phosphine groups into the tetradentate framework. A tetradentate phosphine of this kind may exhibit any one of four possible coordination modes, **A-D** (illustrated for $n = 1$). One interesting possibility for such a ligand is that it can potentially act as a bis-bidentate chelating ligand to two metal centers to form homo- or heterobimetallic complexes. Bimetallic complexes may be formed with either of the two isomeric structures **A** and **B** since such a ligand could coordinate with the formation of two six- or two seven-membered rings. Based on models, a tridentate coordination mode **C** of *fac* geometry is also obtainable. A tetraphosphine based on frameworks **1a-1d** may also form mononuclear transition metal complexes of type **D** where the metal must possess a square planar or square pyramidal geometry. Although the steric bulk



and structural limitations of this framework may not be ideal for the formation of complexes of type **D**, the possibility of forcing square planar geometries on tetrahedral metals such as Ag^+ , Ni^0 , Pd^0 and Pt^0 is an intriguing one.

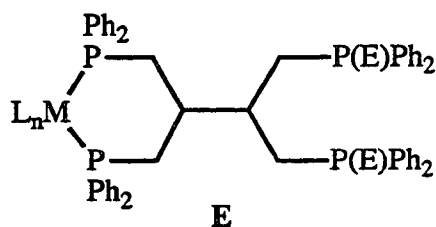
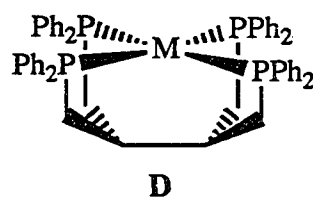
Here we report the synthesis and characterization of the new tetradentate phosphine 2,3-bis(diphenylphosphinomethyl)-1,4-bis(diphenylphosphino)butane (**5**) and its phosphoryl and thiophosphoryl derivatives **6** and **7**. Some of the scope of the transition metal coordination chemistry of **5** is reported here for Cr, Mo, W, Fe, Rh, Ni, Pd and Pt, through the characterization of the new homobimetallic complexes **8-18** of structural type **A**, the monometallic complexes **19-21** of structural type **C**, and the unexpected monometallic complexes **22** and **23** of type **E**. The structures of **6**, **8**, **10** and **11**, as well as the partially oxidized product **23** have been confirmed by X-ray crystallography. Attempts to synthesize mononuclear square planar complexes of type **D** for Rh(I), Ni(II) and Pd(II) are also presented herein.



19 E = lone pair

20 E = O

21 E = S



22 E = lone pair

23 E = O

EXPERIMENTAL SECTION

General Procedures

All reactions were performed under an inert atmosphere of argon or nitrogen using standard inert atmosphere techniques. Toluene, pentane, tetrahydrofuran and diethyl ether were distilled from sodium benzophenone ketyl prior to use. Methylene chloride, acetonitrile, and dimethylsulfoxide were distilled from calcium hydride. Ph_2PH ,⁴ (η^6 -cycloheptatriene) $\text{Mo}(\text{CO})_3$,⁵ (NBD) $\text{Cr}(\text{CO})_4$,⁶ (pip) $_2\text{Mo}(\text{CO})_4$,⁷ (COD) $\text{W}(\text{CO})_4$,⁸ (benzylideneacetone) $\text{Fe}(\text{CO})_3$,⁹ $(\text{PhCN})_2\text{PdCl}_2$,¹⁰ (NBD) PdBr_2 ,¹¹ NiCl_2 (anhydrous),¹² $\text{Rh}_2\text{Cl}_2(\text{COD})_2$,¹³ $\text{Ni}(\text{DMSO})_6(\text{BF}_4)_2$,¹⁴ $(\text{COD})\text{PtCl}_2$ ¹⁵ and 2,3-di(hydroxymethyl)-1,4-butanediol¹⁶ were prepared as previously described. $\text{Pd}(\text{BF}_4)_2 \cdot 4\text{CH}_3\text{CN}$ and AgBF_4 were purchased from Strem and Aldrich, respectively, and used without further purification. Solution NMR spectra were recorded on Nicolet NT 300 (^1H , ^{13}C), Bruker WM200 (^{13}C , ^{31}P), Bruker WM300 (^{13}C , ^{31}P), Varian Unity 500 (^1H , ^{13}C , $^1\text{H}\{^{31}\text{P}\}$), or Varian VXR300 (^1H , ^{13}C , ^{31}P) spectrometers using a deuterated solvent as the internal lock. Chemical shifts are reported relative to TMS (^1H , ^{13}C) or 85% H_3PO_4 (^{31}P). Mass spectra were recorded on Kratos MS-50 (EI, HRMS) or Finnigan 4000 (EI, CI) spectrometers. IR spectra were recorded using an IBM 98 FT-IR spectrometer. Conductance measurements were made with a Markson ElectroMark Analyzer. Microanalyses were carried out by Schwarzkopf Microanalytical Laboratories, Woodside, NY.

Preparation of 2,3-di(chloromethyl)-1,4-dichlorobutane (4)

The title tetrachloride was prepared as previously reported.¹⁶ mp 53-54 °C, lit. mp 52-53 °C; ^1H NMR (CDCl_3) δ 3.90 (dd, $^2J_{\text{HH}} = 11.5$ Hz, $^3J_{\text{HH}} = 2.8$ Hz, 4H, CH_2), 3.73 (dd, $^2J_{\text{HH}} = 11.5$ Hz, $^3J_{\text{HH}} = 6.0$ Hz, 4H, CH_2), 2.29 (m, 2H, CH).

Preparation of 2,3-bis(diphenylphosphinomethyl)-1,4-bis(diphenylphosphino)butane (5)

A red-orange solution of Ph_2PNa was generated *in situ* by stirring Ph_2PH (10.05 g, 54.0 mmol) and sodium metal (1.28 g, 55.6 mmol) in 150 mL of THF overnight. Excess sodium was removed by filtration. The phosphide solution was cooled to 0 °C and was treated dropwise with a solution of **4** (3.00 g, 13.4 mmol) in 50 mL of THF. The reaction mixture was allowed to warm to room temperature with stirring for three hours and was then refluxed for 30 min. Excess phosphide was quenched by the slow addition of water until the red color of the phosphide faded. The volume of the solvent was reduced *in vacuo* to approximately 50 mL and diethyl ether and water were added. The ether layer was separated and the aqueous layer was extracted twice more with 75 mL of diethyl ether. The organic extracts were combined, dried over anhydrous Na_2SO_4 , and the solvent was removed *in vacuo* to yield a thick residue which partially solidified on standing. Recrystallization of this residue from 3:1 MeOH/benzene or from THF/EtOH yielded white needles. The product was isolated by filtration, rinsed with EtOH, and dried *in vacuo*. Yield 8.0 grams (73%). An additional crop of product was isolated upon cooling the filtrate, 1.20 g (10%). Further purification may be achieved by flash chromatographic separation on Kieselgel 60 silica, eluting with benzene.

mp 91-93 °C; HRMS (EI) *m/e* calcd for $\text{C}_{54}\text{H}_{50}\text{P}_4$ (M^+) 821.769, found 821.817; ^{13}C NMR (CDCl_3 , 75 MHz) δ 138.8 (m, Ph-*ipso*), 133.0 (d, $^2J_{\text{PC}} = 20.4$ Hz, Ph-*ortho*), 132.9 (d, $^2J_{\text{PC}} = 19.9$ Hz, Ph-*ortho*), 128.2 (m, Ph-*meta*), 35.1 (tt, CH), 32.0 (m, CH_2); ^1H NMR (CDCl_3 , 500 MHz) δ 7.35-7.10 (m, Ph), 2.26 (dd, $^2J_{\text{HH}} = 13.0$ Hz, $^3J_{\text{HH}} = 7.0$ Hz, 4H, CH_2), 2.12 (m, CH, 2H), 2.03 (dd, $^2J_{\text{HH}} = 13.0$ Hz, $^3J_{\text{HH}} =$

7.0 Hz, 4H, CH₂); Anal. Calcd for C₅₄H₅₀P₄• $\frac{1}{2}$ C₆H₆: C, 79.62; H, 6.68; P, 13.69.

Found: C, 79.56; H, 6.31; P, 13.58.

Preparation of 2,3-bis(diphenylphosphorylmethyl)-1,4-bis(diphenylphosphoryl)butane (6)

Method A. Strong heating (100-130 °C) for 24 h or sonication for 16 h of **5** (0.321 g, 0.391 mmol) in DMSO in the presence of a catalytic amount of water quantitatively yields **6**. Sonication was carried out by immersion of the reaction flask into a Branson 50-60 Hz ultrasonic cleaning bath. The solvent was removed *in vacuo* and the product was recrystallized from CH₃CN to yield 0.331 g of **6** (96%).

Method B. A solution of **5** (0.50 g, 0.61 mmol) in 15 mL of toluene was cooled to 0 °C and was treated with a solution of *t*-BuOOH in toluene (0.8 mL, 3.6 M). The solution was allowed to warm to room temperature while stirring for three hours. Hexane (15 mL) was added and the resulting white solid was isolated by filtration, rinsed with hexane, and dried *in vacuo*. The resulting product is spectroscopically pure, but can be recrystallized from CH₃CN. Yield 0.37 g (70%). mp 243-244 °C; IR(KBr) $\nu_{\text{P=O}}$ 1178, 1117 cm⁻¹; ¹³C NMR (CDCl₃) δ 133.5 (d, ¹J_{PC} = 98 Hz, Ph-*ipso*), 132.9 (d, ¹J_{PC} = 97 Hz, Ph-*ipso*), 131.4 (d, ⁴J_{PC} = 2 Hz, Ph-*para*), 130.65 (d, ²J_{PC} = 8.5 Hz, Ph-*ortho*), 130.60 (d, ²J_{PC} = 8.5 Hz, Ph-*ortho*), 128.6 (d, ³J_{PC} = 11.5 Hz, Ph-*meta*), 34.6 (m, CH), 32.1 (dd, ¹J_{PC} = 69 Hz, ³J_{PC} = 9 Hz, CH₂); ¹H NMR (CDCl₃, 500 MHz) δ 7.69 (ddd, ³J_{PH} = 11.5 Hz, ³J_{HH} = 8.0 Hz, ⁴J_{HH} = 1.5 Hz, 8H, Ph-*ortho*), 7.58 (ddd, ³J_{PH} = 11.5 Hz, ³J_{HH} = 8.5 Hz, ⁴J_{HH} = 1.5 Hz, 8H, Ph-*ortho*), 7.46-7.30 (m, Ph-*meta*, *para*), 2.96 (ddd, ²J_{HH} = 15.0 Hz, ²J_{PH} = 12.5 Hz, ³J_{HH} = 6.5 Hz, 4H, CH₂), 2.70-2.55 (m, 6H, CH, CH₂); Anal. Calcd for C₅₄H₅₀P₄O₄: C, 73.13; H, 5.68; P, 13.97. Found: C, 72.53; H, 5.68; P, 13.67.

Preparation of 2,3-bis(diphenylthiophosphorylmethyl)-1,4-bis(diphenylthiophosphoryl)-butane (7)

A solution of **5** (0.500 g, 0.607 mmol) and **S₈** (0.083 g, 0.32 mmol) in 15 mL of toluene was refluxed for one hour to yield a white mixture. The solid was isolated by filtration and was then eluted on a silica gel column with CH₂Cl₂. The pure product-containing fractions were combined and the solvent was removed *in vacuo*. The product was recrystallized from CH₂Cl₂/hexane to yield white crystals. Yield 0.56 g (96%). mp 275-276 °C; HRMS (EI) *m/e* calcd for C₅₄H₅₀P₄S₄ (M⁺) 950.17461, found 950.17659; ¹³C NMR (CDCl₃) δ 133.7 (d, ¹J_{PC} = 82 Hz, Ph-*ipso*), 131.8 (d, ¹J_{PC} = 78 Hz, Ph-*ipso*), 131.7 (d, ²J_{PC} = 10.5 Hz, Ph-*ortho*), 131.3 (d, ⁴J_{PC} = 2.6 Hz, Ph-*para*), 131.0 (d, ⁴J_{PC} = 2.7 Hz, Ph-*para*), 130.7 (d, ²J_{PC} = 10.5 Hz, Ph-*ortho*), 128.5 (d, ³J_{PC} = 12.2 Hz, Ph-*meta*), 36.9 (m, CH), 35.8 (dd, ¹J_{PC} = 53.4 Hz, ³J_{PC} = 7.3 Hz, CH₂); ¹H NMR (CD₂Cl₂) δ 7.86 (ddd, ³J_{PH} = 13.0 Hz, ³J_{HH} = 7.5 Hz, ⁴J_{HH} = 1.5 Hz, 8H, Ph-*ortho*), 7.59 (ddd, ³J_{PH} = 13.0 Hz, ³J_{HH} = 7.5 Hz, ⁴J_{HH} = 1.5 Hz, 8H, Ph-*ortho*), 7.46-7.33 (m, Ph-*meta*, *para*), 3.22 (m, 4H, CH₂), 2.81 (m, 2H, CH), 2.62 (m, 4H, CH₂); ¹H{³¹P}NMR(CD₂Cl₂, 500 MHz) δ 3.22 (dd, ²J_{HH} = 15.0 Hz, ³J_{HH} = 6.0 Hz, 4H, CH₂), 2.81 (pentet, ³J_{HH} = 6.0 Hz, 2H, CH₂), 2.62 (m, 4H, CH₂); Anal. Calcd for C₅₄H₅₀P₄S₄: C, 68.19; H, 5.30; P, 13.03. Found: C, 67.53; H, 5.12; P, 12.61.

Preparation of Cl₂Pd(PPh₂CH₂)₂CHCH(CH₂Ph₂P)₂PdCl₂ (8)

A solution of **5** (0.240 g, 0.292 mmol) in 20 mL of toluene was added dropwise to a solution of (PhCN)₂PdCl₂ (0.240 g, 0.626 mmol) in 50 mL of toluene. The resulting mixture was stirred for five hours to insure complete reaction. The pale yellow solid was isolated by filtration, rinsed with 10 mL of toluene followed by 10 mL of diethyl ether,

and was dried *in vacuo*. Yield 0.30 g (87%). Recrystallization can be achieved by slow evaporation of a DMSO solution of **8** in air. ^{13}C NMR (d_6 -DMSO) δ 134.4 (d, $^2J_{\text{PC}} = 10$ Hz, Ph-*ortho*), 132.4 (d, $^2J_{\text{PC}} = 8$ Hz, Ph-*ortho*), 131.9 (s, Ph-*para*), 131.4 (d, $^1J_{\text{PC}} = 61$ Hz, Ph-*ipso*), 130.7 (s, Ph-*para*), 128.6 (d, $^3J_{\text{PC}} = 10$ Hz, Ph-*meta*), 128.1 (d, $^3J_{\text{PC}} = 11$ Hz, Ph-*meta*), 127.5 (d, $^1J_{\text{PC}} = 57$ Hz, Ph-*ipso*), 38.2 (m, CH), 28.1 (d, $^1J_{\text{PC}} = 35$ Hz, CH₂); ^1H NMR (d_6 -DMSO) δ 7.70 (m, Ph-*ortho*), 7.5-7.3 (m, Ph-*meta*, *para*), 2.18-2.09 (m, CH, CH₂).

Preparation of $\text{Br}_2\text{Pd}(\text{PPh}_2\text{CH}_2)_2\text{CHCH}(\text{CH}_2\text{Ph}_2\text{P})\text{PdBr}_2$ (**9**)

A solution of **5** (0.33 g, 0.40 mmol) in 5 mL of CH₂Cl₂ was slowly added to a solution of (NBD)PdBr₂ (0.32 g, 0.89 mmol) in 15 mL of CH₂Cl₂ and the resulting mixture was stirred overnight. Filtration yielded a light yellow solid which was washed with CH₂Cl₂ and dried *in vacuo*. Yield 0.40 g (74%). ^{13}C NMR (d_6 -DMSO) δ 134.6 (d, $^2J_{\text{PC}} = 7$ Hz, Ph-*ortho*), 132.5 (d, $^1J_{\text{PC}} = 57$ Hz, Ph-*ipso*), 132.2 (d, $^2J_{\text{PC}} = 8$ Hz, Ph-*ortho*), 131.9 (s, Ph-*para*), 130.6 (s, Ph-*para*), 128.5 (d, $^3J_{\text{PC}} = 11$ Hz, Ph-*meta*), 128.0 (d, $^3J_{\text{PC}} = 11$ Hz, Ph-*meta*), 127.7 (d, $^1J_{\text{PC}} = 52$ Hz, Ph-*ipso*), 28.5 (m, CH₂).

Preparation of $\text{I}_2\text{Pd}(\text{PPh}_2\text{CH}_2)_2\text{CHCH}(\text{CH}_2\text{Ph}_2\text{P})_2\text{PdI}_2$ (**10**)

To a solution of Pd(BF₄)₂·4CH₃CN (0.340 g, 0.766 mmol) in 10 mL of CH₃CN was added a solution of **5** (0.310 g, 0.377 mmol) in 5 mL of CH₂Cl₂. The ^{31}P NMR spectrum of this solution showed a complex mixture to be present, with sharp singlets at 24.0 and 22.5 ppm and broad resonances at 11.0, 7.9, 7.1, and 6.4 ppm. No resonances attributable to free phosphine or phosphine oxide were observed. To this complex solution was added Et₄NI, yielding a deep red solution, the ^{31}P NMR spectrum

of which showed only two singlets at 11.4 and 11.7 ppm in a ratio of approximately 10:1.

Preparation of $\text{Cl}_2\text{Ni}(\text{PPh}_2\text{CH}_2)_2\text{CHCH}(\text{CH}_2\text{Ph}_2\text{P})_2\text{NiCl}_2$ (11)

To a suspension of anhydrous NiCl_2 (0.095 g, 0.73 mmol) in 30 mL of CH_3CN was added a solution of **5** (0.30 g, 0.36 mmol) in 15 mL of CH_2Cl_2 to give a deep orange-red mixture. This mixture was refluxed for 30 min in which time all solids dissolved to give a deep red solution which was cooled and reduced to a volume of 10 mL *in vacuo*. Diethyl ether (5 mL) was added to initiate precipitation and the mixture was cooled overnight. The deep red product was isolated by filtration, washed with two 10 mL portions of diethyl ether, and dried *in vacuo*. Yield 0.31 g (80%). Recrystallization from CH_3CN yields red crystals which crumble to a powder upon removal from their mother liquor.

Preparation of $\text{Cl}_2\text{Pt}(\text{PPh}_2\text{CH}_2)\text{CHCH}(\text{CH}_2\text{Ph}_2\text{P})_2\text{PtCl}_2$ (12)

A solution of **5** (0.300 g, 0.365 mmol) in 5 mL of CH_2Cl_2 was added to a solution of $(\text{COD})\text{PtCl}_2$ (0.270 g, 0.722 mmol) in 15 mL of CH_2Cl_2 and the resulting mixture was stirred overnight. The white product was isolated by filtration, washed with 5 mL of diethyl ether, and dried *in vacuo*. Yield 0.34 g, 71%.

Preparation of $(\text{OC})_4\text{Cr}(\text{PPh}_2\text{CH}_2)_2\text{CHCH}(\text{CH}_2\text{Ph}_2\text{P})_2\text{Cr}(\text{CO})_4$ (13)

(Norbornadiene)tetracarbonylchromium (0.191 g, 0.729 mmol) and **5** (0.300 g, 0.365 mmol) were refluxed in 30 mL of tetrahydrofuran for 30 min to yield a yellow solution. The solvent was removed *in vacuo* to yield a yellow solid which was washed with methanol and dried *in vacuo*. Yield 0.30 g (71%). ^{13}C NMR (CD_2Cl_2) δ 226.1

(at, 17 separation 19 Hz, CO_{eq}), 221.5 (t, $^2J_{PC}$ = 14 Hz, CO_{ax}), 221.4 (t, $^2J_{PC}$ = 14 Hz, CO_{ax}), 139.0 (m, separation 44 Hz, Ph-*ipso*), 136.5 (m, separation 29 Hz, Ph-*ipso*), 132.7 (at, separation 11 Hz, Ph-*ortho*), 131.2 (at, separation 10 Hz, Ph-*ortho*), 130.5 (s, Ph-*para*), 129.7 (s, Ph-*para*), 128.7 (m, Ph-*meta*), 38.5 (tt, $^3J_{PC}$ = 11 Hz, $^2J_{PC}$ = 5 Hz, CH), 34.9 (at, separation 19 Hz, CH₂).

Preparation of (OC)₄Mo(PPh₂CH₂)₂CHCH(CH₂Ph₂P)Mo(CO)₄ (14)

Bis(piperidine)tetracarbonylmolybdenum (0.240 g, 0.610 mmol) and **5** (0.261 g, 0.304 mmol) were refluxed in 25 mL of CH₂Cl₂ for 30 min to yield a bright yellow solution. Volatiles were removed *in vacuo* to yield a pale yellow solid which was rinsed with methanol and dried *in vacuo*. Yield 0.27 g (71%). ^{13}C NMR (CD₂Cl₂) δ 214.8 (m, separation 16 Hz, CO_{eq}), 210.6 (t, $^2J_{PC}$ = 9.5 Hz, CO_{ax}), 210.3 (t, $^2J_{PC}$ = 8.0 Hz, CO_{ax}), 138.9 (m, separation 41 Hz, Ph-*ipso*), 136.1 (m, separation 30 Hz, Ph-*ipso*), 132.8 (at, separation 13 Hz, Ph-*ortho*), 131.3 (at, separation 11 Hz, Ph-*ortho*), 130.6 (s, Ph-*para*), 129.6 (s, Ph-*para*), 128.7 (at, separation 10 Hz, Ph-*meta*), 128.6 (at, separation 10 Hz, Ph-*meta*), 38.77 (tt, $^3J_{PC}$ = 10 Hz, $^2J_{PC}$ = 5 Hz, CH), 35.7 (at, separation 18 Hz, CH₂).

Preparation of (OC)₄W(PPh₂CH₂)₂CHCH(CH₂Ph₂P)₂W(CO)₄ (15)

(Cyclooctadiene)tetracarbonyltungsten (0.200 g, 0.495 mmol) and **5** (0.205 g, 0.248 mmol) were refluxed in 30 mL of tetrahydrofuran for 30 min to yield a pale yellow solution. The solvent was removed *in vacuo* and the resulting yellow solid was washed with methanol and dried *in vacuo*. Yield 0.25 g (71%). ^{13}C NMR (CD₂Cl₂) δ 205.4 (m, separation 17 Hz, CO_{eq}), 203.2 (t, $^2J_{PC}$ = 8 Hz, CO_{ax}), 202.6 (t, $^2J_{PC}$ = 6 Hz, CO_{ax}), 138.5 (m, separation 47 Hz, Ph-*ipso*), 135.7 (m, separation 35 Hz, Ph-*ipso*),

132.9 (at, separation 12 Hz, Ph-*ortho*), 131.4 (at, separation 11 Hz, Ph-*ortho*), 130.8 (s, Ph-*para*), 129.9 (s, Ph-*para*), 128.4 (m, Ph-*meta*), 39.1 (tt, $^3J_{PC} = 10$ Hz, $^2J_{PC} = 4$ Hz, CH), 35.8 (at, separation 30 Hz, CH₂).

Preparation of (OC)₃Fe(PPh₂CH₂)₂CHCH(CH₂Ph₂P)₂Fe(CO)₃ (16)

(Benzylideneacetone)tricarbonyliron (0.450 g, 1.57 mmol) and **5** (0.600 g, 0.729 mmol) were stirred in 20 mL of toluene for four hours at room temperature. The solvent was removed *in vacuo* to yield a red-orange residue. This residue was dissolved in toluene and eluted on a silica gel column to yield a yellow solution. Removal of the solvent *in vacuo* gave the product as a bright yellow solid. ¹³C NMR (CD₂Cl₂, 20 °C) δ 220.2 (t, $^2J_{PC} = 9$ Hz, CO), 140.2 (at, separation 51 Hz, Ph-*ipso*), 134.9 (at, separation 38 Hz, Ph-*ipso*), 133.3 (at, separation 12 Hz, Ph-*ortho*), 131.0 (at, separation 9 Hz, Ph-*ortho*), 130.5 (s, Ph-*para*), 129.9 (s, Ph-*para*), 128.7 (m, Ph-*meta*), 38.9 (m, CH), 34.1 (at, separation 27 Hz, CH₂); ¹H NMR (CD₂Cl₂) δ 7.4-7.1 (m, Ph), 2.13 (m, 4H, CH₂), 1.92 (m, 4H, CH₂), 1.13 (m, 2H, CH).

Preparation of (5)Mo(CO)₃ (19)

A solution of **5** (0.400 g, 0.486 mmol) and (η⁶-cycloheptatriene)Mo(CO)₃ (0.134 g, 0.486 mmol) in 25 mL of toluene was stirred for 30 min at room temperature and was then refluxed for 1.5 hours. The resulting yellow-brown solution was cooled and the solvent was removed *in vacuo*. The remaining residue was dissolved in CH₂Cl₂ and eluted on a silica gel column. A light yellow fraction was collected and the solvent removed *in vacuo* to yield a pale yellow solid.

Preparation of $\text{Cl}_2\text{Pd}(\text{PPh}_2\text{CH}_2)_2\text{CHCH}(\text{CH}_2\text{P}(\text{O})\text{Ph}_2)_2$ (**23**)

A solution of the ligand **5** (0.235 g, 0.286 mmol) in 5 mL of toluene was added to a yellow solution of **8** (0.298 g, 0.253 mmol) in 25 mL of DMSO. This mixture was stirred for three days during which time ^{31}P NMR spectra showed two new resonances at 21.4 and -20.9 ppm assigned to the presence of $\text{Cl}_2\text{Pd}(\text{PPh}_2\text{CH}_2)_2\text{CHCH}(\text{CH}_2\text{PPh}_2)_2$ (**22**). This solution remained unchanged over the next three weeks as indicated by ^{31}P NMR spectra. The solution was then exposed to air and stirred for five days. DMSO was removed from the solution at 40 °C *in vacuo* to yield a yellow solid. This yellow solid was redissolved in 5 mL of CH_2Cl_2 and the resulting yellow solution was treated with 15 mL of MeOH to precipitate 50 mg of unreacted **8** which was isolated by filtration. The solvent was removed from the filtrate to yield a light yellow solid. Remaining traces of **8** were removed by eluting this material on a silica gel column with acetone. Removal of the solvent from the product-containing fractions *in vacuo* yielded 0.260 g of **23** as a creamy white solid, a 60% yield based on the quantity of **8** not recovered. (This is a minimum value for the % yield since the unknown quantity of unreacted **8** not precipitated in the methanol addition step was subsequently removed by chromatography.) A pale yellow crystalline sample of **23** was obtained by layering methanol onto a DMSO solution. IR(KBr) $\nu_{\text{P=O}}$ 1184, 1119 cm^{-1} ; ^{13}C NMR (CD_2Cl_2) δ 134.8 (at, separation 11.2 Hz, PPh_2 -*ortho*), 133.5 (at, separation 10.7 Hz, PPh_2 -*ortho*), 133.1 (d, $^1\text{J}_{\text{PC}} = 98.9$ Hz, $\text{P}(\text{O})\text{Ph}_2$ -*ipso*), 132.7 (d, $^1\text{J}_{\text{PC}} = 98.9$ Hz, $\text{P}(\text{O})\text{Ph}_2$ -*ipso*), 132.2 (d, $^4\text{J}_{\text{PC}} = 2.7$ Hz, $\text{P}(\text{O})\text{Ph}_2$ -*para*), 132.1 (s, $\text{P}(\text{O})\text{Ph}_2$ -*para*), 132.0 (s, PPh_2 -*para*), 131.4 (s, PPh_2 -*para*), 131.2 (d, $^2\text{J}_{\text{PC}} = 9.7$ Hz, $\text{P}(\text{O})\text{Ph}_2$ -*ortho*), 130.8 (d, $^2\text{J}_{\text{PC}} = 9.1$ Hz, $\text{P}(\text{O})\text{Ph}_2$ -*ortho*), 129.0 (d, $^3\text{J}_{\text{PC}} = 11.8$ Hz, $\text{P}(\text{O})\text{Ph}_2$ -*meta*), 129.04 (at, separation 10.7 Hz, PPh_2 -*meta*), 128.9 (d, $^3\text{J}_{\text{PC}} = 11.8$ Hz, $\text{P}(\text{O})\text{Ph}_2$ -*meta*), 128.7 (at, separation 11.8 Hz, PPh_2 -*meta*), 37.4 (tt, $^3\text{J}_{\text{PC}} = 12.0$ Hz, $^2\text{J}_{\text{PC}} = 2.5$ Hz,

CH(CH₂PPh₂)₂), 36.0 (bs, CH(CH₂P(O)Ph₂)₂), 32.0 (dd, ¹J_{PC} = 69.3 Hz, ³J_{PC} = 8.0 Hz, CH₂P(O)Ph₂), 30.9 (m, separation 37.1 Hz, CH₂PPh₂); ¹H NMR (CD₂Cl₂) δ 7.85 (ddd, ³J_{PH} = 11.7 Hz, ³J_{HH} = 7.8 Hz, ⁴J_{HH} = 1.2 Hz, 4H, P(O)Ph₂-ortho), 7.70-7.59 (m, 8H, P(O)Ph₂-ortho, PPh₂-ortho), 7.56-7.26 (m, Ph), 2.75-2.56 (m, CH₂P(O)Ph₂), 2.22 (m, CH), 2.10-1.94 (m, CH₂).

Reaction of **5** with [Ni(CH₃CN)₆][BF₄]₂

A solution of [Ni(CH₃CN)₆][BF₄]₂ was generated by treating [Ni(H₂O)₆][BF₄]₂ (0.083 g, 0.243 mmol) in 10 mL of CH₃CN with 0.5 mL of the dehydrating reagent dimethoxypropane. The resulting blue solution was stirred for fifteen minutes. Addition of a solution of **5** (0.200 g, 0.243 mmol) in 5 mL of CH₂Cl₂ resulted in the formation of a deep brown solution. A ³¹P NMR spectrum of this solution showed only a very broad resonance centered at 5 ppm. No change in this solution was observed by ³¹P NMR spectroscopy over a period of two weeks. Exposure of this solution to oxygen results in a change of color to pale yellow within ten minutes. A ³¹P NMR spectrum of this solution showed only a singlet at 30.9 ppm, indicative of phosphine oxidation. Colorless crystals of **6** were obtained within two days as the solution slowly evaporated. Similar results were also obtained starting from [Ni(DMSO)₆][BF₄]₂ or [Ni(CH₃CN)₆][ClO₄]₂ without the addition of dimethoxypropane.

Preparation of (5)RhCl (**24**)

A solution of **5** (0.830 g, 1.01 mmol) in 15 mL of THF was added to a stirred solution of Rh₂Cl₂(COD)₂ (0.250 g, 0.507 mmol) in 15 mL of THF. Within a few minutes a golden-yellow solid began to precipitate. The mixture was stirred an additional 30 min, and **24** was isolated by filtration, rinsed with THF and dried *in vacuo*. MS

(FAB) *m/e* (relative intensity) 957.1 ($M^+ + 2O$, 6), 925.1 (M^+ , 3), 887.2 (6, 15), 553(28), 286.9(79), 201.0(100). Λ_m (EtOH) = 8.6 ohm⁻¹cm²mol⁻¹; Λ_m (CH₃NO₂) = 37 ohm⁻¹cm²mol⁻¹.

Crystal and Molecular Structure Solution for (Ph₂P(O)CH₂)₂CHCH(CH₂P(O)Ph₂)₂ (6)

A suitable crystal for data collection, approximately 0.10-0.12 mm on a side was selected, placed in a glass capillary and mounted on a standard goniometer. All intensity data were collected at room temperature. The unit cell parameters were initially calculated using an automatic indexing procedure¹⁸ and subsequently verified by oscillation photographs. Final lattice constants were determined by a least-squares fit to the +2 θ values of 14 higher angle reflections. The intensity data were corrected for Lorentz and polarization effects. Table 1 contains a tabulation of the pertinent information relevant to data collection and reduction.

The majority of the non-hydrogen atom positions were identified using direct-methods routines.¹⁹ The remaining non-hydrogen atoms were located via alternate cycles of least-squares calculations²⁰ and electron density difference density calculations.²¹ The atomic scattering factors used were those found in the International Tables.²² Positions of the hydrogen atoms were calculated using an assumed C-H bond distance of 1.0 Å and a C-H bond angle of 109°.

Analysis of residual electron density on an electron density difference map (maximum = 0.4 e/Å³) indicated all atoms were accounted for by the model.

**Crystal and Molecular Structure Solution for
 $\text{Cl}_2\text{Pd}(\text{PPh}_2\text{CH}_2)_2\text{CHCH}(\text{CH}_2\text{Ph}_2\text{P})_2\text{PdCl}_2$ (8)**

A crystal suitable for data collection, approximately 0.08-0.15 mm on a side was selected, attached to a glass fiber and mounted on a standard goniometer. All intensity data were collected at room temperature. The unit cell dimensions and Bravais lattice type were initially calculated using an automatic indexing procedure¹⁸ and subsequently verified by oscillation photographs. The observed systematic absences of $0k0$, $k = 2n + 1$ and $h01$, $h + 1 = 2n + 1$ indicated the space group $\text{P2}_1/n$. Final lattice constants were determined by a least squares fit to the $+2\theta$ values of 12 higher angle reflections. The intensity data were corrected for Lorentz and polarization effects. Table 1 contains a tabulation of the pertinent information relevant to data collection and reduction.

Analysis of palladium-palladium vectors from the three-dimensional Patterson map revealed the appropriate positions for the palladium atoms in the unit cell. The remaining non-hydrogen atoms were located via alternate cycles of least-squares calculations²⁰ and electron density difference density calculation.²¹ The atomic scattering factors used were those found in the International Tables.^{22a} Positions of the hydrogen atoms were calculated using an assumed C-H bond distance of 1.0 Å. Thermal parameters for the phenyl rings and the DMSO atoms were refined isotropically. The data were reweighted prior to the final least squares cycle so that $\omega(|F_o| - |F_c|)^2$ was approximately constant as a function of $\sin\theta$.

Restraints^{22b} were imposed upon the C-C bond distances in the phenyl rings due to the relatively small contribution to the total scattering made by the individual carbon atoms when compared to the scattering power of the molecule and possible disorder in the ring positions. Analytical scattering factors were used, and the targets for the restrained phenyl distances were set to 1.40 Å. Residual electron density found on an

electron density difference map indicated the possible presence of one or more highly disordered DMSO groups and some disorder in the phenyl ring orientations. These artifacts were not modeled due to the small occupancies of these disordered sites (<0.16). Since estimated standard deviations are not obtained from RESLSQ,^{22b} the parameters were used without restraints in a full-matrix least-squares procedure. The esd's were obtained from the inverse of the normal equations matrix and therefore represent maxima for these values.

Crystal and Molecular Structure Solution for $\text{Cl}_2\text{Ni}(\text{PPh}_2\text{CH}_2)_2\text{CHCH}(\text{CH}_2\text{Ph}_2\text{P})_2\text{NiCl}_2$ (11)

An orange-colored crystal of the title compound was set on the tip of a glass fiber and mounted on the diffractometer for data collection at -50 ± 1 °C. The cell constants for data collection were determined from a list of reflections found by an automated search routine. Several crystals were used initially to determine cell constants and none were better than the one chosen for data collection. The error for the c cell parameter is noticeably high at 0.015 Å. Pertinent data collection and reduction information are given in Table 2.

Lorentz and polarization corrections, a correction based on a decay in the standard reflections of 0.8%, and an absorption correction based on a series of psi-scans were applied to the data. The agreement factor for the averaging of observed reflections was 4.2% (based on F). Generally this is twice the average merging agreement factor for CAD4 data collections.

The centric space group $\text{P}\bar{1}$ was indicated initially by intensity statistics,²³ and later confirmed by successful refinement of the structure. About 2/3 of the nonhydrogen atoms were placed directly from the E-map. The remaining nonhydrogen atoms were

found in successive difference Fourier maps. Two cyclohexane and two cyclohexanone solvent molecules were placed in the asymmetric unit. It is suspected that solvent loss and/or disorder is the probable cause of the poor crystal quality discussed above. Only the nonhydrogen atoms of the nickel complex were allowed to refine anisotropically. All hydrogen atoms were placed at calculated positions 0.95 Å from the attached atom with isotropic temperature factors set equal to 1.3 times the isotropic equivalent of that atom. The hydrogen atom positions and isotropic temperature factors were not refined. The thermal ellipsoids for the phenyl rings of the complex visually indicate a high degree of thermal (vibrational) motion. Rigid-body modeling of the eight phenyl rings is in progress. Refinement calculations were performed on a Digital Equipment Corp. Micro VAX II computer using the CAD4-SDP programs.²⁴

Crystal and Molecular Structure Solution for $\text{Cl}_2\text{Pd}(\text{PPh}_2\text{CH}_2)_2\text{CHCH}(\text{CH}_2\text{P}(\text{O})\text{Ph}_2)_2$ (23)

A pale yellow pinacoidal crystal of approximate dimensions 0.20 x 0.20 x 0.60 mm was mounted on a glass fiber in a random orientation. Cell constants and an orientation matrix for data collection were obtained from least-squares refinement, using the setting angles of 25 reflections in the range $22 < 2\theta < 34$. The data were collected using the $\theta - 2\theta$ technique.

A total of 7783 reflections were collected, of which 3896 were unique and not systematically absent. As a check on crystal and electron stability, three representative reflections were measured every 60 minutes. No significant loss of intensity was observed throughout the data collection, so no decay correction was applied. Lorentz and polarization corrections and an empirical absorption correction, based on a series of psi-scans, were applied to the data. Relative transmission coefficients ranged from

0.965 to 0.999 with an average value of 0.987. Intensities of equivalent reflections were averaged. The agreement factors for the averaging of the 3896 observed and accepted reflections was 2.0% based on intensity and 1.7% based on F_o . Table 2 contains a tabulation of the pertinent information relevant to data collection and reduction.

The position of the Pd atom was given by a Patterson interpretation method.²³ The remainder of the non-hydrogen atoms were located from subsequent difference-Fourier and least-squares refinement cycles. Following least-squares refinement of all the non-hydrogen atoms in the Pd complex, the oxygen atom of a water molecule and a partially disordered molecule of DMSO were located in the lattice. The DMSO molecule was disordered such that the oxygen atom and the two methyl groups defined a plane, on either side of which were located half-occupancy atoms. The total occupancy of the solvent molecule refined to a value of 0.88.

The parameters thus defined were refined in full-matrix least-squares calculations. Scattering factors were taken from Cromer and Waber.²⁴ Anomalous dispersion effects were included in F_c ; the values of f and f' were those of Cromer.²⁴ Only those reflections having intensities greater than 3.0 times their standard deviation were used in the refinements. Refinement calculations were performed on a Digital Equipment Corp. Micro VAX II computer using the CAD4-SDP programs.²⁴

Analysis of residual electron density on an electron density difference map (maximum = $2.2e/\text{\AA}^3$, located 0.23 Å from Pd) indicated all atoms were accounted for by the model.

Table 1. Crystallographic data for 6 and 8

	6	8
Formula	C ₅₄ H ₅₀ O ₄ P ₄	C ₅₄ H ₅₀ Cl ₄ P ₄ Pd ₂ ·C ₂ H ₆ SO
Formula weight	886.83	1255.6
Space Group	P $\bar{1}$	P2 ₁ /n
a, Å	11.70(3)	21.798(8)
b, Å	21.80(3)	13.927(5)
c, Å	9.28(6)	22.802(9)
α , deg	94.0(3)	
β , deg	102.7(3)	115.81(4)
γ , deg	88.4(2)	
V, Å ³	2302	6231(4)
<i>d</i> _{calc.} g/cm ³	1.28	1.34
Crystal size, mm	0.10 x 0.10 x 0.12	0.08 x 0.10 x 0.15
μ (MoK α), cm ⁻¹	2.04	8.56
Data collection instrument	DATEX	DATEX
Radiation (monochromated in incident beam)	MoK α (λ = 0.71034 Å)	MoK α (λ = 0.71034 Å)
Orientation reflections, number	14	12
Temperature, °C	17	17
Scan type	ω -scan	ω -scan

$$^a R = \sum |F_o| - |F_c| / \sum |F_o|$$

$$^b R_w = [\sigma(|F_o| - |F_c|)^2 / \sum w F_o^2]^{1/2}; w = 1/\sigma^2(|F_o|)$$

Table 1. Continued

	6	8
Data col. range, 2θ , deg	3.5-40.0	3.5-50.0
No. of total reflections collected	3116	6287
No. of unique reflections		
with $I > 2\sigma(I)$	1207	1996
Number of parameters refined	319	353
R^a	0.065	0.13
R_w^b	0.053	0.11

Table 2. Crystallographic data for **11** and **23**

	11	23
Formula	C ₅₄ H ₅₄ Cl ₄ Ni ₂ P ₄ •2 C ₆ H ₁₂ + 2 C ₆ H ₁₀ O	C ₅₄ H ₅₀ Cl ₂ O ₃ P ₄ Pd •C ₂ H ₆ SO
Formula weight	1090.47 (1455.08)	1126.3
Space Group	P $\bar{1}$	Pna2, No. 33
a, Å	14.320(5)	33.375(5)
b, Å	14.601(2)	11.125(2)
c, Å	19.448(15)	14.886(3)
α , deg	92.39(2)	
β , deg	99.83(4)	
γ , deg	99.00(1)	
V, Å ³	3947.6(31)	5527(3)
Z	4	4
<i>d</i> _{calc.} g/cm ³	1.47	1.35
Crystal size, mm	0.60 x 0.50 x 0.45	0.20 x 0.20 x 0.60
μ (MoK α), cm ⁻¹	9.07	6.2
Data collection instrument	Enraf-Nonius CAD4	Enraf-Nonius CAD4

$$^a R = \sum |F_o| - |F_c| / \sum |F_o|$$

$$^b R_w = [\sum w(|F_o| - |F_c|)^2 / \sum F_o^2]^{1/2}; w = 1/\sigma^2(|F_o|)$$

$$^c \text{Quality-of-fit} = [\sum w(|F_o| - |F_c|)^2 / (N_{\text{obs}} - N_{\text{parameters}})]^{1/2}$$

Table 2. Continued

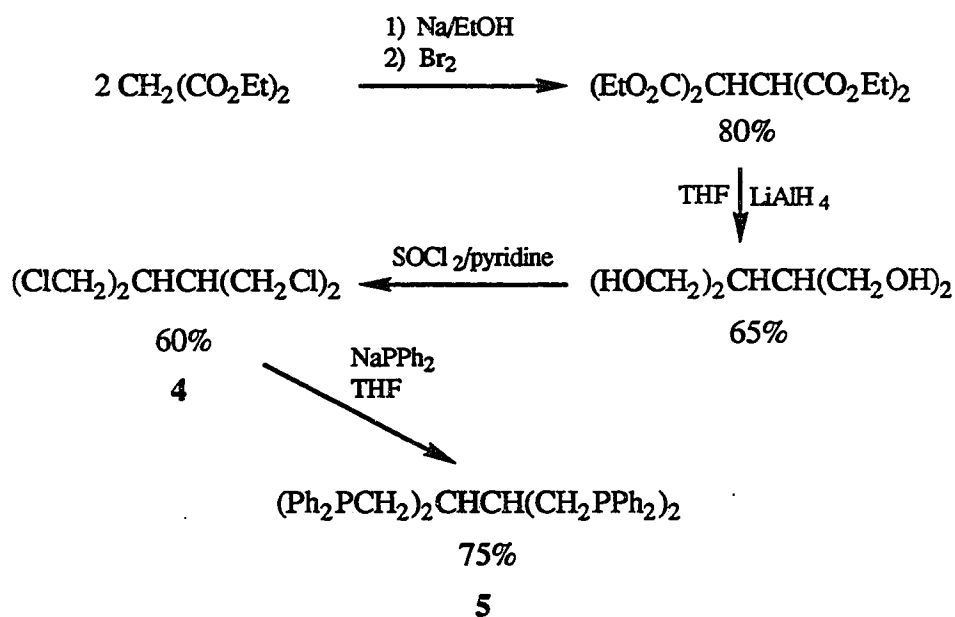
	11	23
Radiation (monochromated in incident beam)	MoK α ($\lambda = 0.71073 \text{ \AA}$)	MoK α ($\lambda = 0.71073 \text{ \AA}$)
Orientation reflections, number, range (2θ)	25, $17.8 < 2\theta < 31.9$	25, 22-34
Temperature, °C	-50(1)	21
Scan method	$\theta-2\theta$	$\theta-2\theta$
Data col. range, 2θ , deg	4.0-45.0	0-50.0
Number of unique data, total:	6554	3896
with $F_o^2 > 3\sigma(F_o^2)$:	5341	3031
Number of parameters refined	681	592
Trans. factors, max., min. (psi-scans)	0.999, 0.699	0.999, 0.965
R ^a	0.096	0.048
R _w ^b	0.131	0.066
Quality-of-fit indicator ^c	2.9	2.07
Largest shift/esd, final cycle	0.01	0.03
Largest peak, e/ \AA^3	1.82(4)	2.2

RESULTS AND DISCUSSION

Ligand Synthesis and Characterization

Previous work by Weinges and Spanig¹⁶ provided a straight-forward synthetic route to the tetrachloride **4** as outlined in Scheme I. Typical yields obtained by us are also given in this scheme. Diphenylphosphido groups are conveniently introduced into this framework by the reaction of **4** with NaPPh₂ in THF. Workup of the reaction mixture, followed by recrystallization of the resulting residue from THF/EtOH gives **5** in yields ranging from 70-83% as an air stable, crystalline white solid readily soluble in diethyl ether, toluene, and methylene chloride. Its constitution was confirmed by both analytical and high-resolution mass spectral data.

Scheme I



A ^{31}P NMR spectrum of **5** reveals a singlet resonance at -22.0 ppm affirming the equivalence of all four phosphorus nuclei. The phenyl region of the ^1H NMR spectrum exhibits only uninformative multiplets from 7.35-7.10 ppm. The methylene protons are diastereotopic and their ^1H NMR resonances appear at 2.26 and 2.03 ppm as part of an ABX spin system ($X = \text{CH}$; $^2J_{\text{HH}} = 13$ Hz, $^3J_{\text{HH}} = 7.0$ Hz). The two methine protons appear as a multiplet at 2.12 ppm. The phosphorus coupling to the methylene protons was small and unresolved as confirmed by a 500 MHz $^1\text{H}\{^{31}\text{P}\}$ NMR spectrum.

Typical of tertiary phosphines, **5** is readily oxidized by *t*-BuOOH or S_8 in toluene to yield the white, crystalline phosphoryl and thiophosphoryl derivatives **6** and **7**, respectively. It was also found that partial oxidation of DMSO solutions of **5** occurs over a period of weeks to months. The oxidation of phosphines by DMSO with the liberation of dimethylsulfide is well documented.²⁵ The reaction is typically quite slow for aryl phosphines but it is subject to acid catalysis. We have found that the rate of DMSO oxidation of **5** can be increased thermally or by sonication.

^{31}P NMR spectra of **6** and **7** exhibit singlet resonances at 30.6 and 40.1 ppm, respectively. In their ^1H NMR spectra the diastereotopic methylene protons exhibit an ABX pattern ($X = \text{CH}$). Unlike **5**, however, these resonances are complicated by strong coupling to the phosphorus nuclei with $^2J_{\text{PH}}$, evaluated with the aid of $^1\text{H}\{^{31}\text{P}\}$ spectra, of 12.5 Hz for one of the two diastereotopic methylene protons in **6**. This complication precludes complete assignment of these resonances. Similar difficulties also limit the utility of ^1H NMR spectroscopy in the characterization of the transition metal complexes of **5**. The ^1H NMR spectra of **6** and **7** each exhibit two doublet of doublet of doublets in the phenyl region in addition to other phenyl proton multiplets. In the 500 MHz ^1H NMR spectrum of **7**, for example, these two unique resonances occur at 7.86 and 7.59 ppm each with the coupling constants $^3J_{\text{HH}} = 7.5$ Hz, $^4J_{\text{HH}} = 1.5$ Hz, and $^3J_{\text{PH}} = 13.0$

Hz. These resonances are assigned to *ortho* phenyl protons based on integration and on the collapse of these resonances to doublet of doublets in the $^1\text{H}\{^{31}\text{P}\}$ NMR spectra. Just as the methylene protons of **5-7** are diastereotopic, the two phenyl substituents on each phosphorus atom are stereochemically nonequivalent and hence give rise to the appearance of two Ph-*ortho* resonances in the ^1H NMR spectra of these compounds. This inequivalence is further demonstrated in the ^{13}C NMR spectra of **6** and **7** which exhibit two phenyl *ipso* and *ortho* carbon resonances as doublets. For **7**, two phenyl *para* resonances are also resolved. As expected for P(V), the Ph-*ipso* carbon resonances each exhibit large one-bond coupling to phosphorus²⁶ with $^1J_{\text{PC}}$ values of 98 and 97 Hz for those in **6**, and 82 and 78 Hz for those in **7**. The methylene carbon resonances appear as doublets of doublets resulting from one bond coupling to phosphorus of 69 and 53 Hz for **6** and **7**, respectively.

The identity of **6** was further confirmed by X-ray crystallography. Selected bond distances and angles are given in Table 3. The unit cell is comprised of two unique molecules of **6** which differ by the orientation of the phenyl rings with respect to the remainder of each molecule. The greatest deviation lies between the pairs of phenyl rings C, D and E, F which are rotated by almost 60° relative to one another. Half of each molecule is related to the second half by an inversion center at the midpoint of the HC-CH vector. The phosphoryl groups are oriented in a paddle wheel fashion around both molecules with P=O distances of 1.468(1), 1.511(1), 1.547(2), 1.515(1) Å at P(1), P(2), P(3), and P(4), respectively. These distances do not differ significantly from the previously observed range of 1.47-1.50 Å for P=O bond distances.²⁷ For example, the distances reported for bis(diphenylphosphoryl)methane, which also crystallizes with two unique molecules in the unit cell, range from 1.484(5) to 1.500(5) Å.^{27a} The paddle wheel orientation of the phosphoryl groups in **6** is presumably the result of crystal

packing forces. It is interesting to note, however, that the phosphoryl oxygen atoms are each directed in the vicinity of a methylene proton of a neighboring "arm". Although the O····C distances between each phosphoryl oxygen atom and a neighboring methylene carbon atom, which range from 3.16(1) to 3.20(1) Å, may potentially be in the range allowable for a weak C-H····O hydrogen bonding interaction,²⁸ we do not believe it to be significant in **6**. (The positions of the hydrogen atoms were not located.)

Table 3. Selected bond distances (Å) and angles (deg) in [(Ph₂P(O)CH₂)₂HC]₂ (**6**)

Bond Distances			
P(1)-O(1)	1.468(1)	P(2)-O(2)	1.511(1)
P(1)-C(1A)	1.814(2)	P(2)-C(1D)	1.819(2)
P(1)-C(1B)	1.816(2)	P(2)-C(1C)	1.825(2)
P(1)-C(11)	1.817(2)	P(2)-C(21)	1.833(2)
P(3)-O(3)	1.547(2)	P(4)-O(4)	1.515(1)
P(3)-C(1E)	1.801(2)	P(4)-C(1G)	1.822(2)
P(3)-C(1F)	1.832(2)	P(4)-C(1H)	1.803(2)
P(3)-C(31)	1.815(2)	P(4)-C(41)	1.771(2)
C(11)-C(12)	1.526(3)	C(31)-C(34)	1.573(3)
C(12)-C(21)	1.558(3)	C(34)-C(41)	1.581(3)
C(12)-C(12)	1.572(3)	C(34)-C(34)	1.573(3)

Table 3. Continued

Bond Angles			
O(1)-P(1)-C(11)	114.2(8)	O(2)-P(2)-C(21)	114.8(8)
O(1)-P(1)-C(1A)	113.5(9)	O(2)-P(2)-C(1C)	113.2(9)
O(1)-P(1)-C(1B)	109.0(8)	O(2)-P(2)-C(1C)	113.2(9)
C(11)-P(1)-C(1A)	103.5(9)	C(21)-P(2)-C(1D)	105.3(9)
C(11)-P(1)-C(1B)	107.7(9)	C(21)-P(2)-C(1D)	104.0(9)
C(1A)-P(1)-C(1B)	108.6(9)	C(1C)-P(2)-C(1D)	105.5(9)
O(3)-P(3)-C(31)	116.3(8)	O(4)-P(4)-C(41)	115.4(8)
O(3)-P(3)-C(1E)	111.6(9)	O(4)-P(4)-C(1G)	110.8(8)
O(3)-P(3)-C(1F)	111.5(9)	O(4)-P(4)-C(1H)	112.8(9)
C(31)-P(3)-C(1E)	103.(1)	C(41)-P(4)-C(1G)	107.2(9)
C(31)-P(3)-C(1F)	106.6(9)	C(41)-P(4)-C(1H)	104.2(9)
C(1E)-P(3)-C(1F)	107.(1)	C(1G)-P(4)-C(1H)	105.8(9)
P(1)-C(11)-C(12)	117.(1)	P(2)-C(21)-C(12)	123.(1)
P(3)-C(31)-C(34)	128.(1)	P(4)-C(41)-C(34)	116.(1)
C(11)-C(12)-C(12)	110.(2)	C(31)-C(34)-C(34)	110.(1)
C(11)-C(12)-C(12)	107.(1)	C(31)-C(34)-C(41)	108.(1)
C(12)-C(12)-C(21)	112.(2)	C(34)-C(34)-C(41)	112.(2)

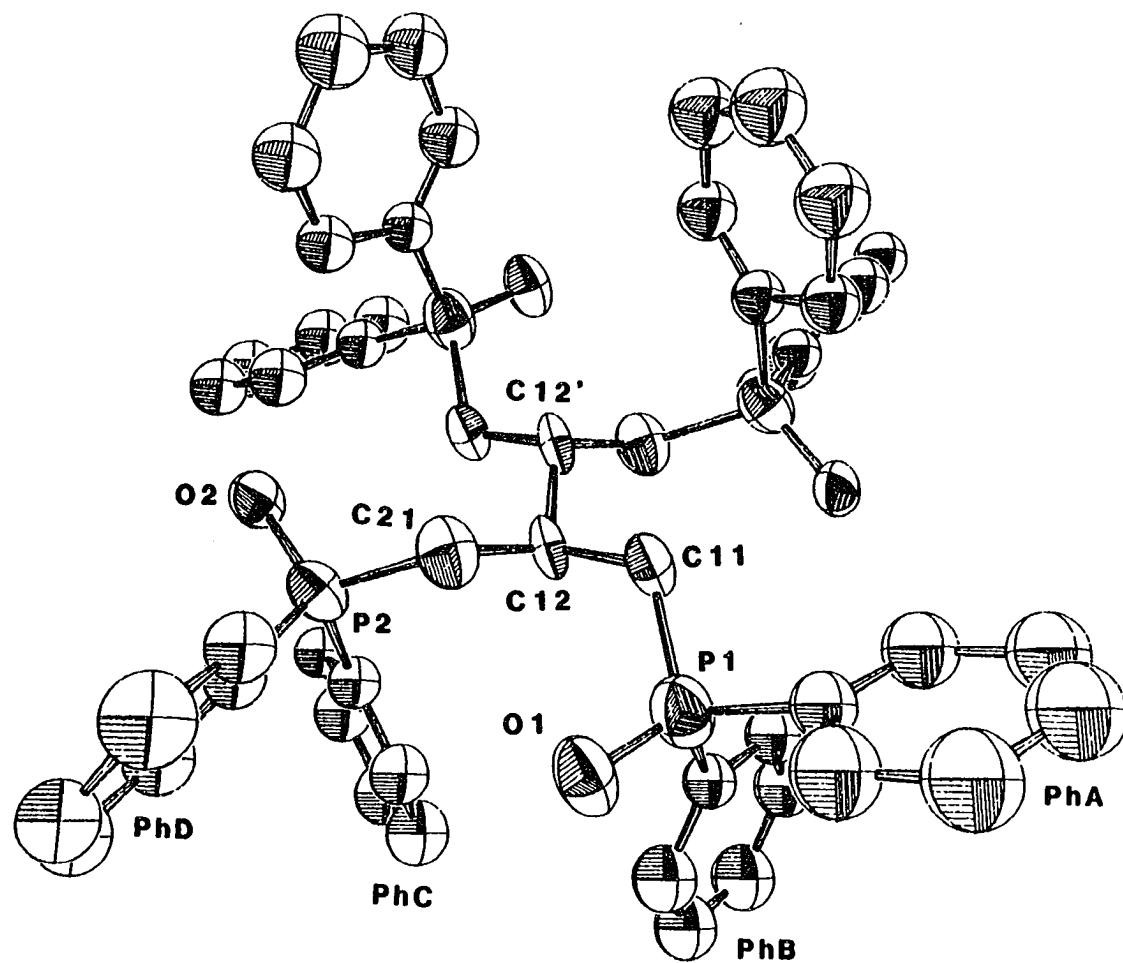


Figure 1a. ORTEP drawing of the first of two independent molecules of **6**. The thermal ellipsoids are drawn at the 50% probability level.

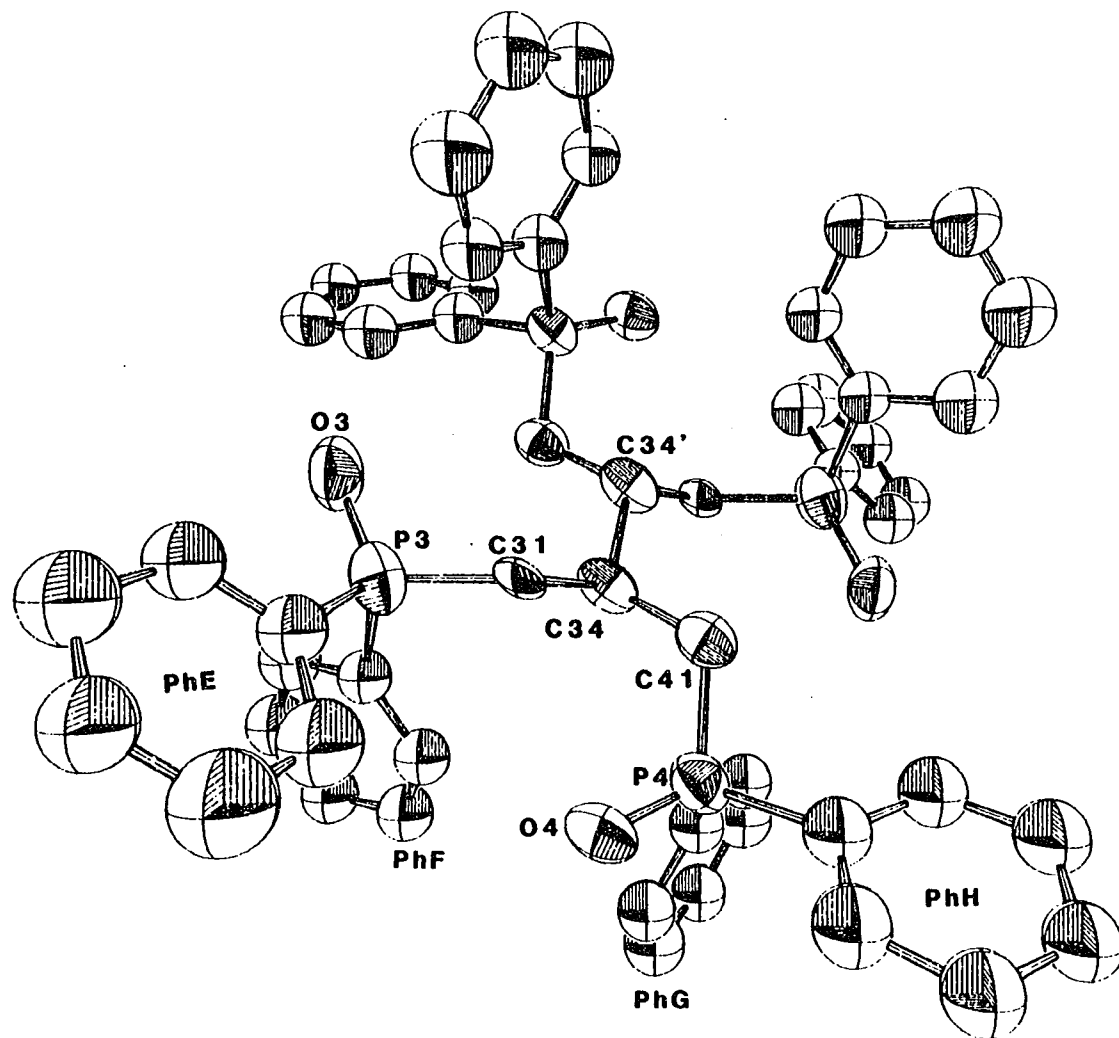


Figure 1b. ORTEP drawing of the second independent molecule of 6. The thermal ellipsoids are drawn at the 50% probability level.

Bimetallic Complexes

In the initial investigations of the transition metal chemistry of **5** it quickly became apparent that this ligand favors bis-bidentate coordination to two metals to form homobimetallic complexes. The addition of **5** to a toluene solution of $(\text{PhCN})_2\text{PdCl}_2$ results in the precipitation of an air stable, pale yellow solid, **8**, regardless of the stoichiometry of the reactants. This product, soluble only in DMSO or pyridine, exhibits a singlet in its ^{31}P NMR spectrum at 21.7 ppm. Analytical data for **8** indicate the

Table 4. Selected bond distances (Å) and angles (deg) in $[\text{Cl}_2\text{Pd}(\text{Ph}_2\text{PCH}_2)_2\text{CH}]_2$ (**8**)

Bond Distances			
Pd(1)-P(7)	2.26(1)	Pd(2)-P(9)	2.23(1)
Pd(1)-P(8)	2.24(1)	Pd(2)-P(10)	2.25(1)
Pd(1)-Cl(3)	2.32(1)	Pd(2)-Cl(5)	2.34(1)
Pd(1)-Cl(4)	2.34(1)	Pd(2)-Cl(6)	2.36(1)
P(7)-C(11)	1.90(4)	P(8)-C(12)	1.82(4)
P(7)-C(1A)	1.84(5)	P(8)-C(1C)	1.87(4)
P(7)-C(1B)	1.83(5)	P(8)-C(1D)	1.81(5)
P(9)-C(14)	1.78(5)	P(10)-C(15)	1.80(4)
P(9)-C(1E)	1.84(5)	P(10)-C(1G)	1.78(4)
P(9)-C(1F)	1.81(5)	P(10)-C(1H)	1.82(5)
C(11)-C(13)	1.50(6)	C(12)-C(13)	1.54(6)
C(13)-C(16)	1.62(6)	C(14)-C(16)	1.61(6)
C(15)-C(16)	1.47(5)		

Table 4. Continued

Bond Angles			
Cl(3)-Pd(1)-Cl(4)	89.6(4)	Cl(5)-Pd(2)-Cl(6)	90.6(6)
Cl(3)-Pd(1)-P(7)	88.0(5)	Cl(5)-Pd(2)-P(9)	86.8(5)
Cl(3)-Pd(1)-P(8)	174.0(4)	Cl(5)-Pd(2)-P(10)	173.5(5)
Cl(4)-Pd(1)-P(7)	176.0(4)	Cl(6)-Pd(2)-P(9)	176.5(6)
Cl(4)-Pd(1)-P(8)	88.4(4)	Cl(6)-Pd(2)-P(10)	87.8(6)
P(7)-Pd(1)-P(8)	93.7(4)	P(9)-Pd(2)-P(10)	94.5(5)
Pd(1)-P(7)-C(11)	118.(1)	Pd(1)-P(8)-C(12)	118.(1)
Pd(1)-P(7)-C(1A)	114.(1)	Pd(1)-P(8)-C(1C)	107.(1)
Pd(1)-P(7)-C(1B)	111.(2)	Pd(1)-P(8)-C(1D)	118.(1)
C(11)-P(7)-C(1A)	98.(2)	C(12)-P(8)-C(1C)	103.(2)
C(11)-P(7)-C(1B)	102.(2)	C(12)-P(8)-C(1D)	103.(2)
C(1A)-P(7)-C(1B)	113.(2)	C(1C)-P(8)-C(1D)	106.(2)
Pd(2)-P(9)-C(14)	119.(2)	Pd(2)-P(10)-C(15)	119.(1)
Pd(2)-P(9)-C(1E)	114.(1)	Pd(2)-P(10)-C(1G)	108.(2)
Pd(2)-P(9)-C(1F)	110.(1)	Pd(2)-P(10)-C(1H)	115.(2)
C(14)-P(9)-C(1E)	100.(2)	C(15)-P(10)-C(1G)	105.(2)
C(14)-P(9)-C(1F)	103.(2)	C(15)-P(10)-C(1H)	96.(2)
C(1E)-P(9)-C(1F)	109.(2)	C(1G)-P(10)-C(1H)	113.(2)
P(7)-C(11)-C(13)	114.(2)	P(9)-C(14)-C(16)	114.(3)
P(8)-C(12)-C(13)	114.(2)	P(10)-C(15)-C(16)	112.(3)
C(11)-C(13)-C(12)	112.(4)	C(13)-C(16)-C(14)	106.(3)

presence of two PdCl₂ units per ligand **5**, suggesting that the ligand coordinates to the PdCl₂ fragments in a bis-bidentate manner. The ¹³C NMR spectrum of **8** is consistent with a structure of either type A or B.

Slow evaporation of a concentrated DMSO solution of **8** yielded crystals suitable for X-ray analysis. The structural solution suffers from highly disordered DMSO molecules and some disorder in the phenyl ring orientations leading to R and R_w values of 0.11 and 0.13, respectively. Despite the disorder present in the structure, the location of the heavy atom positions confirms the presence of two palladium atoms, each in an essentially square planar environment comprised of two chloride ligands and two phosphorus donors from **5**. The Pd-P distances of 2.23(1) to 2.26(1) Å are in the range reported previously for (dppm)PdCl₂, (dppe)PdCl₂, and (dppp)PdCl₂,²⁹ but the P-Pd-P angles of 93.7(4) and 94.5(5)° are significantly larger than those found for (dppp)PdCl₂ and (dppp)Pd(NCS)₂³⁰ of 90.58(5) and 89.32°, respectively. Figure 2 shows that **5** chelates to the two PdCl₂ fragments with the formation of six-membered rings, rather than the isomeric product containing seven-membered chelate rings.

In addition to forming complexes with PdCl₂, the bromide and iodide analogues (μ-**5**)(PdBr₂)₂ (**9**) and (μ-**5**)(PdI₂)₂ (**10**) have been prepared. The physical and spectroscopic characteristics of **9** are similar to those of **8**, but the ³¹P NMR spectrum of **10** reveals resonances at 11.7 and 11.4 ppm in a ratio of 1:10. The solubility of **10** in acetonitrile and methylene chloride allows the separation of these two components by fractional crystallization yielding **10a** (δ 11.7 ppm) as dark red needles and **10b** (δ 11.4 ppm) as orange hexagonal plates. X-ray crystallography reveals that the molecular structure of **10b** is analogous to that for **8** where **5** coordinates to two palladium atoms with the formation of six-membered rings.³¹ It is tempting to speculate that the minor

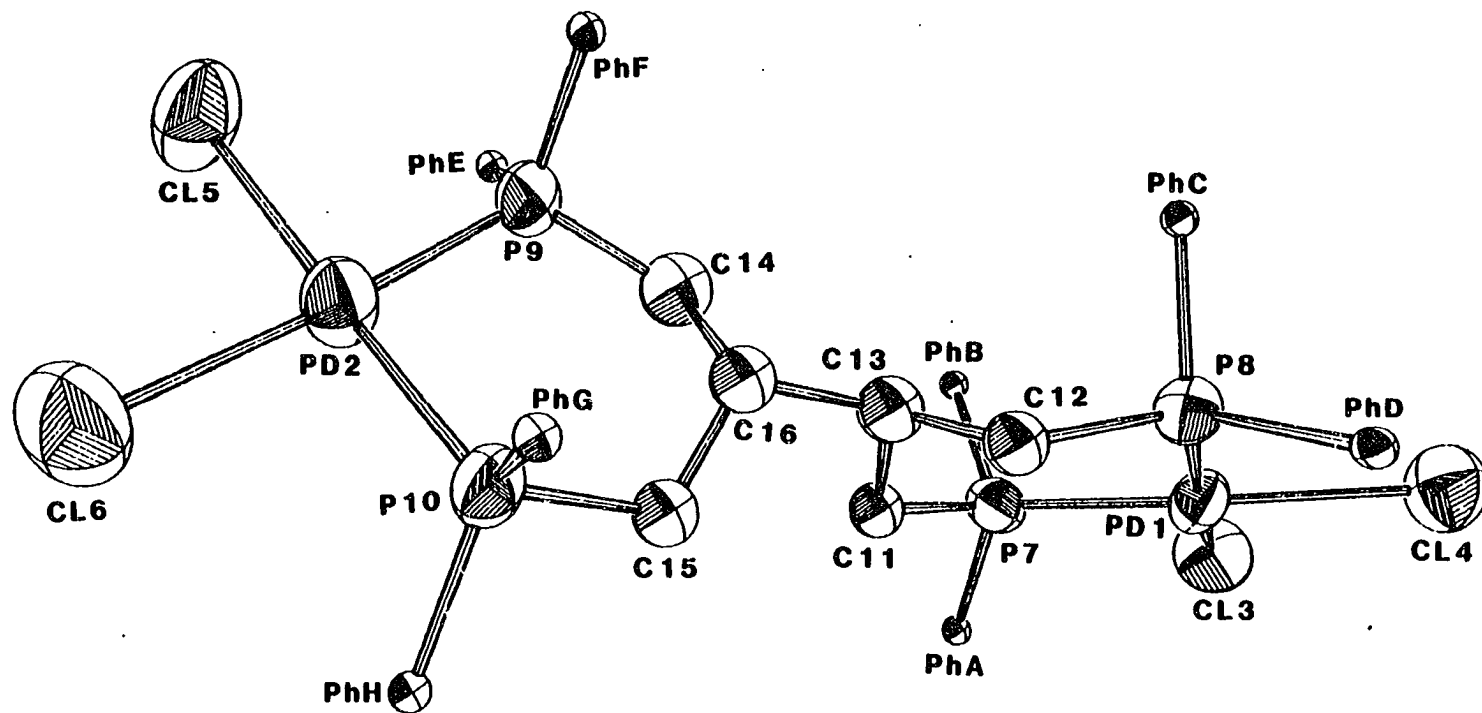


Figure 2. ORTEP drawing of **8** with thermal ellipsoids drawn at the 50% probability level. All phenyl carbons have been omitted for clarity, except for the *Ph-*ipso** carbons which are drawn at an arbitrary size.

component **10a** may be of type **B**, where **5** coordinates to two palladium atoms with the formation of seven-membered chelate rings.

Reaction of **5** with two equivalents of NiCl_2 yields a deep red solid, **11**, whose ^{31}P NMR spectrum exhibits a paramagnetically broadened, almost unobservable resonance at 5 ppm, consistent with a tetrahedral geometry at nickel. Complex **11** dissolves in pyridine to form a bright yellow solution, but the ^{31}P NMR spectrum of this solution indicates dissociation of the ligand has occurred to yield uncoordinated **5**. The nickel-containing material in this solution is presumably $\text{Ni}(\text{py})_4\text{Cl}_2$.³² We are unaware of previous reports concerning the dissociation of nickel phosphine complexes in pyridine, but this observation is consistent with the trend for first row transition metals to prefer "hard" donors such as nitrogen whereas the second and third row transition metals display a preference for "soft" donors such as phosphines. In accord with these trends complex **8** does not dissociate detectably in pyridine. Complex **11** is stable to dissociation in other solvents in which it is soluble (e.g., CH_3CN , DMSO, acetone) and forms red crystals upon concentration of an acetonitrile solution of the complex. Upon removal of these crystals from their mother liquor they immediately lose solvent to form a red powder. Crystals of **11** obtained from acetone were also plagued by rapid solvent loss. However, layering cyclohexane onto a cyclohexanone solution of **11** afforded red crystals stable enough with respect to solvent loss to allow for the structure of this complex to be determined by X-ray crystallography. The molecular structure of **11** is illustrated in Figure 3. Selected bond distances and angles are tabulated in Table 5. Ligand **5** coordinates to two NiCl_2 fragments with the formation of six-membered chelate rings. The nickel atoms adopt a slightly distorted square planar geometry with the sum of the angles around each nickel atom totaling 358° . The P-Ni-P angles are $96.79(9)^\circ$ and $94.52(9)^\circ$. The Ni-P distances of 2.189(3), 2.170(3), 2.181(3), and

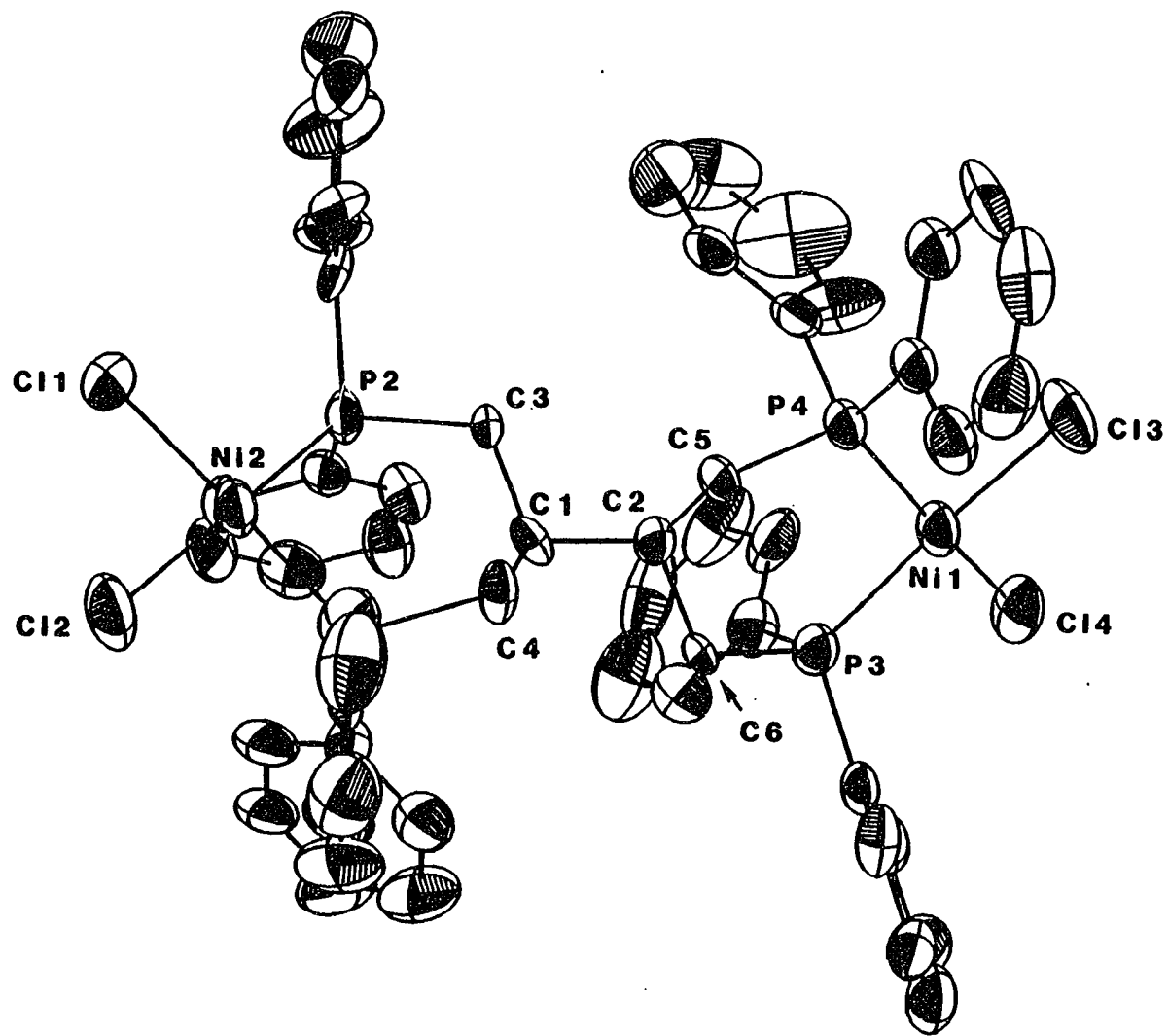


Figure 3a. ORTEP drawing of 11. Thermal ellipsoids are drawn at the 50% probability level.

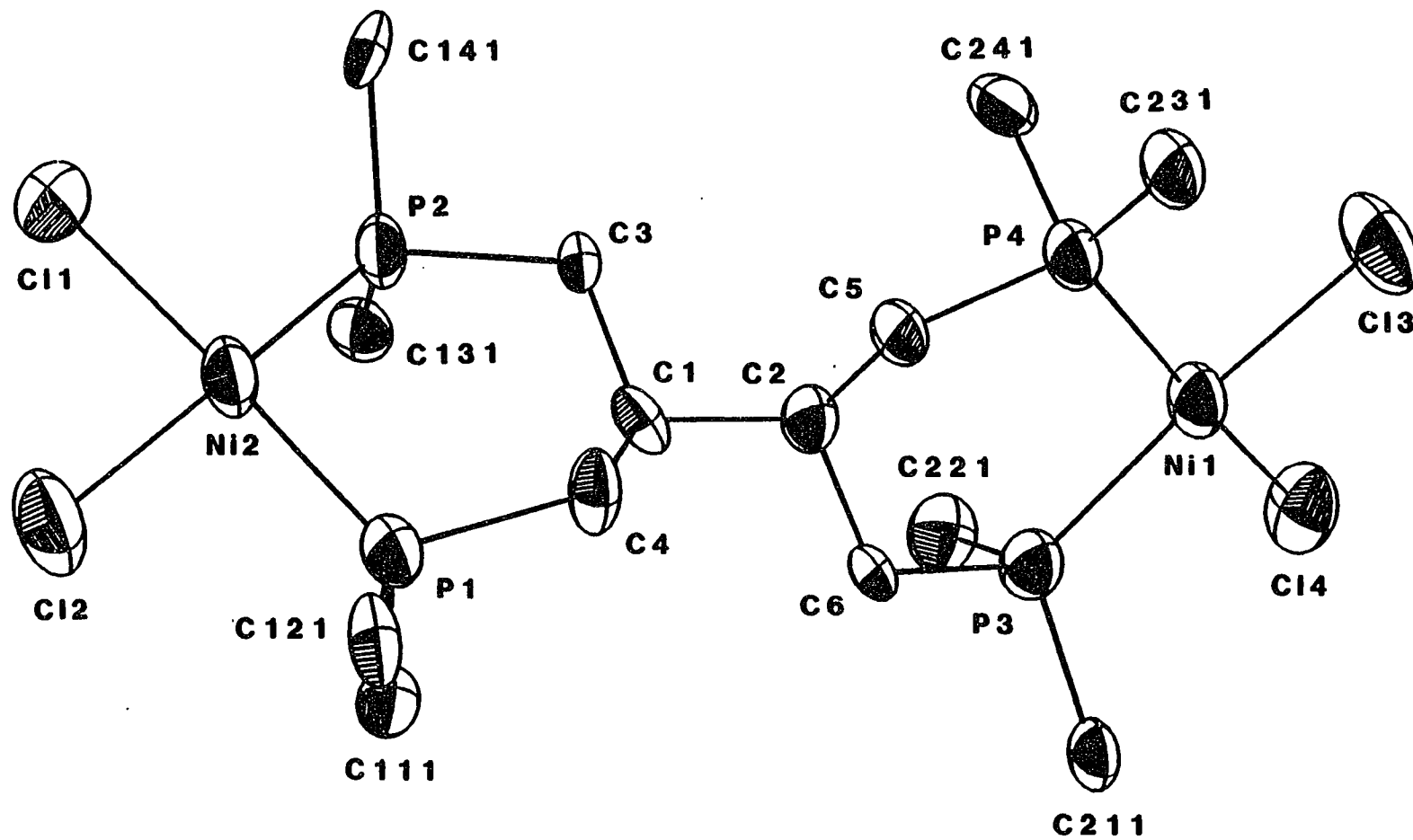


Figure 3b. ORTEP drawing of 11 with all phenyl carbons, except for Ph-*ipso* carbons, omitted for clarity.

2.178(3) Å for P(1), P(2), P(3), and P(4), respectively, fall in the range of 2.145(2) Å - 2.321(3) Å reported previously for (dppe)NiCl₂,^{33a}

{Ph₂P(CH₂)₂O(CH₂)₂PPh₂}NiCl₂,^{33b} and (Ph₃P)₂NiCl₂.^{33c} The square planar geometry around nickel in the solid state and the paramagnetism exhibited in solution are reminiscent of (dppp)NiCl₂ which undergoes a SP ⇌ tetrahedral isomerization in solution, but is square planar in the solid state on the basis of spectroscopic data.³⁴ Also of interest in this structure are the large number of solvent molecules incorporated into

Table 5. Selected bond distances (Å) and angles (deg) in **11**

Bond Distances (Å)			
Ni(1)-P(3)	2.181(3)	Ni(2)-P(1)	2.189(3)
Ni(1)-P(4)	2.178(3)	Ni(2)-P(2)	2.170(3)
Ni(1)-Cl(3)	2.176(3)	Ni(2)-Cl(1)	2.196(3)
Ni(1)-Cl(4)	2.195(3)	Ni(2)-Cl(2)	2.193(3)
Bond Angles (deg)			
P(3)-Ni(1)-P(4)	96.79(9)	P(1)-Ni(2)-P(2)	94.52(9)
P(3)-Ni(1)-Cl(3)	176.0(1)	P(1)-Ni(2)-Cl(1)	176.7(1)
P(3)-Ni(1)-Cl(4)	84.8(1)	P(1)-Ni(2)-Cl(2)	84.7(1)
P(4)-Ni(1)-Cl(3)	86.2(1)	P(2)-Ni(2)-Cl(1)	88.4(1)
P(4)-Ni(1)-Cl(4)	169.7(1)	P(2)-Ni(2)-Cl(2)	170.8(1)
Cl(3)-Ni(1)-Cl(4)	92.7(1)	Cl(1)-Ni(2)-Cl(2)	92.1(1)

the crystalline lattice, two each of cyclohexane and cyclohexanone. This explains why crystals obtained from more common, lower boiling solvents rapidly lose solvent to yield powders.

The platinum chemistry of **5** generally yielded insoluble white precipitates believed to be dimeric or oligomeric in nature when starting from $(\text{PhCN})_2\text{PtCl}_2$, $(\text{PhCN})_2\text{PtI}_2$ or $(\text{Me}_2\text{S})_2\text{PtCl}_2$. The reaction of **5** with two equivalents of $(\text{COD})\text{PtCl}_2$ yields a white solid (**12**) which does, however, exhibit slight solubility in CH_2Cl_2 and DMSO. The ^{31}P NMR spectrum of **12** exhibits a singlet at 2.9 ppm flanked by platinum satellites. The ^{195}Pt - ^{31}P coupling constant of 3456 Hz is typical for a *cis* arrangement of phosphorus donors around platinum.³⁵ As for **8-10**, this data is consistent with a bimetallic complex wherein **5** coordinates to two square planar PtCl_2 units.

Ligand **5** was also found to form bimetallic complexes when Group VI metal carbonyl precursors were employed. Reaction of **5** with two equivalents of $\text{L}_2\text{M}(\text{CO})_4$ where $\text{M} = \text{Cr}, \text{Mo}, \text{W}$ and $\text{L}_2 = \text{NBD}, 2 \text{ piperidine}$ and COD , respectively, yields the creamy white complexes $[\text{CH}(\text{CH}_2\text{PPh}_2)_2\text{M}(\text{CO})_4]_2$, $\text{M} = \text{Cr}$ (**13**), Mo (**14**) and W (**15**). The ^{31}P NMR spectra of these complexes exhibit singlets with the tungsten analogue displaying satellites with $^1\text{J}_{\text{PW}} = 227 \text{ Hz}$ (see Table 6). The carbonyl stretches in the infrared spectra of **13-15** are consistent with those previously reported for *cis* phosphine substituted tetracarbonyl complexes³⁶ and are tabulated in Table 7. The ^{13}C NMR spectra of **13-15** are consistent with a bis-bidentate coordination mode of either type A or B. Complex **15**, for example, exhibits triplet resonances at 203.2 ppm ($^2\text{J}_{\text{PC}} = 8 \text{ Hz}$) and 202.6 ppm ($^2\text{J}_{\text{PC}} = 6 \text{ Hz}$) assigned to the two nonequivalent axial carbonyls. The expected five line multiplet of an AXX' ($\text{A} = ^{13}\text{C}$; $\text{X}, \text{X}' = ^{31}\text{P}$) spin system is observed at 205.4 ppm for the two equivalent equatorial carbonyls. In octahedral metal complexes where **5** coordinates in a bidentate manner, the two axial

sites on each metal are stereochemically nonequivalent owing to the presence of two different exocyclic substituents on the methine carbons. The triplet multiplicities of these resonances as well as their small $^2J_{PC}$ coupling constants³⁷ confirm the orientation of these two carbonyl ligands as *cis* to two phosphorus donors. The appearance of a five-line multiplet³⁷ for the two equivalent equatorial carbonyls and the dependence of the

Table 6. ^{31}P NMR Spectroscopic data^a

	δ (ppm)
5	-22.0
6, (5)O₄	30.6
7, (5)S₄	40.1
8, (μ-5){PdCl₂}₂	21.7 ^b
9, (μ-5){PdBr₂}₂	19.1 ^b
10a, (μ-5){PdI₂}₂	11.4
10b, (μ-5){PdI₂}₂	11.7
11, (μ-5){NiCl₂}₂	5(broad) ^c
12, (μ-5){PtCl₂}₂	2.9, $^1J_{\text{Pt-P}} = 3456$ Hz
13, (μ-5){Cr(CO)₄}₂	49.0
14, (μ-5){Mo(CO)₄}₂	28.4
15, (μ-5){W(CO)₄}₂	8.2, $^1J_{\text{PW}} = 227$ Hz
16, (μ-5){Fe(CO)₃}₂	54.7 ^d
17, (μ-5){Rh(COD)}₂²⁺	36.7(d), $^1J_{\text{Rh-P}} = 165$ Hz

Table 6. Continued

18, (μ -5){Rh(CO) ₂ } ₂ ²⁺	17.3(d), ¹ J _{Rh-P} = 122 Hz
19, (5)Mo(CO) ₃	17.7(t) ^e 15.8(t), 14.2(t), -17.9(s) ^f
20, (5-P,P',P'', P=O)Mo(CO) ₃	20.1(t) ^g , 18.4(t), 16.1(t), 32.7(s) ^h
21, (5-P,P',P'', P=S)Mo(CO) ₃	17.1(t), ⁱ 15.7(t), 13.6(t), 40.5(s) ^j
22, (5-P,P')PdCl ₂	21.4, -20.7 ^f
23, (5,P,P', P=O, P'=O)PdCl ₂	31.4, ^h 20.4

^aSpectra taken in CH₂Cl₂ unless indicated otherwise. ^bDMSO. ^cCH₃CN. ^dToluene.

^e2J_{PP} = 19.6 Hz. ^fCorresponds to uncoordinated PPh₂ group. ^g2J_{PP} = 19.1 Hz.

^hP(O)Ph₂ resonance. ⁱ2J_{PP} = 19.3 Hz. ^jP(S)Ph₂ resonance.

Table 7. Infrared spectroscopic data

		ν _{CO} (cm ⁻¹)		
13, (μ -5){Cr(CO) ₄ } ₂	2004	1919	1879	
14, (μ -5){Mo(CO) ₄ } ₂	2017	1927	1909	
15, (μ -5){W(CO) ₄ } ₂	2014	1917	1880	
16, (μ -5){Fe(CO) ₃ } ₂	1981	1909	1886	1875
19, (5-P,P',P'')Mo(CO) ₃		1934	1830	

appearance of these multiplets on the variation of $^2J_{PP}$ in analogous complexes of chromium, molybdenum and tungsten has been previously discussed for the series $(Ph_2P(CH_2)_nPPh_2)M(CO)_4$ where $n = 1-4$ and $M = Cr, Mo$ and W .³⁹ As was discussed for the phosphoryl and thiophosphoryl derivatives of **5**, the complexes **13-15** exhibit two resonances in their ^{13}C NMR spectra for the phenyl *ipso*, *ortho*, *meta* and *para* carbons of the two stereochemically nonequivalent phenyl substituents on phosphorus. These phenyl resonances for **13-15** appear as "apparent" triplets resulting from phosphorus coupling of the AXX' spin system.³⁷ In contrast, the phenyl resonances for the palladium complexes **8** and **9** appear as slightly broadened doublets, which requires that $^2J_{PP}$ and $^1J_{PC}$ be small. Other complexes of the type $(R_3P)_2PdX_2$ have also been reported to exhibit doublet resonances in their ^{13}C NMR spectra.⁴⁰

The complexes $[CH(CH_2PPh_2)_2Fe(CO)_3]_2$ **16** and $[CH(CH_2PPh_2)Rh(COD)]_2[BF_4]_2$ **17** were also prepared and characterized by infrared and 1H , ^{13}C , and ^{31}P NMR spectroscopies. Their spectral features are similar to the complexes discussed previously. It is worthy to note that the carbonyl ligands in **16** are fluxional on the ^{13}C NMR time scale and exhibit only one triplet resonance down to -60 °C where some broadening of the resonance occurs. Similar behavior has been previously reported for complexes of the type $(R_3P)_2Fe(CO)_3$.⁴¹ Also worthy of note is the reaction of **17** with CO to yield a complex we assign as $[CH(CH_2PPh_2)_2Rh(CO)_2]_2[BF_4]_2$ **18**. This complex, which was not isolated, exhibits a doublet resonance in the ^{31}P NMR spectrum at 17.3 ppm with $^1J_{Rh-P} = 122$ Hz.

Based on the structural results obtained for **8**, **10b** and **11** as well as the infrared and 1H , ^{13}C and ^{31}P NMR spectroscopic data presented, compounds **8-18** are all assigned structure type A where **5** chelates to two metal fragments with the formation of

six-membered chelate rings. The possible exception to this assignment may be the minor component **10a**, although we have no strong evidence to support this claim. Thus, we were interested in finding a spectroscopic tool which could distinguish compounds of type **A** from those of type **B** without having to rely on X-ray crystallography. With this aim we pursued the differentiation of chelate ring size by measuring the phosphorus coordination chemical shift of the complexes, $\Delta(\delta^{31}\text{P})$, which is defined as the difference in the ^{31}P NMR chemical shifts of the complex and the free ligand.⁴² As discussed by Grim et al.,^{42b} ^{31}P NMR chemical shifts for phosphine transition metal complexes vary considerably with chelate size. Five-membered chelate rings exhibit large downfield shifts, four-membered chelate rings are shifted upfield, and six-membered chelate rings display normal chemical shifts behavior in comparison to monodentate phosphine analogues. Literature data for a series of Group VI metal carbonyl chelate complexes as well as data for complexes **13-15** are given in Table 8. This data shows that the

Table 8. Phosphorus coordination chemical shifts^a ($\Delta(\delta^{31}\text{P})$)

M/L	dppm ^b	dppe ^b	dppp ^b	dppb ^b	5 ^c	Ph ₂ PCH ₂ CMe ₂ CH ₂ PPh ₂
Cr	49.6	91.9	58.3	63.0	71.0	–
Mo	25.1	67.2	37.3	44.2	50.4	44.0 ^c
W	0.1	52.6	17.2	26.3	30.2	25.3 ^d

^a $\Delta(\delta^{31}\text{P}) = \delta^{31}\text{P}_{\text{complex}} - \delta^{31}\text{P}_{\text{ligand}}$; see reference 42.

^bValues taken from reference 39.

^cThis work.

^dValue determined from data in reference 36c.

differences in $\Delta(\delta^{31}\text{P})$ values for six- vs. seven-membered rings ranges from only 5-9 ppm with the larger $\Delta(\delta^{31}\text{P})$ values associated with the seven-membered rings. These differences are much smaller than those observed between four-, five- and six-membered rings. Unfortunately, the phosphorus coordination chemical shifts for **13-15** are considerably larger than either those for the six- or seven-membered chelate ring model complexes. Even more unsatisfying are the coordination chemical shifts of 25.3 ppm calculated for $(\text{Ph}_2\text{PCH}_2\text{CMe}_2\text{CH}_2\text{PPh}_2)\text{W}(\text{CO})_4$ based on data reported by Kraihanzel *et al.*^{36c} and the value of 44.0 ppm which we have obtained for its molybdenum analogue. Using these $\Delta(\delta^{31}\text{P})$ values in the usual way would erroneously suggest the presence of seven-membered chelate rings in these two complexes, obviously leading us to discard this method for the differentiation of structural types A and B in our complexes. Unfortunately, we have found no other suitable spectroscopic tool to distinguish these two structural types.

Monometallic Complexes: Tridentate Coordination Mode

Several attempts were made to synthesize complexes of type C utilizing Group VI metal carbonyl precursors. Reactions of **5** with $\text{Mo}(\text{CO})_6$ led to the formation of **14**. The bidentate coordination mode also prevailed when **5** was reacted with one equivalent of $\text{Mo}(\text{CO})_3(\text{NCEt})_3$,⁴² yielding a partially characterized complex of type A (e.g., *{fac-(EtCN)(OC)₃Mo}*₂(μ -**5**)) based on the symmetry implied by its spectroscopic features. Ligand **5** was found, however, to slowly replace cycloheptatriene from $(\eta^6\text{-cycloheptatriene})\text{Mo}(\text{CO})_3$ at 60 °C to yield the new complex **19** as a creamy white solid. The ^{31}P NMR spectrum of **19** is most informative about its structure, exhibiting what appear to be triplets at 17.7, 15.8 and 14.2 ppm and a singlet at -17.9 ppm indicative of an uncoordinated phosphine group, but shifted 4.4 ppm downfield from

uncoordinated **5**. This spectrum is consistent with a complex of type **C** where ligand **5** adopts a tridentate coordination mode. Each of the four phosphine groups are inequivalent, accounting for the appearance of three triplets for the coordinated phosphine groups. The ^{13}C NMR spectrum is very complicated since all eight phenyl rings are inequivalent. An attempt to grow crystals of this complex by layering hexane onto a CH_2Cl_2 solution yielded thin colorless needles of a new complex **20** within three weeks. The ^{31}P NMR spectrum of this new complex shows three triplets, similar to **19**, but the free phosphine group has apparently been oxidized as indicated by a singlet at 32.7 ppm. Presumably this oxidation occurs because of the presence of adventitious oxygen. Darensbourg has similarly reported that upon prolonged standing at room temperature, solutions of $\text{W}(\text{CO})_3(\text{dppm})(\eta^1\text{-dppm})$ yield the new complex $\text{W}(\text{CO})_3(\text{dppm})(\text{Ph}_2\text{PCH}_2\text{P}(\text{O})\text{Ph}_2)$, presumably due to the presence of adventitious oxygen.⁴⁴ Oxidation of the uncoordinated phosphine group in **19** with S_8 in toluene gives the new complex **21**.

Monometallic Complexes: Tetradentate Coordination Mode

Divalent nickel, palladium, and platinum, as well as monovalent rhodium, are known to favor a square planar geometry for phosphine complexes. The square planar complexes $[\text{M}(\text{dppe})_2]^{2+}$ are well known for $\text{M} = \text{Ni}, \text{Pd}$ and Pt and the palladium and platinum complexes have been characterized by X-ray crystallography.⁴⁵ Similarly, the series of square planar complexes $[\{\text{Ph}_2\text{P}(\text{CH}_2)_n\text{PPh}_2\}_2\text{Rh}]^+$ where $n = 2, 3, 4$ have been synthesized and characterized spectroscopically and structurally.⁴⁶ Thus, these metals were chosen to explore the tendency of **5** to form square planar complexes of type **D**.

In our first attempt, complex **8** was reacted with one equivalent of **5** in DMSO in hopes of achieving ligand redistribution. The ^{31}P NMR spectrum of this reaction

solution indicates the presence of a small quantity of unreacted **8** as well as new resonances at 21.4 and -20.7 ppm assigned to the new complex **22**. Occasionally additional resonances in the regions of 32-30, 23-20 and -18 to -23 ppm were observed. The 32-30 ppm region is indicative of phosphine oxidation and most likely arises from the presence of adventitious oxygen. Samples of this reaction solution are stable under argon for up to a month with no evidence of further reaction or oxidation. Exposure of this solution to air results in oxidation within several days to cleanly yield complex **23** exhibiting ^{31}P NMR chemical shifts of 31.4 and 20.4 ppm. This complex was isolated as a pale yellow solid which exhibits good solubility in CH_2Cl_2 . The ^{31}P NMR chemical shift of 31.4 ppm indicates the presence of phosphoryl groups, which are further substantiated by a split phosphoryl stretch in the infrared spectrum at 1184 and 1119 cm^{-1} . For comparison, the phosphoryl compound **6** exhibits a split phosphoryl stretch at 1178 and 1117 cm^{-1} . Such splitting of phosphoryl and thiophosphoryl stretches in infrared spectra is apparently relatively common.⁴⁷

The ^{13}C NMR spectrum of **23** exhibits resonances for four distinct phenyl groups. Two of these obviously belong to a phosphoryl group based on the doublet nature of their resonances and on the large coupling to phosphorus of 99 Hz observed for the two Ph-*ipso* carbons. The two remaining nonequivalent phenyl groups belong to two equivalent phosphine groups coordinated to a single palladium atom. This assignment is based on the "apparent" triplet multiplicity of these resonances indicative of an AXX' spin system. The presence of two phosphine and two phosphoryl groups is also confirmed by the observation of two methylene carbon resonances with the resonance for the methylene carbons adjacent to a phosphoryl group appearing as a doublet of doublets with $^1J_{\text{PC}} = 69$ Hz. Based on the spectroscopic data presented above, **23** is assigned a

structure of type E. The presence of two methine carbon resonances in the ^{13}C NMR spectrum of **23** clearly indicates the structure must contain a six-membered chelate ring.

Crystals of **23** were obtained as a DMSO solvate by slow evaporation of a DMSO solution in air and their structure was confirmed by X-ray crystallography. The ORTEP diagram shown in Figure 4 shows that **23** is comprised of half each of compounds **6** and

Table 9. Selected bond distances (Å) and angles (deg) in
 $\text{Cl}_2\text{Pd}(\text{Ph}_2\text{PCH}_2)_2\text{CHCH}(\text{CH}_2\text{P}(\text{O})\text{Ph}_2)_2$ (**23**)

Bond Distances			
Pd-Cl(1)	2.415(2)	Pd-Cl(2)	2.386(3)
Pd-P(1)	2.243(3)	Pd-P(2)	2.229(3)
P(1)-C(3)	1.84(1)	P(1)-C(7)	1.82(1)
P(1)-C(19)	1.80(1)	P(2)-C(1)	1.81(1)
P(2)-C(13)	1.79(1)	P(2)-C(25)	1.78(1)
P(3)-O(2)	1.480(9)	P(3)-C(5)	1.80(1)
P(3)-C(31)	1.80(1)	P(3)-C(43)	1.78(1)
P(4)-O(1)	1.485(9)	P(4)-C(6)	1.81(1)
P(4)-C(37)	1.81(1)	P(4)-C(49)	1.80(1)
C(1)-P(2)	1.81(1)	C(1)-C(2)	1.54(1)
C(2)-C(3)	1.54(1)	C(2)-C(4)	1.55(1)
C(3)-P(1)	1.84(1)	C(3)-C(2)	1.54(1)

Table 9. Continued

Bond Angles			
Cl(1)-Pd-Cl(2)	92.21(9)	Pd-P(1)-C(3)	120.4(3)
Cl(1)-Pd-P(1)	87.91(9)	Pd-P(1)-C(7)	107.4(4)
Cl(1)-Pd-P(2)	177.3(1)	Pd-P(1)-C(19)	115.7(4)
Cl(2)-Pd-P(1)	174.9(1)	C(3)-P(1)-C(7)	106.3(6)
Cl(2)-Pd-P(2)	85.3(1)	C(3)-P(1)-C(19)	98.9(5)
P(1)-Pd-P(2)	94.6(1)	C(7)-P(1)-C(19)	107.2(6)
Pd-P(2)-C(1)	116.8(3)	O(2)-P(3)-C(5)	114.5(5)
Pd-P(2)-C(13)	112.6(4)	O(2)-P(3)-C(31)	110.2(6)
Pd-P(2)-C(25)	112.3(4)	O(2)-P(3)-C(5)	112.7(5)
C(1)-P(2)-C(25)	106.6(5)	C(5)-P(3)-C(31)	103.8(5)
C(1)-P(2)-C(25)	99.3(6)	C(5)-P(3)-C(43)	106.8(5)
C(13)-P(2)-C(25)	108.0(5)	C(31)-P(3)-C(43)	108.3(6)
O(1)-P(4)-C(6)	113.7(5)	P(2)-C(1)-C(2)	116.2(8)
O(1)-P(4)-C(37)	113.9(6)	C(1)-C(2)-C(3)	110.8(8)
O(1)-P(4)-C(49)	112.3(5)	C(1)-C(2)-C(4)	108.9(8)
C(6)-P(4)-C(37)	105.1(5)	C(3)-C(2)-C(4)	112.7(8)
C(6)-P(4)-C(49)	104.6(5)	P(1)-C(3)-C(2)	118.8(7)
C(37)-P(4)-C(49)	106.4(6)	C(2)-C(4)-C(5)	111.1(8)
C(2)-C(4)-C(6)	111.2(8)	C(5)-C(4)-C(6)	111.6(8)
P(3)-C(5)-C(4)	116.4(7)	P(4)-C(6)-C(4)	113.1(7)

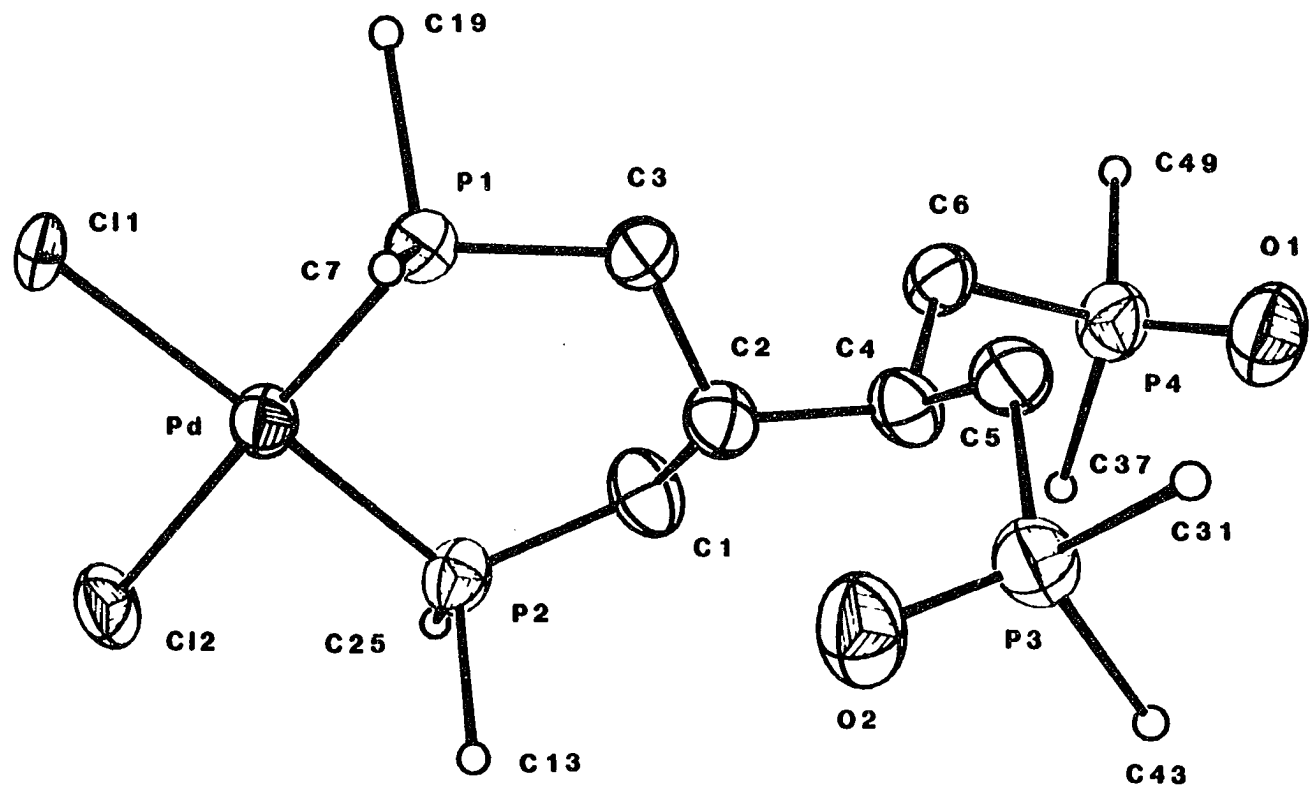


Figure 4. ORTEP drawing of **23** with thermal ellipsoids drawn at the 50% probability level. All phenyl carbons, except for Ph-*ipso* carbons, have been omitted for clarity.

8. Figure 4 also reveals that **5** coordinates to palladium with the formation of a six-membered chelate ring as suggested by ^{13}C NMR spectroscopic data. The palladium atom is square planar and lies 0.034 Å out of the P_2Cl_2 plane. The Pd-P distances of 2.243(3) and 2.229(3) Å as well as the P-Pd-P angle of $94.6(1)^\circ$ are quite similar to the analogous values found for **8**. The P-O distances of 1.480(9) and 1.485(9) Å lie in the normal range discussed earlier. Unlike the molecular structure of **6**, **23** has no close intramolecular contacts between phosphoryl oxygen atoms and neighboring methylene groups. Selected bond distances and angles are given in Table 9.

The formation of **23** upon exposure of the reaction solution of **5** and **8** to air is consistent with a metal-catalyzed oxidation of the uncoordinated phosphine groups. This oxidation does not appear to be the result of reaction with DMSO since solutions of **5** in DMSO exposed to air and the reaction solution of **5** and **8** in DMSO under argon show no oxidation according their ^{31}P NMR spectra. Several other examples of metal-catalyzed oxidation of phosphines have been reported.⁴⁸ The precursor to **23**, formed in the reaction solution of **5** and **8** prior to exposure to air, is presumably $\text{Cl}_2\text{Pd}(\text{Ph}_2\text{PCH}_2)_2\text{CHCH}(\text{CH}_2\text{PPh}_2)_2$, **22**. This assignment is based on the two ^{31}P NMR chemical shifts of 21.4 and -20.7 ppm observed in this solution as well as the fact that exposure of solutions of **22** to air yields **23**. Although we have not yet attempted to isolate this complex, it could provide a convenient entry into heterobimetallic complexes of this ligand.

To avoid the formation of complexes **22** and **23**, we chose a palladium starting material with a non-coordinating anion. Reaction of **5** with one equivalent of $\text{Pd}(\text{BF}_4)_2 \cdot 4\text{CH}_3\text{CN}$ in $\text{CH}_2\text{Cl}_2/\text{CH}_3\text{CN}$ yields a yellow solution whose ^{31}P NMR spectrum consists mainly of a singlet at 6.7 ppm. A shoulder on the upfield side of this resonance as well as a broad peak centered at ~11 ppm were also present. Raising the

temperature of this solution to 325 K results in a sharpening of the resonance at 11 ppm and splitting of the shoulder on the 6.7 ppm resonance into two additional resonances. These additional resonances suggest the presence of more than one species in solution. We have been unable to identify the complex giving rise to the resonance at 6.7 ppm and have been unable to isolate a complex which appears by ^{31}P NMR spectra to consist of only one species in solution.

The addition of one equivalent of **5** to a light blue solution of $[\text{Ni}(\text{NCCH}_3)_6][\text{ClO}_4]_2$ or $[\text{Ni}(\text{DMSO})_6][\text{BF}_4]_2$ in acetonitrile results in the formation of an immediate deep brown solution. The ^{31}P NMR spectrum of this solution exhibits only one small singlet at -22.0 ppm assigned to uncoordinated **5**. The lack of resonances for a nickel complex of **5** indicates the nickel complex may be tetrahedral and paramagnetic, inconsistent with a complex of type **D**. A nickel complex of type **D** would have to be square planar and as such should be diamagnetic. This brown solution is stable indefinitely under argon, but similarly to **22**, this solution undergoes a metal-catalyzed oxidation within ten minutes in the presence of air to yield a light yellow solution. Oxidation is indicated by a ^{31}P NMR chemical shift of 30.9 ppm and the formation of clear crystals of **6** upon allowing this solution to stand for several days.

Reaction of **5** with half an equivalent of $\text{Rh}_2\text{Cl}_2(\text{COD})_2$ in THF yields a pale yellow powder (**24**) which does not contain cyclooctadiene. A FAB mass spectrum of **24** shows a small molecular ion peak for $(\text{5})\text{Rh}^+$ at m/e 925.1 and peaks at m/e 957.1 and 973.1 corresponding to the molecular ion plus two and three oxygen atoms, respectively, arising from oxidation of the complex while in the glycerol matrix. Additionally, numerous smaller peaks corresponding to higher mass fragments were observed above m/e 1000. Conductivity measurements on CH_3NO_2 solutions of **24** provide a molar conductance of only $37 \text{ ohm}^{-1}\text{cm}^2\text{mol}^{-1}$ based on a mononuclear species

of composition [(5)Rh]Cl. This is considerably lower than the commonly accepted range⁴⁹ of 75-95 $\text{ohm}^{-1}\text{cm}^2\text{mol}^{-1}$ for 1:1 electrolytes in CH_3NO_2 and may indicate partial coordination of chloride to rhodium or the presence of dimeric species.

The ^{31}P NMR spectrum of **24** in acetonitrile shows a broadened resonance consisting of two doublets of unequal intensity at 18.3 and 15.9 ppm with coupling to rhodium of 130 and 135 Hz, respectively. In DMSO, **24** exhibits only one very broad resonance centered at 12.7 ppm. Removal of the chloride anion using AgBF_4 had no effect on the ^{31}P NMR spectrum of **24** in either solvent, indicating that chloride is not coordinated to rhodium in solution. Variable temperature ^{31}P NMR spectra taken in $\text{CH}_3\text{CN}/\text{CH}_2\text{Cl}_2$ between 225 K and 325 K shows complicated, unassigned resonances at both extremes. Based on this ^{31}P NMR data as well as the conductivity and mass spectral results, it is clear that **24** is not a mononuclear species of type **D**, and may well be dimeric or oligomeric in solution. We have no information concerning its structure in the solid state.

Based on the results of nickel, palladium and rhodium reactions with an equimolar quantity of **5**, we believe that complex mixtures, which may contain interconverting dimeric or oligomeric complexes as well as solvated species, are present in these reaction solutions. Since we have shown that this ligand is capable of acting as a bidentate ligand to two metals, the formation of oligomeric materials seems quite plausible.

Work by Pignolet and Shaw offers some support for this proposal as well as a rationale for these results. Pignolet^{46a} has published an informative paper concerning the series of complexes $[\text{Rh}(\text{Ph}_2\text{P}(\text{CH}_2)_n\text{PPh}_2)_2]\text{BF}_4$ ($n = 2-4$). These complexes are all reported to exhibit doublet resonances in their ^{31}P NMR spectra with couplings to rhodium of 132-137 Hz. In the low temperature spectra for these complexes, however, only the $n = 2$ complex continued to exhibit a doublet resonance. The $n = 3$ complex

exhibited an A_2B_2X pattern consistent with a five-coordinate solvated complex and for the $n = 4$ complex the low temperature spectrum was complex and unassignable, presumably due to the presence of *solvated and dinuclear species*. The authors concluded that this temperature dependent behavior was the result of *increasing steric interactions with increasing chelate size* throughout the series $n = 2-4$. Consistent with this argument was the appearance of the same trend in the molecular structures of these complexes. Furthermore, in the reaction of CO with the complex in which $n = 4$, a dppb ligand readily dissociates to form the dimeric species $[Rh_2(dppb)_3(CO)_4]^{2+}$, the structure of which has been confirmed by X-ray crystallography.⁵⁰ In solution this complex exhibits two broad ^{31}P NMR resonances at 20 and 23 ppm and its low temperature spectrum becomes complex. These spectra indicate that this complex does not retain its solid state structure in solution. This is of direct relevance to our system since a complex of type **D** would contain both six-membered and seven-membered chelate rings. The results described by Pignolet for the complexes $n = 3,4$ suggest the presence of steric repulsions in our system and they support our proposal for a complex solution chemistry with the potential formation of solvated and oligomeric species. Models indicate that four severe Ph-Ph interactions occur in complexes of type **D**. Unlike the bidentate ligands dppp and dppb, **5** offers little structural flexibility to allow for minimization of these steric interactions when all four phosphine groups are coordinated to a single metal atom. Figure 5 illustrates these potential phenyl interactions.

Work by Shaw, McAuliffe, and others has shown that chelating phosphines of the type $R_2P(CH_2)_nPR_2$ require a minimum of five methylene units ($n = 5$) between the donor atoms in order to span *trans* positions on the same metal.⁵¹ In fact, several structural studies on complexes of the type *trans*- $Cl_2Pd(R_2P(CH_2)_nPR_2)$ where $n > 5$ have shown many of these complexes to be cyclic dimers or trimers forming rings as

large as 45 atoms.^{51h,i,l} In our system, a complex of structural type D has two trans pairs of phosphorus donors labeled as P₁-P₃ and P₂-P₄ in Figure 5. It is apparent from this illustration that there are only four backbone carbon atoms between either trans pair of phosphorus donors in **5**, thereby not fulfilling the minimum requirement proposed by Shaw. This argument is also supported by attempts to build space-filling models of type

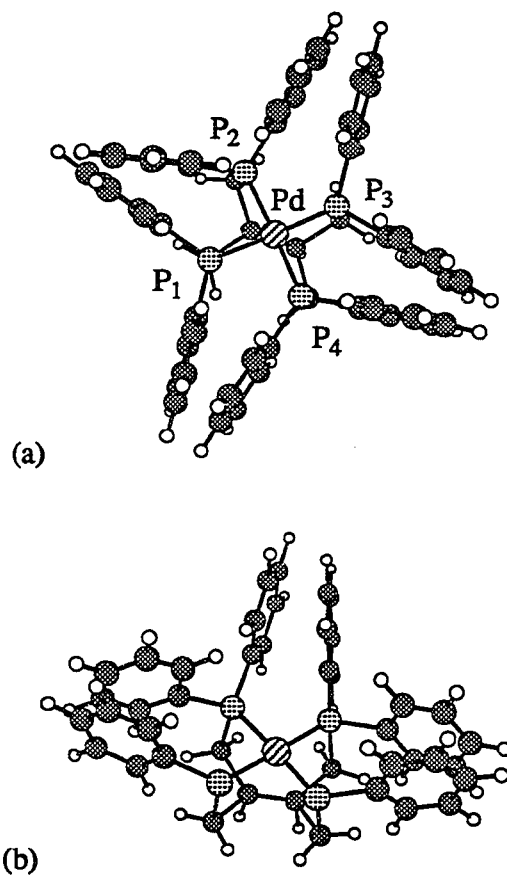


Figure 5. Model of [(**5**)Pd]²⁺ (a) viewed from above to illustrate the steric interactions of the eight phenyl rings, and (b) viewed from the side with two phenyl rings omitted for clarity.

D. Thus is it apparent that attempts to form complexes of type **D** are hindered i) by steric repulsions of the eight phenyl substituents in **5**; ii) by a ligand backbone structurally incapable of spanning two *trans* sites in a metal complex, and iii) by the ease of formation of dinuclear complexes wherein **5** readily acts as a bis-bidentate ligand as in complexes **8-18**.

Conclusions

We have synthesized the new tetratertiary phosphine **5** which readily forms homobimetallic complexes with a variety of transition metals. The formation of **22** in solution may provide a convenient route to the synthesis of heterobimetallic complexes. Ligand **5** also coordinates to molybdenum tricarbonyl fragments as a tridentate ligand with one phosphine group remaining uncoordinated. Steric hindrance and structural limitations were found, however, to preclude the formation of monometallic complexes of Ni(II), Pd(II), and Rh(I) wherein **5** coordinates as a tetradentate ligand. Removal of these steric and structural limitations in derivatives of **5** may yield a novel class of new tetradentate phosphine ligands.

ACKNOWLEDGMENTS

The authors thank the National Science Foundation for grant support of this research and the Department of Energy, Basic Energy Sciences, Material Science Division (Contract No. W-7405-Eng-82) for support to Dr. Robert A. Jacobson. Drs. Lance J. Miller and Tom Hendrixson, formerly of Dr. Robert A. Jacobson's group, and Drs. Victor J. Young, Jr. and Lee M. Daniels of the Iowa State University Molecular Structure Laboratory, are thanked for the X-ray structural analyses for compounds **6** and **8**, **10b**, **11**, and **23**, respectively. Dr. Colleen M. Duff is acknowledged for the initial synthesis and partial characterization of ligand **5**, its tetraphosphoryl derivative **6** via DMSO oxidation, and the palladium dichloride complex **8**, as well as the unexpected isolation of a crystalline sample of **23**. A compilation of supplementary material for the molecular structure solutions of **6**, **8**, and **23** is given in her dissertation.⁵² All other syntheses and all conclusions presented in this section are strictly those of the author.

REFERENCES

1. Davis, R. V.; Wintergrass, D. J.; Janakiraman, M. N.; Hyatt, E. M.; Jacobson, R. A.; Daniels, L. M.; Wroblewski, A.; Padmakumari Amma, J.; Das, S. K.; Verkade, J. G. *Inorg. Chem.*, accepted.
2. Davis, R. V.; Verkade, J. G. *Inorg. Chem.* **1990**, *29*, 4983.
3. de Ruiter, B.; Benson, J. E.; Jacobson, R. A.; Verkade, J. G. *Inorg. Chem.* **1990**, *29*, 1065.
4. Bianco, V. D.; Doronzo, S. *Inorg. Synth.* **1976**, *16*, 161.
5. Cotton, F. A.; McCleverty, J. A.; White, J. E. *Inorg. Synth.* **1967**, *9*, 121.
6. Bennett, M. A.; Pratt, L.; Wilkinson, G. *J. Chem. Soc.* **1961**, 2037.
7. Darensbourg, D. J.; Kump, R. L. *Inorg. Chem.* **1978**, *22*, 2680.
8. King, R. B.; Fronzaglia, A. *Inorg. Chem.* **1966**, *5*, 1837.
9. Howell, J. A. S.; Johnson, B. F. G.; Josty, P. L.; Lewis, J. J. *Organomet. Chem.* **1972**, *39*, 329.
10. Doyle, J. R.; Slade, P. E.; Jonassen, H. B. *Inorg. Synth.* **1960**, *6*, 218.
11. Alexander, R. A.; Baenziger, N. C.; Carpenter, C.; Doyle, J. R. *J. Am. Chem. Soc.* **1960**, *82*, 535.
12. Pray, A. R. *Inorg. Synth.* **1957**, *5*, 154.
13. Chatt, J.; Venanzi, L. M. *J. Chem. Soc.* **1957**, 4735.
14. Selbin, J.; Bull, W. E.; Holmes, Jr., L. H. *J. Inorg. Nucl. Chem.* **1961**, *16*, 219.
15. Drew, D.; Doyle, J. R. *Inorg. Synth.* **1972**, *13*, 48.
16. Weinges, K.; Spanig, R. *Chem. Ber.* **1968**, *101*, 3010.

17. Five-line multiplets of an AXX' ($A = {}^{13}\text{C}$; $X, X' = {}^{31}\text{P}$) spin system where the two outer lines are of low intensity are denoted here as apparent triplets, at. The separation reported is that between lines 2 and 4.
18. Jacobson, R. A. *J. Appl. Crystallogr.* **1976**, *9*, 115.
19. Main, R.; Lessinger, L.; Woolfson, M. M.; Germain, G.; Declercq, J. P. "A System of Computer Programs for the Automatic Solution of Crystal Structures from X-ray Diffraction Data"; University of York, York, England, 1976.
20. Lapp, R. L.; Jacobson, R. A. "Alls: A Generalized Crystallographic Least Squares Program", U.S. DOE Report, IS-4708; Iowa State University: Ames, IA, 1979.
21. Powell, D. R.; Jacobson, R. A. "Four: A Generalized Crystallographic Fourier Program", U.S. DOE Report, IS-4737; Iowa State University: Ames, IA, 1979.
22. (a) Hydrogen scattering factors were taken from: Stewart, R. F.; Davidson, E. R.; Simpson, W. T. *J. Chem. Phys.* **1965**, *42*, 3175. Atomic scattering factors were obtained from: Cromer, D. T.; Waber, J. T. "International Tables for X-ray Crystallography"; Kynoch Press: Birmingham, England, 1974, Vol. IV, Table 2.2a, 71-79. (b) Flippen-Anderson, J. L.; Gilardi, R.; Konnert, J. H. "Restrained Least-Squares Program (RESLSQ)", NRL Memorandum Report, 5042; Naval Research Laboratory: Washington, D.C., 1983.
23. Sheldrick, G. M. "SHELXS-86", Institut für Anorganische Chemie der Universität, Gottingen, F.R.G., 1986.
24. Enraf-Nonius Structure Determination Package; Enraf-Nonius: Delft, Holland. Neutral-atom scattering factors and anomalous scattering corrections were taken from: Cromer, D. T.; Waber, J. T. "International Tables for X-ray Crystallography"; Kynoch Press: Birmingham, England, 1974, Vol. IV, Table 2.2B, Table 2.3.1.

25. (a) Szmant, H.; Cox, O. *J. Org. Chem.* **1966**, *31*, 1595. (b) Amonoo-Neizer, E. H.; Ray, S. K.; Shaw, R. A.; Smith, B. C. *J. Chem. Soc.* **1965**, 4296. (c) Olah, G. A.; Gupta, B. G. B.; Narang, S. C. *Synthesis* **1978**, 137.
26. (a) Modro, T. A. *Can. J. Chem.* **1977**, *55*, 3681. (b) Albright, T. A.; Freeman, W. J.; Schweizer, E. E. *J. Org. Chem.* **1975**, *40*, 3437.
27. (a) Antipin, M. Y.; Struchkov, Y. T.; Pisareva, S. A.; Medved, T. Y.; Kabachnik, M. I. *J. Struct. Chem.* **1980**, *21*, 644. (b) Naae, D. G.; Lin, T. W. *J. Fluorine Chem.* **1979**, *13*, 473. (c) Bandoli, G.; Bortolozzo, G.; Clemente, D. A.; Croatto, U.; Panattoni, C. *J. Chem. Soc. (A)* **1970**, 2778. (d) Ruban, G.; Zabel, V. *Cryst. Struct. Commun.* **1976**, *5*, 671.
28. Hamilton, W. C.; Ibers, J. A. "Hydrogen Bonding in Solids" W. A. Benjamin, New York, NY, 1968, p. 16.
29. Steffen, W. L.; Palenik, G. L. *Inorg. Chem.* **1976**, *15*, 2432.
30. Palenik, G. L.; Mathew, M.; Steffen, W. L.; Beran, G. J. *Am. Chem. Soc.* **1975**, *97*, 1059.
31. Crystals of **10b** are monoclinic, space group C2/c, with unit cell dimensions $a = 37.541 \text{ \AA}$, $b = 14.622 \text{ \AA}$, $c = 27.353 \text{ \AA}$, $\beta = 113.212^\circ$, and $Z = 8$. The crystal had a calculated density of 1.53 g/cm^3 . The structure was refined to $R = 0.129$ on the basis of 9665 reflections of which 2613 were unique with $I > 3\sigma(I)$. Phenyl rings were refined as rigid groups. Disorder in the DMSO molecule of crystallization and the low number of observed reflections presumably are the cause of the poor refinement. Data was collected at $-80 \text{ }^\circ\text{C}$ on a Rigaku AFC6R diffractometer with graphite monochromated $\text{MoK}\alpha$ radiation and a 12KW rotating anode generator.
32. Rowley, D. A.; Drago, R. S. *Inorg. Chem.* **1967**, *6*, 1092.

33. (a) Spek, A. L.; van Eijck, B. P.; Jans, R. J. F.; van Koten, G. *Acta Crystallogr., Sect. C. Cryst. Struct. Commun.* **1987**, *C43*, 1878. (b) Greene, P. T.; Sacconi, L. *J. Chem. Soc. (A)* **1970**, 866. (c) Garton, G.; Henn, D. E.; Powell, H. M.; Venanzi, L. M. *J. Chem. Soc.* **1963**, 3625.
34. Van Hecke, G. R.; Horrocks, Jr., W. D. *Inorg. Chem.* **1966**, *5*, 1968.
35. Pregosin, P. S.; Kunz, R. W. *NMR Basic Princ. Progr.* **1979**, *16*, 43.
36. See for example: (a) Gabelein, H.; Ellermann, J. *J. Organomet. Chem.* **1978**, *156*, 389. (b) Chatt, J.; Watson, H. R. *J. Chem. Soc.* **1961**, 4980. (c) Kraihanzel, C. S.; Ressler, J. M.; Gray, G. M. *Inorg. Chem.* **1982**, *21*, 879.
37. Todd, J. L.; Wilkinson, J. R. *J. Organomet. Chem.* **1974**, *77*, 1.
38. (a) Pregosin, P. S.; Kunz, R. W. *NMR: Basic Princ. Progr.* **1979**, *16*, 65. (b) Redfield, D. A.; Nelson, J. H.; Carey, L. W. *Inorg. Nucl. Chem. Letters* **1974**, *10*, 727.
39. Andrews, G. T.; Colquhoun, I. J.; McFarlane, W. *Polyhedron* **1983**, *2*, 783.
40. (a) Cheney, A. J.; Mann, B. E.; Shaw, B. L. *J. Chem. Soc. Chem. Commun.* **1971**, 431. (b) Cooper, D. G.; Powell, J. *Can. J. Chem.* **1973**, *51*, 1634.
41. See for example: Casey, C. P.; Whiteker, G. T.; Campana, C. F.; Powell, D. R. *Inorg. Chem.* **1990**, *29*, 3376.
42. (a) Mann, B. E.; Masters, C. E.; Shaw, B. L.; Slade, R. M.; Stainbank, R. E. *Inorg. Nucl. Chem. Letters* **1971**, *7*, 881. (b) Grim, S. O.; Briggs, W. L.; Barth, R. C.; Tolman, C. A.; Jesson, J. P. *Inorg. Chem.* **1974**, *13*, 1095.
43. Kubas, G. J. *Inorg. Chem.* **1983**, *22*, 692.
44. Darensbourg, D. J.; Zalewski, D. J.; Plepys, C.; Campana, C. *Inorg. Chem.* **1987**, *26*, 3727.

45. Engelhardt, L. M.; Patrick, J. M.; Raston, C. L.; Twiss, P.; White, A. H. *Aust. J. Chem.* **1984**, *37*, 2193.
46. (a) Anderson, M. P.; Pignolet, L. H. *Inorg. Chem.* **1981**, *20*, 4101. (b) Hall, M. C.; Kilbourn, B. T.; Taylor, K. A. *J. Chem. Soc. (A)*. **1970**, 2539. (c) Doughty, D. H.; Pignolet, L. H. *J. Am. Chem. Soc.* **1978**, *100*, 7083.
47. Emsley, H.; Hall, D. *The Chemistry of Phosphorus*; John Wiley & Sons, New York, 1976; p. 95.
48. (a) Saum, S. E.; Askham, F. R.; Fronczek, F. R.; Stanley, G. G. *Polyhedron* **1988**, *7*, 1785. (b) Hanzlik, R. P.; Williamson, W. D. *J. Am. Chem. Soc.* **1976**, *98*, 6570. (c) Graham, B. W.; Laing, K. R.; O'Connor, C. J.; Roper, W. R. *J. Chem. Soc., Chem. Commun.* **1970**, 1272. (d) Halpern, J.; Pickard, A. L. *Inorg. Chem.* **1970**, *9*, 2798. (e) Otsuka, S.; Nakamura, A.; Tatsuno, Y. *J. Am. Chem. Soc.* **1969**, *91*, 6994. (f) Birk, J. P.; Halpern, J.; Pickard, A. L. *J. Am. Chem. Soc.* **1968**, *90*, 4491.
49. Geary, W. J. *Coord. Chem. Rev.* **1971**, *7*, 81.
50. Pignolet, L. H.; Doughty, D. H.; Nowicki, S. C.; Anderson, M. P.; Casalnuovo, A. L. *J. Organomet. Chem.* **1980**, *202*, 211.
51. (a) Hill, W. E.; Minahan, D. M. A.; McAuliffe, C. A. *Inorg. Chem.* **1983**, *22*, 3382. (b) Hill, W. E.; Minahan, D. M. A.; Taylor, J. G.; McAuliffe, C. A. *J. Am. Chem. Soc.* **1982**, *104*, 6001. (c) Hill, W. E.; McAuliffe, C. A.; Niven, I. E.; Parish, R. V. *Inorg. Chim. Acta* **1980**, *38*, 273. (d) Hill, W. E.; Taylor, J. G.; Falshaw, C. P.; King, T. J.; Beagley, B.; Tongue, D. M.; Pritchard, R. G.; McAuliffe, C. A. *J. Chem. Soc., Dalton Trans.* **1986**, 2289. (e) McAuliffe, C. A.; Souter, H. E.; Levason, W.; Hartley, F. R.; Murray, S. G. *J. Organomet. Chem.* **1978**, *159*, C25. (f) Levason, W.; McAuliffe, C. A.; Murray, S. G. *J.*

- Organomet. Chem.* **1976**, *110*, C25. (g) Sanger, A. R. *J. Chem. Soc., Dalton Trans.* **1977**, 1971. (h) Housecroft, C. E.; Shaykh, B. A. M.; Rheingold, A. L.; Haggerty, B. S. *Inorg. Chem.* **1991**, *30*, 125. (i) Al-Salem, N. A.; Empsall, H. D.; Markham, R.; Shaw, B. L.; Weeks, B. J. *J. Chem. Soc., Dalton Trans.* **1979**, 1972. (j) Shaw, B. L. *J. Organomet. Chem.* **1975**, *94*, 251. (k) Pyrde, A. J.; Shaw, B. L.; Weeks, B. J. *J. Chem. Soc., Chem. Commun.* **1973**, 947. (l) Al-Salem, N. A.; McDonald, W. S.; Markham, R.; Norton, M. C.; Shaw, B. L. *J. Chem. Soc., Dalton Trans.* **1980**, 59.
52. Duff, C. M. Ph.D. Dissertation, Iowa State University, 1987.

SUPPLEMENTARY MATERIAL

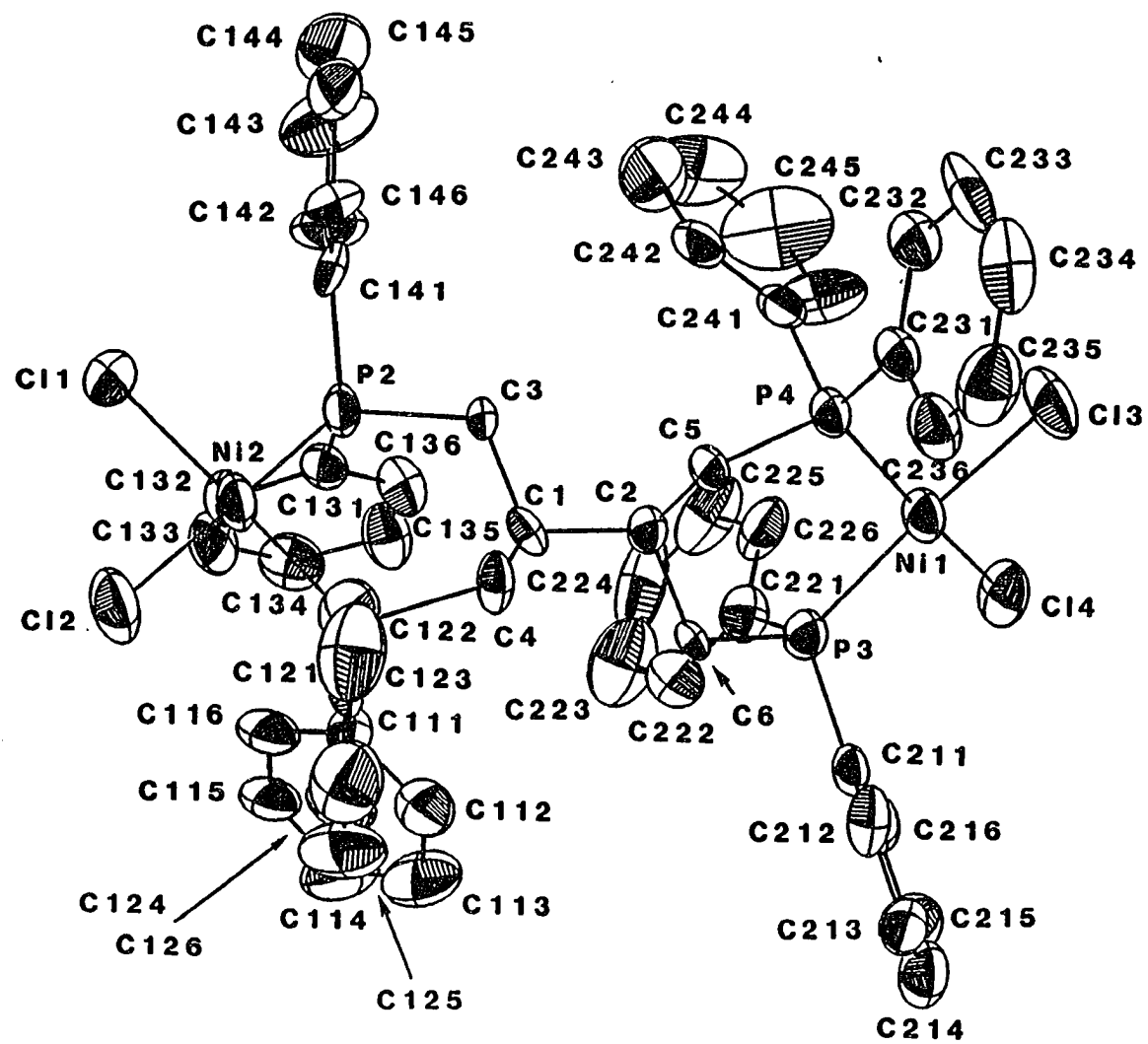


Figure 6. ORTEP drawing and complete labeling scheme for 11.

Table 10. Positional parameters and their estimated standard deviations for **11**

Atom	x	y	z	B(Å ²)
Ni(1)	-0.0078(1)	0.2395(1)	0.0817(1)	3.33(4)
Ni(2)	0.5654(1)	0.3243(1)	0.3692(1)	3.44(5)
P(1)	0.4945(3)	0.4226(3)	0.3056(2)	2.97(9)
P(2)	0.4681(3)	0.2023(3)	0.3177(2)	3.08(9)
P(3)	0.1313(3)	0.2989(3)	0.0574(2)	3.23(9)
P(4)	0.0408(3)	0.2313(3)	0.1933(2)	3.03(9)
Cl(1)	0.6445(3)	0.2313(3)	0.4335(2)	4.4(1)
Cl(2)	0.6765(3)	0.4452(3)	0.4073(3)	5.4(1)
Cl(3)	-0.1511(3)	0.1866(4)	0.1009(2)	5.8(1)
Cl(4)	-0.0545(3)	0.2212(3)	-0.0324(2)	4.7(1)
C(1)	0.3373(9)	0.296(1)	0.2322(7)	2.7(3)
C(2)	0.2350(9)	0.284(1)	0.1882(7)	2.8(3)
C(3)	0.3459(9)	0.217(1)	0.2798(7)	3.0(3)
C(4)	0.3658(9)	0.389(1)	0.2731(7)	3.1(3)
C(5)	0.1576(9)	0.296(1)	0.2327(7)	3.0(3)
C(6)	0.2273(9)	0.348(1)	0.1295(7)	2.9(3)
C(111)	0.543(1)	0.440(1)	0.2269(7)	3.5(4)

Starred atoms were refined isotropically. Anisotropically refined atoms are given in the form of the isotropic equivalent displacement parameter defined as:
 $(4/3) * [a^2*B(1,1) + b^2*B(2,2) + c^2*B(3,3) + ab(\cos \gamma)*B(1,2) + ac(\cos \beta)*B(1,3) + bc(\cos \alpha)*B(2,3)]$

Table 10. Continued

Atom	x	y	z	B(Å ²)
C(112)	0.502(1)	0.482(1)	0.1720(8)	4.8(4)
C(113)	0.537(1)	0.489(1)	0.1109(8)	6.2(5)
C(114)	0.619(1)	0.449(2)	0.104(1)	7.8(6)
C(115)	0.658(1)	0.404(1)	0.157(1)	7.0(5)
C(116)	0.625(1)	0.402(1)	0.2188(8)	4.5(4)
C(121)	0.4953(9)	0.535(1)	0.3499(7)	3.3(4)
C(122)	0.460(1)	0.536(1)	0.4101(8)	4.2(4)
C(123)	0.451(1)	0.618(1)	0.4445(8)	6.1(5)
C(124)	0.484(1)	0.702(1)	0.4149(9)	6.0(5)
C(125)	0.518(1)	0.701(1)	0.3570(9)	5.9(5)
C(126)	0.525(1)	0.619(1)	0.3224(8)	4.5(4)
C(131)	0.519(1)	0.163(1)	0.2463(7)	3.3(4)
C(132)	0.620(1)	0.170(1)	0.2544(8)	4.1(4)
C(133)	0.663(1)	0.146(1)	0.2008(8)	4.8(4)
C(134)	0.609(1)	0.117(1)	0.1354(8)	5.2(5)
C(135)	0.509(1)	0.111(1)	0.1242(8)	4.8(4)
C(136)	0.466(1)	0.132(1)	0.1811(8)	4.2(4)
C(141)	0.438(1)	0.104(1)	0.3676(7)	3.8(4)
C(142)	0.442(1)	0.014(1)	0.3414(9)	6.4(5)
C(143)	0.414(2)	-0.064(1)	0.375(1)	9.1(7)

Table 10. Continued

Atom	x	y	z	B(Å ²)
C(144)	0.378(2)	-0.053(1)	0.436(1)	9.0(7)
C(145)	0.374(1)	0.042(2)	0.4646(9)	8.0(6)
C(146)	0.405(1)	0.117(1)	0.4280(8)	5.3(5)
C(211)	0.1297(9)	0.395(1)	0.0008(7)	3.0(3)
C(212)	0.123(1)	0.481(1)	0.0280(8)	4.5(4)
C(213)	0.122(1)	0.556(1)	-0.0140(9)	4.8(4)
C(214)	0.124(1)	0.545(1)	-0.081(1)	5.7(5)
C(215)	0.126(1)	0.462(1)	-0.1118(9)	6.8(5)
C(216)	0.129(1)	0.384(1)	-0.0693(9)	5.1(5)
C(221)	0.189(1)	0.210(1)	0.0184(8)	4.2(4)
C(222)	0.276(1)	0.236(1)	-0.0009(9)	5.8(5)
C(223)	0.329(2)	0.173(1)	-0.023(1)	8.6(6)
C(224)	0.292(1)	0.086(2)	-0.026(1)	8.8(6)
C(225)	0.204(1)	0.052(1)	-0.008(1)	7.1(5)
C(226)	0.150(1)	0.119(1)	0.0168(9)	5.6(5)
C(231)	-0.034(1)	0.268(1)	0.2527(7)	3.4(4)
C(232)	-0.079(1)	0.208(1)	0.2945(8)	4.4(4)
C(233)	-0.134(1)	0.240(1)	0.3406(8)	5.2(5)
C(234)	-0.145(1)	0.329(1)	0.3408(9)	5.7(5)
C(235)	-0.100(1)	0.389(1)	0.2993(9)	5.7(5)

Table 10. Continued

Atom	x	y	z	B(Å ²)
C(236)	-0.046(1)	0.360(1)	0.2558(8)	4.2(4)
C(241)	0.0554(9)	0.112(1)	0.2065(8)	3.5(4)
C(242)	0.110(1)	0.090(1)	0.2679(9)	4.9(4)
C(243)	0.134(1)	0.002(1)	0.277(1)	7.8(6)
C(244)	0.103(2)	-0.061(1)	0.225(1)	11.1(7)
C(245)	0.043(2)	-0.042(2)	0.162(1)	11.1(8)
C(246)	0.022(2)	0.047(1)	0.1543(9)	6.7(6)
O(1)	0.152(1)	0.527(1)	0.2213(7)	8.8(4)*
C(11)	0.159(1)	0.591(2)	0.265(1)	7.8(6)*
C(12)	0.230(2)	0.616(2)	0.330(1)	8.8(6)*
C(13)	0.184(2)	0.644(2)	0.388(1)	11.2(8)*
C(14)	0.139(2)	0.728(2)	0.369(1)	12.5(9)*
C(15)	0.065(2)	0.703(2)	0.309(1)	10.9(8)*
C(16)	0.102(2)	0.670(2)	0.243(1)	10.3(7)*
O(2)	0.234(1)	0.274(1)	0.4116(9)	12.2(5)*
C(21)	0.209(1)	0.323(2)	0.457(1)	7.6(5)*
C(22)	0.150(2)	0.399(2)	0.437(2)	13(1)*
C(23)	0.076(2)	0.392(2)	0.475(2)	14(1)*
C(24)	0.095(2)	0.390(2)	0.542(1)	11.0(8)*

Table 10. Continued

Atom	x	y	z	B(Å ²)
C(25)	0.145(2)	0.309(3)	0.567(2)	16(1)*
C(26)	0.238(2)	0.304(2)	0.529(1)	10.9(8)*
C(31)	0.369(2)	0.681(2)	0.085(1)	8.6(6)*
C(32)	0.314(2)	0.705(2)	0.142(1)	9.9(7)*
C(33)	0.335(2)	0.803(2)	0.175(1)	9.8(7)*
C(34)	0.333(2)	0.868(2)	0.113(1)	9.8(7)*
C(35)	0.397(2)	0.855(2)	0.058(1)	9.3(7)*
C(36)	0.362(2)	0.752(2)	0.032(1)	8.3(6)*
C(41)	0.152(2)	0.112(2)	0.728(2)	13.0(9)*
C(42)	0.180(2)	0.190(2)	0.786(2)	15(1)*
C(43)	0.277(2)	0.249(2)	0.786(2)	16(1)*
C(44)	0.359(2)	0.200(2)	0.792(2)	15(1)*
C(45)	0.327(3)	0.108(3)	0.736(2)	17(1)*
C(46)	0.214(2)	0.052(3)	0.722(2)	16(1)*

Table 11. Bond distances (Å) in Cl₂Ni(PPh₂CH₂)₂CHCH(CH₂Ph₂P)₂NiCl₂, **11**

Atom1-Atom2	Distance	Atom 1-Atom 2	Distance
Ni(1)-P(3)	2.180(0)	C(111)-C(112)	1.370(0)
Ni(2)-P(4)	2.175(0)	C(111)-C(116)	1.390(0)
Ni(1)Cl(3)	2.176(0)	C(112)-C(113)	1.352(0)
Ni(1)-Cl(4)	2.198(0)	C(113)-C(114)	1.442(0)
Ni(2)-P(1)	2.185(0)	C(114)-C(115)	1.310(0)
Ni(2)-P(2)	2.169(0)	C(115)-C(116)	1.374(0)
Ni(2)-Cl(1)	2.198(0)	C(121)-C(122)	1.354(0)
Ni(2)-Cl(2)	2.195(0)	C(121)-C(126)	1.378(0)
P(1)-C(4)	1.822(0)	C(122)-C(123)	1.412(0)
P(1)-C(111)	1.804(0)	C(123)-C(124)	1.411(0)
P(1)-C(121)	1.812(0)	C(124)-C(125)	1.301(0)
P(2)-C(3)	1.823(0)	C(125)-C(126)	1.390(0)
P(2)-C(131)	1.801(0)	C(131)-C(132)	1.400(0)
P(2)-C(141)	1.804(0)	C(131)-C(136)	1.357(0)
P(3)-C(6)	1.819(0)	C(132)-C(133)	1.359(0)
P(3)-C(211)	1.811(0)	C(133)-C(134)	1.372(0)
P(3)-C(221)	1.846(0)	C(134)-C(135)	1.404(0)
P(4)-C(5)	1.816(0)	C(135)-C(136)	1.414(0)
P(4)-C(231)	1.822(0)	C(141)-C(142)	1.399(0)

Numbers in parentheses are estimated standard deviations in the least significant digits

Table 11. Continued

Atom1-Atom2	Distance	Atom1-Atom2	Distance
P(4)-C(241)	1.801(0)	C(141)-C(146)	1.369(0)
C(1)-C(2)	1.550(0)	C(142)-C(143)	1.362(0)
C(1)-C(3)	1.512(0)	C(143)-C(144)	1.356(0)
C(1)-C(4)	1.504(0)	C(144)-C(145)	1.484(0)
C(2)-C(5)	1.537(0)	C(145)-C(146)	1.378(0)
C(2)-C(6)	1.519(0)	C(211)-C(212)	1.363(0)
C(211)-C(216)	1.358(0)	C(11)-C(16)	1.512(0)
C(212)-C(213)	1.418(0)	C(12)-C(13)	1.486(0)
C(213)-C(214)	1.337(0)	C(13)-C(14)	1.512(0)
C(214)-C(215)	1.316(0)	C(14)-C(15)	1.452(0)
C(215)-C(216)	1.422(0)	C(15)-C(16)	1.576(0)
C(221)-C(222)	1.381(0)	O(2)-C(21)	1.219(0)
C(221)-C(226)	1.363(0)	C(21)-C(22)	1.499(0)
C(222)-C(223)	1.374(0)	C(21)-C(26)	1.486(0)
C(223)-C(224)	1.296(0)	C(22)-C(23)	1.439(0)
C(224)-C(225)	1.379(0)	C(23)-C(24)	1.285(0)
C(225)-C(226)	1.440(0)	C(24)-C(25)	1.499(0)
C(231)-C(232)	1.382(0)	C(25)-C(26)	1.639(0)
C(231)-C(236)	1.373(0)	C(31)-C(32)	1.518(0)

Table 11. Continued

Atom1-Atom2	Distance	Atom1-Atom2	Distance
C(232)-C(233)	1.422(0)	C(31)-C(36)	1.513(0)
C(233)-C(234)	1.319(0)	C(32)-C(33)	1.495(0)
C(234)-C(235)	1.387(0)	C(33)-C(34)	1.586(0)
C(235)-C(236)	1.321(0)	C(34)-C(35)	1.539(0)
C(241)-C(242)	1.368(0)	C(35)-C(36)	1.507(0)
C(241)-C(246)	1.348(0)	C(41)-C(42)	1.536(0)
C(242)-C(243)	1.388(0)	C(41)-C(46)	1.385(0)
C(243)-C(244)	1.340(0)	C(42)-C(43)	1.617(0)
C(244)-C(245)	1.418(0)	C(43)-C(44)	1.463(0)
C(245)-C(246)	1.357(0)	C(44)-C(45)	1.632(0)
O(1)-C(11)	1.222(0)	C(45)-C(46)	1.716(0)
C(11)-C(12)	1.444(0)		

Table 12. Bond angles (deg) for Cl₂Ni(PPh₂CH₂)₂CHCH(CH₂Ph₂P)₂NiCl₂, **11**

Atom1-Atom2-Atom3	Angle	Atom1-Atom2-Atom3	Angle
P(3)-Ni(1)-P(4)	96.(0)	Ni(1)-P(3)-C(211)	115.(0)
P(3)-Ni(1)-Cl(3)	176.(0)	Ni(1)-P(3)-C(221)	111.(0)
P(3)-Ni(1)-Cl(4)	84.(0)	C(6)-P(3)-C(211)	100.(0)
P(4)-Ni(1)-Cl(3)	86.(0)	C(6)-P(3)-C(221)	100.(0)
P(4)-Ni(1)-Cl(4)	169.(0)	C(211)-P(3)-C(221)	107.(0)
Cl(3)-Ni(1)-Cl(4)	92.(0)	Ni(1)-P(4)-C(5)	118.(0)
P(1)-Ni(2)-P(2)	94.(0)	Ni(1)-P(4)-C(231)	117.(0)
P(1)-Ni(2)-Cl(1)	176.(0)	Ni(1)-P(4)-C(241)	107.(0)
P(1)-Ni(2)-Cl(2)	84.(0)	C(5)-P(4)-C(231)	100.(0)
P(2)-Ni(2)-Cl(1)	88.(0)	C(5)-P(4)-C(241)	102.(0)
P(2)-Ni(2)-Cl(2)	170.(0)	C(231)-P(4)-C(241)	109.(0)
Cl(1)-Ni(2)-Cl(2)	92.(0)	C(2)-C(1)-C(3)	110.(0)
Ni(2)-P(1)-C(4)	117.(0)	C(2)-C(1)-C(4)	112.(0)
Ni(2)-P(1)-C(111)	110.(0)	C(3)-C(1)-C(4)	112.(0)
Ni(2)-P(1)-C(121)	116.(0)	C(1)-C(2)-C(5)	112.(0)
C(4)-P(1)-C(111)	103.(0)	C(1)-C(2)-C(6)	113.(0)
C(4)-P(1)-C(121)	99.(0)	C(5)-C(2)-C(6)	109.(0)
C(111)-P(1)-C(121)	109.(0)	P(2)-C(3)-C(1)	115.(0)

Numbers in parentheses are estimated standard deviations in the least significant digits.

Table 12. Continued

Atom1-Atom2-Atom3	Angle	Atom1-Atom2-Atom3	Angle
Ni(2)-P(2)-C(3)	117.(0)	P(1)-C(4)-C(1)	114.(0)
Ni(2)-P(2)-C(131)	106.(0)	P(4)-C(5)-C(2)	111.(0)
Ni(2)-P(2)-C(141)	119.(0)	P(3)-C(6)-C(2)	110.(0)
C(3)-P(2)-C(131)	105.(0)	P(1)-C(111)-C(112)	122.(0)
C(3)-P(2)-C(141)	97.(0)	P(1)-C(111)-C(116)	119.(0)
C(131)-P(2)-C(141)	107.(0)	C(112)-C(111)-C(116)	117.(0)
Ni(1)-P(3)-C(6)	118.(0)	C(111)-C(112)-C(113)	122.(0)
C(112)-C(113)-C(114)	118.(0)	C(143)-C(144)-C(145)	119.(0)
C(113)-C(114)-C(115)	119.(0)	C(144)-C(145)-C(146)	118.(0)
C(114)-C(115)-C(116)	121.(0)	C(141)-C(146)-C(145)	119.(0)
C(111)-C(116)-C(115)	121.(0)	P(3)-C(211)-C(212)	119.(0)
P(1)-C(121)-C(122)	116.(0)	P(3)-C(211)-C(216)	123.(0)
P(1)-C(121)-C(126)	123.(0)	C(212)-C(211)-C(216)	116.(0)
C(122)-C(121)-C(126)	119.(0)	C(211)-C(212)-C(213)	121.(0)
C(121)-C(122)-C(123)	120.(0)	C(212)-C(213)-C(214)	118.(0)
C(122)-C(123)-C(124)	117.(0)	C(213)-C(214)-C(215)	122.(0)
C(123)-C(124)-C(125)	121.(0)	C(214)-C(215)-C(216)	118.(0)
C(124)-C(125)-C(126)	121.(0)	C(211)-C(216)-C(215)	122.(0)
C(121)-C(126)-C(125)	119.(0)	P(3)-C(221)-C(222)	119.(0)

Table 12. Continued

Atom1-Atom2-Atom3	Angle	Atom1-Atom2-Atom3	Angle
P(2)-C(131)-C(132)	118.(0)	P(3)-C(221)-C(226)	120.(0)
P(2)-C(131)-C(136)	122.(0)	C(222)-C(221)-C(226)	120.(0)
C(132)-C(131)-C(136)	118.(0)	C(221)-C(222)-C(223)	123.(0)
C(131)-C(132)-C(133)	121.(0)	C(222)-C(223)-C(224)	115.(0)
C(132)-C(133)-C(134)	120.(0)	C(223)-C(224)-C(225)	126.(0)
C(133)-C(134)-C(135)	120.(0)	C(224)-C(225)-C(226)	117.(0)
C(134)-C(135)-C(136)	117.(0)	C(221)-C(226)-C(225)	116.(0)
C(131)-C(136)-C(135)	121.(0)	P(4)-C(231)-C(232)	121.(0)
P(2)-C(141)-C(142)	119.(0)	P(4)-C(231)-C(236)	119.(0)
P(2)-C(141)-C(146)	118.(0)	C(232)-C(231)-C(236)	119.(0)
C(142)-C(141)-C(146)	121.(0)	C(231)-C(232)-C(233)	120.(0)
C(141)-C(142)-C(143)	121.(0)	C(232)-C(233)-C(234)	118.(0)
C(142)-C(143)-C(144)	120.(0)	C(233)-C(234)-C(235)	120.(0)
C(234)-C(235)-C(236)	123.(0)	O(2)-C(21)-C(26)	120.(0)
C(231)-C(236)-C(235)	118.(0)	C(22)-C(21)-C(26)	115.(0)
P(4)-C(241)-C(242)	120.(0)	C(21)-C(22)-C(23)	115.(0)
P(4)-C(241)-C(246)	119.(0)	C(22)-C(23)-C(24)	116.(0)
C(242)-C(241)-C(246)	119.(0)	C(23)-C(24)-C(25)	113.(0)
C(241)-C(242)-C(243)	122.(0)	C(24)-C(25)-C(26)	109.(0)

Table 12. Continued

Atom1-Atom2-Atom3	Angle	Atom1-Atom2-Atom3	Angle
C(242)-C(243)-C(244)	118.(0)	C(21)-C(26)-C(25)	109.(0)
C(243)-C(244)-C(245)	120.(0)	C(32)-C(31)-C(36)	107.(0)
C(244)-C(245)-C(246)	119.(0)	C(31)-C(32)-C(33)	119.(0)
C(241)-C(246)-C(245)	120.(0)	C(32)-C(33)-C(34)	103.(0)
O(1)-C(11)-C(12)	128.(0)	C(33)-C(34)-C(35)	117.(0)
O(1)-C(11)-C(16)	114.(0)	C(34)-C(35)-C(36)	102.(0)
C(12)-C(11)-C(16)	115.(0)	C(31)-C(36)-C(35)	117.(0)
C(11)-C(12)-C(13)	111.(0)	C(42)-C(41)-C(46)	113.(0)
C(12)-C(13)-C(14)	108.(0)	C(41)-C(42)-C(43)	111.(0)
C(13)-C(14)-C(15)	107.(0)	C(42)-C(43)-C(44)	105.(0)
C(14)-C(15)-C(16)	113.(0)	C(43)-C(44)-C(45)	118.(0)
C(11)-C(16)-C(15)	104.(0)	C(44)-C(45)-C(46)	107.(0)
O(2)-C(21)-C(22)	123.(0)	C(41)-C(46)-C(45)	113.(0)

Table 13. General anisotropic displacement parameter expressions for 11

Name	U(1,1)	U(2,2)	U(3,3)	U(1,2)	U(1,3)	U(2,3)
Ni(1)	0.0298(9)	0.040(1)	0.050(1)	-0.0009(9)	-0.0047(9)	-0.002(1)
Ni(2)	0.0271(9)	0.040(1)	0.056(1)	0.0005(9)	-0.0068(9)	-0.000(1)
P(1)	0.029(2)	0.036(2)	0.043(2)	-0.001(2)	0.000(2)	0.001(2)
P(2)	0.023(2)	0.036(2)	0.054(2)	0.005(2)	-0.006(2)	0.004(2)
P(3)	0.038(2)	0.037(2)	0.044(2)	0.003(2)	-0.003(2)	0.002(2)
P(4)	0.025(2)	0.035(2)	0.050(2)	-0.001(2)	-0.001(2)	0.004(2)
Cl(1)	0.050(2)	0.053(3)	0.061(2)	0.012(2)	-0.000(2)	0.017(2)
Cl(2)	0.040(2)	0.053(3)	0.098(3)	-0.004(2)	-0.013(2)	-0.007(3)
Cl(3)	0.034(2)	0.095(4)	0.076(3)	-0.018(3)	0.001(2)	-0.007(3)
Cl(4)	0.054(2)	0.061(3)	0.054(2)	0.005(2)	-0.015(2)	-0.010(2)
C(1)	0.021(7)	0.032(8)	0.045(8)	-0.007(7)	0.005(6)	-0.004(7)
C(2)	0.030(7)	0.036(8)	0.037(8)	0.001(7)	-0.004(6)	0.003(7)
C(3)	0.018(7)	0.040(9)	0.050(8)	-0.002(7)	-0.007(6)	0.019(7)
C(4)	0.028(7)	0.034(8)	0.047(8)	0.007(7)	-0.011(7)	-0.011(7)
C(5)	0.026(7)	0.029(8)	0.051(9)	-0.009(7)	-0.007(7)	0.006(7)
C(6)	0.018(7)	0.034(8)	0.051(8)	-0.009(7)	-0.004(6)	0.014(7)
C(111)	0.038(8)	0.041(9)	0.049(9)	0.003(8)	-0.005(7)	0.008(8)

The form of the anisotropic displacement parameter is: $\exp[-2\pi^2\{h^2a^2U(1,1) + k^2b^2U(2,2) + l^2c^2U(3,3) + 2hkabU(1,2) + 2hlacU(1,3) + 2klbcU(2,3)\}]$ where a, b, and c are reciprocal lattice constants.

Table 13. Continued

Atom	U(1,1)	U(2,2)	U(3,3)	U(1,2)	U(1,3)	U(2,3)
C(112)	0.054(9)	0.06(1)	0.07(1)	0.006(9)	0.016(8)	0.010(9)
C(113)	0.12(1)	0.08(1)	0.046(9)	0.01(1)	0.023(9)	0.021(9)
C(114)	0.12(1)	0.10(2)	0.09(1)	0.03(1)	0.05(1)	0.01(1)
C(115)	0.10(1)	0.09(1)	0.10(1)	0.04(1)	0.05(1)	0.05(1)
C(116)	0.054(9)	0.06(1)	0.07(1)	-0.000(9)	0.028(7)	0.025(8)
C(121)	0.020(7)	0.06(1)	0.036(8)	0.004(7)	-0.004(6)	-0.007(8)
C(122)	0.06(1)	0.039(9)	0.050(9)	0.001(9)	-0.009(8)	-0.004(8)
C(123)	0.07(1)	0.11(1)	0.05(1)	0.03(1)	-0.002(9)	-0.02(1)
C(124)	0.08(1)	0.06(1)	0.08(1)	0.01(1)	-0.01(1)	-0.01(1)
C(125)	0.10(1)	0.03(1)	0.09(1)	-0.00(1)	0.02(1)	0.01(1)
C(126)	0.06(1)	0.04(1)	0.07(1)	-0.010(9)	0.014(8)	-0.001(9)
C(131)	0.038(8)	0.026(8)	0.055(9)	-0.001(7)	-0.002(7)	0.004(7)
C(132)	0.035(8)	0.05(1)	0.07(1)	0.012(8)	0.003(8)	0.009(9)
C(133)	0.034(8)	0.09(1)	0.07(1)	0.018(9)	0.020(7)	0.01(1)
C(134)	0.08(1)	0.05(1)	0.07(1)	0.00(1)	0.018(9)	-0.005(9)
C(135)	0.048(9)	0.06(1)	0.07(1)	0.003(9)	-0.000(8)	-0.016(9)
C(136)	0.042(9)	0.06(1)	0.06(1)	-0.001(9)	0.005(8)	-0.005(9)
C(141)	0.033(8)	0.06(1)	0.043(8)	0.009(8)	-0.017(7)	0.015(8)
C(142)	0.10(1)	0.06(1)	0.09(1)	0.01(1)	0.03(1)	0.04(1)
C(143)	0.18(2)	0.08(1)	0.10(1)	0.05(1)	0.04(1)	0.03(1)

Table 13. Continued

Atom	U(1,1)	U(2,2)	U(3,3)	U(1,2)	U(1,3)	U(2,3)
C(144)	0.11(2)	0.05(1)	0.15(2)	-0.02(1)	-0.03(1)	0.04(1)
C(145)	0.05(1)	0.19(2)	0.07(1)	0.01(1)	0.005(9)	0.07(1)
C(146)	0.06(1)	0.07(1)	0.06(1)	-0.00(1)	0.000(9)	0.043(9)
C(211)	0.024(7)	0.050(9)	0.035(8)	0.001(7)	-0.005(6)	0.002(7)
C(212)	0.038(9)	0.07(1)	0.06(1)	0.016(8)	-0.010(8)	-0.005(9)
C(213)	0.042(9)	0.05(1)	0.08(1)	0.008(9)	-0.010(9)	0.015(9)
C(214)	0.05(1)	0.05(1)	0.10(1)	0.007(9)	-0.02(1)	0.00(1)
C(215)	0.08(1)	0.12(2)	0.06(1)	0.01(1)	-0.00(1)	0.04(1)
C(216)	0.045(9)	0.07(1)	0.08(1)	0.000(9)	0.001(9)	0.00(1)
C(221)	0.050(9)	0.06(1)	0.050(9)	0.010(9)	0.002(8)	0.003(9)
C(222)	0.06(1)	0.08(1)	0.08(1)	0.01(1)	0.020(9)	0.02(1)
C(223)	0.12(2)	0.10(1)	0.11(2)	0.06(1)	-0.00(1)	-0.02(1)
C(224)	0.09(1)	0.18(2)	0.08(1)	0.09(1)	-0.01(1)	-0.02(1)
C(225)	0.13(1)	0.05(1)	0.08(1)	0.05(1)	-0.02(1)	-0.02(1)
C(226)	0.07(1)	0.05(1)	0.08(1)	0.02(1)	-0.02(1)	0.01(1)
C(231)	0.028(7)	0.040(9)	0.055(9)	-0.005(7)	-0.003(7)	0.004(8)
C(232)	0.038(8)	0.05(1)	0.07(1)	-0.000(8)	0.001(8)	0.010(9)
C(233)	0.022(7)	0.11(1)	0.07(1)	-0.005(9)	0.016(7)	-0.01(1)
C(234)	0.045(9)	0.09(1)	0.07(1)	0.02(1)	-0.003(8)	-0.03(1)
C(235)	0.07(1)	0.06(1)	0.09(1)	0.028(9)	-0.00(1)	0.00(1)

Table 13. Continued

Atom	U(1,1)	U(2,2)	U(3,3)	U(1,2)	U(1,3)	U(2,3)
C(236)	0.035(8)	0.04(1)	0.08(1)	0.001(8)	0.003(8)	-0.005(9)
C(241)	0.033(7)	0.038(9)	0.065(9)	0.003(7)	0.019(7)	0.015(8)
C(242)	0.039(9)	0.04(1)	0.11(1)	-0.002(8)	0.016(9)	0.034(9)
C(243)	0.08(1)	0.06(1)	0.16(2)	0.03(1)	0.02(1)	0.03(1)
C(244)	0.21(2)	0.05(1)	0.22(2)	0.08(1)	0.13(1)	0.05(1)
C(245)	0.24(3)	0.09(2)	0.10(2)	0.03(2)	0.06(2)	-0.02(1)
C(246)	0.16(2)	0.021(9)	0.07(1)	0.00(1)	0.02(1)	-0.002(9)

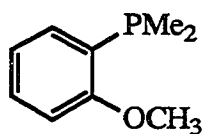
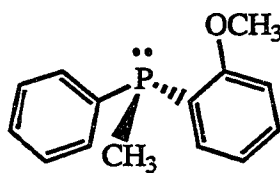
**SECTION III. BIDENTATE AND TRIDENTATE COORDINATION MODES
OF A NOVEL BICYCLIC DITERTIARY PHOSPHINE ETHER**

ABSTRACT

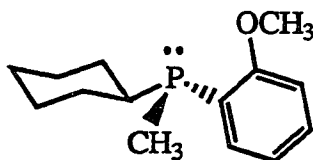
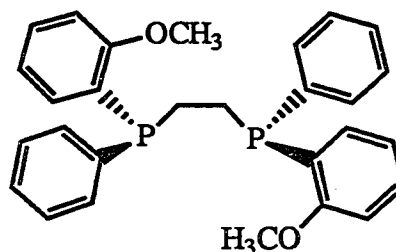
The synthesis and characterization of the new ligand *cis*-1,5-bis(diphenylphosphinomethyl)-3-oxabicyclo[3.3.0]octane (**6**) is reported. Oxidation of **6** with *t*-BuOOH or S₈ yields the phosphoryl and thiophosphoryl derivatives **10a** and **10b**, respectively. The complexes (6-*P,P'*)M(CO)₄ (M = Cr, Mo, W), (6-*P,P'*)PdCl₂, and two diastereomers of *fac*-(6-*P,P'*)Mn(CO)₃Br have been prepared in which **6** coordinates in a bidentate (*P,P'*) fashion. ¹H NMR spectra suggest a ligand conformational preference in these complexes. A tridentate (*P,P',O*) coordination mode has been established for (6-*P,P',O*)M(CO)₃ (M = Mo, W) and [(6-*P,P',O*)Mn(CO)₃]BF₄ on the basis of ¹H, ¹³C, ³¹P and IR spectroscopic data. Single-crystal X-ray diffraction studies on (6-*P,P'*)Mo(CO)₄ and (6-*P,P',O*)W(CO)₃ verify the bidentate and tridentate coordination modes of **6**, respectively. Crystals of (6-*P,P'*)Mo(CO)₄ are triclinic, space group $P\bar{1}$, with unit cell dimensions $a = 15.321(3)$ Å, $b = 22.371(3)$ Å, $c = 11.376(2)$ Å, $\alpha = 90.52(1)^\circ$, $\beta = 91.80(1)^\circ$, $\gamma = 72.07(1)^\circ$, and $Z = 4$. Crystals of (6-*P,P',O*)W(CO)₃ are monoclinic, space group $P2_1/c$ (#14), with unit cell dimensions $a = 12.262(5)$ Å, $b = 17.38(1)$ Å, $c = 16.285(7)$ Å, $\beta = 92.08(4)^\circ$, and $Z = 4$. The structures were refined to $R = 0.059$ and $R_w = 0.079$ for 6702 reflections with $I > 3.0\sigma(I)$ for (6-*P,P'*)Mo(CO)₄ and $R = 0.076$ and $R_w = 0.093$ for 4068 reflections with $I \geq 3.0\sigma(I)$ for (6-*P,P',O*)W(CO)₃.

INTRODUCTION

Because phosphines play an important role in homogeneous transition metal catalyzed reactions of both academic and industrial importance, the synthesis of new phosphine ligands continues to be an area of significant activity. Of particular relevance here are phosphines possessing potentially coordinating ether groups. *o*-Anisole-phosphines (and arsines)¹ were the first such ligands shown to coordinate transition metals via the phosphorus and oxygen atoms. Early on, the weak interactions of the ether oxygen of **1** with the metal centers of square planar rhodium and iridium complexes were shown to increase significantly the rates of oxidative

**1****2**

addition of methyl iodide.² Knowles³ studied the related ligands PAMP (**2**), CAMP (**3**), and DiPAMP (**4**) in the rhodium catalyzed asymmetric hydrogenation of

**3****4**

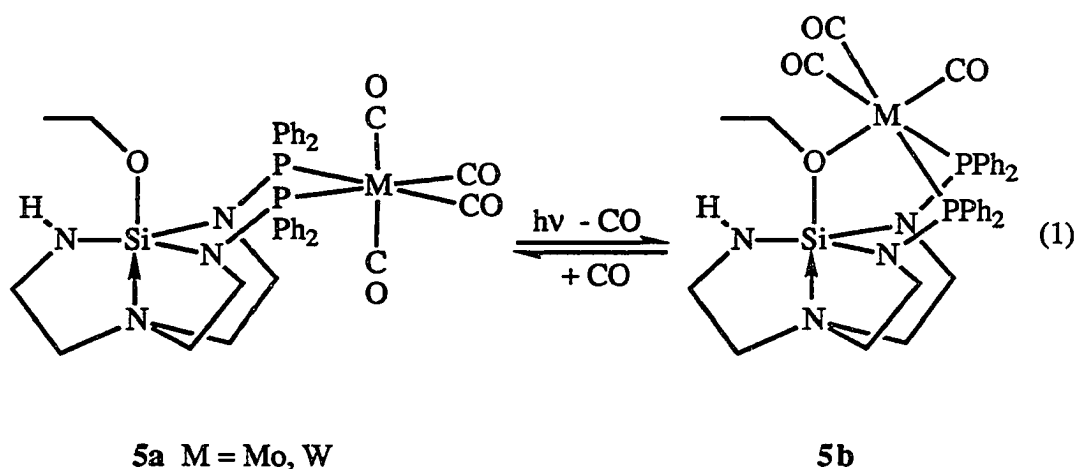
N-acylaminocinnamic acids as part of the L-DOPA synthesis in the 1970's. A weak interaction of the ether oxygen with Rh has been proposed to play an important role in similar reactions.⁴ Coordination of the ether oxygen has now been demonstrated in a variety of metal-ligand systems⁵ and such linkages have been substantiated by X-ray crystallography for $(o\text{-diphenylphosphinoanisole})_2\text{RuCl}_2$,⁶

$(\text{CH}_3\text{OCH}_2\text{CH}_2\text{PPh}_2)_2\text{RuCl}_2$,⁷ $(\text{CH}_3\text{OCH}_2\text{CH}_2\text{PPh}_2)_2\text{Ru}(\text{CO})\text{Cl}_2$,⁷

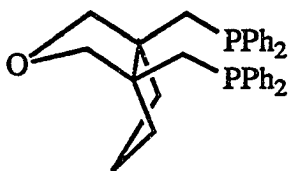
$[\text{Rh}(\text{TMPP})_2]\text{BF}_4$,⁸ $(\text{TMPP})\text{Mo}(\text{CO})_3$,⁹ $\text{Rh}_2(\text{O}_2\text{CCH}_3)_3(\text{TMPP})(\text{MeOH})$,¹⁰ (TMPP = 2,4,6-trimethoxyphenylphosphine) and $[\{(\text{Ph}_2\text{PCH}_2\text{CH}_2)_2\text{O}\}\text{Rh}(\text{CO})]\text{PF}_6$.¹¹

The oxygen ligands in such complexes are sufficiently labile to be displaced by molecules such as phosphines, phosphites,^{5g} nitriles,^{5c,7,9} dialkyl sulfides^{5c} and CO.^{5b,c,g,7} This property renders ether functional groups in phosphines well suited to stabilizing reactive catalytic intermediates having accessible coordination sites. Recently, Lindner¹² utilized a variety of phosphine ethers in rhodium and cobalt-catalyzed methanol carbonylations.

Recently we reported¹³ reversible silyl-ether coordination in Group VI metal



carbonyl complexes of *N,N'*-bis(diphenylphosphino)azasilatrane, **5a**, **5b** (reaction 1). Stimulated by this observation, we synthesized the new chelating ligand *cis*-1,5-bis(diphenylphosphinomethyl)-3-oxabicyclo[3.3.0]octane (**6**) which exhibits much



6

improved stability in solution in comparison to our *N,N'*-bis(diphenylphosphino)-azasilatrane system. Unlike the vast majority of previously reported phosphine ethers, **6** is a bisphosphine capable of adopting only a *fac* geometry when coordinated to an octahedral metal in a tridentate fashion. Furthermore, **6** forms six-membered chelate rings upon ether coordination in contrast to the previously reported ether phosphines, including our azasilatrane system, which coordinate their ether functional groups with the formation of five-membered chelate rings.^{1-12,29} The presence and ring size of chelating ligands, as well as the geometry they impose around a metal center, are important factors in determining the chemistry of metal complexes. Here we report the synthesis of **6** and its ability to coordinate in either a bi- or tridentate mode in octahedral transition metal carbonyl complexes.

EXPERIMENTAL SECTION

General Procedures

All reactions were performed under an inert atmosphere of argon or nitrogen using standard inert atmosphere techniques. Toluene, pentane, tetrahydrofuran and diethyl ether were distilled from sodium benzophenone ketyl prior to use. Methylene chloride was distilled from calcium hydride and stored over 4Å molecular sieves. Ph_2PH ,¹⁴ $\text{Mn}(\text{CO})_5\text{Br}$,¹⁵ $(\eta^6\text{-cycloheptatriene})\text{Mo}(\text{CO})_3$,¹⁶ $(\eta^6\text{-cycloheptatriene})\text{W}(\text{CO})_3$,¹⁷ $(\text{piperidine})_2\text{Mo}(\text{CO})_4$,¹⁸ $(\text{COD})\text{W}(\text{CO})_4$,¹⁹ $(\text{NBD})\text{Cr}(\text{CO})_4$,²⁰ $(\text{PhCN})_2\text{PdCl}_2$ ²¹ and 1,1,2,2-tetrakis(hydroxymethyl)cyclopentane²² were synthesized as described in the literature. $(\eta^6\text{-cycloheptatriene})\text{Cr}(\text{CO})_3$ was purchased from Aldrich and used without further purification. Solution NMR spectra were recorded on Nicolet NT 300 (^1H), Bruker WM 200 (^{31}P), Varian VXR 300 (^1H , ^{13}C , ^{31}P) or Varian Unity 500 (^1H , $^1\text{H}\{^{31}\text{P}\}$) spectrometers using a deuterated solvent as the internal lock. Chemical shifts are reported relative to TMS (^1H , ^{13}C) or 85% H_3PO_4 (^{31}P). Mass spectra were recorded on Kratos MS-50 (EI, HRMS) or Finnigan 4000 (EI, CI) instruments. The masses of metal-containing fragments are reported for the most abundant isotope present, viz. ^{98}Mo and ^{184}W , unless otherwise noted. IR spectra were recorded using an IBM 98 FT-IR spectrometer. Microanalyses were carried out by Schwarzkopf Microanalytical Laboratories, Woodside, NY.

Preparation of *cis*-1,5-di-methanesulfonyloxymethyl-3-oxabicyclo-[3.3.0]octane (9a)

Trimethylorthoacetate (4.35 mL, 34.1 mmol), 1,1,2,2-tetrakis(hydroxymethyl)cyclopentane (5.02 g, 26.4 mmol), and 2 mL of methanol were added to 30 mL of CHCl_3 . A few crystals of *p*-toluenesulfonic acid were added as a

catalyst and the reaction mixture was stirred for 30 minutes to give a clear solution. K_2CO_3 (0.500 g) was added and the mixture was stirred overnight. This mixture was filtered and the volatiles removed *in vacuo* to leave a thick residue. This residue was dissolved twice in 5 mL of methanol which was subsequently removed *in vacuo*. A 1H NMR spectrum identified the residue so obtained as *cis*-1,5-di-hydroxymethyl-3-oxabicyclo[3.3.0]octane (**8b**). This was used in the next step of this synthesis without further purification. 1H NMR ($CDCl_3$) δ 4.19 (br s, 2H, OH), 3.87 (d, 2H, $^2J_{HH} = 9.0$ Hz, OCH_2), 3.53 (d, 2H, $^2J_{HH} = 9.0$ Hz, OCH_2), 3.63 (s, 4H, CH_2OH), 1.7-1.5 (m, 6H, CH_2).

Crude **8b** in 30 mL of pyridine was added dropwise to a cooled ($0\text{ }^\circ\text{C}$) solution of methanesulfonylchloride (6.5 mL, 79 mmol) in 50 mL of pyridine. After the addition was complete, the solution was stirred for one hour at $0\text{ }^\circ\text{C}$ and 4 h at room temperature. The solution was then poured onto a slurry of 600 g ice/150 mL H_2O /75 mL HCl with stirring. After 30 minutes the pale white solid was isolated by filtration, washed with water, and dried *in vacuo*. Recrystallization from EtOH/ CH_3CN (3:1) yielded 5.4 g (62% yield, mp $105\text{ }^\circ\text{C}$) of **9a**. MS (EI) *m/e* (relative intensity) 327 (M^+ , 0.3), 136 (100), 123 (9.1), 106 (48), 93 (61), 79 (57); HRMS (EI) calcd for $C_{11}H_{19}O_7S_2$ (M^+) 327.05722, found 327.05640; ^{13}C NMR ($CDCl_3$) δ 77.8 (CH_2O), 71.2 ($CH_2OSO_2CH_3$), 56.0 (s, C), 37.4 (OSO_2CH_3), 36.2 ($CH_2CH_2CH_2$), 23.4 ($CH_2CH_2CH_2$); 1H NMR ($CDCl_3$) δ 4.25 (s, 4H, $CH_2OSO_2CH_3$), 3.88 (d, 2H, $^2J_{HH} = 9.6$ Hz, OCH_2), 3.61 (d, 2H, $^2J_{HH} = 9.6$ Hz, OCH_2), 3.06 (s, 6H, OSO_2CH_3), 1.9-1.6 (m, 6H, CH_2).

Preparation of *cis*-1,5-bis(diphenylphosphinomethyl)-3-oxabicyclo-[3.3.0]octane (6)

A deep red solution of lithium diphenylphosphide was generated by the addition of *n*-BuLi (6.5 mL, 13 mmol) to a solution of diphenylphosphine (2.25 mL, 12.9 mmol) in 125 mL of THF. This was cooled to 0 °C and treated dropwise with a solution of **9a** (2.11 g, 6.42 mmol) in 45 mL of THF. After the addition was complete, the resulting mixture was stirred for 2 h at room temperature followed by refluxing overnight. After cooling to room temperature, excess phosphide was quenched with the addition of 1 mL of a saturated NH₄Cl(aq) solution. The mixture was filtered and the solvent was removed from the filtrate in vacuo to leave a thick residue. This residue was chromatographed on silica gel with 10% ethyl acetate in toluene to yield a thick oil which readily crystallized at room temperature. These crystals were rinsed with *n*-pentane and dried *in vacuo*. Yield 2.48 g (76%, mp 110-111 °C). MS (EI) *m/e* (relative intensity) 508 (M⁺, 3.6), 431 (100), 323 (23), 183 (31), 108 (19); HRMS (EI) calcd for C₃₃H₃₄OP₂ (M⁺) 508.20849, found 508.20833; IR (KBr) ν (COC) = 1082 cm⁻¹; ³¹P NMR (toluene) δ -19.8 (s); ¹³C NMR (CDCl₃) δ 139.5 (d, ¹J_{PC} = 13.1 Hz, Ph-*ipso*), 139.4 (d, ¹J_{PC} = 13.1 Hz, Ph-*ipso*), 133.1 (d, ²J_{PC} = 19.6 Hz, Ph-*ortho*), 133.0 (d, ²J_{PC} = 19.7 Hz, Ph-*ortho*), 128.7 (s, Ph-*para*), 128.5 (d, ³J_{PC} = 7.1 Hz, Ph-*meta*), 81.6 (d, ³J_{PC} = 12.6 Hz, CH₂O), 56.0 (dd, ²J_{PC} = 6.0 Hz, ³J_{PC} = 12.1 Hz, CC₄), 40.8 (d, ³J_{PC} = 10.6 Hz, CH₂CH₂CH₂), 36.7 (d, ¹J_{PC} = 16.6 Hz, CH₂PPh₂), 24.3 (s, CH₂CH₂CH₂); ¹H NMR (CDCl₃) δ 7.50 - 7.38 (m, Ph), 7.31 (m, Ph), 3.66 (d, ²J_{HH} = 9.2 Hz, CH₂O), 3.48 (d, ²J_{HH} = 9.2 Hz, CH₂O), 2.34 (dd, ²J_{HH} = 13.6 Hz, ²J_{PH} = 2.9 Hz, CH₂PPh₂), 2.28 (dd, ²J_{HH} = 13.6 Hz, ²J_{PH} = 3.0 Hz, CH₂PPh₂), 1.77 (m, CH₂), 1.6 - 1.4 (m, CH₂); Anal. Calcd for C₃₃H₃₄OP₂: C, 77.94; H, 6.74; P, 12.18. Found: C, 77.90; H, 6.74; P, 12.08.

Preparation of *cis*-1,5-bis(diphenylphosphorylmethyl)-3-oxabicyclo-[3.3.0]octane (10a)

A solution of **6** (0.402 g, 0.791 mmol) in 15 mL of toluene was treated with a solution of *t*-BuOOH in toluene (3.6 M, 0.50 mL) at 0 °C. After stirring at room temperature for two hours, the volume of the solution was reduced to 5 mL *in vacuo*. Addition of 5 mL of MeOH followed by the slow addition of 15 mL of hexane yielded the product as a white solid. The product was isolated by filtration, rinsed with 10 mL of pentane and dried *in vacuo*. Recrystallization from hot MeOH (15 mL) yielded 0.38 g (89%, mp 210 °C) of clear colorless crystals. MS (EI) *m/e* (relative intensity) 540 (M^+ , 15), 339 (87), 201 (100); HRMS (EI) calcd for $C_{33}H_{34}O_3P_2$ (M^+) 540.19832, found 540.19883; IR(KBr) 1177 cm^{-1} (P=O); ^{31}P NMR ($CHCl_3$) δ 29.6 (s); ^{13}C NMR ($CDCl_3$) δ 134.5 (d, $^1J_{PC} = 98.2$ Hz, Ph-*ipso*), 134.2 (d, $^1J_{PC} = 97.7$ Hz, Ph-*ipso*), 131.8 (d, $^4J_{PC} = 3.0$ Hz, Ph-*para*), 131.7 (d, $^4J_{PC} = 3.0$ Hz, Ph-*para*), 130.8 (d, $^2J_{PC} = 9.6$ Hz, Ph-*ortho*), 130.6 (d, $^2J_{PC} = 9.1$ Hz, Ph-*ortho*), 128.8 (d, $^3J_{PC} = 11.6$ Hz, Ph-*meta*), 128.7 (d, $^3J_{PC} = 12.1$ Hz, Ph-*meta*), 80.7 (d, $^3J_{PC} = 4.0$ Hz, CH_2O), 55.5 (dd, $^2J_{PC} = 10.1$ Hz, $^3J_{PC} = 4.5$ Hz, CC_4), 39.4 (d, $^3J_{PC} = 3.0$ Hz, $CH_2CH_2CH_2$), 36.8 (d, $^1J_{PC} = 70$ Hz, $CH_2P(O)Ph_2$), 24.7 (s, $CH_2CH_2CH_2$); 1H NMR ($CDCl_3$) δ 7.79 (m, Ph), 7.49 (m, Ph), 3.69 (d, $^2J_{HH} = 9.9$ Hz, CH_2O), 3.60 (d, $^2J_{HH} = 9.9$ Hz, CH_2O), 2.60 (dd, $^2J_{HH} = 15.0$ Hz, $^2J_{PH} = 10.5$ Hz, $CH_2P(O)Ph_2$), 2.49 (dd, $^2J_{HH} = 15.0$ Hz, $^2J_{PH} = 12.5$ Hz, $CH_2P(O)Ph_2$), 1.84 (m, CH_2), 1.7-1.5 (m, CH_2); Anal. Calcd for $C_{33}H_{34}O_3P_2 \cdot 2CH_3OH$: C, 69.52; H, 7.00; P, 10.24. Found: C, 69.74; H, 7.15; P, 10.18.

Preparation of *cis*-1,5-bis(diphenylthiophosphorylmethyl)-3-oxabicyclo-[3.3.0]octane (10b)

A solution of **6** (0.400 g, 0.786 mmol) in 15 mL of toluene was stirred with Sg (0.0582 g, 0.227 mmol) for 4 h at room temperature. The resulting white precipitate was isolated by filtration, rinsed with 10 mL of hexane and dried *in vacuo*.

Recrystallization from CH₂Cl₂/ethanol yielded 0.29 g (64%, mp > 250 °C) of fine white needles. MS (EI) *m/e* (relative intensity) 572 (M⁺, 17), 539 (80), 507 (43), 431 (32), 355 (57), 323 (45), 217 (100), 185 (52), 139 (50), 108 (57); HRMS (EI) calcd for C₃₃H₃₄OP₂S₂ (M⁺) 572.15264, found 572.15105; ³¹P NMR (CD₂Cl₂) δ 38.3 (s); ¹³C NMR (CD₂Cl₂) δ 134.9 (d, ¹J_{PC} = 80.1 Hz, Ph-*ipso*), 134.1 (d, ¹J_{PC} = 79.0 Hz, Ph-*ipso*), 131.7 (s, Ph-*para*), 131.7 (d, ²J_{PC} = 12.1 Hz, Ph-*ortho*), 131.3 (d, ²J_{PC} = 10.1 Hz, Ph-*ortho*), 129.0 (d, ³J_{PC} = 12.1 Hz, Ph-*meta*), 128.9 (d, ³J_{PC} = 11.6 Hz, Ph-*meta*), 80.5 (d, ³J_{PC} = 4.0 Hz, CH₂O), 56.8 (dd, ³J_{PC} = 4.0 Hz, ²J_{PC} = 10.1 Hz, CC₄), 39.6 (d, ¹J_{PC} = 55.4 Hz, CH₂P(S)Ph₂), 39.2 (d, ³J_{PC} = 3.5 Hz, CH₂CH₂CH₂), 25.2 (s, CH₂CH₂CH₂); ¹H NMR (CD₂Cl₂) δ 8.02 - 7.86 (m, Ph), 7.51 (m, Ph), 3.80 (d, ²J_{HH} = 9.9 Hz, CH₂O), 3.68 (d, ²J_{HH} = 9.9 Hz, CH₂O), 3.07 (dd, ²J_{HH} = 14.1 Hz, ²J_{PH} = 12.0 Hz, CH₂P(S)Ph₂), 2.78 (dd, ²J_{HH} = 14.1 Hz, ²J_{PH} = 13.0 Hz, CH₂P(S)Ph₂), 1.65-1.40 (m, CH₂).

Preparation of *cis*-(*cis*-1,5-bis(diphenylphosphinomethyl)-3-oxabicyclo-[3.3.0]octane-*P,P'*)dichloropalladium (11)

A solution of **6** (0.403 g, 0.792 mmol) in 10 mL of toluene was slowly added to a solution of (PhCN)₂PdCl₂ (0.303 g, 0.790 mmol) in 20 mL of toluene and the resulting mixture was stirred overnight. The creamy white solid was isolated by filtration, washed with 5 mL of toluene then 10 mL of hexane, and was then dried *in vacuo*. Yield 0.53 g

(98%). ^{31}P NMR (d_6 -DMSO) δ 22.8 (s); ^{13}C NMR (d_6 -DMSO) δ 134.9 (at,²³ separation 9.5 Hz, Ph-*ortho*), 133.6 (at, separation 8.5 Hz, Ph-*ortho*), 131.0 (s, Ph-*para*), 128.0 (m, Ph-*meta*), 127.9 (m, Ph-*meta*), 80.7 (m, CH₂O), 53.7 (s, CC₄), 34.7 (at, separation 29.7 Hz, CH₂PPh₂), 23.6 (s, CH₂CH₂CH₂); ^1H NMR (d_6 -DMSO) δ 8.07 (m, 4H, Ph-*ortho*), 7.95 (m, 4H, Ph-*ortho*), 7.53 (m, Ph-*meta*, *para*), 3.34 (m, CH₂O), 3.18 (m, CH₂PPh₂), 1.40 - 0.90 (m, 6H, CH₂).

Preparation of *cis*-(*cis*-1,5-bis(diphenylphosphinomethyl)-3-oxabicyclo-[3.3.0]octane-*P,P'*)tetracarbonylchromium (12)

A solution of (norbornadiene)tetracarbonylchromium (0.229 g, 0.894 mmol) and **6** (0.455 g, 0.895 mmol) in 20 mL of toluene was refluxed for 3 hours during which time the deep yellow color of the solution almost dissipated. The solvent was removed *in vacuo* and the residue was chromatographed on silica gel with CH₂Cl₂. Solvent was removed from the product-containing fractions *in vacuo* to yield a light yellow solid. Yield 0.49 g (82%). MS (desorption CI, NH₃) *m/e* (relative intensity) 690 (M + NH₄⁺, 12), 673 (MH⁺, 31), 645 (MH⁺ - CO, 6.5), 578 (6.4), 560 (7.1), 541 (6.0), 509 (100), 431 (11), 323 (6.3); MS (EI) *m/e* (relative intensity) 588 (M⁺ - 3 CO, 0.3), 560 (M⁺ - 4 CO, 7.3), 508 (16), 431 (100), 323 (44); HRMS (EI) calcd for C₃₄H₃₄CrO₂P₂ (M⁺ - 3 CO) 588.14406, found 588.14470, calcd for C₃₃H₃₄CrOP₂ (M⁺ - 4 CO) 560.14915, found 560.15028; ^{31}P NMR (toluene) δ 44.2 (s); ^{13}C NMR (CD₂Cl₂) δ 227.2 (at, separation 20.4 Hz, CO_{eq}) 223.8 (t, $^2J_{\text{PC}} = 13.9$ Hz, CO_{ax}) 217.5 (t, $^2J_{\text{PC}} = 12.1$ Hz, CO_{ax}), 142.4 (m, separation 37.3 Hz, Ph-*ipso*), 138.7 (m, separation 37.3 Hz, Ph-*ipso*), 133.7 (at, separation 10.8 Hz, Ph-*ortho*), 130.9 (at, separation 8.8 Hz, Ph-*ortho*), 130.2 (s, Ph-*para*), 129.1 (s, Ph-*para*), 128.9 (at, separation 8.8 Hz, Ph-*meta*), 128.7 (at, separation 8.4 Hz, Ph-*meta*), 86.2 (at, separation 12.7 Hz, CH₂O), 53.7 (s,

CC₄), 42.4 (at, separation 8 Hz, CH₂CH₂CH₂), 38.4 (at, separation 12.8 Hz, CH₂PPh₂), 24.7 (s, CH₂CH₂CH₂); ¹H NMR (CD₂Cl₂) δ 7.86 (m, Ph), 7.50-7.30 (m, Ph), 3.62 (dd, ²J_{HH} = 9.0 Hz, ⁴J_{HH} = 1.2 Hz, CH₂O), 3.57 (d, ²J_{HH} = 9.0 Hz, CH₂O), 3.02 (dd, ²J_{HH} = 15.6 Hz, ²J_{PH} = 10.5 Hz, CH₂PPh₂), 2.98 (dd, ²J_{HH} = 15.6 Hz, ²J_{PH} = 2.0 Hz, CH₂PPh₂), 1.77 (m, 2H, H_B), 1.51 (m, 1H, H_C), 1.42 (m, 1H, H_D), 1.13 (dd, ²J_{AB} = 12.6 Hz, ³J_{AC} = 5.2 Hz, 2H, H_A); Anal. Calcd for C₃₇H₃₄CrO₅P₂: C, 66.07; H, 5.10; P, 9.21; Found: C, 66.37; H, 5.19; P, 9.13.

Preparation of *cis*-(*cis*-1,5-bis(diphenylphosphinomethyl)-3-oxabicyclo-[3.3.0]octane-*P,P'*)tetracarbonylmolybdenum (13)

Bis(piperidine)tetracarbonylmolybdenum (0.374 g, 0.983 mmol) and **6** (0.506 g, 0.983 mmol) were refluxed in 25 mL of CH₂Cl₂ for 30 minutes. The reaction mixture was cooled to room temperature and the volatiles were removed *in vacuo*. The resulting white solid was purified by elution on a silica gel column with CH₂Cl₂. The solvent was removed from the product-containing fractions to yield a pure white solid (mp 185 °C, dec). MS (desorption CI, NH₃) *m/e* (relative intensity) 719 (MH⁺, 64), 691 (MH⁺ - CO, 64), 509 (29), 262 (31), 187 (100); MS (EI) 690 (M⁺ - CO, 0.4), 662 (M⁺ - 2 CO, 0.6), 634 (M⁺ - 3 CO, 1.0), 606 (M⁺ - 4 CO, 5.9), 508 (5.1), 431 (100), 323 (29), 183 (52), 108 (41); HRMS (EI) calcd for C₃₆H₃₄⁹²MoO₄P₂ (M⁺ - CO) 684.09953, found 684.09961; ³¹P NMR (CD₂Cl₂) δ 22.0 (s); ¹³C NMR (CD₂Cl₂) δ 215.9 (m, separation 15.1 Hz, CO_{eq}), 212.2 (t, ²J_{PC} = 9.5 Hz, CO_{ax}), 206.0 (t, ²J_{PC} = 7.5 Hz, CO_{ax}), 142.3 (m, separation 35.7 Hz, Ph-*ipso*), 138.4 (m, separation 35.3 Hz, Ph-*ipso*), 134.0 (at, separation 12.3 Hz, Ph-*ortho*), 130.9 (at, separation 10.3 Hz, Ph-*ortho*), 130.3 (s, Ph-*para*), 129.1 (s, Ph-*para*), 128.9 (at, separation 9.1 Hz, Ph-*meta*), 128.7 (at, separation 8.3 Hz, Ph-*meta*), 86.3 (at, separation 12.3 Hz, CH₂O), 53.5 (br s, CC₄),

42.8 (br s, CH₂CH₂CH₂), 37.1 (at, separation 14.7 Hz, CH₂PPh₂), 24.9 (s, CH₂CH₂CH₂); ¹H NMR (CD₂Cl₂) δ 7.84 (m, Ph), 7.50-7.30 (m, Ph), 3.60 (dd, ²J_{HH} = 9.0 Hz, ⁴J_{HH} = 2.0 Hz, CH₂O), 3.57 (d, ²J_{HH} = 9.0 Hz, CH₂O), 2.99 (d, ²J_{PH} = 5.7 Hz, CH₂PPh₂), 1.81 (m, 2H, H_B), 1.52 (m, 1H, H_C), 1.41 (m, 1H, H_D), 1.12 (dd, ²J_{AB} = 12.3 Hz, ³J_{AC} = 5.4 Hz, 2H, H_A).

Preparation of *cis*-(*cis*-1,5-bis(diphenylphosphinomethyl)-3-oxabicyclo-[3.3.0]octane-*P,P'*)tetracarbonyltungsten (14)

A solution of (cyclooctadiene)tetracarbonyltungsten (0.374 g, 0.926 mmol) and **6** (0.466 g, 0.916 mmol) in 25 mL of THF was refluxed for 30 minutes. The solvent was removed *in vacuo* and the residue was chromatographed on silica gel with CH₂Cl₂. Solvent was removed from the product-containing fractions to yield a creamy white solid. Yield 0.70 g (95%). MS (desorption CI, NH₃) *m/e* (relative intensity) 806 (MH⁺, 100), 778 (MH⁺ - CO, 8.5), 541 (6.5), 525 (6.9), 509 (12), 317 (26), 263 (19); MS (EI) 804 (M⁺, 2.4), 776 (M⁺ - CO, 13), 748 (M⁺ - 2 CO, 3.0), 720 (M⁺ - 3 CO, 9.4), 692 (M⁺ - 4 CO, 6.6), 508 (6.7), 431 (100), 323 (23); HRMS (EI) calcd for C₃₇H₃₄O₅P₂¹⁸⁴W (M⁺) 804.13911, found 804.13910, calcd for C₃₆H₃₄O₄P₂¹⁸⁴W (M⁺ - CO) 776.14433, found 776.14622; ³¹P NMR (THF) δ 4.5 (s), ¹J_{PW} = 232 Hz; ¹³C NMR (CD₂Cl₂) δ 206.4 (m, separation 16.2 Hz, CO_{eq}), 204.9 (t, ²J_{PC} = 7.1 Hz, CO_{ax}), 198.9 (t, ²J_{PC} = 5.4 Hz, CO_{ax}), 142.1 (m, separation 42.8 Hz, Ph-*ipso*), 138.0 (m, separation 41.3 Hz, Ph-*ipso*), 134.2 (at, separation 12.0 Hz, Ph-*ortho*), 130.9 (at, separation 9.4 Hz, Ph-*ortho*), 130.5 (s, Ph-*para*), 129.3 (s, Ph-*para*), 129.0 (at, separation 10.0 Hz, Ph-*meta*), 128.7 (at, separation 8.4 Hz, Ph-*meta*), 86.3 (at, separation 12.8 Hz, CH₂O), 53.4 (s, CC₄), 42.7 (at, separation 8.0 Hz, CH₂CH₂CH₂), 37.4 (m, separation 18.6 Hz, CH₂PPh₂), 24.9 (s, CH₂CH₂CH₂); ¹H NMR (CD₂Cl₂) δ

7.81 (m, Ph), 7.50-7.30 (m, Ph), 3.60 (dd, $^2J_{\text{HH}} = 9.0$ Hz, $^4J_{\text{HH}} = 1.5$ Hz, CH_2O), 3.57 (d, $^2J_{\text{HH}} = 9.0$ Hz, CH_2O), 3.16 (dd, $^2J_{\text{HH}} = 15.6$ Hz, $^2J_{\text{PH}} = 11.5$ Hz, CH_2PPh_2), 3.06 (dd, $^2J_{\text{HH}} = 15.6$ Hz, $^2J_{\text{PH}} = 2.5$ Hz, CH_2PPh_2), 1.80 (m, 2H, H_B), 1.52 (m, 1H, H_C), 1.43 (m, 1H, H_D), 1.13 (dd, $^2J_{\text{AB}} = 12.6$ Hz, $^3J_{\text{AC}} = 5.3$ Hz, 2H, H_A).

Reaction of **6** with $(\eta^6\text{-cycloheptatriene})\text{Cr}(\text{CO})_3$

A solution of **6** (0.406 g, 0.798 mmol) in 5 mL of toluene was added to a deep red solution of $(\eta^6\text{-cycloheptatriene})\text{tricarboxylchromium}$ (0.185 g, 0.811 mmol) in 20 mL of toluene. After heating at 70 °C for 12 hours no reaction had occurred as indicated by ^{31}P NMR spectroscopy. The solution was then refluxed for 8 hours during which time ^{31}P nmr spectra indicated the presence of a small quantity of **12** (δ 44.2) and unreacted **6**. Similarly, refluxing the two starting materials in xylene for 12 hours led only to an increase in the quantity of **12** produced. There was no evidence for the formation of a chromium tricarbonyl complex of **6**.

Preparation of *fac*-(*cis*-1,5-bis(diphenylphosphinomethyl)-3-oxabicyclo-[3.3.0]octane-*P,P',O*)tricarbonylmolybdenum (**15**)

A solution of **6** (0.410 g, 0.806 mmol) in 5 mL of toluene was added to a red solution of $(\eta^6\text{-cycloheptatriene})\text{tricarbonylmolybdenum}$ (0.222 g, 0.815 mmol) in 20 mL of toluene. Stirring at 50 °C for 1 h yielded a yellow precipitate which was isolated by filtration, washed with 5 mL of toluene and dried *in vacuo*. Yield 0.43 g (78%). MS (desorption CI, NH_3) *m/e* (relative intensity) 691 (MH^+ , 7.5), 509 (29), 323 (37), 263 (75), 247 (92), 202 (47), 187 (100); MS (EI) *m/e* (relative intensity) 690 (M^+ , 0.2), 662 ($\text{M}^+ - \text{CO}$, 0.3), 634 ($\text{M}^+ - 2 \text{CO}$, 0.7), 606 ($\text{M}^+ - 3 \text{CO}$, 4.6), 508 (8.1), 431 (100), 323

(41), 183 (54), 108 (39); HRMS (EI) calcd for $C_{36}H_{34}^{92}MoO_4P_2$ (M^+) 684.09954, found 684.10099; ^{31}P NMR (CD_2Cl_2) δ 12.9 (s); ^{13}C NMR (CD_2Cl_2) δ 229.0 (t, $^2J_{PC}$ = 6.7 Hz, CO_{ax}), 219.9 (m, separation 47 Hz, CO_{eq}), 140.9 (m, separation 34 Hz, Ph-*ipso*), 137.0 (m, separation 35 Hz, Ph-*ipso*), 132.1 (m, separation 12.3 Hz, Ph-*ortho*), 131.5 (m, separation 12.7 Hz, Ph-*ortho*), 129.4 (s, Ph-*para*), 129.3 (s, Ph-*para*), 128.9 (m, separation 9.1 Hz, Ph-*meta*), 128.6 (m, separation 9.1 Hz, Ph-*meta*), 85.4 (m, separation 15.5 Hz, CH_2O), 55.9 (m, separation 6.4 Hz, CC_4), 41.7 (m, separation 8.7 Hz, $CH_2CH_2CH_2$), 36.9 (m, separation 12.7 Hz, CH_2PPh_2), 22.5 (s, $CH_2CH_2CH_2$); 1H NMR (CD_2Cl_2) δ 7.72 (m, Ph), 7.40-7.30 (m, Ph), 6.97 (m, Ph), 4.09 (d, $^2J_{HH}$ = 10.5 Hz, CH_2O), 3.32 (dd, $^2J_{HH}$ = 16.0 Hz, $^2J_{PH}$ = 9.5 Hz, CH_2PPh_2), 3.29 (br d, $^2J_{HH}$ = 10.5 Hz, CH_2O), 2.88 (br dd, $^2J_{HH}$ = 16.0 Hz, $^4J_{HH}$ = 1.3 Hz, CH_2PPh_2), 1.90 (dd, $^2J_{AB}$ = 13.2 Hz, $^3J_{BD}$ = 5.1 Hz, 2H, H_B), 1.71 (dt, $^2J_{CD}$ = 12.2 Hz, $^3J_{AC}$ = 6.3 Hz, 1H, H_C), 1.59 (m, 2H, H_A), 1.48 (m, 1H, H_D).

Preparation of *fac*-(*cis*-1,5-bis(diphenylphosphinomethyl)-3-oxabicyclo-[3.3.0]octane-*P,P',O*)tricarbonyltungsten (16)

A solution of 6 (0.413 g, 0.812 mmol) in 5 mL of toluene was added to a solution of (η^6 -cycloheptatriene)tricarbonyltungsten (0.294 g, 0.818 mmol) in 15 mL of toluene. The solution was stirred at room temperature for 2 h and at 60 °C for 6 h to yield a bright yellow precipitate. This was isolated by filtration, washed twice with 10 mL of toluene and dried *in vacuo*. Recrystallization could be achieved from CH_2Cl_2 at -78 °C. Yield 0.40 g (64%). MS (desorption CI, NH_3) *m/e* (relative intensity) 805 ($MH + NH_4^+$, 11), 777 (MH^+ , 100), 509 (44); MS (EI) 776 (M^+ , 1.1), 748 ($M^+ - CO$, 0.5), 720 ($M^+ - 2 CO$, 2.2), 692 ($M^+ - 3 CO$, 1.6), 431 (26), 221 (59), 108 (100); ^{31}P NMR (CD_2Cl_2) δ 8.4 (s), $^1J_{PW}$ = 228 Hz; ^{13}C NMR (CD_2Cl_2) δ 218.5 (t, $^2J_{PC}$ = 3.9

Hz, CO_{ax}), 216.0 (dd, $^2J_{cis} = 7.3$ Hz, $^2J_{trans} = 35.7$ Hz, CO_{eq}), 140.4 (dd, $^3J_{PC} = 7.5$ Hz, $^1J_{PC} = 33.0$ Hz, Ph-*ipso*), 136.8 (d, $^1J_{PC} = 39.3$ Hz, Ph-*ipso*), 132.0 (d, separation 11.9 Hz, Ph-*ortho*), 131.5 (d, separation 11.9 Hz, Ph-*ortho*), 129.4 (s, Ph-*para*), 128.9 (d, separation 9.5 Hz, Ph-*meta*), 128.6 (d, separation 9.5 Hz, Ph-*meta*), 86.6 (d, separation 15.5 Hz, CH₂O), 55.8 (d, separation 5.9 Hz, CC₄), 41.7 (d, separation 9.1 Hz, CH₂CH₂CH₂), 37.8 (d, separation 15.8 Hz, CH₂PPh₂), 22.4 (s, CH₂CH₂CH₂); ¹H NMR (CD₂Cl₂) δ 7.71 (m, Ph), 7.35 (m, Ph), 6.97 (m, Ph), 4.22 (d, $^2J_{HH} = 10.5$ Hz, CH₂O), 3.65 (dd, $^2J_{HH} = 16.2$ Hz, $^2J_{HP} = 10.5$ Hz, CH₂PPh₂), 3.46 (br d, $^2J_{HH} = 10.5$ Hz, CH₂O), 2.95 (br d, $^2J_{HH} = 16.2$ Hz, CH₂PPh₂), 1.93 (dd, $^2J_{AB} = 13.0$ Hz, $^3J_{BD} = 5.4$ Hz, 2H, H_B), 1.75 (dt, $^2J_{CD} = 12.5$ Hz, $^3J_{AC} = 5.5$ Hz, 1H, H_C), 1.59 (m, 2H, H_A), 1.47 (m, 1H, H_D); Anal. Calcd for C₃₆H₃₄O₄P₂W: C, 55.69; H, 4.41; W, 23.68. Found: C, 55.49; H, 4.63; W, 23.17.

Preparation of *fac*-(*cis*-1,5-bis(diphenylphosphinomethyl)-3-oxabicyclo-[3.3.0]octane-*P,P'*)bromotricarbonylmanganese (isomers 17a, 17b)

A solution of **6** (0.520 g, 1.02 mmol) in 10 mL of toluene was added to a suspension of Mn(CO)₅Br (0.268 g, 0.975 mmol) in 5 mL of toluene. This mixture was refluxed for 20 minutes to yield a yellow precipitate. The mixture was cooled and stirred at room temperature for 30 minutes. Precipitation was completed with the addition of 20 mL of pentane. The product was isolated by filtration, washed twice with 5 mL of pentane, and dried *in vacuo*. Yield 0.56 g (79%). ¹H, ¹³C, and ³¹P NMR showed the presence of two facial isomers (4/1 ratio) which were not separated.

Major isomer (**17a**). ³¹P NMR (CH₂Cl₂) δ 26.9 (s); ¹³C NMR (CD₂Cl₂) δ 139.4 (m, separation 39.7 Hz, Ph-*ipso*), 137.7 (m, separation 38.5 Hz, Ph-*ipso*), 134.0 (at, separation 9.1 Hz, Ph-*ortho*), 132.0 (at, separation 8.7 Hz, Ph-*ortho*), 130.6 (s, Ph-

para), 130.3 (s, Ph-*para*), 128.9 (at, separation 8.4 Hz, Ph-*meta*), 128.6 (at, separation 9.1 Hz, Ph-*meta*), 55.4 (s, CC₄), 39.6 (at, separation 9.4 Hz, CH₂CH₂CH₂), 38.2 (at, separation 14.6 Hz, CH₂PPh₂), 22.5 (s, CH₂CH₂CH₂); ¹H NMR (CD₂Cl₂) δ 8.02 (br, Ph), 3.45 (br m, CH₂O), 3.05 (br m, CH₂PPh₂), 1.8-1.0 (m, CH₂).

Minor isomer (**17b**). ³¹P NMR (CH₂Cl₂) δ 28.7 (s); ¹³C NMR (CD₂Cl₂) δ 133.4 (at, separation 8.3 Hz, Ph-*ortho*), 132.9 (at, separation 9.1 Hz, Ph-*ortho*), 130.6 (s, Ph-*para*), 130.3 (s, Ph-*para*), 128.9 (at, Ph-*meta*), 128.4 (at, separation 8.7 Hz, Ph-*meta*), 55.6 (s, C), 41.2 (m, CH₂CH₂CH₂), 37.2 (m, CH₂PPh₂), 22.5 (s, CH₂CH₂CH₂).

Preparation of *fac*-(*cis*-1,5-bis(diphenylphosphinomethyl)-3-oxabicyclo-[3.3.0]octane-*P,P',O*)tricarbonylmanganese tetrafluoroborate (18**)**

The isomeric mixture **17a**, **17b** (0.296 g, 0.407 mmol) and AgBF₄ (0.090 g, 0.462 mmol) were stirred in 15 mL of CH₂Cl₂ for 1.5 hours. The resulting mixture was filtered through celite to leave a bright yellow filtrate. The volume was reduced to 10 mL *in vacuo* and the product was precipitated by the addition of 20 mL of pentane. The product was isolated by filtration, washed twice with 10 mL of diethyl ether and dried *in vacuo*. Yield 0.25 g (85%). MS (FAB) *m/e* (relative intensity) 647 (M⁺, 71), 591 (M⁺ - 2 CO, 20), 563 (M⁺ - 3 CO, 47); ³¹P NMR (CH₂Cl₂) δ 20.0 (s); ¹³C NMR (CD₂Cl₂) δ 223.2 (t, CO_{ax}), 214.7 (m, CO_{eq}), 137.0 (d, separation 22.6 Hz, Ph-*ipso*), 136.7 (d, separation 21.8 Hz, Ph-*ipso*), 131.4 (at, separation 9.1 Hz, Ph-*ortho*), 131.1 (s, Ph-*para*), 131.0 (s, Ph-*para*), 130.8 (at, separation 9.5 Hz, Ph-*ortho*), 130.0 (at, separation 9.5 Hz, Ph-*meta*), 129.6 (at, separation 9.9 Hz, Ph-*meta*), 86.0 (at, separation 14.6 Hz, CH₂O), 54.8 (s, CC₄), 39.6 (at, separation 10.3 Hz, CH₂CH₂CH₂), 32.7 (at, separation 18.6 Hz, CH₂PPh₂), 22.5 (s, CH₂CH₂CH₂); ¹H NMR (CD₂Cl₂, 500 MHz), δ 7.70 (m, Ph-*ortho*), 7.53 (m, Ph-*meta*), 7.48 (m, Ph-*para*), 7.35 (m, Ph-*ortho*), 7.18

(m, Ph-*para*), 7.04 (m, Ph-*meta*), 3.84 (d, $^2J_{\text{HH}} = 10.5$ Hz, 2H, CH₂O), 3.64 ("filled in" dd, $^2J_{\text{HH}} = 16.5$ Hz, separation 13.5 Hz, 2H, CH₂PPh₂), 3.42 (bd, $^2J_{\text{HH}} = 16.5$ Hz, 2H, CH₂PPh₂), 3.39 (d, $^2J_{\text{HH}} = 10.5$ Hz, 2H, CH₂O), 2.06 (m, 2H, H_B), 1.95 (m, 3H, H_{A,C}), 1.55 (m, 1H, H_D); $\Lambda_{\text{M}}(\text{CH}_2\text{Cl}_2) = 27.0 \text{ ohm}^{-1}\text{cm}^2\text{mol}^{-1}$ at 2.29 mM.

Crystal and Molecular Structure Solution of (6)Mo(CO)₄ (13)

A colorless crystal of the title compound was attached to the tip of a glass fiber, moved into the cold stream of the low-temperature device on the diffractometer, and cooled to -10 °C. The cell constants for data collection were determined from a list of reflections found by an automated search routine. The final cell constants were determined after data collection using 25 well-centered high-angle reflections. Pertinent data collection and reduction information is given in Table 1.

A total of 10,108 reflections were collected in the $\pm h, k, \pm l$ hemisphere. Lorentz and polarization corrections, and an absorption correction based on a series of psi-scans were applied. The agreement factor for the averaging of 642 observed reflections was 1.7% (based on I).

The centric space group $\text{P}\bar{1}$ was initially chosen, as suggested by intensity statistics; this choice was verified by the successful solution and refinement of the structure. The positions of the two independent Mo atoms were taken from a Patterson map. The remaining non-hydrogen atoms were then found through subsequent sets of difference Fourier maps and least-squares refinement. Two molecules of CH₂Cl₂ were also located in the lattice. The occupancies of the two solvent molecules were included in the refinement; the final occupancy values were 0.80(2) and 0.88(2). In the final stages of refinement, all of the non-hydrogen atoms except for the phenyl carbon atoms and the solvent carbon atoms were refined with anisotropic temperature factors. Hydrogen

atoms were added in idealized positions with isotropic temperature factors set equal to 1.3 times the isotropic equivalent of the attached carbon atom. An analysis of the environment around each complex verified the independence of the two molecules.

There was a potential ambiguity in the identity of the two unique atoms (one carbon and one oxygen) of the two fused five-membered rings in each complex. The initial identification was made by observation of the refined values of the isotropic thermal parameters. This assignment was later confirmed by using carbon scattering factors for both atoms, fixing isotropic B values at 4.0 for each atom, and refining the positions and occupancy of each atom. For each of the two molecules, the occupancy of the atom previously assigned as oxygen refined to approximately 0.8 and the other occupancy to about 1.2, confirming the initial assignment. Refinement calculations were performed on a Digital Equipment Corp. Micro VAXII computer using the CAD4-SDP programs.²⁴

Crystal and Molecular Structure Solution of (6)W(CO)₃ (16)

A yellow crystal of **16** was mounted on a glass fiber and centered on a Rigaku AFC6R diffractometer with graphite monochromated MoK α radiation and a 12KW rotating anode generator. Cell dimensions and the orientation matrix were obtained from least-squares refinement using setting angles of 25 carefully centered reflections in the range $12.52 < 2\theta < 15.17^\circ$. Since the intensities of three representative reflections measured after every 150 reflections remained constant throughout data collection, no decay correction was applied. Lorentz and polarization corrections were applied to the data. Refinement of the structure was performed using the TEXSAN crystallographic software package.²⁵ Scattering factors were obtained from Cromer and Waber.²⁶ The space group P2₁/c (#14) was initially chosen and subsequently verified by the successful solution and refinement of the structure. The non-hydrogen atoms were

refined anisotropically. The final cycle of full-matrix least-squares refinement, which was based on 4068 observed reflections with $I > 3\sigma(I)$ and 460 variable parameters, converged with unweighted and weighted agreement factors of 0.076 and 0.093, respectively.

Table 1. Crystallographic Data for (6)Mo(CO)₄, 13 and (6)W(CO)₃, 16

	13	16
Formula	C ₃₇ H ₃₄ O ₅ P ₂ Mo •CH ₂ Cl ₂	C ₃₆ H ₃₄ O ₄ P ₂ W •CH ₂ Cl ₂
Formula weight	801.50	861.39
Space Group	P $\bar{1}$	P2 ₁ /c (#14)
a, Å	15.321(3)	12.262(5)
b, Å	22.371(3)	17.38(1)
c, Å	11.376(2)	16.285(7)
α , deg	90.52(1)	
β , deg	91.80(1)	92.08(4)
γ , deg	72.07(1)	
V, Å ³	3708(1)	3468(3)

$$^aR = \sum |F_o| - |F_c| / \sum |F_o|$$

$$^bR_w = [\sum w(|F_o| - |F_c|)^2 / \sum F_o^2]^{1/2}; w = 1/\sigma^2(|F_o|)$$

$$^c\text{Quality-of-fit} = [\sum w(|F_o| - |F_c|)^2 / (N_{\text{obs}} - N_{\text{parameters}})]^{1/2}$$

Table 1. Continued

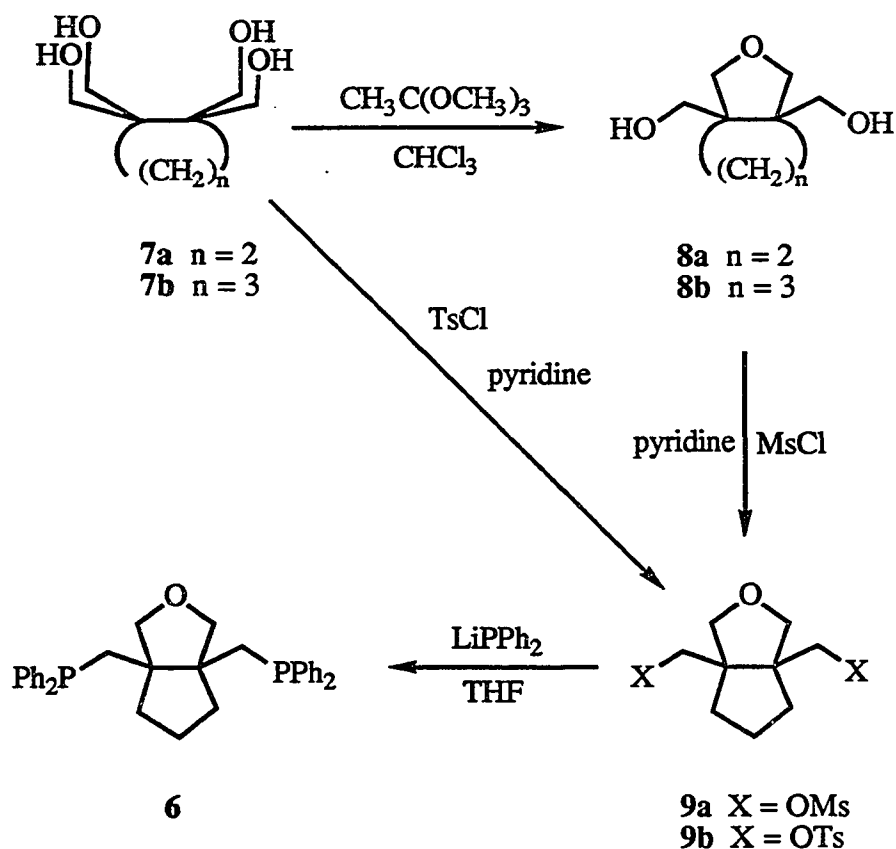
	13	16
Z	4	4
d_{calc} , g/cm ³	1.436	1.650
Crystal size, mm	0.48 x 0.24 x 0.18	0.30 x 0.45 x 0.50
$\mu(\text{MoK}\alpha)$, cm ⁻¹	6.15	36.85
Data collection instrument	Enraf-Nonius CAD4	Rigaku AFC6R
Radiation (monochromated in incident beam)	MoK α ($\lambda = 0.71073 \text{ \AA}$)	MoK α ($\lambda = 0.71069 \text{ \AA}$)
Orientation reflections, number, range (2θ)	25, 21-34	25, 12.5-15.2
Temperature, °C	-10(1)	-15
Scan method	θ - 2θ	ω - 2θ
Data col. range, 2θ , deg	4.0-45.0	0-55.2
No. unique data, total:	9667	8290
with $F_0^2 > 3\sigma(F_0^2)$:	6702	4068
Number of parameters refined	615	460
Trans. factors, max., min. (psi-scans)	0.999, 0.947	
R^a	0.059	0.076
R_w^b	0.079	0.093
Quality-of-fit indicator ^c	2.10	2.53
Largest shift/esd, final cycle	0.03	0.36
Largest peak, e/ \AA^3	1.2(1)	6.09

RESULTS AND DISCUSSION

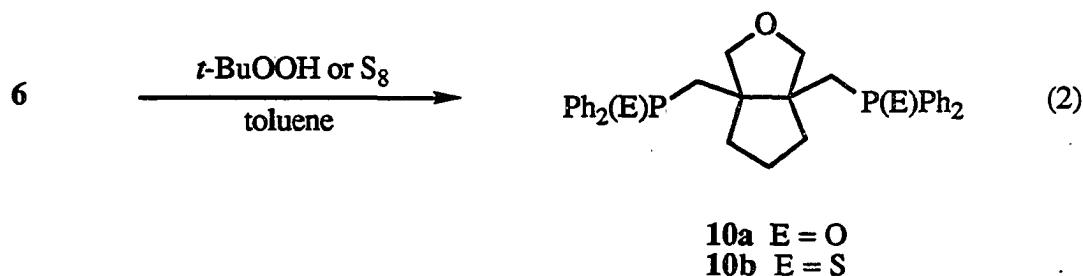
Synthesis of Ligand 6

Previous work from our group²⁷ showed that reaction of the tetrol 7a with trimethylorthoacetate in chloroform unexpectedly yielded the diol-ether 8a in the presence of an acid catalyst. A similar procedure starting with 7b, followed by reaction with methanesulfonyl chloride in pyridine yielded the dimesylate-ether 9a. The tosylate derivative 9b has previously been synthesized²⁸ directly from 7b, but in our hands the yield was low.

Scheme I



Substitution of the mesylate groups in **9a** by PPh₂ moieties was achieved using LiPPh₂ in THF. The residue obtained after workup was chromatographed on silica gel with 10% EtOAc/toluene to give pure **6**. This new diphosphine ether is a crystalline air stable white solid which is soluble in toluene, tetrahydrofuran, diethyl ether and CH₂Cl₂. Typical of tertiary phosphines, **6** is readily oxidized with *t*-BuOOH or S₈ in toluene giving **10a** or **10b**, respectively (reaction 2). These compounds were isolated as stable white solids and their constitutions were confirmed by NMR and HRM spectroscopies.

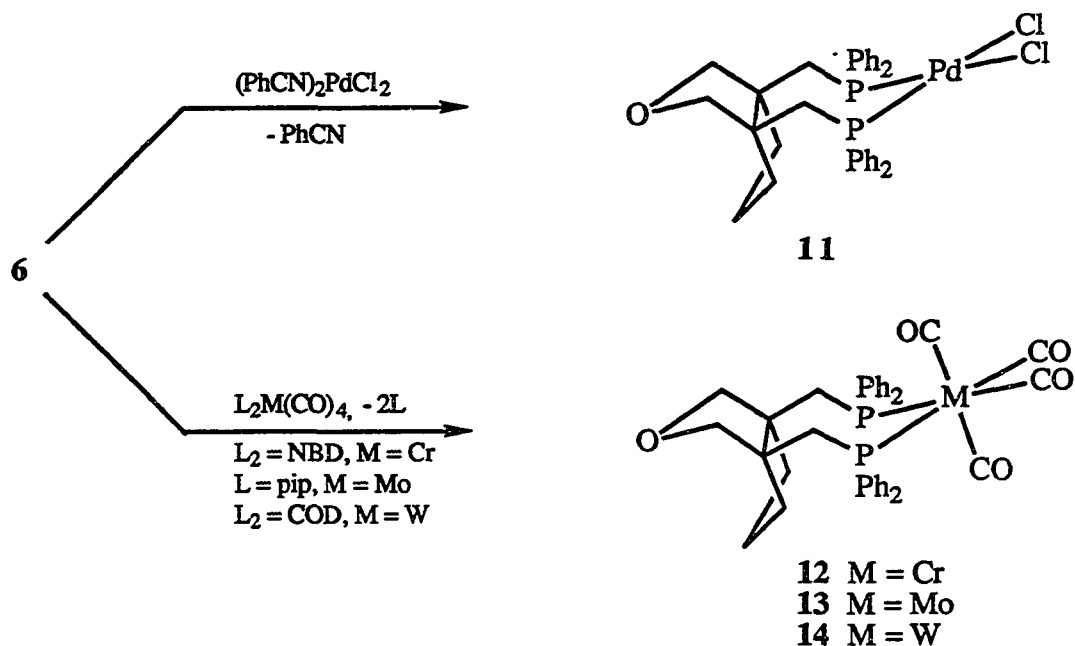


Coordination Chemistry of **6**

Addition of **6** to (PhCN)₂PdCl₂ in toluene resulted in the precipitation of **11** in Scheme II as a creamy white solid in almost quantitative yield. This compound is insoluble in most organic solvents but exhibits moderate solubility in DMSO. Solutions of **11** in DMSO exhibit a singlet in the ³¹P NMR spectrum at 22.8 ppm and resonances in the ¹H and ¹³C NMR spectra consistent with the formulation of **11** as a *cis*-square planar complex wherein **6** is coordinated through the two phosphorus atoms.

Addition of **6** to CH₂Cl₂ solutions of *cis*-L₂Mo(CO)₄ (L₂ = NBD, (piperidine)₂, COD; M = Cr, Mo, W) yields the complexes **12-14** in Scheme II as pale white to lightly yellow solids. In contrast to **11**, these complexes exhibit high solubility in CH₂Cl₂ and THF, allowing purification by column chromatography and easy spectroscopic

Scheme II



identification. These complexes exhibit singlets in their ^{31}P NMR spectra except for **14** which also shows satellites for $^{31}\text{P} - ^{183}\text{W}$ coupling with a value of 232 Hz. The four strong carbonyl stretches in the infrared spectra of **12-14** (Table 2) are in a range consistent with *cis* phosphine-substituted tetracarbonyls. An X-ray crystallographic study of **13** confirms this assignment. ^1H and ^{13}C NMR spectral evidence for these complexes will be discussed later.

In addition to a bidentate phosphine coordination mode (*P,P*) for **6** as in complexes **11-14**, a tridentate coordination mode (*P,P,O*) is also accessible via coordination of the ether oxygen. Heating solutions of **6** and $(\eta^6\text{-cycloheptatriene})\text{Mo}(\text{CO})_3$ or $(\eta^6\text{-cycloheptatriene})\text{W}(\text{CO})_3$ in toluene at 40-60 °C results in the precipitation of **15** or **16** as bright yellow solids in 70-80% yield (reaction

3). These complexes are moderately air stable as solids but their CH_2Cl_2 solutions rapidly decompose upon exposure to air.

The constitutions of **15** and **16** were confirmed by their mass spectra as well as their IR and NMR spectroscopic properties. Both **15** and **16** show strong molecular ion peaks (MH^+) in their desorption CI mass spectra at m/e 690 and 777, respectively. In addition, **15** shows a molecular ion peak (M^+) in its EI mass spectrum and its molecular formula was confirmed by high resolution measurement. The appearance of three strong carbonyl stretches in the IR spectra of **15** and **16** supports a facial tricarbonyl species (Table 2). Strong evidence for coordination of the ether functionality is also provided by

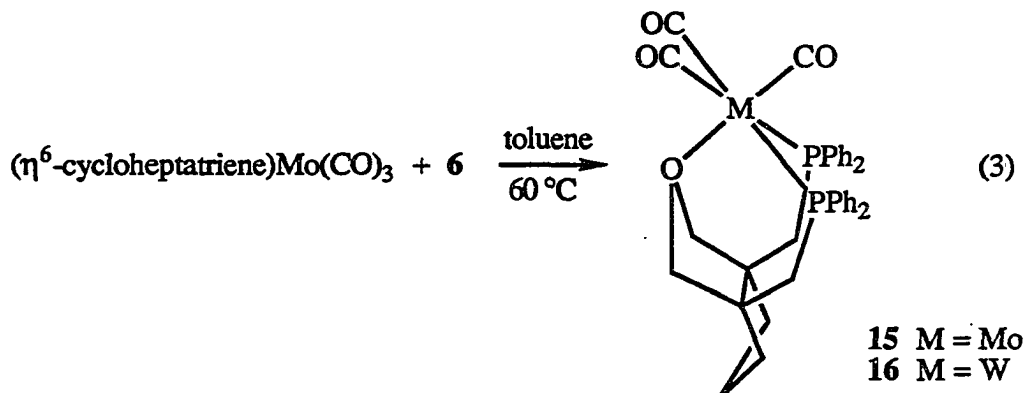
Table 2. Infrared spectroscopic data^a.

	ν_{CO} (cm^{-1})			
12 , (6)Cr(CO) ₄	2014	1925	1877	1863
13 , (6)Mo(CO) ₄	2027	1934	1886	1869
14 , (6)W(CO) ₄	2021	1917	1892	1863
15 , (6)Mo(CO) ₃		1921	1826	1763
16 , (6)W(CO) ₃		1913	1819	1757
17a , ^b <i>fac</i> -(6)Mn(CO) ₃ Br	2023	1956	1911	
18 , ^c [(6)Mn(CO) ₃]BF ₄	2044	1981	1931	

^a Samples prepared as Nujol mulls except where indicated.

^b IR bands for the minor isomer **17b** were not observed in this mixture of isomers.

^c CH_2Cl_2 solution.



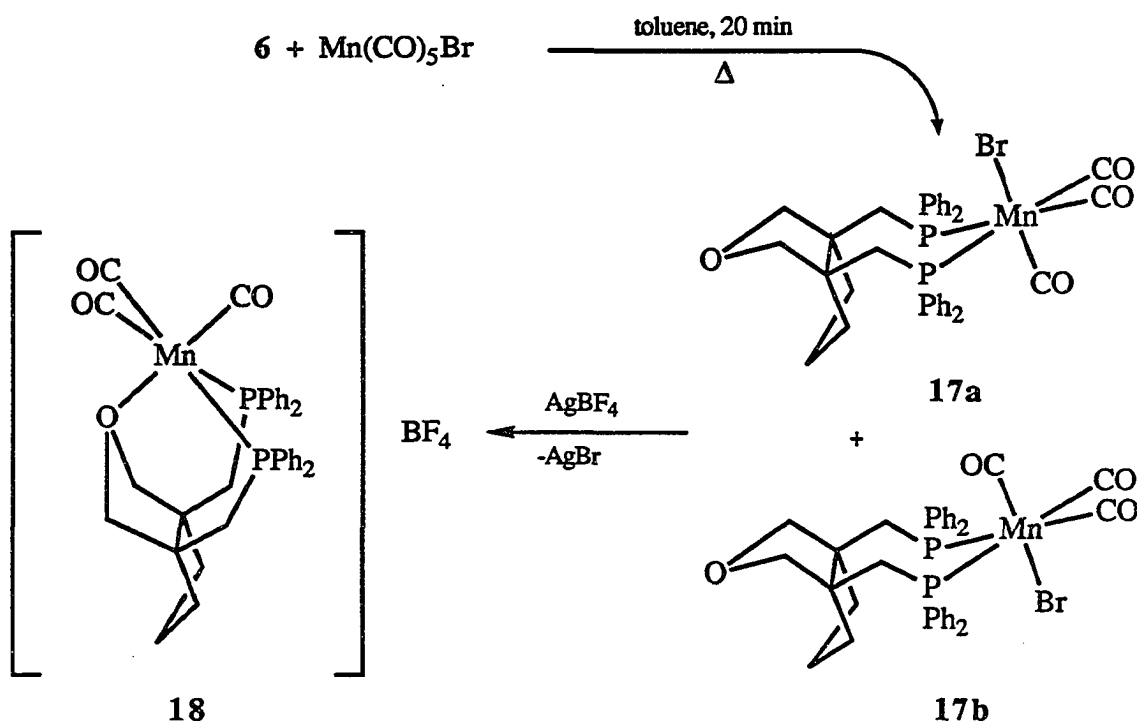
the large shift of carbonyl stretching frequencies to as low as 1763 cm^{-1} for **15** and 1757 cm^{-1} for **16**. Such a shift to lower frequency is expected based on the lack of π acceptor capability of ether donors, resulting in an increase in the strength of M-C backbonding, especially for the carbonyl *trans* to the ether oxygen. An attempt was also made to assign the asymmetric $\nu_{\text{C-O-C}}$ mode for the coordinated ether. Lindner^{7,29} has reported that upon ether coordination in metal complexes of ether-substituted phosphines, $\nu_{\text{C-O-C}}$ shifts to lower frequency by $30\text{-}40\text{ cm}^{-1}$. Although **6** exhibits a weak asymmetric $\nu_{\text{C-O-C}}$ band at 1082 cm^{-1} , the low intensity of this stretch did not allow for a reliable assignment to be made in the spectra of **15** and **16**.

Attempts to prepare the chromium analogue of **15** and **16** were unsuccessful. No reaction was observed when solutions of $(\eta^6\text{-cycloheptatriene})\text{Cr}(\text{CO})_3$ and **6** were heated in toluene at temperatures up to 100°C for 12 h. Lower temperatures and longer reaction times also yielded no reaction. Refluxing the two starting materials in xylene yielded only decomposition and disproportionation products. Analysis of this solution by ^{31}P NMR spectroscopy revealed the two major products to be unreacted ligand **6** and the tetracarbonyl derivative **12**.

Mn(CO)₅Br was found to react with **6** in refluxing toluene to give (6)Mn(CO)₃Br as a mixture of two *fac* isomers **17a** and **17b** which was confirmed by ³¹P and ¹³C NMR spectroscopy. Here the isomerism arises from the inequivalency of the two axial sites due to the lack of symmetry of the ligand **6**.

Removal of bromide from a mixture of **17a** and **17b** was achieved by reaction with a slight excess of AgBF₄ in CH₂Cl₂ (Scheme III). Following filtration, precipitation with pentane yielded **18** as a bright yellow solid which was highly soluble in CH₂Cl₂. FAB MS revealed a large molecular ion peak (excluding BF₄⁻) at *m/e* 647. The ionic nature of **18** is shown by its conductivity in CH₂Cl₂ $\Lambda_m = 27 \text{ ohm}^{-1}\text{cm}^2 \text{mol}^{-1}$. Although this conductance seems low, it is in the range of 20-30 $\text{ohm}^{-1}\text{cm}^2\text{mol}^{-1}$ observed previously for other 1:1 electrolytes in CH₂Cl₂.³⁰ This conductivity, as well as ¹H and ¹³C NMR data confirms the coordination of the ether oxygen to manganese. Infrared data are also consistent with a facial tricarbonyl species. Whereas coordination of the ether oxygen in **15** and **16** significantly lowers the carbonyl stretching frequencies to as low as ~1760 cm^{-1} , they remain in the region of 2044-1931 cm^{-1} in the case of **18**. Presumably this arises from the formation of a positive charge on manganese which offsets the expected increase in M-CO backbonding anticipated for the axial carbonyl upon ether coordination.

Scheme III



Crystallographic Studies

Slow evaporation of a CH₂Cl₂ solution of **13** yielded clear colorless crystals suitable for X-ray analysis. In addition to two solvent molecules, the unit cell contains two independent molecules of the complex each with the same overall geometry but differing by small variations in bond distances and angles (Figure 1). The distorted octahedral geometry around Mo is comprised of two *cis* phosphorus atoms from **6** and four carbonyl ligands. The average Mo-P distance of 2.543(2) Å is in the range reported previously for other phosphine complexes of molybdenum carbonyls.³¹ The Mo-C distances for the carbonyls *trans* to phosphorus average 1.977(9) Å. This is shorter than

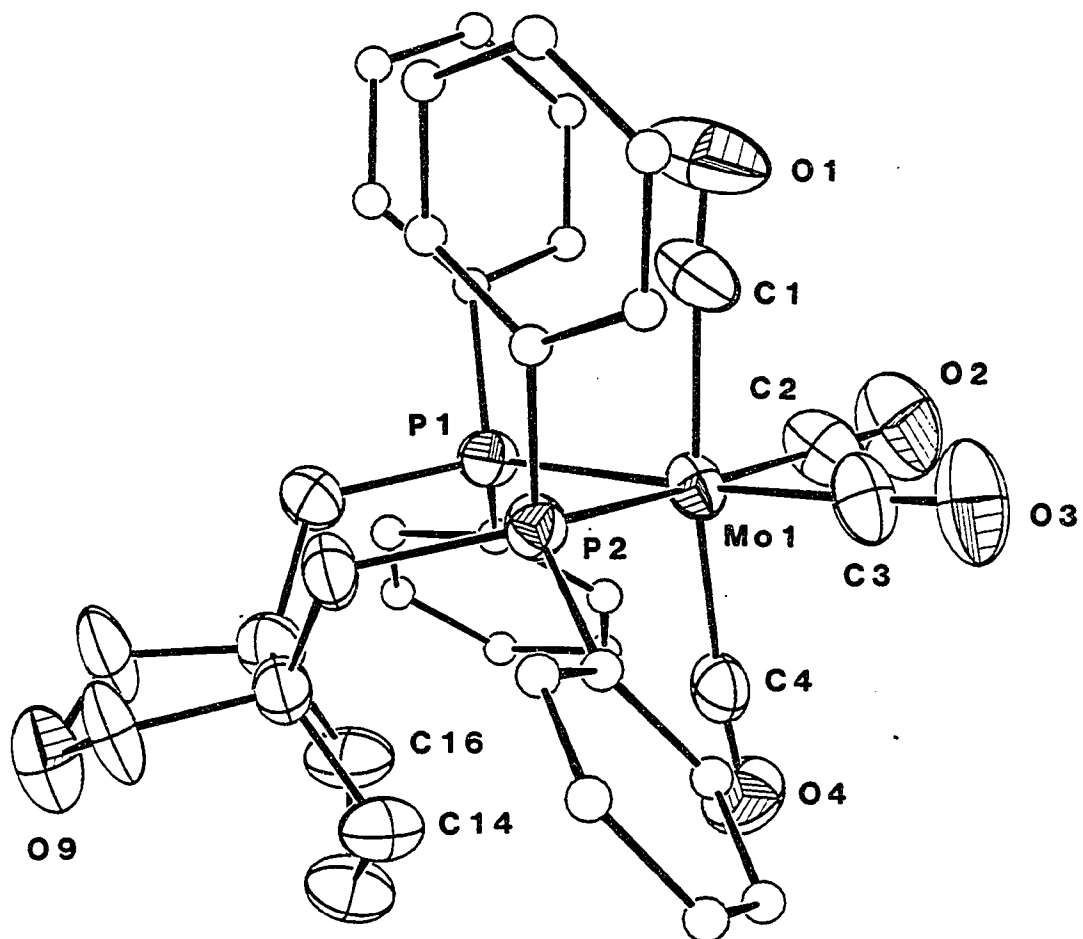


Figure 1a. ORTEP diagram of the first of two independent molecules of 13 with ellipsoids drawn at the 50% probability level.

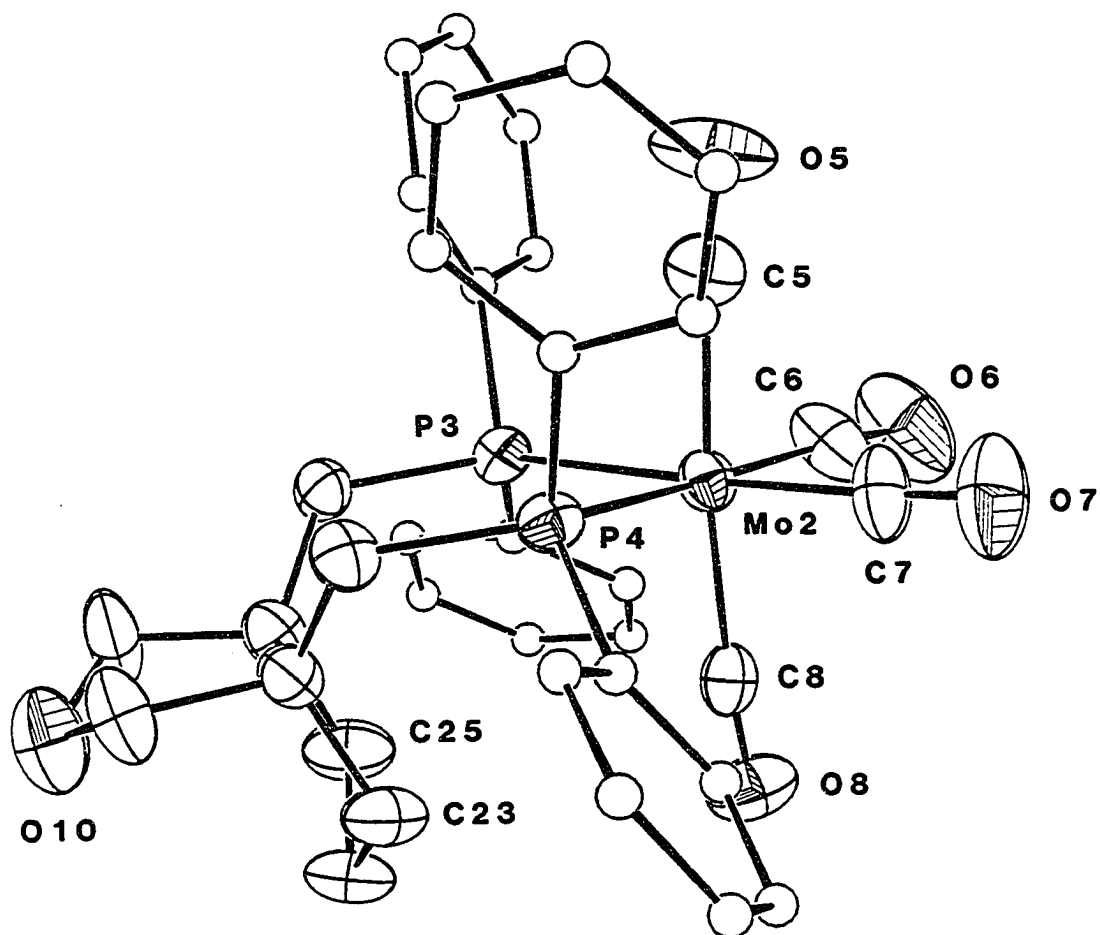


Figure 1b. ORTEP drawing of the second independent molecule of 13 with ellipsoids drawn at the 50% probability level.

the Mo–C distances for the mutually *trans* axial carbonyls, as is expected for the poorer π acceptor ability of P compared with CO. Furthermore, the mutually *trans* carbonyls occupy stereochemically nonequivalent axial sites which is reflected in the Mo–C bond distances. The Mo–C distances of 2.061(9) and 2.048(8) Å for C-1 and C-5, which occupy the axial positions nearest two phenyl rings, are significantly elongated compared with 2.021(8) and 2.011(7) Å for C-4 and C-8 which are nearest the cyclopentane ring of ligand **6** (See Tables 3 and 4)

The geometry around Mo reveals a distortion of the carbonyls away from the phosphine ligand presumably due to steric hindrance. The average P–Mo–P angle has been opened up to 93.5°. Most P–Mo–C angles also slightly exceed 90°, with the largest deviations being 96.8(2)° and 96.9(2)° for P(4)–Mo(2)–C(8) and P(2)–Mo(1)–C(4), respectively. However, P(2)–Mo(1)–C(3) exhibits a much smaller angle of 84.8°(2). To offset the slightly larger-than-ideal P–Mo–C angles, the C–Mo–C angles are slightly less than 90° with an average value of 87.9°. The distortion from an idealized octahedral geometry is also readily apparent by noting that the *trans* C–Mo–C and P–Mo–C angles

Table 3. Selected bond distances (Å) for **13**•CH₂Cl₂

Mo(1)–P(1)	2.544(2)	Mo(1)–C(3)	1.981(9)
Mo(1)–P(2)	2.546(2)	Mo(1)–C(4)	2.021(8)
Mo(2)–P(3)	2.543(2)	Mo(2)–C(5)	2.048(8)
Mo(2)–P(4)	2.539(2)	Mo(2)–C(6)	1.980(9)
Mo(1)–C(1)	2.061(9)	Mo(2)–C(7)	1.965(8)
Mo(1)–C(2)	1.983(8)	Mo(2)–C(8)	2.011(7)

Table 4. Bond angles (deg)^a for 13•CH₂Cl₂

P(1)-Mo(1)-P(2)	93.05(6)	P(3)-Mo(2)-P(4)	94.00(7)
P(1)-Mo(1)-C(1)	90.0(3)	P(3)-Mo(2)-C(5)	89.9(2)
P(1)-Mo(1)-C(2)	92.8(3)	P(3)-Mo(2)-C(6)	91.4(3)
P(1)-Mo(1)-C(3)	176.0(2)	P(3)-Mo(2)-C(7)	177.4(2)
P(1)-Mo(1)-C(4)	93.2(2)	P(3)-Mo(2)-C(8)	92.3(2)
P(2)-Mo(1)-C(1)	89.4(2)	P(4)-Mo(2)-C(5)	88.5(3)
P(2)-Mo(1)-C(2)	173.0(3)	P(4)-Mo(2)-C(6)	173.5(3)
P(2)-Mo(1)-C(3)	84.8(2)	P(4)-Mo(2)-C(7)	87.0(3)
P(2)-Mo(1)-C(4)	96.9(2)	P(4)-Mo(2)-C(8)	96.8(2)
C(1)-Mo(1)-C(2)	86.7(3)	C(5)-Mo(2)-C(6)	88.0(4)
C(1)-Mo(1)-C(3)	86.6(4)	C(5)-Mo(2)-C(7)	87.7(3)
C(1)-Mo(1)-C(4)	172.7(3)	C(5)-Mo(2)-C(8)	174.1(4)
C(2)-Mo(1)-C(3)	89.1(4)	C(6)-Mo(2)-C(7)	87.4(4)
C(2)-Mo(1)-C(4)	86.6(3)	C(6)-Mo(2)-C(8)	86.5(3)
C(3)-Mo(1)-C(4)	90.3(3)	C(7)-Mo(2)-C(8)	90.0(3)

^aNumbers in parentheses are estimated standard deviations in the least significant digits.

vary from 172.7(3) to 177.4(2)°. An important feature to note in this structure is the orientation of one methylene proton towards the face of a phenyl ring on each of carbons 14, 16 and 23, 25 in the cyclopentane ring. The implications of such a conformation and its effect on ^1H and ^{13}C NMR spectra of these complexes will be discussed later. Also, of the two five-membered rings in **6**, it should be noted that the ether-containing ring is pointed away from the metal center.

Slow evaporation of a CH_2Cl_2 solution of **16** yielded yellow crystals of X-ray quality as a CH_2Cl_2 solvate (Figure 2). The distorted octahedral coordination sphere around tungsten is comprised of three carbonyls in a *fac* arrangement as well as an oxygen and two phosphorus donors verifying the tridentate coordination mode for **6** in **16**. The P(1)-W(1)-P(2) angle has decreased upon ether coordination to 83.2°, an angle considerably less than the 93.5° angle observed in **13**. All C-W-C angles between carbonyls as well as P-W-O angles of **6** are less than 90° whereas all P-W-C and O-W-C angles exceed 90°, indicating the expected distortion of the carbonyls away from the steric bulk of **6**. The largest deviations from an ideal octahedron are observed for P(2)-W(1)-O(4), P(2)-W(1)-C(1) and P(2)-W(1)-C(2) with angles of 83.2(3), 98.7(6) and 98.8(6)°, respectively (See Table 5).

Two W-C distances are observed for the two types of non-equivalent carbonyls in **16**. The two carbonyls *trans* to phosphorus atoms exhibit a W-C distance of 1.98(2) Å in agreement with the analogous Mo-C distances in **13**.³² The W-C distance of 1.91(2) Å observed for the carbonyl *trans* to the coordinated ether represents a considerable bond shortening when compared to the Mo-C distances for the mutually *trans* carbonyls in **13** which range from 2.011(7) to 2.061(9) Å. This decrease in W-C bond distance in **16** is consistent with an increase in W-C π bonding for the carbonyl *trans* to the poor π accepting ether oxygen, as is further substantiated by the low ν_{CO} value of 1757 cm^{-1} in

the infrared spectrum. The W-O distance of 2.33(1) Å is considerably longer than the sum of the covalent radii (2.19 Å) as is expected for a weak ether-metal interaction. This distance is in agreement with Mo-O distances of 2.363(6) and 2.337(7) Å reported for (TMPP)Mo(CO)₃.⁹ The W-P distances of 2.558(5) and 2.550(5) Å are quite normal.

Table 5. Selected bond distances (Å) and angles (deg) for 16•CH₂Cl₂

Bond Distances			
W(1)-P(1)	2.558(5)	W(1)-C(3)	1.98(2)
W(1)-P(2)	2.550(5)	O(1)-C(1)	1.19(2)
W(1)-O(4)	2.33(1)	O(2)-C(2)	1.15(3)
W(1)-C(1)	1.91(2)	O(3)-C(3)	1.12(3)
W(1)-C(2)	1.98(2)		

Bond Angles			
P(1)-W(1)-P(2)	83.2(2)	P(2)-W(1)-C(3)	170.5(6)
P(1)-W(1)-O(4)	88.6(4)	O(4)-W(1)-C(1)	178.0(7)
P(1)-W(1)-C(1)	92.1(7)	O(4)-W(1)-C(2)	91.5(7)
P(1)-W(1)-C(2)	178.1(6)	O(4)-W(1)-C(3)	88.9(7)
P(1)-W(1)-C(3)	91.4(6)	C(1)-W(1)-C(2)	87.7(9)
P(2)-W(1)-O(4)	83.2(3)	C(1)-W(1)-C(3)	89.3(9)
P(2)-W(1)-C(1)	98.7(6)	C(2)-W(1)-C(3)	86.7(9)
P(2)-W(1)-C(2)	98.8(6)		

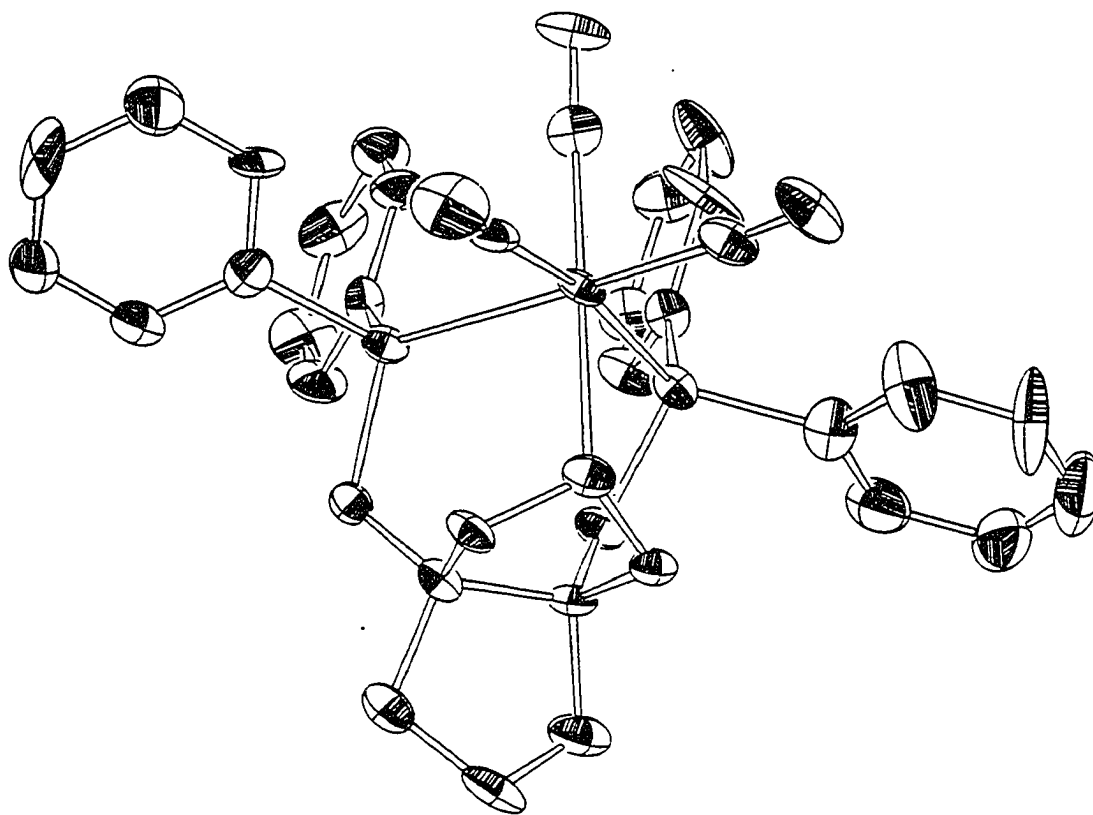


Figure 2a. ORTEP drawing of 16 with ellipsoids drawn at the 50% probability level.

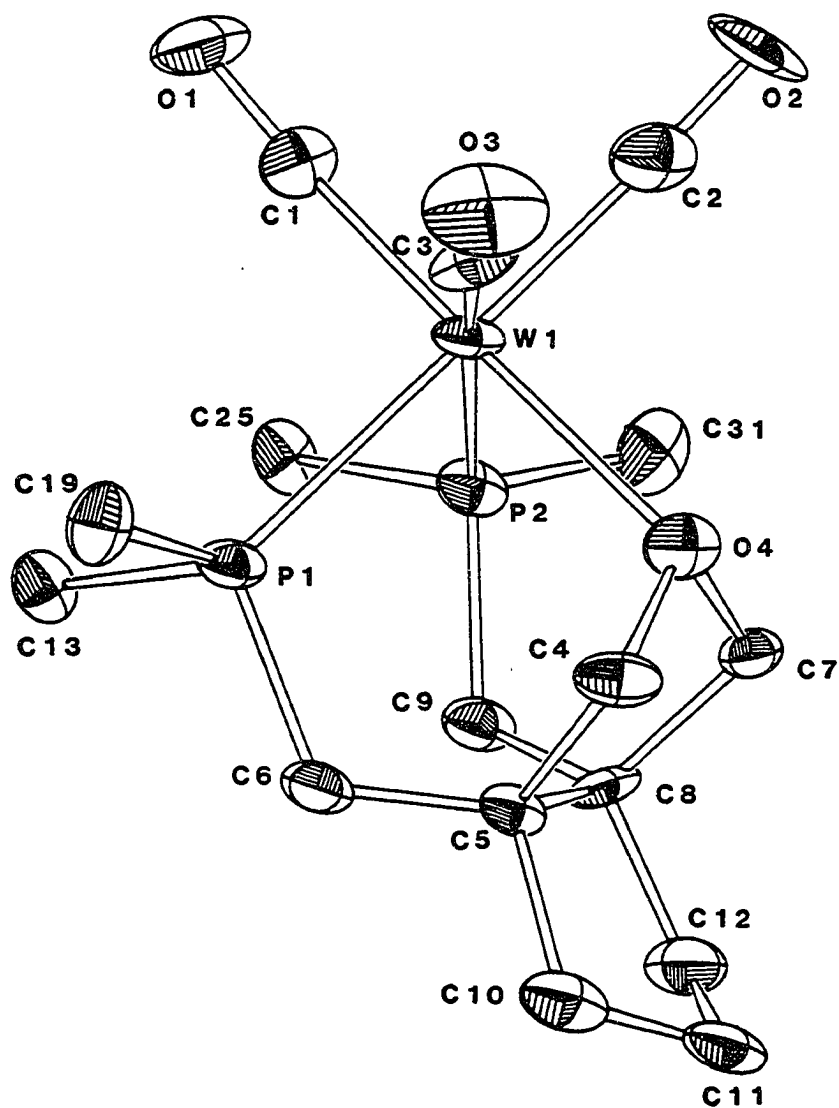


Figure 2b. ORTEP drawing of **16** with ellipsoids drawn at the 50% probability level. All phenyl carbons, except for Ph-*ipso* carbons, have been omitted for clarity.

¹H NMR Spectroscopic Characterization

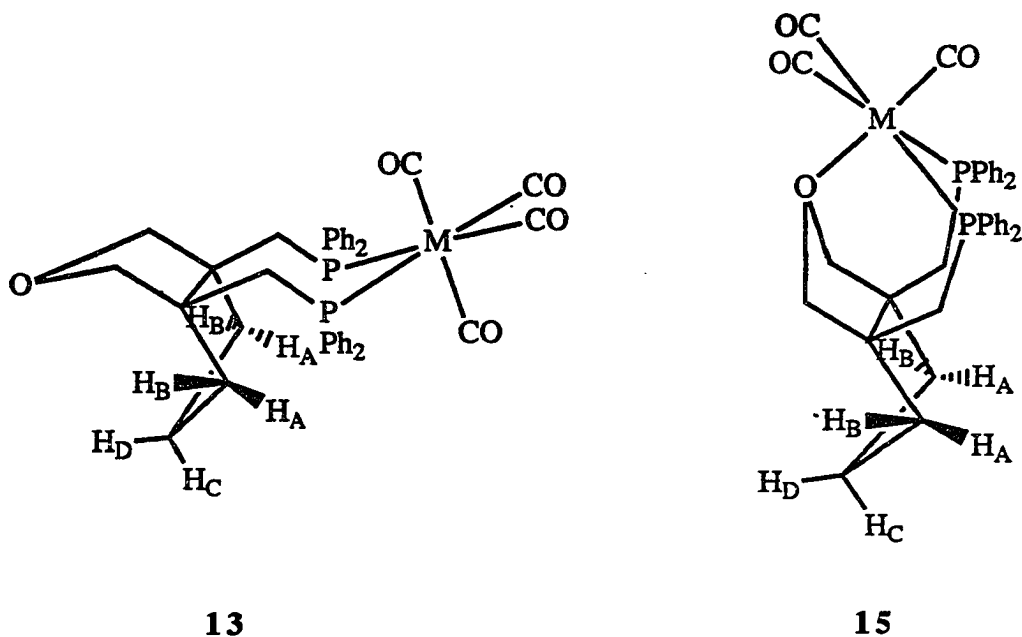
Compound **6** exhibits resonances in three distinct regions of its ¹H NMR spectrum that are useful in the characterization of the metal complexes of this ligand. These regions are comprised of the phenyl protons, the CH₂O and CH₂PPh₂ methylene protons, and the methylene protons of the cyclopentane ring. Assignments discussed below were aided by the use of ¹H {³¹P} spectra obtained on a 500 MHz spectrometer to assure correct assignment of couplings due to phosphorus nuclei.

The phenyl region in **6** shows two multiplets, one centered at 7.46 ppm assigned to the *ortho* protons and the other at 7.31 ppm assigned to the *meta* and *para* protons. The multiplet at 7.46 ppm actually corresponds to two sets of inequivalent *ortho* protons owing to the presence of two sets of stereochemically non-equivalent phenyls, one each per phosphorus atom. In fact, the 500 MHz ¹H NMR spectrum of **10a** shows two well resolved multiplets at 7.82 and 7.76 ppm for these two types of *ortho* protons. These multiplets are assigned to the phenyl *ortho* protons based on integrations and on the collapse of these multiplets to doublets (with fine structure) upon phosphorus irradiation in the ¹H {³¹P} NMR spectrum.

Compound **6** also exhibits an AB quartet centered at 3.57 ppm and an ABX pattern (X = P) centered at 2.31 ppm for the diastereotopic methylene protons adjacent to the ether-oxygen and the PPh₂ groups respectively. The region from 1.4-1.8 ppm is marked by complex multiplets due to the A₂B₂CD spin system for the six cyclopentane ring protons. The derivatives **10a** and **10b** display the same basic features discussed above for their parent compound **6**.

Upon coordination of **6** to an octahedral metal fragment in **12-14**, the cyclopentane portion of the spectrum features well separated resonances. In **13** for example, a doublet of doublets at 1.12 ppm and a multiplet at 1.81 ppm are assigned to

the geminal protons H_A and H_B as shown in Figure 3. The resonance at 1.12 ppm for H_A appears as a doublet of doublets due to a strong geminal coupling to H_B of 12.3 Hz and a vicinal *cis* coupling to H_C of 5.4 Hz. A vicinal *trans* coupling of H_A to H_D is not observed as is sometimes the case for cyclopentane rings.³³ These assignments agree with the results of a COSY experiment for **12**, and ^1H $\{^{31}\text{P}\}$ spectra for **12-14** which show that none of the couplings in this region arise from P-H coupling.



In Figure 3 it is noted that the position of H_A in **13** has been shifted significantly upfield compared with the chemical shift of H_B and compared with the corresponding resonances for **6**, **10a** and **10b**. Presumably this upfield shift has been induced by a neighboring phenyl ring. The crystal structure of **13** indeed shows that H_A is oriented towards the face of a phenyl ring on phosphorus in the solid state. In solution one might expect fluxionality between conformations wherein the two five-membered rings switch

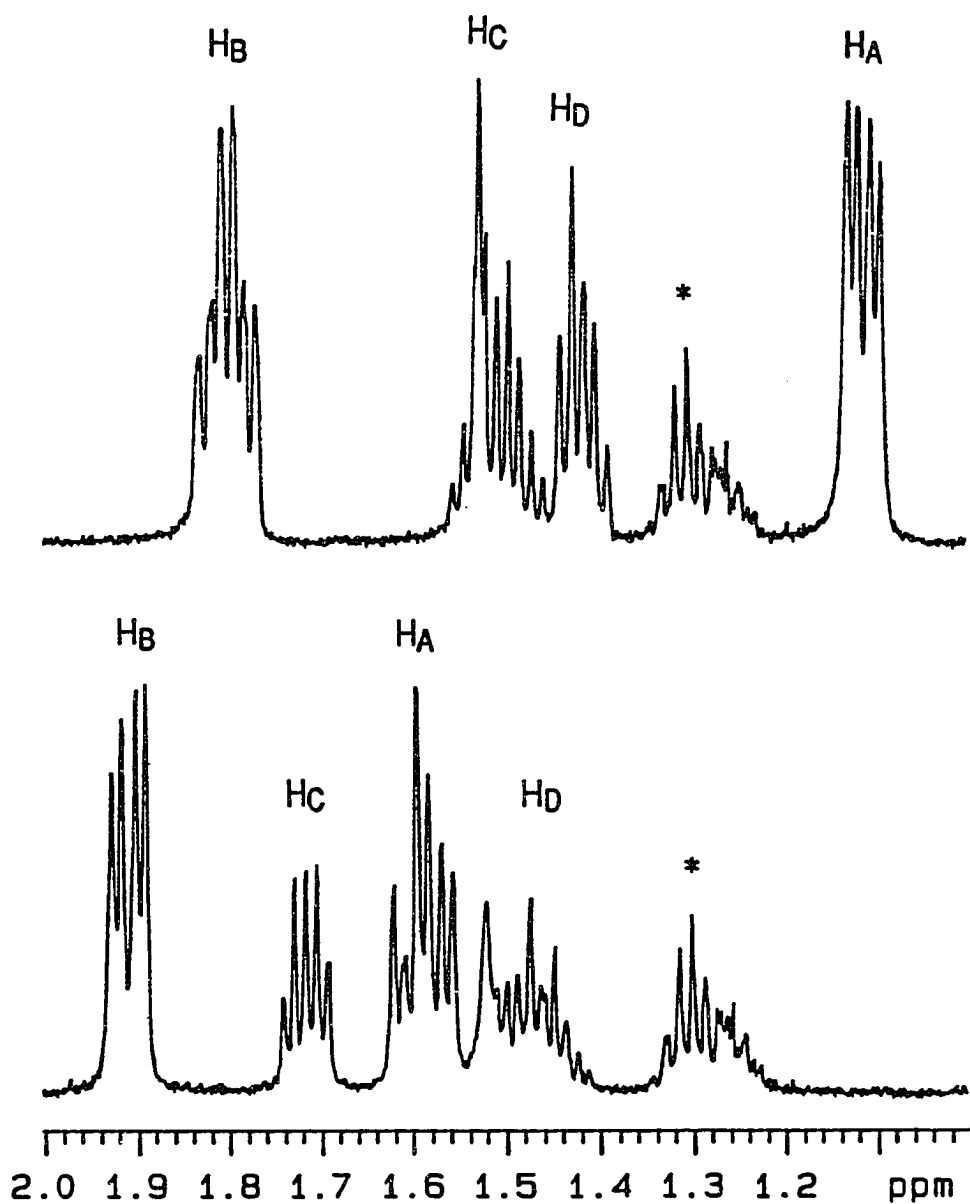
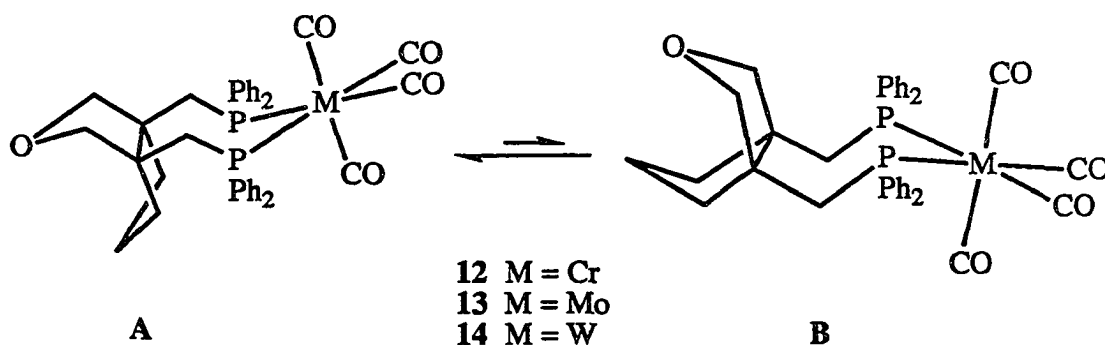


Figure 3. The cyclopentane region of the ^1H NMR (500 MHz, CD_2Cl_2) spectra of $(\delta)\text{Mo}(\text{CO})_4$, **13**, (above) and $(\delta)\text{Mo}(\text{CO})_3$, **15**, (below). The asterisks indicate resonances due to pentane present as an impurity.

positions as in equation 4. If such a conformational equilibrium exists, noticeable shielding should also be observed for two of the four diastereotopic CH₂O protons. However, the ¹H NMR spectrum of **13** shows an AB system centered at 3.59 ppm ($\Delta\delta_{AB} = 0.03$ ppm) for the CH₂O protons and a partially collapsed ABX pattern at 2.99 ppm for the CH₂PPh₂ protons. Thus no significant shielding in this region is observed, prompting us to speculate that in solution the conformations of **12-14** closely resemble that found in the solid state for **13** where the ether oxygen in **6** is removed as far as possible from the metal center. Variable temperature ¹H NMR spectra of **14** in d₅-pyridine lend further support to this argument. With increasing temperature, the doublet of doublets resonance at 1.24 ppm assigned to H_A at 20 °C gradually shifts downfield to 1.38 ppm at 110 °C. Similarly the difference in chemical shifts for the CH₂O proton resonances steadily increases from 0.07 ppm at 20 °C to 0.20 ppm at 110 °C. This can be explained by a shift in equilibrium toward conformation **B** with increasing temperature, allowing for decreased shielding at H_A and an increase in shielding for two of the four CH₂O protons.



Upon coordination of the ether-oxygen in **15**, a doublet of doublets resonance appears in the ¹H NMR spectrum at 1.90 ppm (${}^2J_{AB} = 13.2$ Hz, ${}^3J_{BD} = 5.1$ Hz) assigned to H_B. H_A has shifted downfield to 1.58 ppm, a change of 0.46 ppm from

assigned to H_B. H_A has shifted downfield to 1.58 ppm, a change of 0.46 ppm from the resonance for H_A in **13**. This is consistent with structural data for **16** which show that upon ether coordination, none of the phenyl rings on phosphorus are oriented in a manner conducive to shielding any of the cyclopentane protons. Resonances for the diastereotopic CH₂O protons of **15** are observed as doublets ($^2J_{\text{HH}} = 10.5$ Hz) at 4.09 ppm and 3.29 ppm, a separation of 0.8 ppm compared with a separation of only 0.03 ppm in **13**. Similarly a much larger separation of the CH₂PPh₂ methylene protons is also observed for **15**, **16** and **18** compared with **12-14**. For example, a separation of 0.44 ppm is observed for the diastereotopic CH₂PPh₂ methylene protons of **15**, whereas in **13** the CH₂PPh₂ methylene resonance appears as a doublet with coupling only to phosphorus.

Coordination of the ether to a metal also increases the resolution of the phenyl protons. ¹H {³¹P} spectra of **15**, **16** and **18** clearly show well-resolved resonances for each of the two nonequivalent *ortho*, *meta* and *para* protons in a window spanning, for example from 6.98 to 7.72 ppm for **16**. Overlap of some of these resonances occurs for the non-ether coordinated complexes **12-14**.

¹³C NMR Spectroscopic Characterization

In the free ligand **6**, inequivalence of the two phenyl rings is indicated by the observance of two doublets for the *ipso* carbons and two doublets for the *ortho* carbons. The difference between the chemical shifts of the phenyl carbons increases upon oxidation as two doublets each are observed for the *ipso*, *ortho*, *meta* and *para* carbons in **10a** and **10b**. Also, the oxidation of phosphorus in **10a** and **10b** is supported by the large ¹J_{PC-*ipso*} values³⁴ of 98 and 80 Hz, respectively.

In the ^{13}C NMR spectra of **12-14**, resonances are also observed for two nonequivalent phenyl rings. The multiplicities of these resonances vary, however. The *ortho* and *meta* resonances are "apparent" triplets with two much smaller, but observable, satellites. The couplings in these virtually coupled triplets are reported here as the separation between lines 2 and 4 (counting the smaller 2 satellites as 1 and 5) and these separations represent the sum of two coupling constants, $|^nJ_{\text{PC}} + {}^{n+2}J_{\text{PC}}|$. Phenyl *ipso* carbon resonances appear as five-line multiplets³⁵ for **12** and **13** but as doublets with a small center line for **14**. These multiplicities follow the trend expected for a decreasing value of $J_{\text{P-P}}$ for the heavier metals in Group VI for an AXX' spin system.³⁶ This spin system and its relevance to Group VI metal carbonyl complexes³⁷ has been fully detailed previously. All of the methylene carbons of ligand **6** exhibit similar five-line patterns, usually as "apparent" triplets, except for the central methylene in the cyclopentane ring which appears as a singlet in all metal complexes reported here.

The symmetry of **6** imposes an inequivalency upon the axial positions of octahedral metal complexes of this ligand. This asymmetry is revealed in the ^{13}C NMR spectra of **12-14**. In the spectrum of **13** for instance, three carbonyl resonances are observed. Two triplets of equal intensity at 212.0 and 206.0 ppm are assigned to two nonequivalent axial carbonyls. For the two equatorial carbonyls a five-line multiplet of the virtual type is observed at 215.9 ppm with twice the intensity of an axial carbonyl resonance.

As expected, the phenyl resonances for **15**, **16** and **18** show the presence of two nonequivalent phenyl rings, with multiplicities similar to those described for **12-14**. Also, the carbonyl regions of these spectra show only two resonances. In the ^{13}C NMR spectrum of **15** a five-line multiplet is observed at 219.9 ppm for the two equatorial carbonyls and a triplet with only half the intensity of the first resonance is observed at 229.0 for the axial carbonyl. This represents a considerable downfield shift of this

resonance upon coordination of the ether oxygen compared with the axial carbonyl chemical shifts for **13**. The lack of resonances corresponding to an additional axial carbonyl (or some other additional ligand) supports the assignment of a structure wherein **6** binds in a tridentate (*P,P,O*) manner. The changes observed in the CH₂O chemical shift upon coordination of the ether oxygen in **12-14** to the metal in **15**, **16** and **18** were small. Thus no diagnostic trend is apparent in these particular resonances for differentiating the bidentate (*P,P*) from tridentate (*P,P,O*) coordination modes.

Conclusions

We have synthesized a new diphosphine ether, **6**, capable of coordinating to metal carbonyl complexes in either a bidentate (*P,P*) or a tridentate (*P,P,O*) coordination mode as shown from the analysis of spectroscopic and structural data. The ¹H NMR spectra for the (*P,P*)-coordinated octahedral metal complexes of **6** studied here are consistent with the presence of a ligand whose conformational preference in solution is similar to that observed in the crystal structure of **13**.

The weak metal-O(ether) interactions in complexes such as **15**, **16** and **18** are expected to be quite labile. Results of substitution reactions of these complexes will be reported shortly. Further studies concerning the chemistry of **6** and its potential in catalytic systems are in progress.

ACKNOWLEDGMENTS

The authors thank the National Science Foundation and the Mallinckrodt Chemical Company for grant support of this research and the Department of Energy, Basic Energy Sciences, Materials Science Division (Contract No. W-7405-Eng-82) for support to Robert A. Jacobson. We also thank Dr. Lee M. Daniels of the Iowa State University Molecular Structure Laboratory and Yingzhong Su for the structural determinations of **13** and **16** respectively.

REFERENCES

1. Graziani, R.; Bombieri, G.; Yolponi, L.; Panattoni, C.; Clark, R. J. H. *J. Chem. Soc. (A)* **1969**, 1236.
2. (a) Miller, E. M.; Shaw, B. L. *J. Chem. Soc., Dalton Trans.* **1974**, 480. (b) Empsall, H. D.; Hyde, E. M.; Jones, C. E.; Shaw, B. L. *J. Chem. Soc., Dalton Trans.* **1974**, 1980.
3. (a) Knowles, W. S.; Sabacky, M. J.; Vineyard, B. D. *Chem. Commun.* **1972**, 10. (b) Vineyard, B. D.; Knowles, W. S.; Sabacky, M. J.; Bachman, G. L.; Weinkauff, D. J. *J. Am. Chem. Soc.* **1977**, *99*, 5946. (c) Knowles, W. S. *Acc. Chem. Res.* **1983**, *16*, 106.
4. (a) Horner, L.; Simmons, G. *Z. Naturforsch.* **1984**, *39b*, 497. (b) Brown, J. M.; Maddox, P. J. *J. Chem. Soc., Chem. Commun.* **1987**, 1276.
5. (a) Reddy, V. V. S.; Varshney, A.; Gray, G. M. *J. Organomet. Chem.* **1990**, *391*, 259. (b) Rauchfuss, T. B.; Patino, F. T.; Roundhill, D. M. *Inorg. Chem.* **1975**, *14*, 652. (c) Anderson, G. K.; Kumar, R. *Inorg. Chem.* **1984**, *23*, 4064. (d) Lindner, E.; Meyer, S. *J. Organomet. Chem.* **1988**, *339*, 193. (e) Lindner, E.; Schober, V.; Stangle, M. *J. Organomet. Chem.* **1987**, *331*, C13. (f) Lindner, E.; Schober, V. *Inorg. Chem.* **1988**, *27*, 212. (g) Lindner, E.; Mayer, H. A.; Wegner, P. *Chem. Ber.* **1986**, *119*, 2616. (h) Lindner, E.; Rauleder, H.; Scheytt, C.; Mayer, H. A.; Hiller, W.; Fawzi, R.; Wegner, P. *Z. Naturforsch.* **1984**, *39b*, 632. (i) Lindner, E.; Speidel, R. *Z. Naturforsch.* **1989**, *44b*, 437.
6. Jeffrey, J. C.; Rauchfuss, T. B. *Inorg. Chem.* **1979**, *18*, 2658.
7. Lindner, E.; Schober, V.; Fawzi, R.; Hiller, W.; Englert, V.; Wegner, P. *Chem. Ber.* **1987**, *120*, 1621.

8. Dunbar, K. R.; Haefner, S. C.; Pence, L. E. *J. Am. Chem. Soc.* **1989**, *111*, 5504.
9. Dunbar, K. R.; Haefner, S. C.; Burzynski, D. J. *Organometallics* **1990**, *9*, 1347.
10. Chen, S. J.; Dunbar, K. R. *Inorg. Chem.* **1990**, *29*, 588.
11. Alcock, N. W.; Brown, J. M.; Jeffrey, J. C. *J. Chem. Soc., Dalton Trans.* **1976**, 583.
12. (a) Lindner, E.; Bader, A.; Braunling, H.; Reinhard, J. *J. Mol. Catal.* **1990**, *57*, 291. (b) Lindner, E.; Norz, H. *Chem. Ber.* **1990**, *123*, 459. (c) Lindner, E.; Glaser, E. *J. Organomet. Chem.* **1990**, *391*, C37. (d) Lindner E.; Andres, B. *Chem. Ber.* **1988**, *121*, 829. (e) Lindner, E.; Sickinger, A.; Wegner, P. *J. Organomet. Chem.* **1988**, *349*, 75. (f) Lindner, E.; Schober, V.; Glaser, E.; Norz, H.; Wegner, P. *Z. Naturforsch.* **1987**, *42b*, 1527. (g) Lindner, E.; Andres, B. *Chem. Ber.* **1987**, *120*, 761. (h) Lindner, E.; Sickinger, A.; Wegner, P. *J. Organomet. Chem.* **1986**, *312*, C37.
13. Gudat, D.; Daniels, L. M.; Verkade, J. G. *Organometallics* **1990**, *9*, 1464.
14. Bianco, V. D.; Doronzo, S. *Inorg. Synth.* **1976**, *16*, 161.
15. Quick, M. H.; Angelici, R. J. *Inorg. Synth.* **1979**, *19*, 160.
16. Cotton, F. A.; McCleverty, J. A.; White, J. E. *Inorg. Synth.* **1967**, *9*, 121.
17. Kubas, G. J. *Inorg. Chem.* **1983**, *22*, 692.
18. Darensbourg, D. J.; Kump, R. L. *Inorg. Chem.* **1978**, *22*, 2680.
19. King, R. B.; Fronzaglia, A. *Inorg. Chem.* **1966**, *5*, 1837.
20. Bennett, M. A.; Pratt, L.; Wilkinson, G. *J. Chem. Soc.* **1961**, 1027.
21. Doyle, J. R.; Slade, P. E.; Jonassen, H. B. *Inorg. Synth.* **1960**, *6*, 218.
22. Weinges, K.; Klessing, K.; Kolb, R. *Chem. Ber.* **1973**, *106*, 2298.

23. Multiplets of an AXX' (A = ^{13}C ; X,X' = ^{31}P) spin system which resemble triplets are denoted as apparent triplets. See Discussion.
24. Enraf-Nonius Structure Determination Package; Enraf-Nonius: Delft, Holland.
25. TEXSAN-TEXRAY Structure Analysis Package, Molecular Structure Corporation (1985).
26. Cromer, D. T.; Waber, J. T. *International Tables for X-ray Crystallography*; The Kynoch Press: Birmingham, England, 1974; Vol. IV.
27. Wroblewski, A.; Verkade, J. G., to be published.
28. Weinges, K.; Wiesenhutter, A. *Liebigs Ann. Chem.* **1971**, *746*, 70.
29. (a) Lindner, E.; Andres, B. *Chem. Ber.* **1988**, *121*, 829. (b) McCann, G. M.; Carvill, A.; Lindner, E.; Karle, B.; Mayer, H. A. *J. Chem. Soc., Dalton Trans.* **1990**, 3107.
30. (a) Uguagliati, P.; Deganello, G.; Busetto, L.; Belluco, U. *Inorg. Chem.* **1969**, *8*, 1625. (b) Rosenthal, M. R.; Drago, R. S. *Inorg. Chem.* **1965**, *4*, 840.
31. Bernal, I.; Reisner, G. M.; Dobson, G. R.; Dobson, C. B. *Inorg. Chim. Acta.* **1986**, *121*, 199 and references therein.
32. The covalent radii of tungsten and molybdenum are approximately the same, 1.46 Å and 1.45 Å, respectively. See Pauling, L. *Nature of the Chemical Bond*; 3rd ed.; Cornell University Press: Ithaca, NY, 1960; pp 224-249.
33. Silverstein, R. M.; Bassler, G. C.; Morrill, T. C. *Spectrometric Identification of Organic Compounds*, 4th ed.; John Wiley and Sons, New York, 1981; p 209.
34. (a) Modro, T. A. *Can. J. Chem.* **1977**, *55*, 3681. (b) Albright, T. A.; Freeman, W. J.; Schweizer, E. E. *J. Org. Chem.* **1975**, *40*, 3437.
35. The small central line of these five-line multiplets is actually comprised of two lines which are resolved in some spectra. Six lines are expected for the X portion of an

- ABX system. See: Pople, J. A.; Schneider, W. G.; Bernstein, H. J. *High Resolution Nuclear Magnetic Resonance*; McGraw-Hill Book Co., New York, 1959; pp 132-135.
36. (a) Pregosin, P. S.; Kunz, R. W. *NMR: Basic Princ. Progr.* **1979**, *16*, 65. (b) Redfield, D. A.; Nelson, J. H.; Carey, L. W. *Inorg. Nucl. Chem. Letters* **1974**, *10*, 727.
37. Andrews, G. T.; Colquhoun, I. J.; McFarlane, W. *Polyhedron* **1983**, *2*, 783.

SUPPLEMENTARY MATERIAL

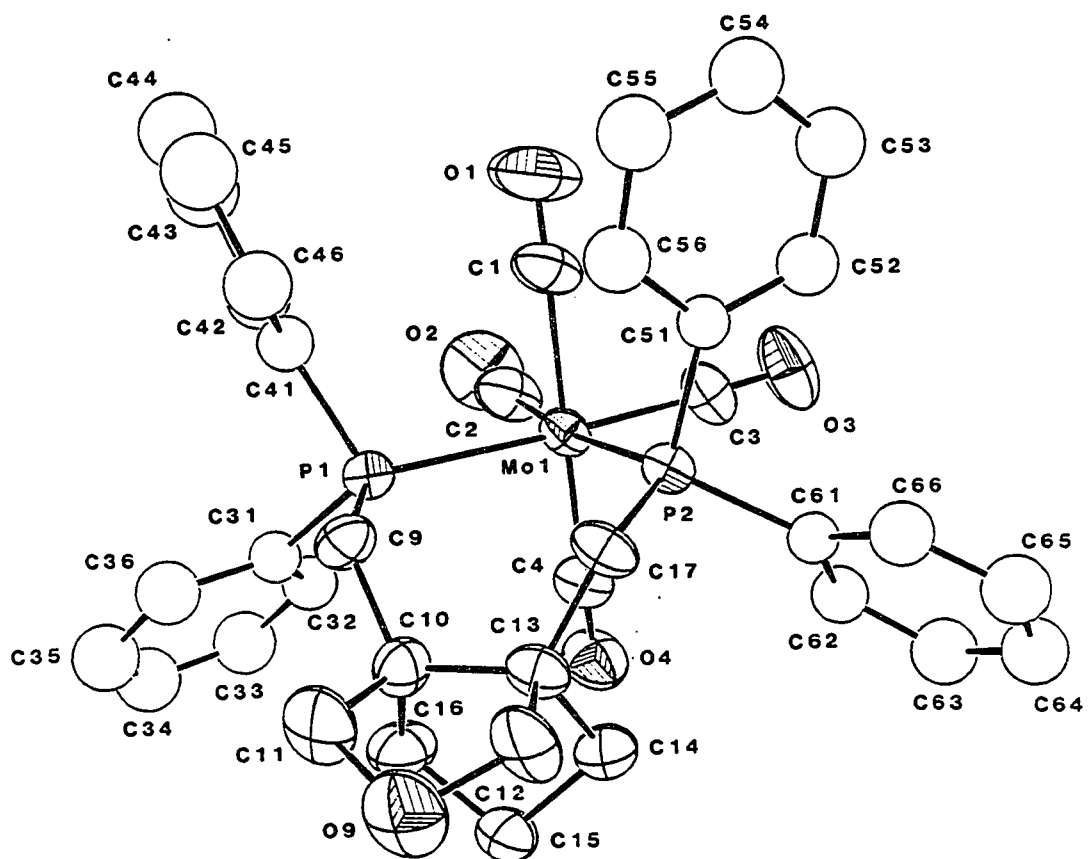


Figure 1. ORTEP drawing and complete labeling scheme of the first of two independent molecules of **13**

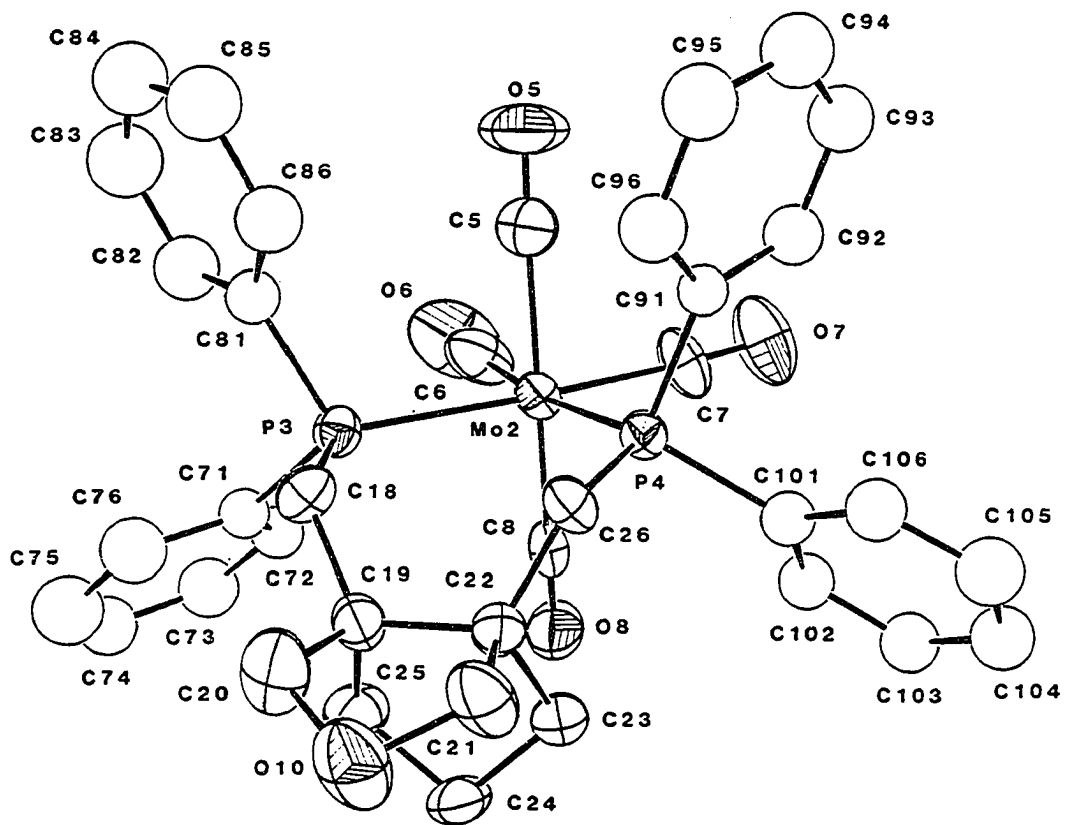


Figure 2. ORTEP drawing and complete labeling scheme of the second independent molecule of 13.

Table 1. Bond distances (Å) for (6)Mo(CO)₄, 13

Mo(1)-P(1)	2.544(2)	P(4)-C(26)	1.851(8)
Mo(1)-P(2)	2.546(2)	P(4)-C(91)	1.832(7)
Mo(1)-C(1)	2.061(9)	P(4)-C(101)	1.866(6)
Mo(1)-C(2)	1.983(8)	O(9)-C(11)	1.41(1)
Mo(1)-C(3)	1.981(9)	O(9)-C(12)	1.41(1)
Mo(1)-C(4)	2.021(8)	O(10)-C(20)	1.41(1)
Mo(2)-P(3)	2.543(2)	O(10)-C(21)	1.44(1)
Mo(2)-P(4)	2.539(2)	C(9)-C(10)	1.55(1)
Mo(2)-C(5)	2.048(8)	C(10)-C(11)	1.54(1)
Mo(2)-C(6)	1.980(9)	C(10)-C(13)	1.59(1)
Mo(2)-C(7)	1.965(8)	C(10)-C(16)	1.55(1)
Mo(2)-C(8)	2.011(7)	C(12)-C(13)	1.55(1)
P(1)-C(9)	1.840(7)	C(13)-C(14)	1.55(1)
P(1)-C(31)	1.842(8)	C(13)-C(17)	1.52(1)
P(1)-C(41)	1.838(8)	C(14)-C(15)	1.54(1)
P(2)-C(17)	1.853(7)	C(15)-C(16)	1.52(1)
P(2)-C(51)	1.843(7)	C(18)-C(19)	1.55(1)
P(2)-C(61)	1.839(8)	C(19)-C(20)	1.53(1)
P(3)-C(18)	1.845(8)	C(19)-C(22)	1.58(1)
P(3)-C(71)	1.837(7)	C(19)-C(25)	1.55(1)
P(3)-C(81)	1.840(7)	C(21)-C(22)	1.57(1)

Table 1. Continued

C(22)-C(26)	1.54(1)	C(61)-C(62)	1.38(1)
C(23)-C(24)	1.49(1)	C(61)-C(66)	1.40(1)
C(24)-C(25)	1.50(1)	C(62)-C(63)	1.37(1)
C(31)-C(32)	1.38(1)	C(63)-C(64)	1.38(1)
C(31)-C(36)	1.39(1)	C(64)-C(65)	1.40(1)
C(32)-C(33)	1.40(1)	C(65)-C(66)	1.36(1)
C(33)-C(34)	1.35(1)	C(71)-C(72)	1.38(1)
C(34)-C(35)	1.36(1)	C(71)-C(76)	1.39(1)
C(35)-C(36)	1.39(1)	C(72)-C(73)	1.40(1)
C(41)-C(42)	1.37(1)	C(73)-C(74)	1.35(1)
C(41)-C(46)	1.38(1)	C(74)-C(75)	1.35(1)
C(42)-C(43)	1.43(1)	C(75)-C(76)	1.38(1)
C(43)-C(44)	1.33(2)	C(81)-C(82)	1.38(1)
C(44)-C(45)	1.35(1)	C(81)-C(86)	1.37(1)
C(45)-C(46)	1.43(1)	C(82)-C(83)	1.42(1)
C(51)-C(52)	1.36(1)	C(83)-C(84)	1.38(1)
C(51)-C(56)	1.38(1)	C(84)-C(85)	1.37(1)
C(52)-C(53)	1.40(1)	C(85)-C(86)	1.42(1)
C(53)-C(54)	1.37(1)	C(91)-C(92)	1.37(1)
C(54)-C(55)	1.37(1)	C(91)-C(96)	1.38(1)
C(55)-C(56)	1.40(1)	C(92)-C(93)	1.40(1)

Table 1. Continued

C(93)-C(94)	1.33(1)	C(104)-C(105)	1.37(1)
C(94)-C(95)	1.39(1)	C(105)-C(106)	1.40(1)
C(95)-C(96)	1.41(1)	C(S1)-Cl(1)	1.78(2)
C(101)-C(102)	1.37(1)	C(S1)-Cl(2)	1.61(2)
C(101)-C(106)	1.37(1)	C(S2)-Cl(3)	1.44(3)
C(102)-C(103)	1.39(1)	C(S2)-Cl(4)	1.53(4)
C(103)-C(104)	1.37(1)		

Table 2. Bond angles (deg) for (6)Mo(CO)₄, 13

P(1)-Mo(1)-P(2)	93.05(6)	C(5)-Mo(2)-C(7)	87.7(3)
P(1)-Mo(1)-C(1)	90.0(3)	C(5)-Mo(2)-C(8)	174.1(4)
P(1)-Mo(1)-C(2)	92.8(3)	C(6)-Mo(2)-C(7)	87.4(4)
P(1)-Mo(1)-C(3)	176.0(2)	C(6)-Mo(2)-C(8)	86.5(3)
P(1)-Mo(1)-C(4)	93.2(2)	C(7)-Mo(2)-C(8)	90.0(3)
P(2)-Mo(1)-C(1)	89.4(2)	Mo(1)-P(1)-C(9)	119.7(3)
P(2)-Mo(1)-C(2)	173.0(3)	Mo(1)-P(1)-C(31)	119.6(3)
P(2)-Mo(1)-C(3)	84.8(2)	Mo(1)-P(1)-C(41)	109.9(3)
P(2)-Mo(1)-C(4)	96.9(2)	C(9)-P(1)-C(31)	102.3(3)
C(1)-Mo(1)-C(2)	86.7(3)	C(9)-P(1)-C(41)	101.6(4)
C(1)-Mo(1)-C(3)	86.6(4)	C(31)-P(1)-C(41)	100.8(4)
C(1)-Mo(1)-C(4)	172.7(3)	Mo(1)-P(2)-C(17)	125.1(3)
C(2)-Mo(1)-C(3)	89.1(4)	Mo(1)-P(2)-C(51)	107.8(2)
C(2)-Mo(1)-C(4)	86.6(3)	Mo(1)-P(2)-C(61)	117.8(2)
C(3)-Mo(1)-C(4)	90.3(3)	C(17)-P(2)-C(51)	100.3(3)
P(3)-Mo(2)-P(4)	94.00(7)	C(17)-P(2)-C(61)	100.3(3)
P(3)-Mo(2)-C(5)	89.9(2)	C(51)-P(2)-C(61)	102.1(3)
P(3)-Mo(2)-C(6)	91.4(3)	Mo(2)-P(3)-C(18)	120.2(2)
P(3)-Mo(2)-C(7)	177.4(2)	Mo(2)-P(3)-C(71)	118.3(2)
P(3)-Mo(2)-C(8)	92.3(2)	Mo(2)-P(3)-C(81)	111.9(3)
P(4)-Mo(2)-C(5)	88.5(3)	C(18)-P(3)-C(71)	103.5(4)
P(4)-Mo(2)-C(6)	173.5(3)	C(18)-P(3)-C(81)	99.1(3)
P(4)-Mo(2)-C(7)	87.0(3)	C(71)-P(3)-C(81)	100.5(3)

Table 2. Continued

P(4)-Mo(2)-C(8)	96.8(2)	Mo(2)-P(4)-C(26)	124.6(2)
C(5)-Mo(2)-C(6)	88.0(4)	Mo(2)-P(4)-C(91)	109.3(2)
Mo(2)-P(4)-C(101)	117.3(3)	P(3)-C(18)-C(19)	123.1(5)
C(26)-P(4)-C(91)	100.6(3)	C(18)-C(19)-C(20)	106.9(6)
C(26)-P(4)-C(101)	101.9(3)	C(18)-C(19)-C(22)	118.7(6)
C(91)-P(4)-C(101)	99.2(3)	C(18)-C(19)-C(25)	112.7(6)
C(11)-O(9)-C(12)	104.4(6)	C(20)-C(19)-C(22)	103.1(6)
C(20)-O(10)-C(21)	103.8(7)	C(20)-C(19)-C(25)	110.8(7)
P(1)-C(9)-C(10)	121.5(6)	C(22)-C(19)-C(25)	104.1(5)
C(9)-C(10)-C(11)	106.0(7)	O(10)-C(20)-C(19)	107.8(6)
C(9)-C(10)-C(13)	117.8(6)	O(10)-C(21)-C(22)	107.3(6)
C(9)-C(10)-C(16)	114.3(6)	C(19)-C(22)-C(21)	101.4(6)
C(11)-C(10)-C(13)	102.0(6)	C(19)-C(22)-C(23)	104.1(6)
C(11)-C(10)-C(16)	111.1(7)	C(19)-C(22)-C(26)	118.7(6)
C(13)-C(10)-C(16)	105.1(7)	C(21)-C(22)-C(23)	109.3(6)
O(9)-C(11)-C(10)	107.1(7)	C(21)-C(22)-C(26)	106.6(6)
O(9)-C(12)-C(13)	107.9(6)	C(23)-C(22)-C(26)	115.8(6)
C(10)-C(13)-C(12)	101.9(6)	C(22)-C(23)-C(24)	106.1(6)
C(10)-C(13)-C(14)	104.6(6)	C(23)-C(24)-C(25)	103.0(6)
C(10)-C(13)-C(17)	119.0(6)	C(19)-C(25)-C(24)	105.9(6)
C(12)-C(13)-C(14)	109.9(6)	P(4)-C(26)-C(22)	119.2(5)
C(12)-C(13)-C(17)	106.7(6)	P(1)-C(31)-C(32)	121.1(6)

Table 2. Continued

C(14)-C(13)-C(17)	114.0(7)	P(1)-C(31)-C(36)	120.7(6)
C(13)-C(14)-C(15)	104.4(7)	C(32)-C(31)-C(36)	118.3(7)
C(14)-C(15)-C(16)	102.6(6)	C(31)-C(32)-C(33)	120.7(8)
C(10)-C(16)-C(15)	105.6(6)	C(32)-C(33)-C(34)	119.7(9)
P(2)-C(17)-C(13)	120.1(5)	C(33)-C(34)-C(35)	120.9(9)
C(34)-C(35)-C(36)	120(1)	C(61)-C(66)-C(65)	122.6(8)
C(31)-C(36)-C(35)	119.9(8)	P(3)-C(71)-C(72)	121.4(6)
P(1)-C(41)-C(42)	117.5(7)	P(3)-C(71)-C(76)	120.9(6)
P(1)-C(41)-C(46)	123.7(5)	C(72)-C(71)-C(76)	117.6(7)
C(42)-C(41)-C(46)	118.6(8)	C(71)-C(72)-C(73)	121.2(7)
C(41)-C(42)-C(43)	121.1(8)	C(72)-C(73)-C(74)	119.9(8)
C(42)-C(43)-C(44)	118.1(8)	C(73)-C(74)-C(75)	119.6(8)
C(43)-C(44)-C(45)	124.(1)	C(74)-C(75)-C(76)	121.6(9)
C(44)-C(45)-C(46)	118(1)	C(71)-C(76)-C(75)	120.0(9)
C(41)-C(46)-C(45)	120.1(7)	P(3)-C(81)-C(82)	120.1(6)
P(2)-C(51)-C(52)	121.3(6)	P(3)-C(81)-C(86)	119.7(6)
P(2)-C(51)-C(56)	119.4(6)	C(82)-C(81)-C(86)	120.0(7)
C(52)-C(51)-C(56)	118.9(7)	C(81)-C(82)-C(83)	119.5(8)
C(51)-C(52)-C(53)	120.7(8)	C(82)-C(83)-C(84)	120.3(9)
C(52)-C(53)-C(54)	119.4(9)	C(83)-C(84)-C(85)	120.0(8)
C(53)-C(54)-C(55)	121.2(9)	C(84)-C(85)-C(86)	119.6(9)
C(54)-C(55)-C(56)	118.6(9)	C(81)-C(86)-C(85)	120.4(8)

Table 2. Continued

C(51)-C(56)-C(55)	121.3(8)	P(4)-C(91)-C(92)	119.2(5)
P(2)-C(61)-C(62)	121.2(5)	P(4)-C(91)-C(96)	123.0(6)
P(2)-C(61)-C(66)	122.1(6)	C(92)-C(91)-C(96)	117.8(7)
C(62)-C(61)-C(66)	116.7(7)	C(91)-C(92)-C(93)	121.5(7)
C(61)-C(62)-C(63)	121.7(7)	C(92)-C(93)-C(94)	120.0(8)
C(62)-C(63)-C(64)	120.7(9)	C(93)-C(94)-C(95)	121.7(9)
C(63)-C(64)-C(65)	118.5(9)	C(94)-C(95)-C(96)	117.4(8)
C(64)-C(65)-C(66)	119.8(8)	C(91)-C(96)-C(95)	121.7(8)
P(4)-C(101)-C(102)	121.1(5)	C(103)-C(104)-C(105)	120.2(7)
P(4)-C(101)-C(106)	119.2(5)	C(104)-C(105)-C(106)	120.1(8)
C(102)-C(101)-C(106)	119.7(6)	C(101)-C(106)-C(105)	119.7(7)
C(101)-C(102)-C(103)	121.0(7)	Cl(1)-C(S1)-Cl(2)	114.(1)
C(102)-C(103)-C(104)	119.2(8)	Cl(3)-C(S2)-Cl(4)	135.(2)

Table 3. Positional parameters and thermal parameters for (6)Mo(CO)₄, 13

Atom	x	y	z	B, b(Å ²)
Mo(1)	0.14772(4)	0.27904(3)	0.08485(6)	2.75(1)
Mo(2)	0.67550(4)	0.25534(3)	-0.35070(5)	2.54(1)
P(1)	0.2753(1)	0.32355(9)	0.1514(2)	2.78(4)
P(2)	0.2589(1)	0.18276(9)	-0.0085(2)	2.64(4)
P(3)	0.8379(1)	0.21541(8)	-0.4259(2)	2.59(4)
P(4)	0.7019(1)	0.34917(8)	-0.2456(2)	2.49(4)
O(1)	0.1215(5)	0.3550(3)	-0.1559(6)	7.4(2)
O(2)	-0.0106(5)	0.3947(3)	0.1704(7)	7.2(2)
O(3)	-0.0056(4)	0.2262(3)	-0.0152(6)	6.1(2)
O(4)	0.1331(4)	0.2205(3)	0.3322(5)	4.9(1)
O(5)	0.7361(5)	0.1747(3)	-0.1163(6)	7.2(2)
O(6)	0.6212(5)	0.1419(3)	-0.4588(7)	8.0(2)
O(7)	0.4780(4)	0.2962(3)	-0.2510(6)	6.7(2)
O(8)	0.5930(4)	0.3216(3)	-0.5912(5)	4.7(2)
O(9)	0.5767(4)	0.1316(3)	0.2240(6)	5.9(2)
O(10)	0.9646(4)	0.4110(3)	-0.4608(6)	5.9(2)

^a Atoms with an asterisk were refined isotropically.

^b Anisotropically refined atoms are given in the form of the isotropic equivalent displacement parameter defined as: $4/3[a^2B(1,1) + b^2B(2,2) + c^2B(3,3) + ab(\cos \gamma)B(1,2) + ac(\cos \beta)B(1,3) + bc(\cos \alpha)B(2,3)]$.

Table 3. Continued

Atom	x	y	z	B, ^b (Å ²)
C(1)	0.1349(6)	0.3260(4)	-0.0729(8)	4.4(2)
C(2)	0.0503(6)	0.3534(4)	0.1419(7)	4.5(2)
C(3)	0.0514(5)	0.2443(4)	0.0218(7)	4.0(2)
C(4)	0.1437(5)	0.2399(4)	0.2432(7)	3.3(2)
C(5)	0.7182(6)	0.2043(4)	-0.1996(7)	4.1(2)
C(6)	0.6454(6)	0.1820(4)	-0.4183(8)	4.9(2)
C(7)	0.5514(5)	0.2828(4)	-0.2879(7)	4.1(2)
C(8)	0.6262(5)	0.2994(3)	-0.5033(7)	3.0(2)
C(9)	0.3959(5)	0.2747(3)	0.1422(7)	3.2(2)
C(10)	0.4330(5)	0.2115(3)	0.2086(7)	3.2(2)
C(11)	0.5376(6)	0.1976(4)	0.2191(9)	5.2(2)
C(12)	0.5260(5)	0.1090(4)	0.1392(8)	4.5(2)
C(13)	0.4241(5)	0.1503(3)	0.1444(7)	3.0(2)
C(14)	0.3727(5)	0.1213(4)	0.2322(7)	3.8(2)
C(15)	0.3974(6)	0.1433(4)	0.3535(7)	4.0(2)
C(16)	0.3914(6)	0.2112(4)	0.3308(7)	4.3(2)
C(17)	0.3848(5)	0.1556(3)	0.0191(7)	3.1(2)
C(18)	0.9159(5)	0.2636(3)	-0.4084(7)	2.9(2)
C(19)	0.8936(5)	0.3306(3)	-0.4597(7)	3.0(2)
C(20)	0.9843(6)	0.3452(4)	-0.4654(9)	4.9(2)

Table 3. Continued

Atom	x	y	z	B, ^b (Å ²)
C(21)	0.8959(6)	0.4302(4)	-0.3724(8)	4.3(2)
C(22)	0.8312(5)	0.3879(3)	-0.3874(7)	2.8(2)
C(23)	0.7517(5)	0.4197(3)	-0.4733(7)	3.7(2)
C(24)	0.7882(6)	0.4046(3)	-0.5932(7)	3.8(2)
C(25)	0.8453(6)	0.3372(4)	-0.5825(7)	4.3(2)
C(26)	0.8038(5)	0.3757(3)	-0.2632(6)	2.9(2)
C(31)	0.2728(5)	0.3586(3)	0.2989(7)	3.1(1)*
C(32)	0.1988(5)	0.3664(4)	0.3698(7)	3.7(2)*
C(33)	0.1985(6)	0.3913(4)	0.4828(9)	5.1(2)*
C(34)	0.2721(6)	0.4067(4)	0.5239(8)	5.0(2)*
C(35)	0.3451(6)	0.4007(4)	0.4554(9)	5.3(2)*
C(36)	0.3461(6)	0.3772(4)	0.3419(8)	4.3(2)*
C(41)	0.2729(5)	0.3909(3)	0.0585(7)	3.4(2)*
C(42)	0.2023(6)	0.4454(4)	0.0728(8)	4.6(2)*
C(43)	0.1909(7)	0.4981(5)	-0.0023(9)	5.9(2)*
C(44)	0.2509(7)	0.4930(5)	-0.086(1)	6.2(2)*
C(45)	0.3221(7)	0.4408(5)	-0.104(1)	6.1(2)*
C(46)	0.3336(6)	0.3881(4)	-0.0294(8)	4.8(2)*
C(51)	0.2539(5)	0.1959(3)	-0.1686(6)	2.8(1)*
C(52)	0.1917(5)	0.1796(4)	-0.2398(7)	3.8(2)*

Table 3. Continued

Atom	x	y	z	B, b(Å ²)
C(53)	0.1835(6)	0.1945(4)	-0.3602(8)	4.6(2)*
C(54)	0.2372(6)	0.2270(4)	-0.4054(8)	4.9(2)*
C(55)	0.2985(6)	0.2455(4)	-0.3352(8)	5.0(2)*
C(56)	0.3064(6)	0.2296(4)	-0.2157(8)	4.2(2)*
C(61)	0.2338(5)	0.1077(3)	0.0013(6)	2.7(1)*
C(62)	0.1761(5)	0.0981(3)	0.0847(7)	3.5(2)*
C(63)	0.1611(6)	0.0412(4)	0.0971(8)	4.6(2)*
C(64)	0.2006(6)	-0.0081(4)	0.0222(8)	4.7(2)*
C(65)	0.2573(6)	0.0011(4)	-0.0650(8)	4.6(2)*
C(66)	0.2728(6)	0.0574(4)	-0.0739(7)	4.0(2)*
C(71)	0.8535(5)	0.1878(3)	-0.5786(6)	2.6(1)*
C(72)	0.7829(5)	0.1770(3)	-0.6443(7)	3.3(2)*
C(73)	0.7959(6)	0.1540(4)	-0.7595(8)	4.2(2)*
C(74)	0.8789(6)	0.1428(4)	-0.8085(8)	4.2(2)*
C(75)	0.9489(6)	0.1530(4)	-0.7449(9)	5.4(2)*
C(76)	0.9386(6)	0.1740(4)	-0.6298(8)	4.8(2)*
C(81)	0.9074(5)	0.1445(3)	-0.3468(7)	3.0(1)*
C(82)	0.9173(6)	0.0860(4)	-0.3939(8)	4.5(2)*
C(83)	0.9683(7)	0.0317(5)	-0.3302(9)	5.9(2)*
C(84)	1.0065(6)	0.0374(4)	-0.2208(9)	5.2(2)*

Table 3. Continued

Atom	x	y	z	B, b(Å ²)
C(85)	0.9940(6)	0.0955(4)	-0.1725(9)	5.3(2)*
C(86)	0.9429(6)	0.1500(4)	-0.2366(8)	4.5(2)*
C(91)	0.7079(5)	0.3357(3)	-0.0865(6)	2.5(1)*
C(92)	0.6300(5)	0.3364(4)	-0.0304(7)	3.6(2)*
C(93)	0.6315(6)	0.3243(4)	0.0899(7)	4.1(2)*
C(94)	0.7101(6)	0.3111(4)	0.1523(8)	4.7(2)*
C(95)	0.7918(6)	0.3101(4)	0.1011(8)	5.0(2)*
C(96)	0.7887(6)	0.3226(4)	-0.0203(8)	4.0(2)*
C(101)	0.6066(5)	0.4249(3)	-0.2526(6)	2.8(1)*
C(102)	0.5385(5)	0.4354(3)	-0.3375(7)	3.3(2)*
C(103)	0.4672(5)	0.4917(4)	-0.3422(7)	3.9(2)*
C(104)	0.4633(6)	0.5359(4)	-0.2572(7)	4.0(2)*
C(105)	0.5303(6)	0.5252(4)	-0.1698(8)	4.4(2)*
C(106)	0.6038(5)	0.4698(4)	-0.1690(7)	3.8(2)*
C(S1)	0.510(1)	0.9135(8)	0.330(2)	11.3(5)*
Cl(1)	0.4330(4)	0.9274(3)	0.2061(4)	12.4(2)
Cl(2)	0.5631(4)	0.9652(2)	0.3480(5)	12.4(2)
C(S2)	0.249(2)	0.015(1)	0.490(3)	20(1)*
Cl(3)	0.2030(4)	0.0640(3)	0.4069(4)	13.5(2)
Cl(4)	0.2240(5)	-0.0075(3)	0.6068(5)	17.8(2)

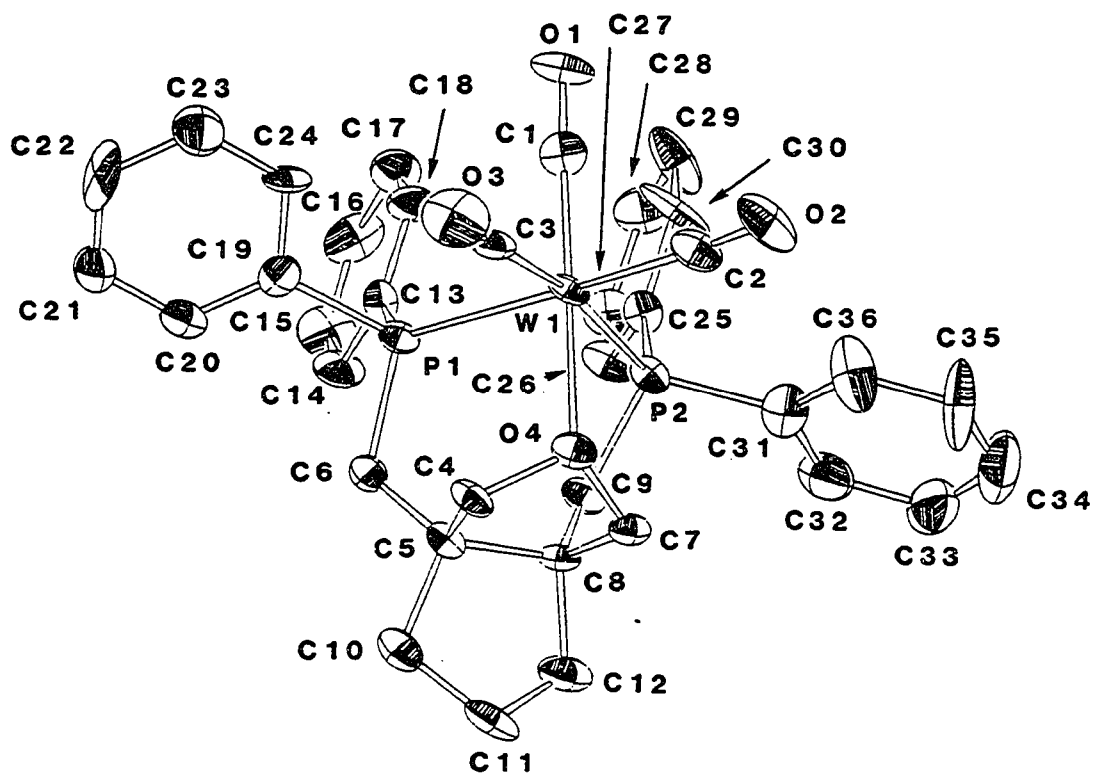


Figure 3. ORTEP drawing and complete labeling scheme for 16.

Table 4. Bond distances (Å)^a for (6)W(CO)₃, 16

W(1)-P(1)	2.558(5)	C(6)-H(4)	0.950
W(1)-P(2)	2.550(5)	C(7)-C(8)	1.55(3)
W(1)-O(4)	2.33(1)	C(7)-H(5)	0.950
W(1)-C(1)	1.91(2)	C(7)-H(6)	0.950
W(1)-C(2)	1.98(2)	C(8)-C(9)	1.54(3)
W(1)-C(3)	1.98(2)	C(8)-C(12)	1.55(3)
Cl(1)-C(37)	1.72(4)	C(9)-H(7)	0.950
Cl(2)-C(37)	1.62(4)	C(9)-H(8)	0.950
P(1)-C(6)	1.86(2)	C(10)-C(11)	1.50(3)
P(1)-C(13)	1.83(2)	C(10)-H(9)	0.950
P(1)-C(19)	1.85(2)	C(10)-H(10)	0.950
P(2)-C(9)	1.84(2)	C(11)-C(12)	1.54(3)
P(2)-C(25)	1.84(2)	C(11)-H(11)	0.950
P(2)-C(31)	1.82(2)	C(11)-H(12)	0.950
O(1)-C(1)	1.19(2)	C(12)-H(13)	0.950
O(2)-C(2)	1.15(3)	C(12)-H(14)	0.950
O(3)-C(3)	1.12(3)	C(13)-C(14)	1.45(3)
O(4)-C(4)	1.46(2)	C(13)-C(18)	1.41(3)
O(4)-C(7)	1.45(2)	C(14)-C(15)	1.40(3)

^a Numbers in parentheses are estimated standard deviations in the least significant digits.

Table 4. Continued

C(4)-C(5)	1.55(3)	C(14)-H(15)	0.950
C(4)-H(1)	0.950	C(15)-C(16)	1.34(3)
C(4)-H(2)	0.950	C(15)-H(16)	0.950
C(5)-C(6)	1.52(3)	C(16)-C(17)	1.41(3)
C(5)-C(8)	1.62(3)	C(16)-H(17)	0.950
C(5)-C(10)	1.56(3)	C(17)-C(18)	1.35(3)
C(6)-H(3)	0.950	C(17)-H(18)	0.950
C(18)-H(19)	0.950	C(28)-C(29)	1.42(3)
C(19)-C(20)	1.38(3)	C(28)-H(27)	0.950
C(19)-C(24)	1.37(3)	C(29)-C(30)	1.35(3)
C(20)-C(21)	1.37(3)	C(29)-H(28)	0.950
C(20)-H(20)	0.949	C(30)-H(29)	0.950
C(21)-C(22)	1.35(4)	C(31)-C(32)	1.38(3)
C(21)-H(21)	0.950	C(31)-C(36)	1.36(4)
C(22)-C(23)	1.38(4)	C(32)-C(33)	1.43(3)
C(22)-H(22)	0.950	C(32)-H(30)	0.949
C(23)-C(24)	1.37(3)	C(33)-C(34)	1.40(4)
C(23)-H(23)	0.950	C(33)-H(31)	0.950
C(24)-H(24)	0.950	C(34)-C(35)	1.30(4)
C(25)-C(26)	1.41(3)	C(34)-H(32)	0.950
C(25)-C(30)	1.41(3)	C(35)-C(36)	1.41(4)

Table 4. Continued

C(26)-C(27)	1.37(3)	C(35)-H(33)	0.950
C(26)-H(25)	0.951	C(36)-H(34)	0.950
C(27)-C(28)	1.39(3)	C(37)-H(35)	0.952
C(27)-H(26)	0.951	C(37)-H(36)	0.946

Table 5. Bond angles (deg)^a for (6)W(CO)₃, 16

P(1)-W(1)-P(2)	83.2(2)	C(25)-P(2)-C(31)	99.8(9)
P(1)-W(1)-O(4)	88.6(4)	W(1)-O(4)-C(4)	114(1)
P(1)-W(1)-C(1)	92.1(7)	W(1)-O(4)-C(7)	119(1)
P(1)-W(1)-C(2)	178.1(6)	C(4)-O(4)-C(7)	101(1)
P(1)-W(1)-C(3)	91.4(6)	W(1)-C(1)-O(1)	176(2)
P(2)-W(1)-O(4)	83.2(3)	W(1)-C(2)-O(2)	175(2)
P(2)-W(1)-C(1)	98.7(6)	W(1)-C(3)-O(3)	176(2)
P(2)-W(1)-C(2)	98.8(6)	O(4)-C(4)-C(5)	105(1)
P(2)-W(1)-C(3)	170.5(6)	O(4)-C(4)-H(1)	110.65
O(4)-W(1)-C(1)	178.0(7)	O(4)-C(4)-H(2)	110.54
O(4)-W(1)-C(2)	91.5(7)	C(5)-C(4)-H(1)	110.58
O(4)-W(1)-C(3)	88.9(7)	C(5)-C(4)-H(2)	110.55
C(1)-W(1)-C(2)	87.7(9)	H(1)-C(4)-H(2)	109.47
C(1)-W(1)-C(3)	89.3(9)	C(4)-C(5)-C(6)	112(1)
C(2)-W(1)-C(3)	86.7(9)	C(4)-C(5)-C(8)	103(1)
W(1)-P(1)-C(6)	113.7(6)	C(4)-C(5)-C(10)	110(1)
W(1)-P(1)-C(13)	118.9(7)	C(6)-C(5)-C(8)	119(2)
W(1)-P(1)-C(19)	116.0(7)	C(6)-C(5)-C(10)	109(2)
C(6)-P(1)-C(13)	105.5(9)	C(8)-C(5)-C(10)	104(1)

^a Numbers in parentheses are estimated standard deviations in the least significant digits.

Table 5. Continued

C(6)-P(1)-C(19)	104.0(9)	P(1)-C(6)-C(5)	117(1)
C1(3)-P(1)-C(19)	96.3(9)	P(1)-C(6)-H(3)	107.62
W(1)-P(2)-C(9)	107.9(6)	P(1)-C(6)-H(4)	107.62
W(1)-P(2)-C(25)	118.9(6)	C(5)-C(6)-H(3)	107.63
W(1)-P(2)-C(31)	121.2(7)	C(5)-C(6)-H(4)	107.61
C(9)-P(2)-C(25)	104.3(9)	H(3)-C(6)-H(4)	109.48
C(9)-P(2)-C(31)	102(1)	O(4)-C(7)-C(8)	105(1)
O(4)-C(7)-H(5)	110.62	C(12)-C(11)-H(11)	110.94
O(4)-C(7)-H(6)	110.65	C(12)-C(11)-H(12)	110.95
C(8)-C(7)-H(5)	110.64	H(11)-C(11)-H(12)	109.44
C(8)-C(7)-H(6)	110.60	C(8)-C(12)-C(11)	105(2)
H(5)-C(7)-H(6)	109.44	C(8)-C(12)-H(13)	110.66
C(5)-C(8)-C(7)	101(1)	C(8)-C(12)-H(14)	110.70
C(5)-C(8)-C(9)	116(2)	C(11)-C(12)-H(13)	110.70
C(5)-C(8)-C(12)	105(1)	C(11)-C(12)-H(14)	110.73
C(7)-C(8)-C(9)	113(1)	H(13)-C(12)-H(14)	109.46
C(7)-C(8)-C(12)	109(2)	P(1)-C(13)-C(14)	124(2)
C(9)-C(8)-C(12)	112(2)	P(1)-C(13)-C(18)	119(2)
P(2)-C(9)-C(8)	116(1)	C(14)-C(13)-C(18)	117(2)
P(2)-C(9)-H(7)	107.77	C(13)-C(14)-C(15)	118(2)
P(2)-C(9)-H(8)	107.76	C(13)-C(14)-H(15)	120.97

Table 5. Continued

C(8)-C(9)-H(7)	107.75	C(15)-C(14)-H(15)	120.87
C(8)-C(9)-H(8)	107.74	C(14)-C(15)-C(16)	122(2)
H(7)-C(9)-H(8)	109.48	C(14)-C(15)-H(16)	118.95
C(5)-C(10)-C(11)	106(2)	C(16)-C(15)-H(16)	118.95
C(5)-C(10)-H(9)	110.30	C(15)-C(16)-C(17)	120(2)
C(5)-C(10)-H(10)	110.31	C(15)-C(16)-H(17)	119.93
C(11)-C(10)-H(9)	110.29	C(17)-C(16)-H(17)	119.89
C(11)-C(10)-H(10)	110.29	C(16)-C(17)-C(18)	120(2)
H(9)-C(10)-H(10)	109.44	C(16)-C(17)-H(18)	119.88
C(10)-C(11)-C(12)	104(2)	C(18)-C(17)-H(18)	119.98
C(10)-C(11)-H(11)	110.94	C(13)-C(18)-C(17)	122(2)
C(10)-C(11)-H(12)	110.94	C(13)-C(18)-H(19)	119.07
C(17)-C(18)-H(19)	119.07	C(26)-C(27)-H(26)	119.82
P(1)-C(19)-C(20)	121(2)	C(28)-C(27)-H(26)	119.84
P(1)-C(19)-C(24)	119(2)	C(27)-C(28)-C(29)	121(2)
C(20)-C(19)-C(24)	120(2)	C(27)-C(28)-H(27)	119.53
C(19)-C(20)-C(21)	120(2)	C(29)-C(28)-H(27)	119.50
C(19)-C(20)-H(20)	119.75	C(28)-C(29)-C(30)	119(2)
C(21)-C(20)-H(20)	119.76	C(28)-C(29)-H(28)	120.54
C(20)-C(21)-C(22)	120(2)	C(30)-C(29)-H(28)	120.57
C(20)-C(21)-H(21)	120.26	C(25)-C(30)-C(29)	120(2)

Table 5. Continued

C(22)-C(21)-H(21)	119.98	C(25)-C(30)-H(29)	119.82
C(21)-C(22)-C(23)	120(2)	C(29)-C(30)-H(29)	119.75
C(21)-C(22)-H(22)	120.03	P(2)-C(31)-C(32)	123(2)
C(23)-C(22)-H(22)	119.95	P(2)-C(31)-C(36)	122(2)
C(22)-C(23)-C(24)	121(2)	C(32)-C(31)-C(36)	115(2)
C(22)-C(23)-H(23)	119.56	C(31)-C(32)-C(33)	123(2)
C(24)-C(23)-H(23)	119.53	C(31)-C(32)-H(30)	118.51
C(19)-C(24)-C(23)	119(2)	C(33)-C(32)-H(30)	118.49
C(19)-C(24)-H(24)	120.51	C(32)-C(33)-C(34)	119(2)
C(23)-C(24)-H(24)	120.54	C(32)-C(33)-H(31)	120.65
P(2)-C(25)-C(26)	117(1)	C(34)-C(33)-H(31)	120.62
P(2)-C(25)-C(30)	123(1)	C(33)-C(34)-C(35)	118(2)
C(26)-C(25)-C(30)	120(2)	C(33)-C(34)-H(32)	121.28
C(25)-C(26)-C(27)	119(2)	C(35)-C(34)-H(32)	121.17
C(25)-C(26)-H(25)	120.57	C(34)-C(35)-C(36)	124(3)
C(27)-C(26)-H(25)	120.58	C(34)-C(35)-H(33)	118.01
C(26)-C(27)-C(28)	120(2)	C(36)-C(35)-H(33)	118.04
C(31)-C(36)-C(35)	122(2)	Cl(1)-C(37)-H(36)	108.17
C(31)-C(36)-H(34)	119.20	Cl(2)-C(37)-H(35)	108.40
C(35)-C(36)-H(34)	119.14	Cl(2)-C(37)-H(36)	108.77
Cl(1)-C(37)-Cl(2)	114(3)	H(35)-C(37)-H(36)	109.58
Cl(1)-C(37)-H(35)	107.84		

Table 6. Positional parameters for (6)W(CO)₃, 16

Atom	x	y	z	B, ^a (Å ²)
W(1)	0.13538(7)	0.32882(5)	0.07148(4)	1.68(3)
Cl(1)	0.674(1)	0.1708(9)	0.2691(8)	13(1)
Cl(2)	0.478(1)	0.102(1)	0.2138(6)	12.9(9)
P(1)	0.2949(4)	0.3235(3)	-0.0253(3)	1.8(2)
P(2)	0.0471(4)	0.2368(3)	-0.0332(3)	1.9(2)
O(1)	0.241(1)	0.2108(9)	0.1928(8)	3.6(8)
O(2)	-0.051(1)	0.341(1)	0.1979(9)	4.2(8)
O(3)	0.242(2)	0.460(1)	0.177(1)	5(1)
O(4)	0.055(1)	0.4225(7)	-0.0134(8)	2.2(6)
C(1)	0.202(2)	0.255(1)	0.144(1)	2(1)
C(2)	0.015(2)	0.335(1)	0.149(1)	2.8(9)
C(3)	0.207(2)	0.412(1)	0.137(1)	3(1)
C(4)	0.133(2)	0.467(1)	-0.059(1)	2.1(9)
C(5)	0.160(2)	0.416(1)	-0.134(1)	1.6(8)
C(6)	0.270(2)	0.377(1)	-0.123(1)	2.2(9)
C(7)	-0.021(2)	0.399(1)	-0.079(1)	1.9(8)

^a Anisotropically refined atoms are given in the form of the isotropic equivalent displacement parameter defined as $4/3[a^2B(1,1) + b^2B(2,2) + c^2B(3,3) + ab(\cos \gamma)B(1,2) + ac(\cos \beta)B(1,3) + bc(\cos \alpha)B(2,3)]$.

Table 6. Continued

Atom	x	y	z	B, a(Å ²)
C(8)	0.051(2)	0.364(1)	-0.146(1)	1.8(8)
C(9)	0.067(2)	0.276(1)	-0.136(1)	2.0(8)
C(10)	0.159(2)	0.467(1)	-0.214(1)	3(1)
C(11)	0.043(2)	0.468(1)	-0.246(1)	3(1)
C(12)	0.002(2)	0.386(1)	-0.232(1)	3(1)
C(13)	0.348(2)	0.230(1)	-0.055(1)	2.1(9)
C(14)	0.374(2)	0.210(1)	-0.139(1)	3(1)
C(15)	0.416(2)	0.137(1)	-0.154(1)	4(1)
C(16)	0.431(2)	0.085(1)	-0.094(1)	4(1)
C(17)	0.406(2)	0.103(1)	-0.012(1)	3(1)
C(18)	0.362(2)	0.172(1)	0.005(1)	2.9(9)
C(19)	0.426(2)	0.363(1)	0.016(1)	2.4(9)
C(20)	0.505(2)	0.388(1)	-0.037(1)	3(1)
C(21)	0.605(2)	0.411(2)	-0.006(1)	4(1)
C(22)	0.628(2)	0.408(1)	0.076(2)	5(1)
C(23)	0.551(2)	0.381(2)	0.128(1)	4(1)
C(24)	0.451(2)	0.358(1)	0.099(1)	3(1)
C(25)	0.099(2)	0.138(1)	-0.039(1)	2.0(8)
C(26)	0.109(2)	0.097(1)	0.036(1)	4(1)
C(27)	0.143(2)	0.022(1)	0.034(2)	4(1)

Table 6. Continued

Atom	x	y	z	B, ^a (Å ²)
C(28)	0.169(2)	-0.013(1)	-0.039(1)	4(1)
C(29)	0.162(2)	0.029(1)	-0.114(1)	3(1)
C(30)	0.126(2)	0.102(1)	-0.114(1)	3(1)
C(31)	-0.099(2)	0.218(1)	-0.035(1)	3(1)
C(32)	-0.153(2)	0.183(2)	-0.100(1)	4(1)
C(33)	-0.268(2)	0.169(2)	-0.103(2)	5(1)
C(34)	-0.328(2)	0.190(2)	-0.035(2)	6(2)
C(35)	-0.276(2)	0.223(2)	0.026(2)	6(2)
C(36)	-0.162(2)	0.236(2)	0.029(2)	5(1)
C(37)	0.610(3)	0.094(2)	0.222(2)	11(3)
H(1)	0.1024	0.5146	-0.0772	2.6
H(2)	0.1976	0.4767	-0.0266	2.6
H(3)	0.3242	0.4155	-0.1260	2.7
H(4)	0.2766	0.3415	-0.1667	2.7
H(5)	-0.0708	0.3613	-0.0595	2.2
H(6)	-0.0614	0.4417	-0.1000	2.2
H(7)	0.1390	0.2646	-0.1510	2.4
H(8)	0.0163	0.2517	-0.1732	2.4
H(9)	0.1838	0.5172	-0.2010	3.1
H(10)	0.2050	0.4443	-0.2531	3.1

Table 6. Continued

Atom	x	y	z	B, ^a (Å ²)
H(11)	0.0012	0.5045	-0.2170	3.4
H(12)	0.0394	0.4809	-0.3032	3.4
H(13)	0.0286	0.3520	-0.2728	3.7
H(14)	-0.0750	0.3842	-0.2329	3.7
H(15)	0.3623	0.2459	-0.1823	3.5
H(16)	0.4338	0.1233	-0.2081	4.6
H(17)	0.4602	0.0354	-0.1060	4.3
H(18)	0.4187	0.0665	0.0302	3.8
H(19)	0.3409	0.1823	0.0593	3.5
H(20)	0.4893	0.3895	-0.0941	4.0
H(21)	0.6589	0.4293	-0.0423	4.9
H(22)	0.6976	0.4245	0.0971	6.1
H(23)	0.5681	0.3786	0.1856	5.0
H(24)	0.3983	0.3380	0.1350	4.1
H(25)	0.0924	0.1209	0.0863	5.2
H(26)	0.1482	-0.0068	0.0841	5.1
H(27)	0.1921	-0.0650	-0.0395	4.2
H(28)	0.1813	0.0052	-0.1644	3.1
H(29)	0.1195	0.1305	-0.1635	3.2
H(30)	-0.1127	0.1671	-0.1461	5.0

Table 6. Continued

Atom	x	y	z	B, \AA^2
H(31)	-0.3030	0.1450	-0.1494	6.2
H(32)	-0.4048	0.1820	-0.0346	6.7
H(33)	-0.3160	0.2380	0.0723	6.9
H(34)	-0.1293	0.2585	0.0773	5.6
H(35)	0.6367	0.0895	0.1678	13.0
H(36)	0.6270	0.0491	0.2521	13.0

Table 7. General anisotropic displacement parameters for (6)W(CO)₃, 16

Atom	U(1,1)	U(2,2)	U(3,3)	U(1,2)	U(1,3)	U(2,3)
W(1)	0.0344(4)	0.0190(3)	0.0107(3)	-0.0002(6)	0.0052(2)	-0.0004(1)
Cl(1)	0.20(1)	0.12(1)	0.17(1)	-0.01(1)	0.00(1)	-0.03(1)
C1(2)	0.120(9)	0.30(2)	0.071(7)	0.08(1)	-0.004(6)	-0.07(1)
P(1)	0.031(3)	0.024(2)	0.013(2)	0.001(3)	0.003(2)	-0.003(1)
P(2)	0.032(3)	0.019(3)	0.021(2)	-0.002(2)	0.006(2)	-0.002(1)
O(1)	0.07(1)	0.04(1)	0.023(8)	0.007(9)	-0.004(7)	0.012(1)
O(2)	0.08(1)	0.05(1)	0.035(8)	0.01(1)	0.039(8)	-0.000(1)
O(3)	0.08(1)	0.05(1)	0.04(1)	-0.01(1)	-0.00(1)	-0.020(1)
O(4)	0.038(9)	0.018(7)	0.026(7)	0.002(7)	0.001(6)	0.002(1)
C(1)	0.04(1)	0.02(1)	0.03(1)	0.00(1)	0.00(1)	-0.006(1)
C(2)	0.06(1)	0.02(1)	0.03(1)	-0.00(1)	0.006(9)	0.00(1)
C(3)	0.04(1)	0.04(1)	0.02(1)	-0.01(1)	-0.01(1)	0.01(1)
C(4)	0.04(1)	0.02(1)	0.02(1)	-0.01(1)	0.003(9)	0.003(1)
C(5)	0.03(1)	0.01(1)	0.016(9)	0.001(8)	0.008(8)	-0.004(1)
C(6)	0.03(1)	0.04(1)	0.02(1)	0.00(1)	0.005(8)	0.002(1)
C(7)	0.03(1)	0.03(1)	0.02(1)	0.008(9)	0.001(8)	0.001(1)
C(8)	0.03(1)	0.02(1)	0.013(9)	0.001(9)	-0.003(8)	0.003(1)

The form of the anisotropic displacement parameter is: $\exp[-2\pi^2\{h^2a^2U(1,1) + k^2b^2U(2,2) + l^2c^2U(3,3) + 2hkabU(1,2) + 2hlacU(1,3) + 2klbcU(2,3)\}]$ where a, b, and c are reciprocal lattice parameters.

Table 7. Continued

Atom	U(1,1)	U(2,2)	U(3,3)	U(1,2)	U(1,3)	U(2,3)
C(9)	0.04(1)	0.03(1)	0.02(1)	0.00(1)	0.007(8)	-0.002(1)
C(10)	0.04(1)	0.03(1)	0.02(1)	-0.00(1)	0.01(1)	-0.000(1)
C(11)	0.06(2)	0.03(1)	0.02(1)	0.01(1)	0.02(1)	0.008(1)
C(12)	0.05(1)	0.05(1)	0.02(1)	0.01(1)	0.01(1)	0.01(1)
C(13)	0.02(1)	0.02(1)	0.04(1)	-0.002(9)	0.008(9)	-0.002(1)
C(14)	0.05(1)	0.05(2)	0.01(1)	0.01(1)	0.01(1)	-0.00(1)
C(15)	0.06(2)	0.06(2)	0.03(1)	0.01(1)	0.01(1)	-0.02(1)
C(16)	0.05(2)	0.04(2)	0.05(1)	0.02(1)	-0.01(1)	-0.02(1)
C(17)	0.04(1)	0.04(1)	0.04(1)	0.01(1)	0.00(1)	0.00(1)
C(18)	0.03(1)	0.05(1)	0.03(1)	0.02(1)	0.005(8)	0.01(1)
C(19)	0.03(1)	0.02(1)	0.04(1)	0.00(1)	-0.00(1)	-0.00(1)
C(20)	0.04(1)	0.05(2)	0.03(1)	-0.01(1)	-0.00(1)	0.01(1)
C(21)	0.04(2)	0.07(2)	0.04(1)	-0.03(1)	-0.01(1)	0.01(1)
C(22)	0.03(1)	0.05(2)	0.11(2)	-0.04(1)	-0.01(1)	-0.00(2)
C(23)	0.05(2)	0.08(2)	0.03(1)	-0.01(1)	0.00(1)	-0.01(1)
C(24)	0.04(1)	0.07(2)	0.02(1)	-0.01(1)	-0.01(1)	0.02(1)
C(25)	0.03(1)	0.01(1)	0.03(1)	-0.002(9)	0.005(9)	-0.005(1)
C(26)	0.12(2)	0.02(1)	0.03(1)	-0.00(1)	0.03(1)	0.01(1)
C(27)	0.07(2)	0.02(1)	0.07(2)	0.00(1)	0.05(1)	0.01(1)
C(28)	0.05(2)	0.03(1)	0.05(2)	0.01(1)	-0.00(1)	0.00(1)
C(29)	0.04(1)	0.02(1)	0.03(1)	0.00(1)	-0.00(1)	-0.011(1)

Table 7. Continued

Atom	U(1,1)	U(2,2)	U(3,3)	U(1,2)	U(1,3)	U(2,3)
C(30)	0.06(2)	0.02(1)	0.02(1)	-0.00(1)	0.00(1)	-0.007(1)
C(31)	0.04(1)	0.02(1)	0.06(2)	0.00(1)	0.01(1)	-0.01(1)
C(32)	0.07(2)	0.05(2)	0.04(1)	-0.03(1)	-0.01(1)	0.01(1)
C(33)	0.05(2)	0.06(2)	0.08(2)	-0.02(2)	-0.01(1)	0.03(2)
C(34)	0.03(1)	0.06(2)	0.12(3)	-0.01(1)	0.00(2)	0.01(2)
C(35)	0.03(1)	0.06(2)	0.13(3)	-0.02(1)	0.04(2)	-0.04(2)
C(36)	0.06(2)	0.05(2)	0.07(2)	-0.03(1)	0.03(1)	-0.04(1)
C(37)	0.15(4)	0.15(4)	0.10(3)	0.11(3)	-0.04(3)	-0.09(3)
H(1)	0.0326					
H(2)	0.0326					
H(3)	0.0340					
H(4)	0.0340					
H(5)	0.0282					
H(6)	0.0282					
H(7)	0.0310					
H(8)	0.0310					
H(9)	0.0387					
H(10)	0.0387					
H(11)	0.0430					
H(12)	0.0430					
H(13)	0.0467					

Table 7. Continued

Atom	U(1,1)	U(2,2)	U(3,3)	U(1,2)	U(1,3)	U(2,3)
H(14)	0.0467					
H(15)	0.0448					
H(16)	0.0582					
H(17)	0.0539					
H(18)	0.0476					
H(19)	0.0448					
H(20)	0.0510					
H(21)	0.0619					
H(22)	0.0771					
H(23)	0.0628					
H(24)	0.0513					
H(25)	0.0662					
H(26)	0.0644					
H(27)	0.0535					
H(28)	0.0390					
H(29)	0.0400					
H(30)	0.0634					
H(31)	0.0779					
H(32)	0.0852					
H(33)	0.0872					

Table 7. Continued

Atom	U(1,1)	U(2,2)	U(3,3)	U(1,2)	U(1,3)	U(2,3)
H(34)	0.0714					
H(35)	0.1649					
H(36)	0.1649					

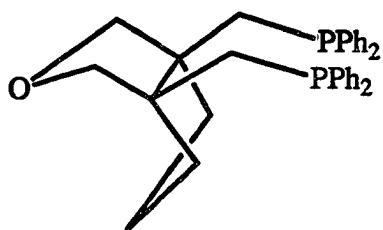
**SECTION IV. UNAMBIGUOUS DEMONSTRATION OF VACANT SITE
INVERSION IN A *cis*-P₂M(CO)₃ INTERMEDIATE**

ABSTRACT

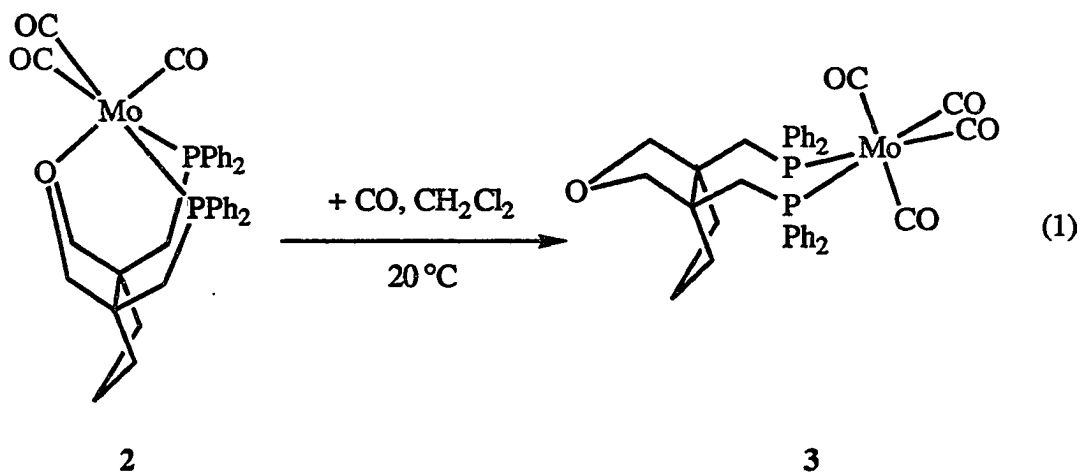
Reaction of *fac*-(1-*P,P',O*)Mo(CO)₃ (1 = *cis*-1,5-bis(diphenylphosphinomethyl)-3-oxa-bicyclo[3.3.0]octane) with ¹³C¹⁸O was found to proceed via substitution of the coordinated ether oxygen. ¹³C NMR spectroscopy revealed that the ¹³C¹⁸O was incorporated into nonequivalent axial sites yielding two diastereomers of *fac*-(1-*P,P'*)Mo(CO)₃(¹³C¹⁸O). No *mer* product could be detected. The formation of the two *fac* products is discussed in terms of isomerization of the initially formed square pyramidal intermediate generated by dissociation of the ether oxygen.

COMMUNICATION

Ligand substitution reactions of octahedral metal carbonyl complexes have been intensely studied over the past 25 years. A wealth of evidence suggests the formation of reactive five-coordinate intermediates in these reactions.¹ Matrix isolation studies and elegant kinetic and flash photolysis studies by Dobson indicate rapid solvolysis of these species even in poorly coordinating solvents such as toluene.² Collapse of the non-solvated five-coordinate intermediates to fluxional TBP species is often proposed to account for isotopic scrambling of ^{13}CO observed in these substitution reactions.¹ It has also been noted that many ligand substitution reactions of octahedral metal carbonyl complexes are stereospecific with a strong preference for the formation of *fac* products from *fac* reactants.³ Despite this observed stereospecificity, it has not been demonstrated whether the incoming ligand coordinates to the axial site vacated by the departing ligand and/or to the one *trans* to this site, since these axial sites have been equivalent in all previously studied cases. For example, studies by Dobson^{2a} and Angelici⁴ have shown that reactions of *fac*-(py)(diphos)Mo(CO)₃ with phosphites and the reaction of [(Ph₂PCH₂CH₂)₂NEt]Mo(CO)₃ with ^{13}CO , respectively, yield only *fac* products upon displacement of the coordinated py and nitrogen in the corresponding starting materials. Even though the site *trans* to the departing nitrogen ligand presumably also became available in both cases via fluxionality of the five-coordinate intermediate, the mirror symmetry of the chelating ligand with respect to the P₂M plane precluded confirmation of the hypothesis that both axial sites are involved. We report here that by utilizing ligand **1**, diastereomeric *fac* products are obtained in which one diastereomer contains the attacking ligand in the site vacated by the departing ligand, whereas in the other the new ligand occupies the site *trans* to the departing ligand.

**1**

We recently synthesized the new ligand **1** which reacts with $(\eta^6\text{-cycloheptatriene})\text{Mo}(\text{CO})_3$ to yield *fac*-(1-*P,P'*,*O*) $\text{Mo}(\text{CO})_3$ (**2**) in which all three donor atoms are coordinated.⁵ Solutions of complex **2** in CH_2Cl_2 react with CO to yield *cis*-(1-*P,P'*) $\text{Mo}(\text{CO})_4$ (**3**) via displacement of the coordinated ether (eq. 1). A ^{13}C NMR spectrum⁶ of **3** clearly shows two non-equivalent axial⁷ carbonyls due to the symmetry of **1**. The ratio of intensities of the equatorial to axial carbonyl resonances is approximately 2:1:1. In the presence of ^{13}CO , **2** forms two diastereomers of *fac*-(1-*P,P'*) $\text{Mo}(\text{CO})_3(^{13}\text{CO})$ with no ^{13}C NMR evidence for the formation of a *mer*



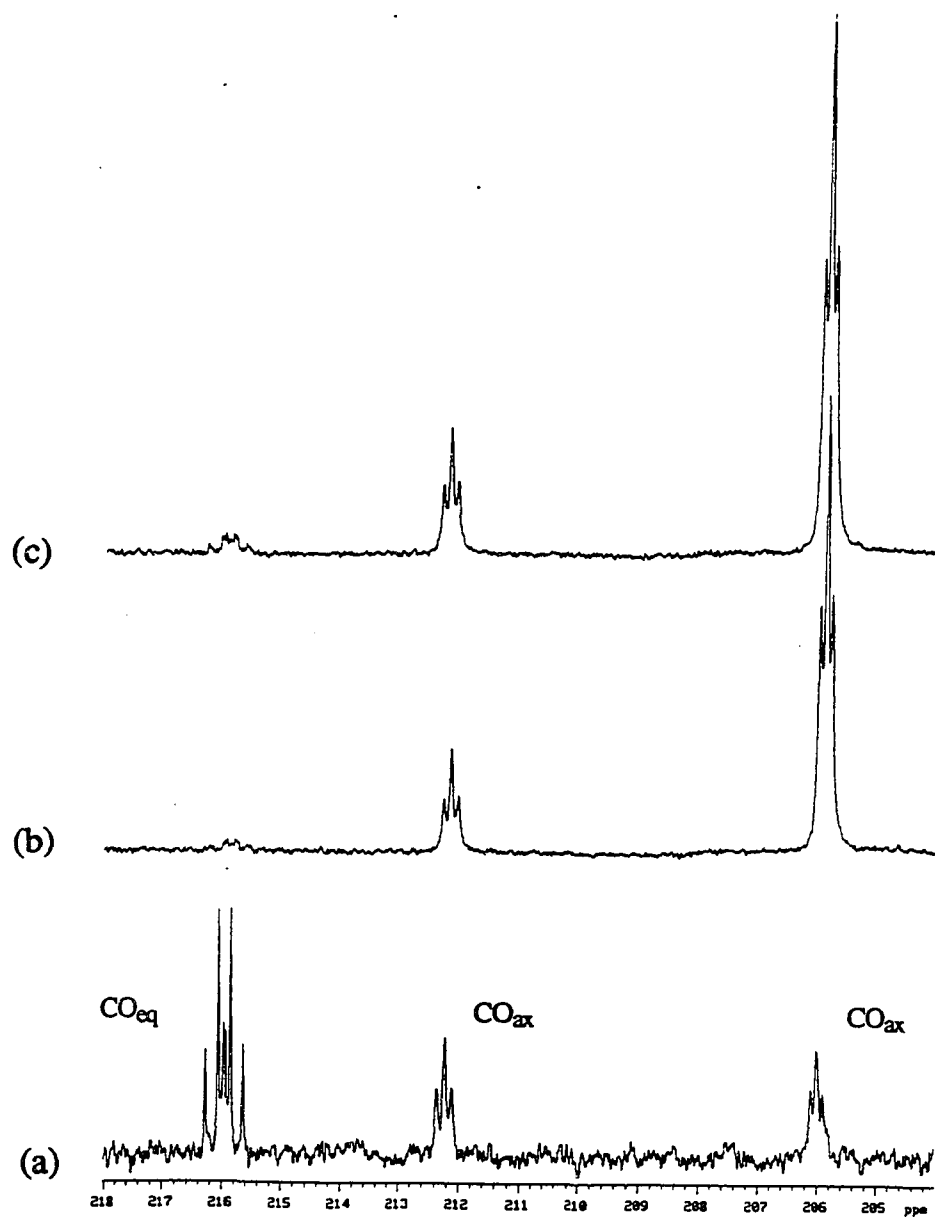


Figure 1. ^{13}C NMR Spectra (CD₂Cl₂): (a) (1-*P,P'*)Mo(CO)₄, natural abundance spectrum; (b) *fac*-(1-*P,P',O*)Mo(CO)₃ + ^{13}C O; (c) *fac*-(1-*P,P',O*)Mo(CO)₃ + ^{13}C O after 17 days

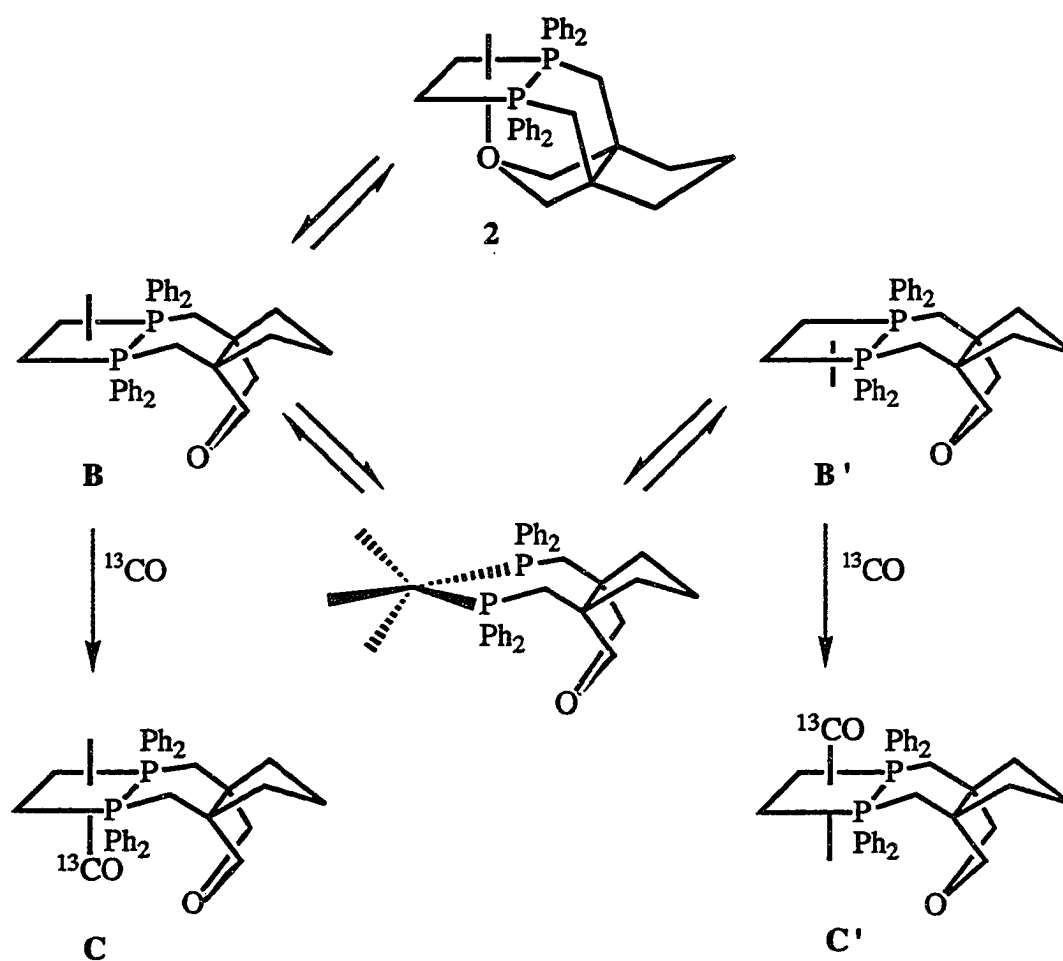
complex in which ^{13}CO has been incorporated into an equatorial site.⁸ As shown in Figure 1, the initial *fac* diastereomer ratio of 4:1 remained stable over a period of 17 days, indicating that no isomerization process was occurring.

The rationale we offer to account for the formation of two diastereomeric *fac* products is illustrated in Scheme I. Dissociation of the ether donor of **1** from **2** yields the five-coordinate intermediate **B** of approximately square pyramidal geometry.⁹ Unsaturated five-coordinate intermediates, such as $[\text{Cr}(\text{CO})_5]$, have been shown to be solvated within picoseconds after their formation.^{2e,f} Based on calculations by Davy and Hall,¹⁰ this process is too rapid to allow isomerization of **B** to provide an equatorial vacancy. Thus, no *mer* products should be formed in accord with the observed stereospecificity in this type of substitution reaction. Lichtenberger and Brown¹¹ have proposed a mechanism whereby, in a five-coordinate intermediate, the vacant site may be interchanged between two sites *cis* to a noncarbonyl ligand, but *trans* to each other, without the intermediate formation of a vacant site *trans* to the noncarbonyl ligand. In Scheme I, inversion of the vacant site to the position *trans* to itself would involve the migration of the axial carbonyl, *trans* to the vacant site, to an equatorial site with the simultaneous migration of the equatorial carbonyl to the initially vacant axial site. Calculations by Davy and Hall¹⁰ show that such a rearrangement has an activation barrier of less than 1 kcal/mol for $\text{Cr}(\text{CO})_4\text{PH}_3$ and can occur within the timeframe of solvation. In our case, this rearrangement would isomerize the two five-coordinate intermediates **B** and **B'**. These two intermediates are diastereomeric and should not be degenerate in energy. Thus, the rate of interconversion of **B** and **B'** relative to their rates of reaction with ^{13}CO may account for the 4:1 ratio of diastereomeric products observed.

Our observation of two diastereomers of *fac*-(1-*P,P'*) $\text{Mo}(\text{CO})_3(^{13}\text{CO})$ constitutes the first direct evidence that in substitution reactions of *fac* complexes, the incoming

ligand may occupy the site initially *trans* to the departing ligand as well as the same site vacated by the departing ligand. The stereochemical course of the reactions of **2** with other ligands is presently under investigation.

Scheme I



ACKNOWLEDGMENTS

The authors are grateful to the National Science Foundation and the donors of the Petroleum Research Foundation, administered by the American Chemical Society, for support of this research. The authors also thank R. J. Angelici for valuable discussions and Drs. Winfried Plass and Martina Schmidt for instruction on the manipulation of gases by vacuum-line techniques.

REFERENCES

1. For a review see: Howell, J. A. S.; Burkinshaw, P. M. *Chem. Rev.* **1983**, *83*, 557.
2. (a) Asali, K. J.; van Zyl, G. J.; Dobson, G. R. *Inorg. Chem.* **1988**, *27*, 3314.
(b) Asali, K. J.; Basson, S. S.; Tucker, J. S.; Hester, B. C.; Cortes, J. E.; Awad, H. H.; Dobson, G. R. *J. Am. Chem. Soc.* **1987**, *109*, 5386. (c) Dobson, G. R.; Hodges, P. M.; Healy, M. A.; Paliakoff, M.; Turner, J. J.; Firth, S.; Asali, K. J. *J. Am. Chem. Soc.* **1987**, *109*, 4218. (d) Welch, J. A.; Peters, K. S.; Vaida, V. *J. Phys. Chem.* **1982**, *86*, 1941. (e) Simon, J. D.; Peters, K. S. *Chem. Phys. Lett.* **1983**, *98*, 53. (f) Simon, J. D.; Xie, X. *J. Phys. Chem.* **1986**, *90*, 6715. (g) Langford, C. H.; Moralejo, C.; Sharma, D. K. *Inorg. Chim. Acta* **1987**, *126*, L11. (h) Simon, J. D.; Xie, X. *J. Phys. Chem.* **1987**, *91*, 5538.
3. Dobson, G. R. *Inorg. Chem.* **1980**, *19*, 1413 and references therein.
4. Knebel, W. J.; Angelici, R. J.; Gansow, O. A.; Darensbourg, D. J. *J. Organomet. Chem.* **1974**, *66*, C11.
5. Mason, M. R.; Su, Y.; Jacobson, R. A.; Verkade, J. G. *Organometallics*, accepted.
6. **3**, ^{13}C NMR (CD_2Cl_2 , 75.4 MHz) δ 215.9 (m, CO_{eq}), 212.2 (t, $^2J_{\text{PC}} = 9.5$ Hz, CO_{ax}), 206.0 (t, $^2J_{\text{PC}} = 7.5$ Hz, CO_{ax}). Approximate ratio of 2:1:1.
7. In this context axial refers to a site *cis* to both phosphorus donors and equatorial refers to a site *trans* to a phosphorus donor.
8. A deep yellow solution of 2^5 (21 mg) in ~0.5 mL CD_2Cl_2 was prepared in a 5 mm NMR tube under argon. ^{13}CO (99%, Cambridge Isotope Laboratories) was bubbled through the solution for 5 min resulting in a colorless solution. A small

quantity of decomposition product precipitated initially, but ^1H and ^{13}C NMR spectra of the supernatant liquid showed only the presence of two diastereomers of *fac*-(1-*P,P*) $\text{Mo}(\text{CO})_3(^{13}\text{CO})$ in an approximately 4:1 ratio. As an internal standard, the intensity of the CO_{eq} resonance remained approximately the same as that for the *ipso*-Ph resonances, just as is observed in the natural abundance spectrum of 3. The NMR tube was then sealed and the reaction monitored by ^{13}C NMR spectroscopy over the course of 17 days.

9. We propose square pyramidal intermediates based on the conclusions of Dobson^{2a,b,c} and on the results of molecular orbital calculations (Elian, M.; Hoffman, R. *Inorg. Chem.* **1975**, *14*, 1058) which suggest that the ground state for a $d^6\text{M}(\text{CO})_5$ complex should be a square pyramid. Alternatively, preferential attack at two positions adjacent to the equatorial phosphorus in a distorted TBP intermediate can also account for our results. The energy difference between these two geometries is expected to be small.
10. Davy, R. D.; Hall, M. B. *Inorg. Chem.* **1989**, *28*, 3524.
11. Lichtenberger, D. L.; Brown, T. L. *J. Am. Chem. Soc.* **1978**, *100*, 366.

**SECTION V. LIGAND SUBSTITUTION REACTIONS IN GROUP VI METAL
CARBONYL COMPLEXES OF A NOVEL BICYCLIC
DITERTIARY PHOSPHINE ETHER**

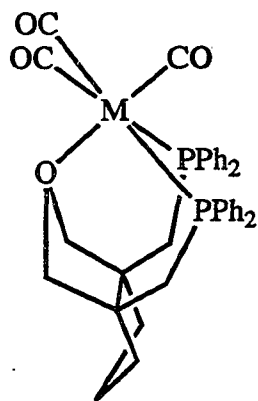
ABSTRACT

The complexes $fac-(1-P,P',O)M(CO)_3$, where $M = Mo, W$ and **1** is *cis*-1,5-bis(diphenylphosphinomethyl)-3-oxabicyclo[3.3.0]octane, were found to react with the ligands (L) acetonitrile, piperidine, pyridine and $P(OCH_2)_3CCH_3$ to yield two diastereomers of $fac-(1-P,P')M(CO)_3(L)$ in each case. 1H and ^{13}C NMR spectroscopic data suggest that the major isomer in each product is that in which the added ligand occupies the site originally occupied by the ether oxygen of **1** and that the minor isomer contains the new ligand in the position *trans* to this site. Carbon monoxide reacts with the complexes $fac-(1-P,P'O)M(CO)_3$ ($M = Mo, W$) to yield $(1-P,P')M(CO)_4$. Using ^{13}CO these reactions stereospecifically yield two diastereomers of $fac-(1-P,P')M(CO)_3(^{13}CO)$ in ratios of approximately 5:1 and 7:1 for $M = Mo$ and W , respectively. A scheme involving the isomerization of diastereomeric five-coordinate square pyramidal intermediates is discussed. The N-donor complexes $fac-(1-P,P')M(CO)_3L$, where $M = Mo, W$ and $L =$ acetonitrile, pyridine and piperidine, were observed by infrared, 1H and ^{31}P NMR spectroscopies to partially dissociate in solution, equilibrating with free L and $fac-(1-P,P'O)M(CO)_3$. This equilibrium was further substantiated by monitoring the exchange reaction between free and coordinated CD_3CN in the presence of $fac-(1-P,P')Mo(CO)_3(NCCH_3)$ using 2H NMR spectroscopy.

INTRODUCTION

There has recently emerged considerable interest in phosphines possessing ether functional groups capable of coordinating to transition metals.¹⁻¹⁴ This interest is based on the lability of the metal-ether interaction which can provide metal center sites for binding additional ligands. This lability has been demonstrated in several metal systems for a variety of ether-containing phosphines by substitution of the coordinated ether with ethylene (Rh),² acetylenes (Rh),² phosphites (Mo, W),³ nitriles (Mo,⁴ Ru⁵), dimethylsulfide (Pt),⁶ pyridine (Pt),⁶ isocyanides (Ru),⁵ and carbon monoxide (Mo,³ W,^{3,7} Rh,^{2,8} Ru,^{5,9} Pt⁶).

We are presently investigating the new ditertiary phosphine ether *cis*-1,5-bis(diphenylphosphinomethyl)-3-oxabicyclo[3.3.0]octane, **1**. This ligand was shown to coordinate to transition metals in either a tridentate (*P,P',O*) or bidentate (*P,P'*) manner as shown by spectroscopic and structural data for **2** and **3**, and for **4-6**, respectively.¹⁰ Ligand **1** differs

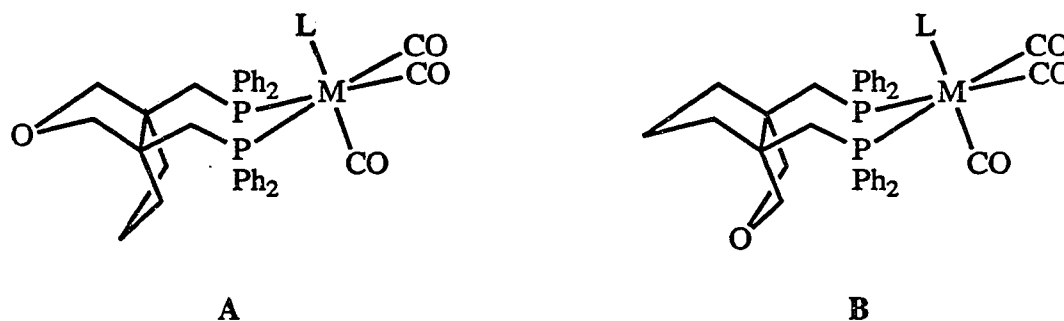


(*P, P', O*) Coordination Mode of **1**

2 M = Mo
3 M = W

from previously reported ether-containing phosphines in that it is a chelating bidentate phosphine capable of forming only *fac* complexes upon coordination of the ether.

Most of the ligands in this class are monotertiary phosphines with the exception of $(\text{Ph}_2\text{PCH}_2\text{CH}_2)_2\text{O}$,¹¹ DIPAMP,¹² and a few analogues of DIPAMP studied by Lindner.¹³ These few exceptions are bidentate phosphines which contain one or more ether donors each and are not restricted to *fac* complex formation upon coordination of the ether. Additionally, ligand **1** is unique in that it forms six-membered chelate rings upon ether coordination, in contrast to the vast majority of previously reported ligands which form five-membered chelate rings (often achieved by making use of 2-methoxyphenyl substituents on phosphorus). Furthermore, the low symmetry of **1** allows differentiation of the two axial¹⁵ sites in its octahedral transition metal complexes when the (*P,P'*) coordination mode is utilized. These factors may play



(*P,P'*) Coordination Mode of **1**

	<u>M</u>	<u>L</u>
4	Cr	CO
5	Mo	CO
6	W	CO
7a	Mo	$\text{P}(\text{OCH}_2)_3\text{CCH}_3$
8a	W	$\text{P}(\text{OCH}_2)_3\text{CCH}_3$
9a	Mo	py
10a	W	py
11a	Mo	NCMe
12a	W	NCMe
13a	W	pip

	<u>M</u>	<u>L</u>
7b	Mo	$\text{P}(\text{OCH}_2)_3\text{CCH}_3$
8b	W	$\text{P}(\text{OCH}_2)_3\text{CCH}_3$
9b	Mo	py
10b	W	py
11b	Mo	NCMe
12b	W	NCMe
13b	W	pip

significant roles in the chemistry of transition metal complexes of **1**.

Based on the literature cited above, it was anticipated that the metal-ether interaction in complexes wherein **1** adopts a (*P,P',O*) coordination mode would be quite weak, thus permitting facile ligand substitution reactions. Here we report the results of ligand substitution reactions of **2** and **3** leading to diastereomeric products **7a**, **7b** to **13a**, **13b** having a *fac* geometry. A preliminary communication described a portion of this work.¹⁴

EXPERIMENTAL SECTION

General Procedures

All reactions were performed under an inert atmosphere of argon using standard inert atmosphere techniques. Toluene, tetrahydrofuran, pentane and diethyl ether were distilled from sodium benzophenone ketyl. Methylene chloride, acetonitrile and pyridine were distilled from calcium hydride prior to use. Compounds 2, 3, 5 and 6,¹⁰ and $\text{P}(\text{OCH}_2)_3\text{CCH}_3$ ¹⁶ were prepared as previously described. ^{13}C O (99%) was purchased from Cambridge Isotope Laboratories. Solution NMR spectra were recorded on Bruker WM200 (^{31}P), Varian VXR 300 (^1H , ^2H , ^{13}C , ^{31}P) or Varian Unity 500 (^1H , ^1H { ^{31}P }) spectrometers using a deuterated solvent as the internal lock. ^2H NMR spectra were obtained by locking on the ^1H resonance of CH_2Cl_2 . The natural abundance resonance for CHDCl_2 (5.3 ppm, $^2\text{J}_{\text{HD}} = 0.9$ Hz) was used as the reference and internal standard for the ^2H NMR experiment. All chemical shifts are reported relative to TMS (^1H , ^2H , ^{13}C) or 85% H_3PO_4 (^{31}P). Mass spectra were recorded on a Finnegan 4000 instrument using chemical ionization and ammonia as the carrier gas. The masses of metal-containing fragments are reported for the most abundant isotope present, viz. ^{98}Mo and ^{184}W , unless otherwise noted. IR spectra were recorded using an IBM 98 FT-IR spectrometer and CaF_2 cells. Microanalyses were carried out by Schwarzkopf Microanalytical Laboratories, Woodside, NY.

Preparation of *fac*-(*cis*-1,5-bis(diphenylphosphinomethyl)-3-oxabicyclo-[3.3.0]octane-*P,P'*)-tricarbonyl-(1-methyl-4-phospha-3,5,8-trioxabicyclo-[2.2.2]octane-*P*)molybdenum (7a, 7b)

The ligand $P(OCH_2)_3CCH_3$ (0.0421 g, 0.284 mmol) in 5 mL of CH_2Cl_2 was added to a solution of **2** (0.183 g, 0.266 mmol) in 10 mL of CH_2Cl_2 . The reaction mixture was stirred for 20 min during which time the yellow solution became colorless. The solution was filtered through celite to remove traces of insoluble material. The solvent was removed *in vacuo* from the clear filtrate to leave a white solid. Spectral data clearly showed the presence of two facial isomers in a 4/1 ratio by integration of CH_3 and CH_2OP resonances in the 1H NMR spectrum. Recrystallization from CH_2Cl_2 yielded fine white needles of the product as an isomeric mixture. Anal. Calcd for $C_{41}H_{43}O_7P_3Mo$: C, 58.86; H, 5.18; Mo, 11.47. Found: C, 59.18; H, 5.23; Mo, 11.54.

Major isomer (7a). MS (desorption CI, NH_3) m/e (relative intensity) 811 ($MH^+ - CO$, 4.9), 719 (6.4), 691 (66), 509 (100); ^{31}P NMR (CD_2Cl_2) δ 86.9 (t, $^2J_{PP}$ 32 Hz, $POCH_2$), 20.2 (d, $^2J_{PP}$ 32 Hz, PPh_2); ^{13}C NMR (CD_2Cl_2) δ 220.5 (dt, $^2J_{PC}^{trans} = 49$ Hz, $^2J_{PC}^{cis} = 9.5$ Hz, CO_{ax}), 218.3 (m, CO_{eq}), 144.3 (m, Ph-*ipso*), 139.6 (m, Ph-*ipso*), 134.3 (at, 17 separation 12.3 Hz, Ph-*ortho*), 132.1 (at, separation 9.6 Hz, Ph-*ortho*), 129.7 (s, Ph-*para*), 128.6 (at, separation 9.1 Hz, Ph-*meta*), 127.8 (s, Ph-*para*), 127.3 (at, separation 7.9 Hz, Ph-*meta*), 87.6 (at, separation 12.3 Hz, CH_2OCH_2), 73.3 (d, $^2J_{PC} = 6.0$ Hz, $POCH_2$), 41.7 (at, separation 8.4 Hz, $CH_2CH_2CH_2$), 35.8 (at, separation 12.7 Hz, CH_2PPh_2), 31.6 (d, $^3J_{PC} = 32.1$ Hz, $POCH_2C$), 24.6 (s, $CH_2CH_2CH_2$), 15.6 (s, CH_3); 1H NMR (CD_2Cl_2) δ 7.90 (m, Ph), 7.44-7.15 (m, Ph), 3.69 (d, $^2J_{HH} = 9.0$ Hz, CH_2OCH_2), 3.63 (dd, $^2J_{HH} = 9.0$ Hz, $^4J_{HH} = 1.5$ Hz, CH_2OCH_2), 3.15 (d, $^3J_{PH} = 3.9$ Hz, CH_2OP), 2.9 (m, CH_2PPh_2), 1.64 (CH_2), 1.35 (m, CH_2), 0.81 (dd, $^2J_{HH} = 12.9$ Hz, $^3J_{HH-cis} = 5.4$ Hz, (CH_2), 0.31 (s, CH_3).

Minor isomer (7b). ^{31}P NMR (CD_2Cl_2) δ 85.9 (t, $^2J_{\text{PP}}$ 31.8 Hz, POCH_2), 18.9 (d, $^2J_{\text{PP}}$ = 31.8 Hz, PPh_2); ^{13}C NMR (CD_2Cl_2) δ 133.7 (at, separation 12.3 Hz, Ph-*ortho*), 132.0 (at, separation 9.5 Hz, Ph-*ortho*), 129.9 (s, Ph-*para*), 128.8 (at, separation 9.1 Hz, Ph-*meta*), 127.9 (s, Ph-*para*), 127.4 (at, separation 7.8 Hz, Ph-*meta*), 81.4 (at, separation 10.3 Hz, CH_2O), 73.6 (d, $^2J_{\text{PC}}$ = 5.6 Hz, POCH_2), 49.3 (at, separation 8.3 Hz, $\text{CH}_2\text{CH}_2\text{CH}_2$), 36.8 (at, separation 11.1 Hz, CH_2PPh_2), 26.2 (s, $\text{CH}_2\text{CH}_2\text{CH}_2$), 15.4 (s, CH_3); ^1H NMR¹⁸ (CD_2Cl_2) δ 3.25 (d, $^3J_{\text{PH}}$ = 3.9 Hz, CH_2OP), 0.36 (s, CH_3).

Preparation of *fac*-(*cis*-1,5-bis(diphenylphosphinomethyl)-3-oxabicyclo[3.3.0]octane-*P,P'*)-tricarbonyl-(1-methyl-4-phospha-3,5,8-trioxabicyclo[2.2.2]-octane-*P*)tungsten (8a, 8b)

A solution of $\text{P}(\text{OCH}_2)_3\text{CCH}_3$ (0.0622 g, 0.420 mmol) in 5 mL of CH_2Cl_2 was added to a solution of **3** (0.257 g, 0.331 mmol) in 10 mL of CH_2Cl_2 resulting in a loss of color within ten minutes. After one hour the volume was reduced to 5 mL *in vacuo* and pentane (10 mL) was added to complete the precipitation. The white solid was isolated by filtration, washed with 5 mL of pentane, and dried *in vacuo* (yield 0.24 g, 78%). Spectral data showed the presence of two *fac* isomers in a ratio of 6:1. Recrystallization from CH_2Cl_2 yielded fine white needles of the product as an isomeric mixture. Anal. Calcd for $\text{C}_{41}\text{H}_{43}\text{O}_7\text{P}_3\text{W}$: C, 53.26; H, 4.69; W, 19.88. Found: C, 52.95; H, 4.67; W, 19.69.

Major isomer (8a). ^{31}P NMR (CD_2Cl_2) δ 111.8 (t, $^2J_{\text{PP}}$ 25 Hz, $^1J_{\text{PW}}$ = 382 Hz, POCH_2), 1.4 (d, $^2J_{\text{PP}}$ = 25 Hz, $^1J_{\text{PW}}$ = 225 Hz, PPh_2); ^{13}C NMR (CD_2Cl_2) δ 212.2(m, CO_{ax}), 209.2 (m, CO_{eq}), 144.4 (m, Ph-*ipso*), 139.3 (m, Ph-*ipso*), 134.6 (at, separation 10.7 Hz, Ph-*ortho*), 132.1 (at, separation 9.1 Hz, Ph-*ortho*), 129.9 (s, Ph-*para*), 128.6 (at, separation 9.5 Hz, Ph-*meta*), 127.9 (s, Ph-*para*), 127.2 (at, separation

8.4 Hz, Ph-*meta*), 87.6 (at, separation 12.7 Hz, CH₂OCH₂), 73.6 (d, ²J_{PC} = 6.0 Hz, POCH₂), 53.3 (s, CC₄), 41.5 (at, separation 7.5 Hz, CH₂CH₂CH₂), 36.2 (at, separation 17.1 Hz, CH₂PPh₂), 31.5 (d, ³J_{PC} = 33.0 Hz, POCH₂C), 24.6 (s, CH₂CH₂CH₂), 15.7 (s, CH₃); ¹H NMR (CD₂Cl₂) δ 7.89 (m, Ph), 7.41 (m, Ph), 7.32-7.15 (m, Ph), 3.69 (d, ²J_{HH} = 9.0 Hz, 2H, CH₂OCH₂), 3.63 (dd, ²J_{HH} = 9.0 Hz, ⁴J_{HH} = 2.0 Hz, 2H, CH₂OCH₂), 3.15 (d, ³J_{PH} = 4.2 Hz, 6H, POCH₂), 3.13 (dd, ²J_{HH} = 15.0 Hz, ²J_{PH} = 12.5 Hz, CH₂PPh₂), 2.96 (d, ²J_{HH} = 15.0 Hz, CH₂PPh₂), 1.6 (m, 2H, CH₂), 1.4-1.2 (m, 2H, CH₂), 0.82 (dd, ²J_{HH} = 12.6 Hz, ³J_{HH-*cis*} = 5.4 Hz, 2H, CH₂), 0.31 (s, 3H, CH₃).

Minor isomer (8b). ³¹P NMR (CD₂Cl₂) δ 113.0 (t, ²J_{PP} = 24 Hz, POCH₂), 0.1 (d, ²J_{PP} = 24 Hz, PPh₂); ¹³C NMR (CD₂Cl₂) δ 134.1 (at, Ph-*ortho*), 131.9 (at, separation 9.1 Hz, Ph-*ortho*), 130.1 (s, Ph-*para*), 128.8 (at, separation 9.6 Hz, Ph-*meta*), 128.0 (s, Ph-*para*), 127.3 (Ph-*meta*), 81.1 (at, separation 9.6 Hz, Ph-*meta*), 73.8 (d, ²J_{PC} = 6.0 Hz, POCH₂), 53.5 (s, CC₄), 49.7 (at, separation 9.5 Hz, CH₂CH₂CH₂), 37.1 (at, separation 13.5 Hz, CH₂PPh₂), 26.6 (s, CH₂CH₂CH₂), 15.7 (s, CH₃); ¹H NMR¹⁸ (CD₂Cl₂) δ 3.48 (d, ²J_{HH} = 9.0 Hz, CH₂OCH₂), 3.28 (dd, ²J_{HH} = 15.5 Hz, ³J_{PH} = 12.5 Hz, CH₂PPh₂), 3.22 (d, ³J_{PH} = 3.9 Hz, POCH₂), 3.09 (d, ²J_{HH} = 15.5 Hz, CH₂PPh₂), 2.90 (d, ²J_{HH} = 9.0 Hz, CH₂OCH₂), 0.34 (s, CH₃).

Preparation of *fac*-(*cis*-1,5-bis(diphenylphosphinomethyl)-3-oxabicyclo-[3.3.0]octane-*P,P'*)-tricarbonyl(η¹-*N*-pyridine)molybdenum (9a, 9b)

This product was prepared as described below for the tungsten analogues 10a and 10b.

Major isomer (9a). ³¹P NMR (CD₂Cl₂) δ 20.7(s); ¹³C NMR (CD₂Cl₂) δ 226.3 (t, ²J_{PC} = 8 Hz, CO_{ax}), 219.9 (m, separation 24 Hz, CO_{eq}), 154.9 (t, ³J_{PC} = 3 Hz, pyridine-C1), 139.2 (m, separation 35 Hz, Ph-*ipso*), 138.1 (m, separation 26 Hz, Ph-

ipso), 134.9 (s, pyridine-C3), 134.7 (at, separation 12 Hz, Ph-*ortho*), 131.6 (at, separation 10 Hz, Ph-*ortho*), 129.6 (s, Ph-*para*), 128.5 (at, separation 9.1 Hz, Ph-*meta*), 128.2 (s, Ph-*para*), 128.1 (at, separation 7 Hz, Ph-*meta*), 122.5 (s, pyridine-C2), 87.8 (at, separation 12 Hz, CH₂OCH₂), 41.5 (at, separation 8 Hz, CH₂CH₂CH₂) 35.8 (at, separation 13 Hz, CH₂PPh₂), 24.8 (s, CH₂CH₂CH₂); ¹H NMR (CD₂Cl₂) δ 8.02 (m, Ph-*ortho*), 7.6-7.2 (m, Ph), 6.90 (m, Ph), 6.15 (m, pyridine - C2), 3.74 (d, ²J_{HH} = 9.3 Hz, CH₂OCH₂), 3.69 (dd, ²J_{HH} = 9.3 Hz, ⁴J_{HH} = 1.8 Hz, CH₂OCH₂), 3.00 (dd, ²J_{HH} = 15.3 Hz, CH₂PPh₂) 2.80 (d, ²J_{HH} = 15.3 Hz, CH₂PPh₂), 2.13 (m, CH₂), 0.90 (dd, ²J_{HH} = 12.0 Hz, ³J_{HH-cis} = 5.4 Hz, CH₂).

Minor isomer (9b). ³¹P NMR (CD₂Cl₂) δ 19.4(s); ¹³C NMR (CD₂Cl₂) δ 134.4 (at, separation 12 Hz, Ph-*ortho*), 131.4 (at, Ph-*ortho*), 122.6 (s, pyridine-C2), 81.1 (m, CH₂OCH₂), 50.4 (at, CH₂CH₂CH₂), 26.2 (s, CH₂CH₂CH₂); ¹H NMR¹⁸ (CD₂Cl₂) δ 4.05 (d, ²J_{HH} = 9.0 Hz, CH₂OCH₂), 3.17 (dd, ²J_{HH} = 15.3 Hz, ²J_{PH} = 11.3 Hz, CH₂PPh₂), 2.91 (d, ²J_{HH} = 15.3 Hz, CH₂PPh₂).

Preparation of *fac*-(*cis*-1,5-bis(diphenylphosphinomethyl)-3-oxabicyclo-[3.3.0]octane-*P,P'*)-tricarbonyl(η¹-*N*-pyridine)tungsten (10a, 10b)

To a solution of **3** (0.305g, 0.393 mmol) in 10 mL of CH₂Cl₂ was added 0.5 mL of pyridine. The addition resulted in an immediate color change to a pale lemon yellow. A ³¹P NMR spectrum of this solution showed only the presence of **10a** and **10b**. After 20 minutes at room temperature, stirring was discontinued. Diethyl ether (30 mL) was slowly added on top of the CH₂Cl₂, and the reaction flask was cooled in the freezer overnight to yield light yellow crystals which were collected by filtration and dried *in vacuo* (yield 0.22 g 65%). Anal. Calcd for C₄₁H₃₉NO₄P₂W: C, 57.56; H, 4.59; W, 21.49. Found: C, 57.12; H, 4.55; W, 21.50.

Major isomer (10a). ^{31}P NMR (CD_2Cl_2) δ 12.9(s), $^1\text{J}_{\text{PW}} = 232$ Hz; ^{13}C NMR (CD_2Cl_2) δ 217.2 (t, $^2\text{J}_{\text{PC}} = 9.9$ Hz, CO_{ax}), 214.1 (dd, $^2\text{J}_{\text{PC-trans}} = 37$ Hz, $^2\text{J}_{\text{PC-cis}} = 10.0$ Hz, CO_{eq}), 156.1 (t, $^3\text{J}_{\text{PC}} = 7.1$ Hz, pyridine-C1), 139.1 (m, separation 42.0 Hz, Ph-*ipso*), 137.6 (m, separation 34.2 Hz, Ph-*ipso*), 135.1 (at, separation 11.9 Hz, Ph-*ortho*), 134.8 (s, pyridine-C3), 131.6 (br, Ph-*ortho*), 129.8 (s, Ph-*para*), 128.7 (at, separation 9.5 Hz, Ph-*meta*), 128.5 (s, Ph-*para*), 128.3 (at, separation 7.5 Hz, Ph-*meta*), 123.2 (s, pyridine-C2), 87.8 (at, separation 12.7 Hz, CH_2OCH_2), 53.3 (at, separation 3.2 Hz, CC_4), 41.3 (at, separation 7.5 Hz, $\text{CH}_2\text{CH}_2\text{CH}_2$), 36.2 (m, separation 17.4 Hz, CH_2PPh_2), 24.8 (s, $\text{CH}_2\text{CH}_2\text{CH}_2$); ^1H NMR (CD_2Cl_2 , 500 MHz) δ 7.99 (m, 4H, Ph-*ortho*), 7.68 (m, 2H, pyridine-HC1), 7.42-7.28 (m, Ph), 6.91 (m, Ph), 6.10 (m, 2H, pyridine-HC2), 3.74 (d, $^2\text{J}_{\text{HH}} = 9.0$ Hz, 2H, CH_2OCH_2), 3.69 (dd, $^2\text{J}_{\text{HH}} = 9.0$ Hz, $^4\text{J}_{\text{HH}} = 2.0$ Hz, 2H, CH_2OCH_2), 3.18 (dd, $^2\text{J}_{\text{HH}} = 15.0$ Hz, $^2\text{J}_{\text{PH}} = 12.6$ Hz, 2H, CH_2PPh_2), 2.83 (d, $^2\text{J}_{\text{HH}} = 15.0$ Hz, 2H, CH_2PPh_2), 2.11 (m, 2H, CH_2), 1.50 (m, 1H, CH_2), 1.45 (m, 1H, CH_2), 0.91 (dd, $^2\text{J}_{\text{HH}} = 12.5$ Hz, $^3\text{J}_{\text{HH-cis}} = 5.5$ Hz, 2H, CH_2).

Minor isomer (10b). ^{31}P NMR (CD_2Cl_2) δ 11.6(s), $^1\text{J}_{\text{PW}} = 232$ Hz; ^{13}C NMR (CD_2Cl_2) δ 123.2 (s, pyridine-C2), 81.0 (at, separation 9.5 Hz, CH_2OCH_2), 50.4 (at, separation 9.1 Hz, $\text{CH}_2\text{CH}_2\text{CH}_2$), 37.5 (m, CH_2PPh_2); ^1H NMR¹⁸ (CD_2Cl_2 , 500 MHz) δ 4.04 (dd, $^2\text{J}_{\text{HH}} = 9.5$ Hz, $^4\text{J}_{\text{HH}} = 1.5$ Hz, CH_2OCH_2), 3.35 (dd, $^2\text{J}_{\text{HH}} = 15.5$ Hz, $^2\text{J}_{\text{PH}} = 12.5$ Hz, CH_2PPh_2), 2.99 (d, $^2\text{J}_{\text{HH}} = 9.5$ Hz, CH_2OCH_2), 2.93 (d, $^2\text{J}_{\text{HH}} = 15.5$ Hz, CH_2PPh_2).

Preparation of *fac*-acetonitrile(*cis*-1,5-bis(diphenylphosphinomethyl)-3-oxabicyclo[3.3.0]octane-*P,P'*)tricarbonylmolybdenum (11a, 11b)

This product was prepared as described below for the tungsten analogues 12a and 12b.

Major isomer (11a). ^{31}P NMR (CH_2Cl_2) δ 27.1(s); ^{13}C NMR (CD_2Cl_2) 223.2 (t, $^2J_{\text{PC}} = 8.4$ Hz, CO_{ax}), 219.8 (m, separation 23.0 Hz, CO_{eq}), 139.8 (m, separation 27.4 Hz, Ph-*ipso*), 138.8 (m, separation 35.7 Hz, Ph-*ipso*), 135.4 (at, separation 12.7 Hz, Ph-*ortho*), 131.4 (at, separation 9.1 Hz, Ph-*ortho*), 130.0 (s, Ph-*para*), 128.6 (at, separation 9.5 Hz, Ph-*meta*), 128.2 (at, separation 7.1 Hz, Ph-*meta*), 127.9 (s, Ph-*para*), 120.8 (s, CH_3CN), 87.4 (at, separation 12.3 Hz, CH_2OCH_2), 53.4 (s, CC_4), 41.3 (at separation 8.7 Hz, $\text{CH}_2\text{CH}_2\text{CH}_2$), 36.8 (at, separation 13.9 Hz, CH_2PPh_2), 24.8 (s, $\text{CH}_2\text{CH}_2\text{CH}_2$), 1.5 (s, CH_3CN); ^1H NMR (CD_2Cl_2) δ 8.01 (m, Ph-*ortho*), 7.40 (m, Ph), 7.35-7.15 (m, Ph), 3.64 (d, $^2J_{\text{HH}} = 9.0$ Hz, CH_2OCH_2), 3.56 (dd, $^2J_{\text{HH}} = 9.0$ Hz, $^4J_{\text{HH}} = 1.8$ Hz, CH_2OCH_2), 2.87 (d, $^3J_{\text{PH}} = 5.4$ Hz, CH_2PPh_2), 2.06 (m, CH_2), 1.44 (m, CH_2), 0.91 (dd, $^2J_{\text{HH}} = 13.1$ Hz, $^3J_{\text{HH-cis}} = 4.5$ Hz, CH_2), 0.80 (s, CH_3CN).

Minor isomer (11b). ^{31}P NMR (CD_2Cl_2) δ 25.4(s); ^{13}C NMR (CD_2Cl_2) δ 134.8 (at, Ph-*ortho*), 130.2 (s, Ph-*para*), 128.7 (at, Ph-*meta*), 81.5 (m, CH_2OCH_2), 49.3 (m, $\text{CH}_2\text{CH}_2\text{CH}_2$), 37.9 (at, separation 11.1 Hz, CH_2PPh_2), 26.0 (s, $\text{CH}_2\text{CH}_2\text{CH}_2$), 1.7 (s, CH_3CN); ^1H NMR¹⁸ (CD_2Cl_2) δ 3.96 (d, $^2J_{\text{HH}} = 9.3$ Hz, CH_2OCH_2), 3.02 (d, $^2J_{\text{HH}} = 9.3$ Hz, CH_2OCH_2), 2.98 (br s, CH_2PPh_2), 0.93 (s, CH_3CN).

Preparation of *fac*-acetonitrile(*cis*-1,5-bis(diphenylphosphinomethyl)-3-oxabicyclo[3.3.0]octane-*P,P'*)tricarbonyltungsten (12a, 12b)

To a solution of 3 (0.227 g, 0.292 mmol) in 5 mL of CH_2Cl_2 was added 0.5 mL of CH_3CN which resulted in a decrease in color to yield a very pale yellow solution. ^{31}P NMR spectroscopy showed only the presence of 12a and 12b in this solution. After stirring the reaction mixture at room temperature for 10 minutes, pentane (10 mL) was slowly added. Within 10 minutes a creamy white precipitate had formed and an additional 10 mL of pentane was added to complete the precipitation. The solid was

isolated by filtration, washed with 5 mL of pentane and dried *in vacuo*, (yield 0.23 g, 96%). The product was obtained as pale yellow crystals by layering diethyl ether onto a CH₂Cl₂ solution of the complex and cooling overnight.

Major isomer (12a). ³¹P NMR (CH₂Cl₂) δ 14.8(s), ¹J_{PW} = 231 Hz; ¹³C NMR (CD₂Cl₂) δ 213.9 (t, ²J_{PC} = 5.9 Hz, CO_{ax}), 212.5 (m, separation 24.9 Hz, CO_{eq}), 139.0 (m, separation 32.9 Hz, Ph-*ipso*), 138.3 (m, separation 38.8 Hz, Ph-*ipso*), 135.7 (at, separation 12.2 Hz, Ph-*ortho*), 131.3 (at, separation 8.7 Hz, Ph-*ortho*), 130.1 (s, Ph-*para*), 128.6 (at, separation 9.9 Hz, Ph-*meta*), 128.3 (at, separation 7.5 Hz, Ph-*meta*), 128.1 (s, Ph-*para*), 119.0 (s, CH₃CN), 87.4(at, separation 13.0 Hz, CH₂OCH₂), 41.1 (at, separation 8.3 Hz, CH₂CH₂CH₂), 37.3 (m, separation 17.8 Hz, CH₂PPh₂), 24.8 (s, CH₂CH₂CH₂), 1.5 (s, CH₃CN); ¹H NMR (CD₂Cl₂) δ 8.00 (m, Ph), 7.45 (m, Ph), 7.31 (m, Ph), 7.20 (m, Ph), 3.64 (d, ²J_{HH} = 8.7 Hz, CH₂OCH₂), 3.57 (dd, ²J_{HH} = 8.7 Hz, ⁴J_{HH} = 1.2 Hz, CH₂OCH₂), 3.08 (dd, ²J_{HH} = 15.6 Hz, ³J_{PH} = 13.3 Hz, CH₂PPh₂), 2.92 (d, ²J_{HH} = 15.6 Hz, CH₂PPh₂), 2.09 (m, CH₂), 1.47 (m, CH₂), 0.94 (m, CH₂), 0.83 (t, ⁵J_{PH} = 1.5 Hz, CH₃CN).

Minor isomer (12b). ³¹P NMR (CH₂Cl₂) δ 13.4(s), ¹J_{PW} = 229 Hz; ¹³C NMR (CD₂Cl₂) δ 135.3 (at, Ph-*ortho*), 131.2 (m, Ph-*ortho*), 130.2 (s, Ph-*para*), 125.6(s, CH₃CN), 81.1 (at, CH₂OCH₂), 49.7 (m, CH₂CH₂CH₂), 38.4 (m, CH₂PPh₂), 26.4 (s, CH₂CH₂CH₂), 1.7 (s, CH₃CN); ¹H NMR¹⁸ (CD₂Cl₂) δ 4.00 (d, ²J_{HH} = 9.3 Hz, CH₂OCH₂), 3.22 (dd, ²J_{HH} = 15.6 Hz, ³J_{PH} = 12.3 Hz, CH₂PPh₂), 3.06 (d, ²J_{HH} = 15.6 Hz, CH₂PPh₂), 2.99 (d, ²J_{HH} = 9.3 Hz, CH₂OCH₂), 0.92 (s, CH₃CN).

Preparation of *fac*-(*cis*-1,5-bis(diphenylphosphinomethyl)-3-oxabicyclo[3.3.0]octane-*P,P'*)tricarbonyl(η^1 -*N*-piperidine)tungsten (13a, 13b).

To a deep yellow solution of **3** (0.214 g, 0.275 mmol) in 5 mL of CH₂Cl₂ was added 0.15 mL of piperidine which resulted in an immediate change of color to a light lemon yellow. This solution was stirred for 10 minutes and then treated with 10 mL of pentane. Within 10 minutes a pale yellow precipitate began to appear and an additional 15 mL of pentane was added to complete the precipitation. The solid was isolated by filtration, rinsed with 5 mL of pentane and dried *in vacuo* (yield 0.22 g, 98%).

Major isomer (13a). ³¹P NMR (CDCl₂) δ 10.9(s), ¹J_{PW} = 230 Hz; ¹³C NMR (CD₂Cl₂) δ 215.3 (t, ²J_{PC} = 5.1 Hz, CO_{ax}), 214.4 (m, separation 26.6 Hz, CO_{eq}), 141.5 (m, separation 27.8 Hz, Ph-*ipso*), 138.7 (d, separation 42.4 Hz, Ph-*ipso*), 135.1 (at, separation 9.9 Hz, Ph-*ortho*), 131.2 (at, separation 8.4 Hz, Ph-*ortho*), 129.8 (s, Ph-*para*), 129.3 (at, separation 7.1 Hz, Ph-*meta*), 129.1 (s, Ph-*para*), 128.6 (at, separation 9.5 Hz, Ph-*meta*), 87.6 (at, separation 12.7 Hz, CH₂OCH₂), 56.1 (t, ³J_{PC} = 2.0 Hz, pip-C1), 41.3 (at, separation 7.2 Hz, CH₂CH₂CH₂), 37.0 (at, separation 16.3 Hz, CH₂PPh₂), 28.6 (s, pip-C2), 24.7 (s, CH₂CH₂CH₂), 22.9 (s, pip-C3); ¹H NMR (CD₂Cl₂) δ 8.01 (m, Ph-*ortho*), 7.53 (m, Ph-*ortho*), 7.50-7.25 (m, Ph), 3.70 (d, ²J_{HH} = 9.0 Hz, 2H, CH₂OCH₂), 3.63 (dd, ²J_{HH} = 9.0 Hz, ⁴J_{HH} = 1.5 Hz, 2H, CH₂OCH₂), 3.24 (dd, ²J_{HH} = 15.0 Hz, ²J_{PH} = 12.6 Hz, 2H, CH₂PPh₂), 2.83 (d, ²J_{HH} = 15.0 Hz, 2H, CH₂PPh₂), 2.75 (m, uncoordinated pip NCH₂), 2.0-1.0 (m, CH₂, pip), 0.80 (dd, ²J_{HH} = 12.9 Hz, ³J_{HH} = 5.4 Hz, 2H, CH₂).

Minor isomer (13b). ³¹P NMR (CD₂Cl₂) δ 9.4 (s), ¹J_{PW} = 230 Hz; ¹³C NMR (CD₂Cl₂) δ 134.7 (at, Ph-*ortho*), 13.1 (at, Ph-*ortho*), 130.0 (s, Ph-*para*), 128.9 (at, separation 9.1 Hz, Ph-*meta*), 80.9 (at, separation 8.7 Hz, CH₂OCH₂), 50.2 (at, separation 9.1 Hz, CH₂CH₂CH₂), 37.9 (at, separation 13.8 Hz, CH₂PPh₂), 26.6 (s,

CH₂CH₂CH₂); ¹H NMR¹⁸ (CD₂Cl₂) δ 3.72 (d, ²J_{HH} = 9.0 Hz, CH₂OCH₂), 2.87 (d, ²J_{HH} = 9.0 Hz, CH₂O), 3.40 (m, CH₂PPh₂), 2.92 (d, ²J_{HH} = 15.3 Hz, CH₂PPh₂).

Thermolysis of (1)W(CO)₄, (6)

Complex 6 (0.206 g, 0.256 mmol) was dissolved in 15 mL of toluene and the solution was refluxed for 16 hours during which time no precipitate had formed. A ³¹P NMR spectrum of this reaction solution showed only the presence of the starting complex, 6 (δ 4.5(s), ¹J_{PW} = 232 Hz).

Photolysis of (1)Mo(CO)₄, (5) and (1)W(CO)₄, (6)

Complex 5 (0.050 g, 0.070 mmol) was dissolved in 2 mL of THF and the solution was irradiated at 254 nm for 4 hours. A very faint yellowing of the solution occurred, but ³¹P NMR spectroscopy showed only the presence of the starting complex, 5 (δ 22.0(s)). Similarly, a solution of complex 6 (0.218 g, 0.272 mmol) in 15 mL of toluene was irradiated with a 275 W UV lamp for 3 hours during which time the solution became brown and a brown decomposition product had precipitated. A ³¹P NMR spectrum of the supernatant showed the presence of unreacted starting material as the only phosphorus-containing species in solution.

Exchange reaction between *fac*-(1)W(CO)₃(NCCH₃) and CD₃CN

Approximately 25 mg of *fac*-(1)W(CO)₃(NCCH₃) (12a, 12b) was dissolved in 0.5 mL of CH₂Cl₂ in a 5 mm NMR tube. CD₃CN was then added and the tube immediately placed in the spectrometer. The exchange reaction was monitored by ²H NMR spectroscopy over the course of two hours.

Reaction of ^{13}CO with *fac*-(1) $\text{M}(\text{CO})_3$ where $\text{M} = \text{Mo}$ (2) and W (3)

Compounds 2 and 3 (~ 20-30 mg) were dissolved in CD_2Cl_2 in separate 5 mm NMR tubes under argon. ^{13}CO was bubbled through the yellow solutions for 10 min resulting in near colorless solutions. A small quantity of decomposition product precipitated initially for the reaction involving 2, but ^1H and ^{13}C NMR spectra showed only the presence of *fac*-(1) $\text{Mo}(\text{CO})_3(^{13}\text{CO})$. The NMR tubes were then sealed and the reactions were monitored by ^{13}C NMR spectroscopy.

RESULTS AND DISCUSSION

Substitution by Phosphorus and Nitrogen Donors

Reaction of **2** or **3** with $\text{P}(\text{OCH}_2)_3\text{CCH}_3$ proceeds cleanly in CH_2Cl_2 at room temperature by displacement of the coordinated ether yielding products of the stoichiometry $(1)\text{M}(\text{CO})_3[\text{P}(\text{OCH}_2)_3\text{CCH}_3]$ where $\text{M} = \text{Mo}$ (**7a**, **7b**) and W (**8a**, **8b**) as shown by mass spectral and analytical data. In both cases two isomeric products were obtained. Starting from complex **2**, the two products **7a** and **7b** were isolated as a mixture in approximately a 4:1 ratio as shown by ^1H NMR spectroscopy. Attempts to separate these two products by column chromatography and fractional recrystallization were unsuccessful. In the ^{31}P NMR spectrum of this product mixture, a triplet at 86.9 ppm ($^2J_{\text{PP}} = 32$ Hz) for the phosphite resonance and a doublet at 20.2 ppm ($^2J_{\text{PP}} = 32$ Hz) for the phosphine resonance of the major isomer and similar resonances for the minor product suggest a *fac* geometry for both. A *fac* geometry for **7a** is also substantiated in the ^{13}C NMR spectrum by a doublet of triplets resonance at 220.5 ppm ($^2J_{\text{PC-trans}} = 49$ Hz, $^2J_{\text{PC-cis}} = 9.5$ Hz) for the axial carbonyl and a complex multiplet at 218.3 ppm for the two equivalent equatorial carbonyls. The signal-to-noise ratio of the spectrum was insufficient to assign the carbonyl resonances of the minor isomer **7b**. Remaining ^{13}C NMR resonances for both isomers indicate the presence of a plane of symmetry consistent with a *fac*, but not a *mer*, arrangement of ligands. On this basis the compounds **7a** and **7b** are assigned as a pair of *fac* diastereomers.

Two diastereomers of *fac* geometry may arise because of the inequivalence of the two axial sites in octahedral metal complexes of ligand **1**. The axial sites above and below the P_2M plane are differentiated by the symmetry of **1**. This has been demonstrated previously¹⁰ for the complexes $(1)\text{M}(\text{CO})_4$ where $\text{M} = \text{Cr}$ (**4**), Mo (**5**), W

(6), by the presence of two axial carbonyl resonances in the ^{13}C NMR spectra of these complexes. Analysis of the ^{31}P and ^{13}C NMR spectra for the tungsten analogues **8a** and **8b** reveals the same features noted above and hence they are assigned as two *fac* diastereomers of $(1)\text{W}(\text{CO})_3[\text{P}(\text{OCH}_2)_3\text{CCH}_3]$.

The reactions of **2** and **3** with acetonitrile, pyridine and piperidine also yield two *fac* diastereomers in each case (**9a,b-13a,b**). Piperidine was included in this study in hopes that intramolecular hydrogen bonding between the N–H of piperidine and the ether of ligand **1** would be favorable in one of the two *fac* diastereomers **13a**, **13b** thus aiding in their separation. Darensbourg has previously noted hydrogen bonding between the N–H of piperidine and the oxygen of $\text{P}(\text{OMe})_3$ in the X-ray structure¹⁹ of *cis*- $\text{Mo}(\text{CO})_4(\text{pip})[\text{P}(\text{OMe})_3]$ as well as hydrogen bonding to THF in solution.²⁰ Unfortunately complexes **13a** and **13b** are labile to piperidine dissociation as will be discussed shortly, thus precluding separation.

The products **9a,b-13a,b** exhibit singlets in their ^{31}P NMR spectra, ruling out substitution in an equatorial site to yield *mer* complexes for which an AB pattern would be expected for the phosphorus nuclei. The ^{31}P NMR resonances of the tungsten complexes exhibit satellites due to $^1\text{J}_{31\text{P}-183\text{W}}$ in the range 229-232 Hz. The ^{13}C NMR spectra of **9a,b-13a,b** indicate the presence of a plane of symmetry in these molecules as discussed above for **7a,b** and **8a,b**. The major isomers **9a-13a** also each exhibit a triplet resonance and a five-line multiplet for the single axial carbonyl and the two equivalent equatorial carbonyls, respectively, as expected for an AXX' spin system.²¹

The major substitution products **7a-13a** all exhibit three strong carbonyl stretches in their infrared spectra, consistent with their assignment as *fac* tricarbonyl complexes (see Table 1). Unfortunately, the carbonyl stretches for the minor

diastereomers could not be resolved from those of the major products in these spectra. Thus, based on infrared, ^{31}P and ^{13}C NMR spectroscopic data, all of the substitution products discussed above are assigned a *fac* geometry.

Table 1. Infrared spectroscopic data^a

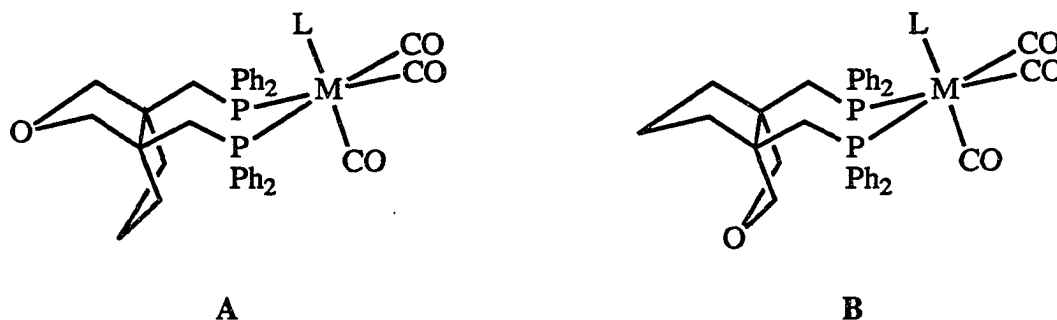
	ν_{CO} (cm^{-1})			
2^b, <i>fac</i>-(1)Mo(CO)₃	1921	1826	1763	
3^b, <i>fac</i>-(1)W(CO)₃	1913	1819	1757	
5^b, (1)Mo(CO)₄	2027	1934	1886	1869
6^b, (1)W(CO)₄	2021	1917	1892	1863
7a, <i>fac</i>-(1)Mo(CO)₃[P(OCH₂)₃CCH₃]	1942	1850		
8a, <i>fac</i>-(1)W(CO)₃[P(OCH₂)₃CCH₃]	1942	1846	1828	
9a, <i>fac</i>-(1)Mo(CO)₃(py)	1929	1830	1801	
10a, <i>fac</i>-(1)W(CO)₃(py)	1921	1825	1796	
11a, <i>fac</i>-(1)Mo(CO)₃(NCCH₃)				
12a, <i>fac</i>-(1)W(CO)₃(NCCH₃)	1929	1836	1805	
13a, <i>fac</i>-(1)W(CO)₃(pip)	1923	1825	1790	

^aSpectra were obtained on CH_2Cl_2 solutions.

^bSpectra were obtained on Nujol mulls.

Stereochemical Assignment of the *fac* Diastereomeric Products

Although spectroscopic data confirm a *fac* geometry for all diastereomeric products **7a,b-13a,b** there are important spectroscopic distinctions that differentiate the class of major diastereomers **7a-13a** from the minor diastereomers **7b-13b** (Table 2). Previously, our X-ray structural analysis of $(1)\text{Mo}(\text{CO})_4$, **5**, revealed a conformation as illustrated for **A** ($L = \text{CO}$) wherein the ether oxygen of **1** is oriented away from the metal center.¹⁰ In addition, a strong ring current effect was observed in the ^1H NMR spectrum of **5** for two methylene protons adjacent to the bridgehead carbons of the cyclopentane ring, which strongly argued for a similar conformation in solution. Analogously, the ^1H NMR spectra for each of the major diastereomers



contain a doublet of doublets in the vicinity of 1.0 ppm, also consistent with shielding of two cyclopentane methylene protons by neighboring phenyl substituents on phosphorus. Furthermore, the CH_2OCH_2 region in the ^1H NMR spectra of the major diastereomers exhibit resonances analogous to those found for **5** and **6** with no indication of a ring current effect.

In the ^{13}C NMR spectra of **7a,b-13a,b** differences between the groups of major and minor products are observed only in the CH_2O and $\text{CH}_2\text{CH}_2\text{CH}_2$ resonances. All the other ^{13}C NMR resonances of these complexes are quite similar. The CH_2O and

Table 2. Selected ^1H and ^{13}C NMR spectroscopic data^b

	δ	δ	δ	$\Delta \delta$
	$\text{O}(\text{CH}_2)_2$	$\text{CH}_2(\text{CH}_2)_2$	$\text{O}(\text{CH}_2)_2$	$\text{O}(\text{CH}_2)_2$
<u>major isomers</u>				
5 , (1)Mo(CO) ₄	86.3	42.8	3.60, 3.57	0.03
7 , (1)W(CO) ₄	86.3	42.7	3.60, 3.57	0.03
6a , <i>fac</i> -(1)Mo(CO) ₃ [P(OCH ₂) ₃ CCH ₃]	87.6	41.7	3.69, 3.63	0.06
8a , <i>fac</i> -(1)W(CO) ₃ [P(OCH ₂) ₃ CCH ₃]	87.6	41.5	3.69, 3.63	0.06
9a , <i>fac</i> -(1)Mo(CO) ₃ (py)	87.8	41.5	3.74, 3.69	0.05
10a , <i>fac</i> -(1)W(CO) ₃ (py)	87.8	41.3	3.74, 3.69	0.05
11a , <i>fac</i> -(1)Mo(CO) ₃ (NCCH ₃)	87.4	41.3	3.64, 3.56	0.08
12a , <i>fac</i> -(1)W(CO) ₃ (NCCH ₃)	87.4	41.1	3.64, 3.57	0.08
13a , <i>fac</i> -(1)W(CO) ₃ (pip)	87.6	41.3	3.70, 3.63	0.07
<u>minor isomers</u>				
7b , <i>fac</i> (1)Mo(CO) ₃ [P(OCH ₂) ₃ CCH ₃]	81.4	49.3		
8b , <i>fac</i> -(1)W(CO) ₃ [P(OCH ₂) ₃ CCH ₃]	81.1	49.7	3.48, 2.90	0.58
9b , <i>fac</i> -(1)Mo(CO) ₃ (py) ^a	81.1	50.4		
10b , <i>fac</i> -(1)W(CO) ₃ (py)	81.0	50.4	4.04, 2.99	1.05
11b , <i>fac</i> -(1)Mo(CO) ₃ (NCCH ₃)	81.5	49.3	3.96, 3.02	0.94
12b , <i>fac</i> -(1)W(CO) ₃ (NCCH ₃)	81.1	49.7	4.00, 2.99	1.01
13b , <i>fac</i> -(1)W(CO) ₃ (pip)	80.9	50.2	3.72, 2.87	0.85

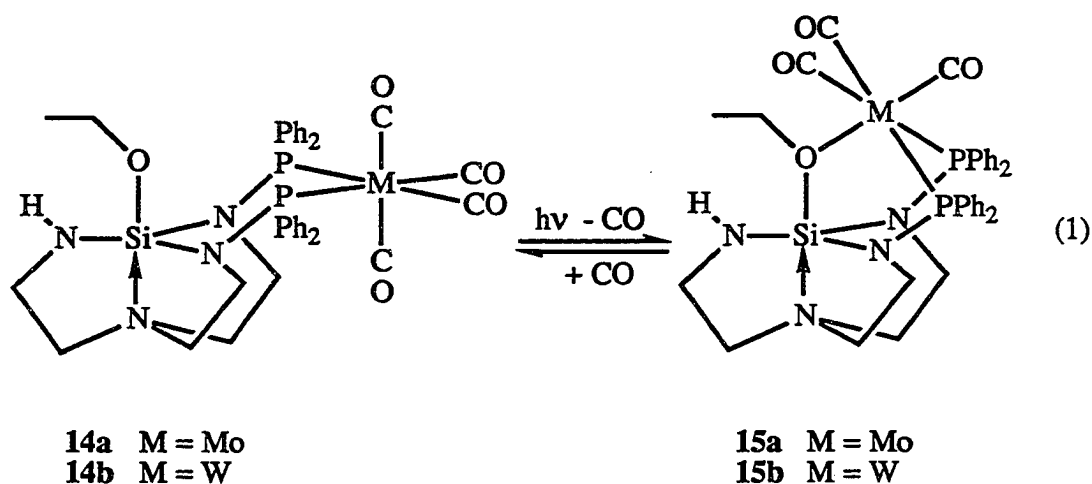
^aDue to the overlap of some resonances, definite assignments could not be made for **7b** and **9b**. ^bCD₂Cl₂ solvent; 20 °C.

$\text{CH}_2\text{CH}_2\text{CH}_2$ resonances of the major diastereomers are analogous to those found in the ^{13}C NMR spectra of **5** and **6**. On the basis of the similarity of ^1H and ^{13}C NMR spectral data for **7a-13a** to those for **5** and **6**, the major diastereomers are assigned structure **A** wherein the new ligand occupies the axial site previously occupied by the ether oxygen of **1** in the starting materials **2** and **3**. In contrast to the major diastereomers, the minor diastereomers **7a-13b** differ significantly in their ^1H and ^{13}C NMR spectra from those of **5** and **6**. These compounds experience a downfield shift of 7.6-9.1 ppm for their $\text{CH}_2\text{CH}_2\text{CH}_2$ ^{13}C NMR resonances, and an upfield shift of 6.0-6.5 ppm for their CH_2OCH_2 resonances in comparison to the major isomers. Again, no significant differences are found for the other carbon resonances. Based on molecular models, these two types of carbons are closest to neighboring phenyl rings and may experience ring current effects depending on the conformation of the ligand. These spectroscopic differences suggest a change in configuration from **A** to **B** where the new ligand now occupies an axial site *trans* to that previously occupied by the ether oxygen in the starting complexes **2** and **3**. Of the two five-membered rings in **1**, the ether-containing ring is now the closest to the metal center. Shielding is thus experienced at the CH_2O sites and not at the $\text{CH}_2\text{CH}_2\text{CH}_2$ positions. ^1H NMR spectroscopy provides some additional evidence for this conclusion. ^1H and $^1\text{H}\{^{31}\text{P}\}$ NMR spectra (500 MHz) have allowed accurate assignment of the CH_2OCH_2 protons for the minor isomers **8b**, **10b**, **11b**, and **12b**. For **10b** two doublet resonances are observed at 4.04 and 2.99 ppm, a separation of 1.05 ppm. Similarly for **8b**, **11b** and **12b**, these resonances are separated by 0.58, 0.94, and 1.01 ppm, respectively, with the upfield resonances occurring between 2.90 and 3.02 ppm in all cases. In contrast, the major diastereomers **7a-13a** exhibit AB quartets with resonances separated by only 0.06 to 0.08 ppm. This large chemical shift separation for the minor isomers as well as the

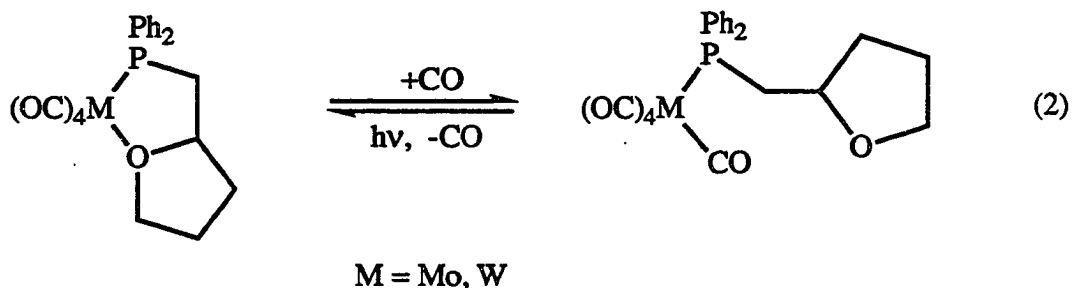
upfield shift of one of the two CH_2OCH_2 resonances strongly argues for a shielding effect at this position caused by a neighboring phenyl ring. Such shielding for two of the four CH_2OCH_2 protons is plausible only for structure B.

Reactions with carbon monoxide

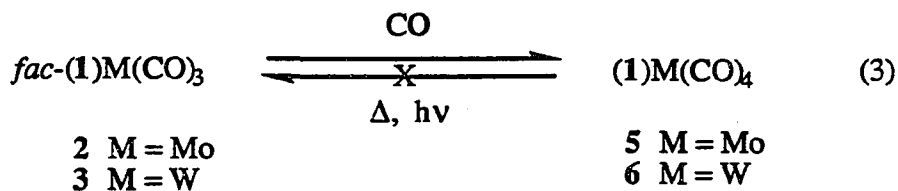
We have reported²² earlier that our $\text{N,N}'$ -bis(diphenylphosphino)azasilatrane complexes **14a** and **14b** react with carbon monoxide to form the tetracarbonyl species



15a and **15b** (reaction 1). This reaction was found to be reversible under photolytic as well as thermal conditions. Similarly, Rauchfuss⁵ reported reversible CO binding



for ruthenium complexes of *o*-(diphenylphosphino)anisole under both thermal and photolytic conditions, and Lindner³ reported reaction 2 to be reversible under photolytic conditions. When carbon monoxide was bubbled through a CH₂Cl₂ solution of **2** or **3**, substitution of the coordinated ether was completed within ten minutes as indicated by loss of the yellow color of the solution (reaction 3). ³¹P NMR and IR spectroscopic data allowed identification of the products as the previously characterized complexes **5** and **6**.¹⁰ In contrast to the above cited examples,



however, this reaction is not reversible. Refluxing **5** or **6** in toluene for as long as 16 hours or photolysis of **5** in THF for four hours yielded no observable reaction. Photolysis of **6** in toluene resulted in the precipitation of some decomposition material, but only starting material was identified in the supernatant by ³¹P NMR spectroscopy.

We recently reported¹⁴ the results of a ¹³CO labeling study which probed the stereospecificity of reaction 3. Reaction of **2** with ¹³CO was found to proceed with stereospecific incorporation of ¹³CO into axial sites yielding two diastereomers of *fac*-(1)Mo(CO)₃(¹³CO) as the sole products. Monitoring the reaction by ¹³C NMR spectroscopy revealed no ¹³CO incorporation into an equatorial site with the approximately 4:1 ratio of diastereomers remaining stable over a period of 17 days.

Darensbourg has reported²³ that reaction of (dppm)W(CO)₃(NCCH₃) with ¹³CO stereospecifically yields *fac*-(dppm)W(CO)₃(¹³CO) by incorporation of the ¹³CO into an axial site. Over the course of two weeks, however, a subsequent intramolecular

rearrangement process led to scrambling of the ^{13}CO between equatorial and axial sites. Thus, it was of interest to extend our ^{13}CO labeling study to include the tungsten analogue, **3**.

^{13}CO was bubbled through a solution of **3** in CD_2Cl_2 for 10 minutes during which time the characteristic yellow color of **3** had dissipated. The ^{13}C NMR spectrum of this solution showed two intense carbonyl resonances at 204.7 and 198.8 ppm with an intensity ratio of 0.16:1.00. The triplet resonance at 198.8 ppm showed well resolved tungsten satellites with $^1J_{^{183}\text{W}-^{13}\text{C}} = 124 \text{ Hz}$.²⁴ The natural abundance spectrum of $(1)\text{W}(\text{CO})_4$ (**6**) exhibits carbonyl resonances at 206.4, 204.9 and 198.9 ppm with the latter two assigned to the two nonequivalent axial carbonyls. The relative intensities of these resonances are 1.0:0.47:0.52, respectively. As in our molybdenum case, this result demonstrates stereospecific introduction of ^{13}CO exclusively into either of the two axial sites yielding two diastereomers of *fac*- $(1)\text{W}(\text{CO})_3(^{13}\text{CO})$. Over the course of two weeks, ^{13}C NMR spectroscopy revealed a slow equilibration of ^{13}CO between axial and equatorial sites. After 27 days, however, the relative intensities of the equatorial and axial carbonyl resonances had only attained a ratio of 1:1.2:3.4, far from the ratio observed in the natural abundance ^{13}C NMR spectrum of $(1)\text{W}(\text{CO})_4$ as illustrated in Figure 1. As in Darensbourg's case, our system apparently undergoes a slow *fac* to *mer* intramolecular rearrangement process, but at a rate much slower than that observed for *fac*-(dppm) $\text{W}(\text{CO})_3(^{13}\text{CO})$. This large difference in rates for the two systems is most likely related to the presence of a seven- vs. four-membered chelate ring. This isomerization may proceed via a slow dissociation of a chelating PPh_2 group, followed by subsequent isomerization and rechelation, in which case the stability of the chelate will determine the rate of equilibration.

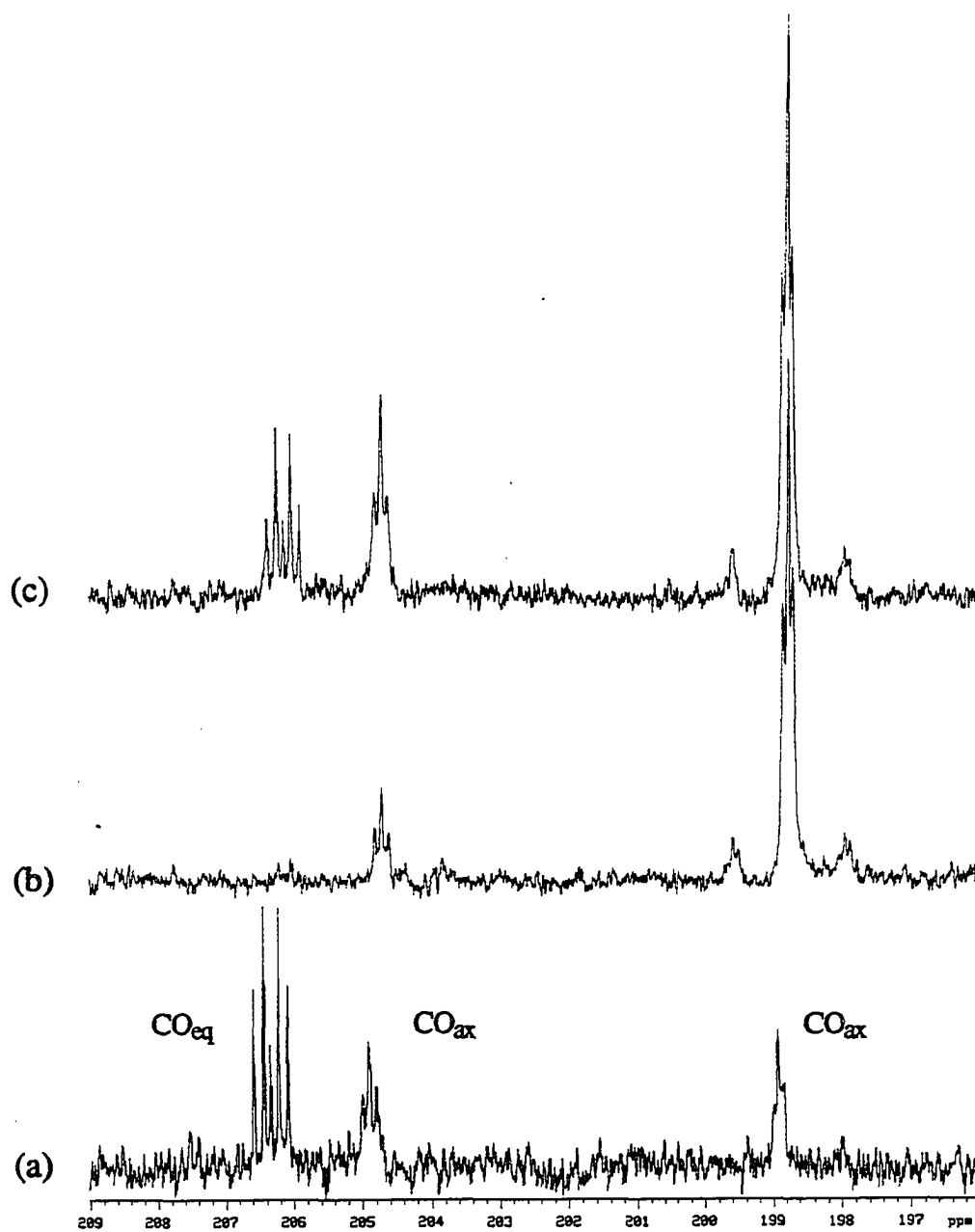


Figure 1. Carbonyl regions of the ^{13}C NMR (CD_2Cl_2) spectra of (a) $(1)\text{W}(\text{CO})_4$, natural abundance spectrum; (b) $\text{fac-}(1)\text{W}(\text{CO})_3 + ^{13}\text{CO}$; (c) $\text{fac-}(1)\text{W}(\text{CO})_3 + ^{13}\text{CO}$ after 27 days.

Previous ^{13}C O labeling studies on ligand substitution reactions of metal carbonyl complexes have also demonstrated stereospecificity in such reactions.²⁵ In addition to the work by Darensbourg cited above, Angelici reported²⁶ that the reaction of $[(\text{Ph}_2\text{PCH}_2\text{CH}_2)_2\text{NEt}]\text{Mo}(\text{CO})_3$ with ^{13}C O stereospecifically yielded *fac*- $[(\text{Ph}_2\text{PCH}_2\text{CH}_2)_2\text{NEt}]\text{Mo}(\text{CO})_3(^{13}\text{C}\text{O})$. Our study differs from these previous examples in that for metal complexes wherein **1** coordinates as a bidentate (*P,P'*) ligand, a plane of symmetry does not exist in the P_2M plane, thus differentiating the two axial sites. Our results demonstrate that the incoming ^{13}C O not only has access to the axial site vacated by the dissociated ether group of **1**, but also has access to the other nonequivalent axial site thus accounting for the minor diastereomeric products *fac*-**(1)** $\text{Mo}(\text{CO})_3(^{13}\text{C}\text{O})$ (ca. 20%) and *fac*-**(1)** $\text{W}(\text{CO})_3(^{13}\text{C}\text{O})$ (~14%).

The mechanism we propose to account for this result is outlined in Scheme I. Dissociation of the ether donor of **1** from **2** or **3** yields the five-coordinate intermediate **B** of approximately square pyramidal geometry. Unsaturated five-coordinate intermediates, such as $[\text{Cr}(\text{CO})_5]$, have been shown to be solvated within picoseconds after their formation.^{27,28} Based on calculations by Davy and Hall,²⁹ this process is too rapid to allow isomerization of **B** to provide an equatorial vacancy. Thus, no *mer* products should be formed in accord with the observed stereospecificity in this type of substitution reaction. Lichtenberger and Brown³⁰ have proposed a mechanism whereby, in a five-coordinate intermediate, the vacant site may be interchanged between two sites *cis* to a noncarbonyl ligand, but *trans* to each other, without the intermediate formation of a vacant site *trans* to the noncarbonyl ligand. In Scheme I, inversion of the vacant site to the position *trans* to itself would involve the

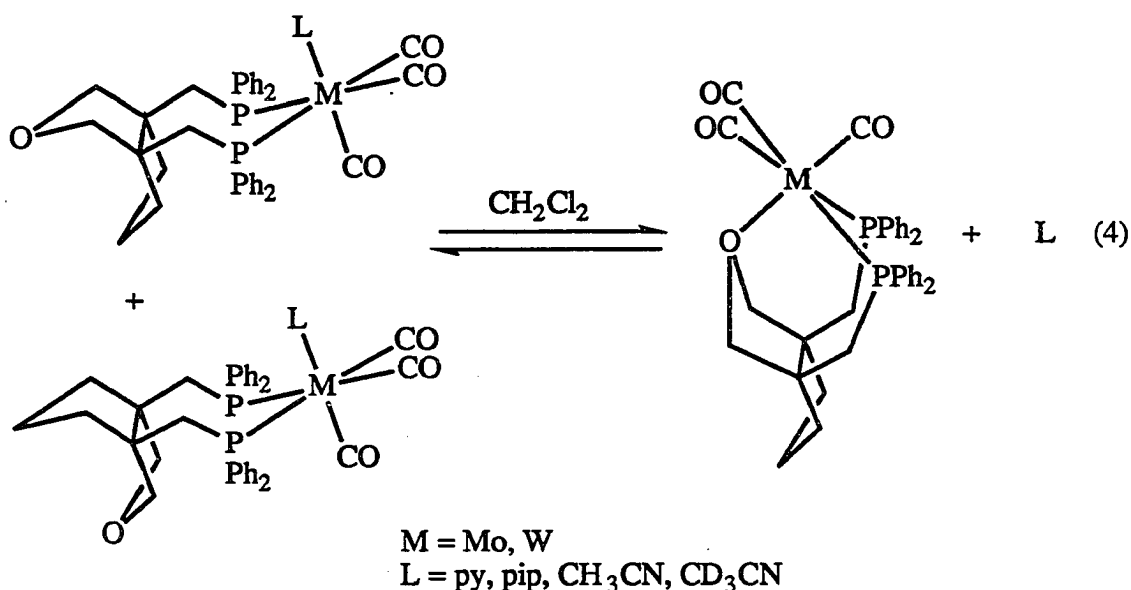
intermediates **B** and **B'**. These two intermediates are diastereomeric and should not be degenerate in energy. Thus, the rate of interconversion of **B** and **B'** relative to their rates of reaction with additional ligands may account for the unequal ratio of diastereomeric products observed.

The results of the reactions of **2** and **3** with acetonitrile, pyridine, piperidine and $\text{P}(\text{OCH}_2)_3\text{CCH}_3$ also indicate stereospecific incorporation of these ligands into axial sites to yield two *fac* diastereomers in each case. Thus the proposed scheme seems to be general for the ligands we have investigated.

Lability of the N-donor complexes

As discussed earlier, reaction of **2** or **3** with $\text{P}(\text{OCH}_2)_3\text{CCH}_3$ cleanly yields the *fac* diastereomeric products **7a-8b**. The results obtained when using pyridine, piperidine and acetonitrile were analogous with one notable distinction. The products obtained when using these N-donor ligands partially dissociate in solution unless excess N-donor ligand is present. For example, **3** reacts with excess pyridine yielding only the two *fac* diastereomers **10a** and **10b** which are isolated as an analytically pure, yellow solid. However, ^{31}P NMR and IR spectroscopies show not only the presence of **10a** and **10b**, but also the presence of the starting complex **3** when this solid sample is redissolved in methylene chloride. Additionally, a ^1H NMR spectrum of a solution of this redissolved material shows not only resonances due to a small quantity of **3**, but also resonances assigned to an equimolar amount of uncoordinated pyridine. ^{31}P NMR spectra of redissolved samples of **9a,b** and **11a,b-13a,b** also show the presence of the ether-coordinated complexes **2** or **3** unless excess N-donor ligand is present. For the complex *fac*-(**1**) $\text{W}(\text{CO})_3(\text{pip})$, **13a,b**, piperidine dissociation occurs to such an extent that **3** accounts for approximately 40% of the mixture in solution as shown by ^{31}P

NMR spectroscopy. These results suggest an equilibrium as shown in equation 4 wherein the ether of **1**, obviously aided by chelation, effectively competes with the N-donor ligands for coordination sites on the metal.



This equilibrium is supported by the results of an exchange reaction involving **12a,b** and CD_3CN monitored by 2H NMR spectroscopy. A solution of *fac*-(**1**) $W(CO)_3(NCCH_3)$ in CH_2Cl_2 was treated with an excess of CD_3CN . As can be seen in Figure 2, 2H NMR of the reaction solution after five minutes showed, in addition to free CD_3CN at 1.93 ppm, two singlets at 0.88 and 0.78 ppm in approximately a 1:4 ratio assigned to coordinated CD_3CN . The proton resonances for coordinated CH_3CN in the 1H NMR spectrum of **12a,b** experience an upfield shift due to neighboring phenyl rings and appear at 0.83 and 0.92 ppm, respectively. This assignment is verified by noting that for **12a** the resonance is split into a well resolved triplet with

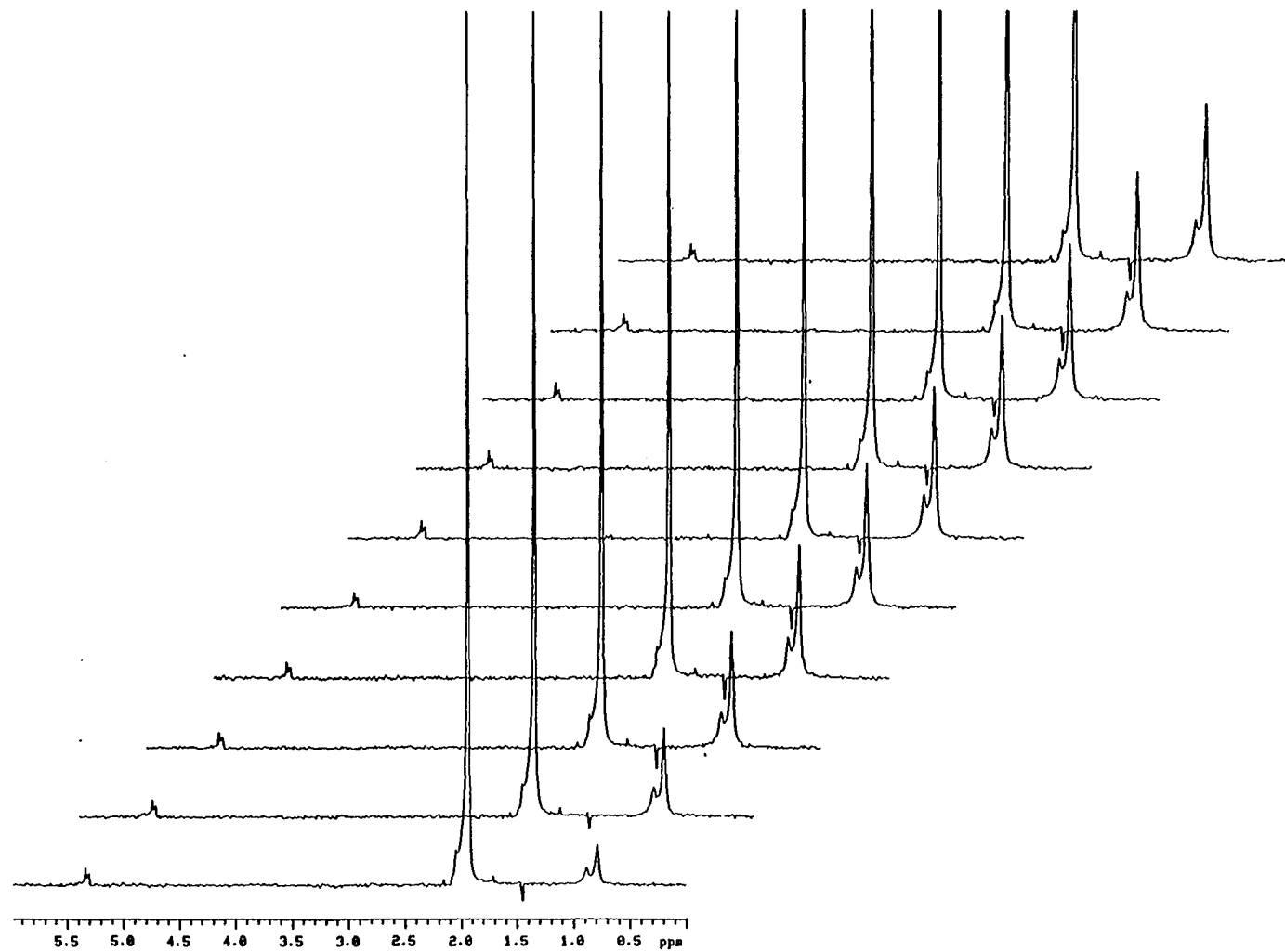


Figure 2. ^2H NMR spectra monitoring the exchange reaction between CD_3CN and $\text{fac}-(1)\text{W}(\text{CO})_3$.

$^5J_{\text{PH}} = 1.5$ Hz. Monitoring this exchange reaction over the period of two hours by ^2H NMR spectroscopy shows a steady increase in the intensity of the coordinated CD_3CN resonances as compared to the intensity of the CH_2Cl_2 resonance. Although the reaction was monitored for two hours, it appears to reach completion within approximately 50 minutes. This confirms that an exchange process does occur between coordinated and non-coordinated acetonitrile and that analogous exchange processes presumably occur for our piperidine and pyridine complexes according to the ^{31}P and ^1H NMR spectroscopic data presented above.

Regarding equilibrium 4, it should be noted that neither **2** nor **3** react with PPh_3 at ambient temperatures, in contrast to results obtained by Darensbourg²³ and Dobson^{25c} for the reactions of PPh_3 with *fac*-(dppm) $\text{W}(\text{CO})_3(\text{NCCH}_3)$ and *fac*-(dppe) $\text{Mo}(\text{CO})_3(\text{pip})$, respectively. Thus, in addition to steric crowding at the axial site hindering our reaction of **2** or **3** with PPh_3 , the ether of ligand **1** may also effectively compete with PPh_3 for coordination to the metal. We also note that neither **2** nor **3** react with ethylene or THF.

Conclusions

We have demonstrated that the metal-ether interactions of **2** and **3** are indeed labile to displacement by a variety of ligands. However, this coordinated ether is not as labile as might initially be expected for a coordinated ether, presumably because of a favorable chelation effect. Evidence for this conclusion is the presence of an equilibrium for the N-donor ligands wherein the ether of **1** effectively competes for coordination sites on the metal. We have also shown that all of the substitution reactions studied are stereospecific yielding two *fac* diastereomers in each case with the major substitution product arising from coordination of the new ligand to the site

vacated by the ether of **1**. Now that we have achieved a better understanding of the basic coordination modes and substitution reactions of these Group VI metal complexes, we shall be exploring the chemistry of **1** in metal systems that are potentially more significant catalytically.

ACKNOWLEDGMENTS

The authors thank the National Science Foundation and the Mallinckrodt Chemical Company for grant support of this research to J.G.V. We also thank Drs. Winfried Plass and Martina Schmidt for experimental assistance in the ^{13}C O labeling experiments.

REFERENCES

1. (a) Reddy, V. V. S.; Varshney, A.; Gray, G. M. *J. Organomet. Chem.* **1990**, *391*, 259. (b) Chen, S. J.; Dunbar, K. R. *Inorg. Chem.* **1990**, *29*, 588. (c) Lindner, E.; Norz, H. *Chem. Ber.* **1990**, *123*, 459. (d) Lindner, E.; Glaser, E. *J. Organomet. Chem.* **1990**, *391*, C37. (e) Lindner, E.; Speidel, R. *Z. Naturforsch.* **1989**, *44b*, 437. (f) Dunbar, K. R.; Haefner, S. C.; Pence, L. E. *J. Am. Chem. Soc.* **1989**, *111*, 5504. (g) Lindner, E.; Andres, B. *Chem. Ber.* **1988**, *121*, 829. (h) Lindner, E.; Sickinger, A.; Wegner, P. *J. Organomet. Chem.* **1988**, *349*, 75. (i) Lindner, E.; Sickinger, A.; Wegner, P. *J. Organomet. Chem.* **1986**, *312*, C37. (j) Lindner, E.; Meyer, S. *J. Organomet. Chem.* **1988**, *339*, 193. (k) Lindner, E.; Schober, V. *Inorg. Chem.* **1988**, *27*, 212. (l) Lindner, E.; Schober, V.; Stangle, M. *J. Organomet. Chem.* **1987**, *331*, C13. (m) Brown, J. M.; Maddox, P. J. *J. Chem. Soc., Chem. Commun.* **1987**, 1276. (n) Horner, L.; Simmons, G. *Z. Naturforsch.* **1984**, *39b*, 497. (o) Lindner, E.; Rauleder, H.; Scheytt, C.; Mayer, H. A.; Hiller, W.; Fawzi, R.; Wegner, P. *Z. Naturforsch.* **1984**, *39b*, 632. (p) Miller, E. M.; Shaw, B. L. *J. Chem. Soc., Dalton Trans.* **1974**, 480. (q) Empsall, H. D.; Hyde, E. M.; Jones, C. E.; Shaw, B. L. *J. Chem. Soc., Dalton Trans.* **1974**, 1980.
2. Werner, H.; Hampp, A.; Peters, K.; Peters, E. M.; Walz, L.; von Schnering, H. G. *Z. Naturforsch.* **1990**, *45b*, 1548.
3. Lindner, E.; Mayer, H. A.; Wegner, P. *Chem. Ber.* **1986**, *119*, 2616.
4. Dunbar, K. R.; Haefner, S. C.; Burzynski, D. J. *Organometallics* **1990**, *9*, 1347.
5. Jeffrey, J. C.; Rauchfuss, T. B. *Inorg. Chem.* **1979**, *18*, 2658.
6. Anderson, G. K.; Kumar, R. *Inorg. Chem.* **1984**, *23*, 4064.

7. Lindner, E.; Meyer, S.; Wegner, P.; Karle, B.; Sickinger, A.; Steger, B. *J. Organomet. Chem.* **1987**, *335*, 59.
8. Lindner, E.; Andres, B. *Chem. Ber.* **1987**, *120*, 761.
9. (a) Rauchfuss, T. B.; Patino, F. T.; Roundhill, D. M. *Inorg. Chem.* **1975**, *14*, 652.
(b) Lindner, E.; Schober, V.; Fawzi, R.; Hiller, W.; Englert, V.; Wegner, P. *Chem. Ber.* **1987**, *120*, 1621.
10. Mason, M. R.; Su, Y.; Jacobson, R. A.; Verkade, J. G. *Organometallics*, accepted.
11. Alcock, N. W.; Brown, J. M.; Jeffrey, J. C. *J. Chem. Soc., Dalton Trans.* **1976**, 583.
12. (a) Knowles, W. S.; Sabacky, M. J.; Vineyard, B. D. *Chem. Commun.* **1972**, 10.
(b) Vineyard, B. D.; Knowles, W. S.; Sabacky, M. J.; Bachman, G. L.; Weinkauff, D. J. *J. Am. Chem. Soc.* **1977**, *99*, 5946. (c) Knowles, W. S. *Acc. Chem. Res.* **1983**, *16*, 106.
13. (a) Lindner, E.; Bader, A.; Braunling, H.; Reinhard, J. *J. Mol. Catal.* **1990**, *57*, 291. (b) Lindner, E.; Schober, U.; Glaser, H.; Norz, H.; Wegner, P. *Z. Naturforsch.* **1987**, *42b*, 1527.
14. Mason, M. R.; Verkade, J. G. *J. Am. Chem. Soc.*, submitted.
15. In this context axial refers to a site *cis* to both phosphorus donors and equatorial refers to a site *trans* to a phosphorus donor.
16. Heitsch, C. W.; Verkade, J. G. *Inorg. Chem.* **1962**, *1*, 392.
17. The five line multiplets of an AXX' ($A = {}^{13}\text{C}$; $X, X' = {}^{31}\text{P}$) spin system which resemble triplets are denoted here as "apparent" triplets, at.

18. Due to the overlap of some resonances for the two diastereomers present, not all assignments could be made in the phenyl and cyclopentane methylene regions of the ^1H NMR spectra for the minor isomers.
19. Atwood, J. L.; Darensbourg, D. J. *Inorg. Chem.* **1977**, *16*, 2314.
20. Ewen, J.; Darensbourg, D. J. *J. Am. Chem. Soc.* **1975**, *97*, 6874.
21. (a) Pregosin, P. S.; Kunz, R. W. *NMR: Basic Princ. Progr.* **1979**, *16*, 65. (b) Redfield, D. A.; Nelson, J. H.; Carey, L. W. *Inorg. Nucl. Chem. Letters* **1974**, *10*, 727. (c) Andrews, G. T.; Colquhoun, I. J.; McFarlane, W. *Polyhedron* **1983**, *2*, 783.
22. Gudat, D.; Daniels, L. M.; Verkade, J. G. *Organometallics* **1990**, *9*, 1464.
23. Darensbourg, D. J.; Zalewski, D. J.; Plepys, C.; Campana, C. *Inorg. Chem.* **1987**, *26*, 3727.
24. $^1\text{J}_{183\text{W}-13\text{C}}$ values typically range from 120-145 Hz for carbonyl ligands in tungsten complexes. We believe that the $^1\text{J}_{183\text{W}-13\text{C}}$ values of 70.4 and 62.5 Hz reported in reference 21 may have been misstated and might actually be 140.8 and 125 Hz, respectively. See (a) Mann, B. E. *Adv. Organomet. Chem.* **1974**, *12*, 135. (b) Todd, L. J.; Wilkinson, J. R. *J. Organomet. Chem.* **1974**, *77*, 1.
25. (a) Darensbourg, D. J.; Kudarowski, R.; Schenk, W. *Inorg. Chem.* **1982**, *21*, 2488. (b) Darensbourg, D. J. *Inorg. Chem.* **1979**, *18*, 2821. (c) Dobson, G. R.; Asali, K. J.; Marshall, J. L.; McDaniel, C. R. *J. Am. Chem. Soc.* **1977**, *99*, 8100. (d) Darensbourg, D. J.; Kump, R. L. *J. Organomet. Chem.* **1977**, *140*, C29. (e) Darensbourg, D. J.; Dobson, G. R.; Muradi-Araghi, A. *J. Organomet. Chem.* **1976**, *116*, C17. (f) Hyde, C. L.; Darensbourg, D. J. *Inorg. Chem.* **1973**, *12*, 1286. (g) Darensbourg, D. J.; Graves, A. H. *Inorg. Chem.* **1979**, *18*, 1257.

26. Knebel, W. J.; Angelici, R. J.; Gansow, O. A.; Darensbourg, D. J. *J. Organomet. Chem.* **1974**, *66*, C11.
27. Simon, J. D.; Peters, K. S. *Chem. Phys. Lett.* **1983**, *98*, 53.
28. Simon, J. D.; Xie, X. *J. Phys. Chem.* **1986**, *90*, 6715.
29. Davy, R. D.; Hall, M. B. *Inorg. Chem.* **1989**, *28*, 3524.
30. Lichtenberger, D. L.; Brown, T. L. *J. Am. Chem. Soc.* **1978**, *100*, 366.

**SECTION VI. FLUORIDE-ASSISTED REDUCTION OF PALLADIUM(II)
PHOSPHINE COMPLEXES**

ABSTRACT

In the presence of 2.5 equivalents of *n*-Bu₄NF·3H₂O, PdCl₂ reacts with five equivalents of PPh₃ or three equivalents of a chelating diphosphine ((Ph₂PCH₂)₂, (Ph₂PCH₂)₂CH₂, (Ph₂PCH₂CH₂)₂, (Ph₂P)₂CH₂ and (Ph₂PCH₂)₂CMe₂) to give 70-90 % yields of the corresponding Pd(0) complexes and O=PPh₃ or diphosphine monoxide, respectively. Difluorophosphorane (F₂PPh₃ or Ph₂PF₂(CH₂)_xPPh₂) is detected as an intermediate prior to hydrolysis, suggesting that fluoride attacks a coordinated phosphorus, followed by electron transfer from phosphorus to palladium.

COMMUNICATION

Zerovalent palladium phosphine complexes have been extensively studied since their synthesis was first reported by Maletesta in 1957.¹ These compounds are commonly made via the reduction of palladium(II) complexes using NaBH₄, hydrazine or KOH/phosphine (for representative examples, see references 1-5). Although numerous other synthetic routes have been reported, there have been to the best of our knowledge no reports of the reduction of palladium(II) phosphine complexes involving fluoride ion. In this communication we report that palladium(II) in the presence of aryl phosphines and fluoride yields zerovalent palladium phosphine complexes via a novel fluoride-assisted redox reaction.

Addition of *n*-Bu₄NF·3H₂O (1.41 mmol) to a solution of (Ph₂PCH₂)₂CH₂ (1.69 mmol) and PdCl₂ (0.564 mmol) in DMSO at 130 °C resulted in the formation of an orange-red solution which rapidly changed to yellow (reaction 1). Upon cooling to room



temperature, a yellow precipitate formed which was isolated by filtration. The product, obtained in 91 % yield, was identified as Pd[(Ph₂PCH₂)₂CH₂]₂ by comparison of its ³¹P and ¹³C NMR spectra to those of an authentic sample prepared as described previously.^{2,3} This assignment was further confirmed crystallographically.⁶ Other aryl phosphine ligands employed in this reaction gave the known complexes Pd(PPh₃)₄,^{4,7} Pd[(Ph₂PCH₂)₂]₂,^{5,8} Pd[(Ph₂PCH₂CH₂)₂]₂⁹ and Pd₂[(Ph₂P)₂CH₂]₃,^{8,10} as well as the new complex Pd[(Ph₂PCH₂)₂CMe₂]₂.¹¹ These complexes, ranging in yield from

70-90 %, were characterized by ^{31}P , ^{13}C and ^1H NMR spectroscopy. In all cases the NMR data corresponded with published data.

The nature of the reducing agent is of interest since reduction does not occur in the absence of fluoride, whether or not water is present. For example, reaction of excess $(\text{Ph}_2\text{PCH}_2)_2$ with PdCl_2 gave $\{\text{Pd}[(\text{Ph}_2\text{PCH}_2)_2]_2\}\text{Cl}_2$ ^{8,12} in 96% yield. Similarly $(\text{Ph}_3\text{P})_2\text{PdCl}_2$ was isolated in 90 %yield when excess PPh_3 was reacted with PdCl_2 . Moreover, reduction failed to take place when water was added to a mixture of PPh_3 and PdCl_2 , but did occur when fluoride ion was added. The addition of less than a stoichiometric amount of fluoride results in only partial reaction, presumably owing to the formation of the exceedingly stable HF_2^- ion from the protons liberated in the reaction (Scheme I). Analysis of the filtrate of reaction 1 by ^{31}P NMR spectroscopy gave evidence for the formation of the phosphine monoxide $\text{Ph}_2\text{P}(\text{CH}_2)_3\text{P}(\text{O})\text{Ph}_2$ (δ ^{31}P 31.0, -17.2) as one of two observable oxidation products. The other bidentate phosphines employed also yielded the phosphine monoxides (and not the dioxides) as the final oxidation products. This assignment is unambiguous since $\text{Ph}_2\text{P}(\text{O})\text{CH}_2\text{CH}_2\text{P}(\text{O})\text{Ph}_2$ and $\text{Ph}_2\text{P}(\text{O})\text{CH}_2\text{P}(\text{O})\text{Ph}_2$ exhibit singlet ^{31}P NMR resonances whereas the monoxides $\text{Ph}_2\text{PCH}_2\text{P}(\text{O})\text{Ph}_2$ and $\text{Ph}_2\text{PCH}_2\text{CH}_2\text{P}(\text{O})\text{Ph}_2$ each exhibit two doublets.¹³ The filtrates of reactions of the type exemplified by reaction 1 also contained a difluorophosphorane product. For $(\text{Ph}_2\text{PCH}_2)_2$, $\text{Ph}_2\text{PCH}_2\text{CH}_2\text{PF}_2\text{Ph}_2$ was identified by comparison of its ^{31}P and ^{19}F NMR spectroscopic parameters¹⁴ to those previously reported.¹⁵ The difluorophosphorane products for the other ligands employed were similarly identified.^{16,17}

A plausible reaction pathway is proposed in Scheme I. Nucleophilic attack of fluoride on phosphorus followed by transfer of two electrons from phosphorus to palladium yields the palladium(0) complex and a fluorophosphonium salt. Although we

ACKNOWLEDGMENT

We thank donors of the Petroleum Research Fund, administered by the American Chemical Society, and the Mallinckrodt Chemical Company for support of this research.

REFERENCES

1. Malatesta, L.; Angoletta, M. *J. Chem. Soc.* **1957**, 1186.
2. Clark, H.C.; Kapoor, P.N.; McMahon, I.J. *J. Organomet. Chem.* **1984**, *265*, 107.
3. Laing, K.R.; Robinson, S.D.; Uttley, M.F. *J. Chem. Soc. Dalton Trans.* **1974**, 1205.
4. Coulson, D.R. *Inorg. Synth.* **1972**, *13*, 121.
5. Chatt, J.; Hart, F.A.; Watson, H.R. *J. Chem. Soc.* **1962**, 2537.
6. Mason, M.R.; Verkade, J.G. manuscript in progress.
7. Tolman, C.A.; Seidel, W.C.; Gerlach, D.H. *J. Am. Chem. Soc.* **1972**, *94*, 2669.
8. Lindsay, C.H.; Benner, L.S.; Balch, A.L. *Inorg. Chem.* **1980**, *19*, 3503.
9. Kumobayashi, H.; Mitsunashi, S.; Akutagawa, S.; Ohtsuka, S. *Chem. Lett.* **1986**, 157.
10. Stern, E.W.; Maples, P.K. *J. Catal.* **1972**, *27*, 120.
11. The ligand $(\text{Ph}_2\text{PCH}_2)_2\text{CMe}_2$ was synthesized as described by Kraihanzel, C.S.; Ressler, J.M.; Gray, G.M. *Inorg. Chem.* **1982**, *21*, 879.
12. Westland, A.D. *J. Chem. Soc.* **1965**, 3060.
13. ^{31}P NMR (DMSO): $\text{Ph}_2\text{PCH}_2\text{P}(\text{O})\text{Ph}_2$ δ 28.8(d), -27.1(d), $^2J_{\text{PP}} = 50.5$ Hz; $\text{Ph}_2\text{PCH}_2\text{CH}_2\text{P}(\text{O})\text{Ph}_2$ δ 32.3(d), -12.4(d), $^3J_{\text{PP}} = 47.3$ Hz. For literature values see (a) Grim, S.O.; Walton, E.D. *Inorg. Chem.* **1980**, *19*, 1982. (b) Berners-Price, S.J.; Johnson, R.K.; Mirabelli, C.K.; Faucette, L.F.; McCabe, F.L.; Sadler, P.J. *Inorg. Chem.* **1987**, *26*, 3383.
14. ^{31}P NMR (DMSO): δ -12.4 (d, $^3J_{\text{PP}} = 69$ Hz), -40.5 (td, $^1J_{\text{PF}} = 644$ Hz, $^3J_{\text{PP}} = 69$ Hz); ^{19}F NMR (DMSO): δ 125.3 (d, $^1J_{\text{PF}} = 644$ Hz).
15. Ruppert, I. *Z. Naturforsch., B: Anorg. Chem., Org. Chem.* **1979**, *34B*, 662.

16. Compound, δ $^{31}\text{P}(\text{III})$, δ $^{31}\text{P}(\text{V})$, $^1\text{J}_{\text{PF}}$, $^n\text{J}_{\text{PP}}$, δ ^{19}F , $^3\text{J}_{\text{PF}}$: $\text{Ph}_2\text{PCH}_2\text{PF}_2\text{Ph}_2$,
-23.9(dt), -41.9(td), 643 Hz, 63.9 Hz, 136.1 (ddt), 22.5 Hz; $\text{Ph}_2\text{P}(\text{CH}_2)_3\text{PF}_2\text{Ph}_2$,
-17.3(s), -42.4(t), 643 Hz, -125.8(d); $\text{Ph}_2\text{P}(\text{CH}_2)_4\text{PF}_2\text{Ph}_2$, -15.6(s), -40.8(t), 639
Hz; $\text{Ph}_2\text{PCH}_2\text{CMe}_2\text{CH}_2\text{PF}_2\text{Ph}_2$, -23.6(s), -44.4(t), 657 Hz; Ph_3PF_2 , -54.0(t), 657
Hz.
17. Ruppert, I.; Bastian, V. *Angew. Chem. Int. Ed., Engl.* **1977**, *16*, 718.
18. Seel, V.F.; Bassler, H.J. *Z. Anorg. Allg. Chem.* **1975**, *418*, 263.

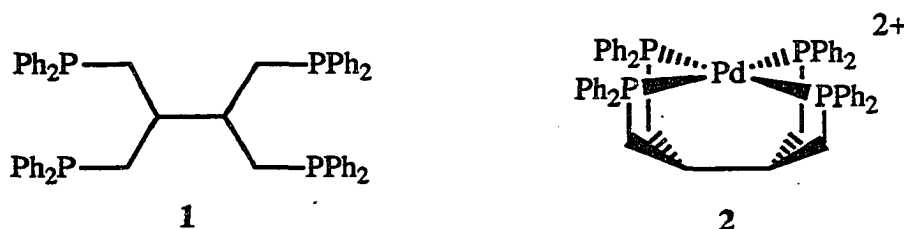
**SECTION VII. A NEW REDOX REACTION INVOLVING FLUORIDE AND
PHOSPHINE COMPLEXES OF GROUP X METALS. CRYSTAL
AND MOLECULAR STRUCTURE OF Pd(dppp)₂**

ABSTRACT

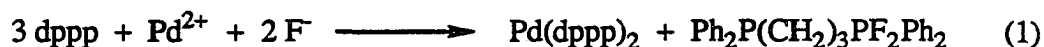
A new redox reaction involving phosphine complexes of palladium(II) and fluoride is reported. The scope of this reaction has been investigated using the ligands PPh_3 , $\text{Ph}_2\text{P}(\text{CH}_2)_n\text{PPh}_2$ ($n = 1-4$), $\text{Ph}_2\text{PCH}_2\text{C}(\text{CH}_3)_2\text{CH}_2\text{PPh}_2$, Ph_2PCH_3 , and $\text{P}(\text{CH}_2\text{CH}_2\text{CN})_3$; several solvents including DMSO, pyridine, acetonitrile, and THF; and either $n\text{-Bu}_4\text{NF}\cdot 3\text{H}_2\text{O}$ or $\text{KF}/18\text{-crown-6}$ as the fluoride source. The reduction products are palladium(0) phosphine complexes. ^{31}P and ^{19}F NMR spectra permitted identification of the initial oxidation products as difluorophosphoranes (R_3PF_2), which subsequently hydrolyze forming phosphine oxides if a hydrated fluoride source is used. Substantial quantities of the difluorophosphorane products are observed when anhydrous KF is utilized. This redox reaction was initially discovered as a side reaction between dppp and $\text{Pd}(\text{BF}_4)_2\cdot 4\text{CH}_3\text{CN}$ implicating BF_4^- as a fluoride source for the reaction. Results implicating this fluoride-induced redox reaction in the thermal decomposition of $[(\text{Ph}_3\text{P})_3\text{PdCl}]\text{BF}_4$ to yield $[\text{Pd}_3\text{Cl}(\text{PPh}_2)_2(\text{PPh}_3)_3]\text{BF}_4$ are also presented. Preliminary results indicate that platinum complexes also undergo this reaction, but nickel complexes yield NiF_2 . Crystals of $\text{Pd}(\text{dppp})_2$ were obtained, space group C2/c (No.15), with unit cell dimensions $a = 18.396(2) \text{ \AA}$, $b = 13.290(1) \text{ \AA}$, $c = 20.186(2) \text{ \AA}$, $\beta = 109.383(5)^\circ$, and $Z = 4$. The structure was refined to $R = 0.0225$ and $R_w = 0.0341$ for 4431 unique reflections with $F_o^2 > 3\sigma(F_o^2)$.

INTRODUCTION

Recently, we reported¹ the synthesis and some of the coordination chemistry of the new tetratertiary phosphine **1**, including unsuccessful attempts to synthesize the monopalladium complex **2**. Presumably the formation of **2** is precluded by steric factors and an unsuitable ligand backbone, incapable of chelating two *trans* positions. The complexes $[\{\text{Ph}_2\text{P}(\text{CH}_2)_n\text{PPh}_2\}_2\text{Pd}]^{2+}$ ($n = 2-4$) are potential models for **2** and we thus sought information concerning the steric interactions of the eight phenyl substituents in



these complexes. Although numerous references were found concerning the chemistry of $[\text{Pd}(\text{dppe})_2]^{2+}$ ($n = 2$),² only a brief reference to $[\text{Pd}(\text{dppp})_2]\text{Cl}_2$ ($n = 3$) has appeared³ and $[\text{Pd}(\text{dppb})_2]^{2+}$ ($n = 4$) has not been reported previously. Since we were most interested in the model complexes containing six- and seven-membered chelate rings, we attempted to prepare $[\text{Pd}(\text{dppp})_2][\text{BF}_4]_2$ by reacting $\text{Pd}(\text{BF}_4)_2 \cdot 4\text{CH}_3\text{CN}$ and dppp . As discussed herein, this synthetic approach unexpectedly yielded, as a minor product, the reduced complex $\text{Pd}(\text{dppp})_2$ formed via a fluoride-induced redox reaction:



Preliminary observations concerning this reaction have been previously communicated.⁴ Here we present these and additional results in detail, including the relevance of reaction

1 to the synthesis of the triangular cluster $[\text{Pd}_3\text{Cl}(\text{PPh}_2)_2(\text{PPh}_3)_3][\text{BF}_4]$ reported by Dixon et al.⁵ The molecular structure of $\text{Pd}(\text{dppp})_2$ and preliminary results concerning attempts to reduce $\text{Ni}(\text{II})$ and $\text{Pt}(\text{II})$ by this method are also discussed.

EXPERIMENTAL SECTION

General Procedures

All reactions were performed under an argon atmosphere using standard inert atmosphere techniques. Tetrahydrofuran, benzene, and diethyl ether were distilled from sodium benzophenone ketyl prior to use. Pyridine, dimethylsulfoxide, methylene chloride, and acetonitrile were distilled from calcium hydride. The following were prepared as described in the literature; $(\text{Ph}_3\text{P})_2\text{PdCl}_2$,⁶ $(\text{dppp})\text{PdCl}_2$,⁷ $(\text{dppe})\text{PdCl}_2$,⁷ $(\text{PhCN})_2\text{PdCl}_2$,⁸ $[(\text{dppe})_2\text{Pd}]\text{Cl}_2$,^{2a} $[(\text{Ph}_3\text{P})_3\text{PdCl}]\text{BF}_4$ ⁹ and $\text{Ph}_2\text{PCH}_2\text{C}(\text{CH}_3)_2\text{CH}_2\text{PPh}_2$.¹⁰ $\text{Pd}(\text{BF}_4)_2 \cdot 4\text{CH}_3\text{CN}$ was purchased from Strem. All other reagents were purchased from Strem or Aldrich and were used without further purification, except for 18-crown-6, which was purified by a previously reported method¹¹ and was as a THF solution over 4Å molecular sieves. NMR spectra were recorded on Nicolet NT-300 (¹H, ¹³C), Bruker WM200 (¹³C, ³¹P), and Bruker WM300 (¹³C, ¹⁹F, ³¹P) spectrometers using a deuterated solvent as the internal lock. Chemical shifts are reported relative to TMS (¹H, ¹³C), C₆F₆ (¹⁹F), or 85% H₃PO₄ (³¹P). Elemental analyses were performed by Schwarzkopf Microanalytical Laboratories, Woodside, NY.

Reaction of (dppp)PdCl₂ with dppp

A mixture of $(\text{dppp})\text{PdCl}_2$ (0.20 g, 0.34 mmol) and dppp (0.14 g, 0.34 mmol) in 5 mL of pyridine and 30 mL of acetonitrile was refluxed for four hours to yield a yellow solution. The ³¹P NMR spectrum of this solution showed only broadened resonances for the two starting materials at 11.9 and -16.9 ppm.^{2c}

Reaction of dppp with $\text{Pd}(\text{BF}_4)_2 \cdot 4\text{CH}_3\text{CN}$

A solution of dppp (0.35 g, 0.86 mmol) in 2 mL of CH_2Cl_2 was added to a yellow solution of $\text{Pd}(\text{BF}_4)_2 \cdot 4\text{CH}_3\text{CN}$ (0.19 g, 0.43 mmol) in 20 mL of acetonitrile. Within ten minutes a cream-colored precipitate began to appear. After stirring the mixture overnight the product was isolated by filtration and dried *in vacuo*. Yield 0.27 g, 57% based on $[\text{Pd}(\text{dppp})_2][\text{BF}_4]_2$. The product is poorly soluble in THF, CH_2Cl_2 , DMSO, and CH_3CN . Upon standing overnight, the filtrate yielded yellow crystals of $\text{Pd}(\text{dppp})_2$ in approximately 5% yield. A suitable crystal was analyzed by X-ray diffraction.

Preparation of $(\text{Ph}_2\text{PCH}_2\text{C}(\text{CH}_3)_2\text{CH}_2\text{PPh}_2)\text{PdCl}_2$

A solution of $\text{Ph}_2\text{PCH}_2\text{C}(\text{CH}_3)_2\text{CH}_2\text{PPh}_2$ (0.34 g, 0.78 mmol) in 15 mL of benzene was added dropwise to a solution of $(\text{PhCN})_2\text{PdCl}_2$ (0.30 g, 0.78 mmol) in 40 mL of benzene. The resulting mixture was stirred overnight. The light tan precipitate was isolated by filtration, rinsed with 10 mL of benzene followed by 10 mL of diethyl ether, and dried *in vacuo*. Yield 0.45 g, 95%. ^{31}P NMR (DMSO) δ 19.1 (s).

Preparation of $\text{Pd}(\text{PPh}_3)_4$

Method A. A mixture of PdCl_2 (0.11 g, 0.62 mmol) and PPh_3 (0.77g, 2.9 mmol) was heated to 140 °C in 15 mL of DMSO to give a yellow solution. Heating was discontinued and a solution of *n*- $\text{Bu}_4\text{NF} \cdot 3\text{H}_2\text{O}$ (0.47 g, 1.7 mmol) in 10 mL of DMSO was added to give a dark orange-red solution which rapidly turned bright yellow. The solution was cooled to room temperature with stirring during which time a yellow solid precipitated. Ethanol (20 mL) was added to complete precipitation and the mixture was stirred for an additional 30 min. The product was isolated by filtration, rinsed with two

10 mL portions of ethanol and one of diethyl ether, and was dried *in vacuo*. Yield 0.57 g, 80%. mp 190 - 194 °C (dec); ^{31}P NMR (CH_2Cl_2) δ 15.5 (br); lit δ 15.0 (toluene, 90 °C).¹² Analysis of the filtrate by ^{31}P NMR spectroscopy revealed the presence of the following: $\text{Ph}_3\text{P}=\text{O}$ δ 29.5 (s), *trans*-(Ph_3P) $_2\text{Pd}(\text{Ph})\text{Cl}$ δ 25.1 (s), and $[\text{Ph}_4\text{P}]\text{Cl}$ δ 23.7 (s), the assignments of which were confirmed by the addition of authentic samples.

Method B. A solution of PdCl_2 (0.10 g, 0.56 mmol) and PPh_3 (0.74 g, 2.82 mmol) in 15 mL of DMSO was heated to 140 °C. Anhydrous KF (0.080 g, 1.4 mmol) was added and the resulting yellow solution was heated at 120 °C for ten minutes to dissolve most of the remaining undissolved KF. The solution was cooled to room temperature yielding a precipitate identified as $\text{Pd}(\text{PPh}_3)_4$. The product was isolated by filtration, washed with diethyl ether and dried *in vacuo*. Yield 0.35 g, 54%. The ^{31}P NMR spectrum of the filtrate revealed the presence of $\text{Ph}_3\text{P}=\text{O}$, $[\text{Ph}_4\text{P}]\text{Cl}$, PPh_3 and a much larger quantity of *trans*-(Ph_3P) $_2\text{Pd}(\text{Ph})\text{Cl}$ than was observed using method A. Clear crystals of *trans*-(Ph_3P) $_2\text{Pd}(\text{Ph})\text{Cl}$ were obtained from the filtrate upon standing several days. mp 210 °C; ^{31}P NMR (CH_2Cl_2) δ 24.4 (s); ^1H NMR (CDCl_3) δ 7.6 - 7.2 (m, PPh_3), 6.71 (d, $^3J_{\text{HH}} = 7$ Hz, 2H, Ph-*ortho*), 6.35 (t, $^3J_{\text{HH}} = 7$ Hz, 1H, Ph-*para*), 6.22 (t, $^3J_{\text{HH}} = 7$ Hz, 2H, Ph-*meta*).

Preparation of $\text{Pd}_2(\text{dppm})_3$

PdCl_2 (0.10 g, 0.56 mmol), dppm (0.65 g, 1.7 mmol), and *n*- $\text{Bu}_4\text{NF}\cdot 3\text{H}_2\text{O}$ (0.47 g, 1.5 mmol) were reacted using method A given above to yield an orange-red solid. Yield 0.33 g, 86%. mp 195-215 °C (dec); ^{31}P NMR (C_6H_6) δ 14.4 (s).¹³ Analysis of the filtrate by ^{31}P NMR spectroscopy revealed the presence of the following: $\text{Ph}_2\text{PCH}_2\text{P}(\text{O})\text{Ph}_2$ δ 28.8 (d, $^2J_{\text{PP}} = 50.5$ Hz, $\text{P}(\text{O})\text{Ph}_2$), -27.0 (d, $^2J_{\text{PP}} = 50.5$ Hz, PPh_2);¹⁴ dppm δ -22.3 (s); $\text{Ph}_2\text{PCH}_2\text{PF}_2\text{Ph}_2$ δ -23.9 (dt, $^2J_{\text{PP}} = 63.9$ Hz, $^3J_{\text{PF}} = 22.5$

Hz, PPh₂), -41.9 (td, ¹J_{PF} = 643 Hz, ²J_{PP} = 63.9 Hz, PF₂Ph₂).¹⁵ ¹⁹F NMR δ 136.1 (ddt, ¹J_{PF} = 644 Hz, ³J_{PF} = 22 Hz, ³J_{HF} = 15 Hz, Ph₂PCH₂PF₂Ph₂).

Preparation of Pd(dppe)₂

PdCl₂ (0.10 g, 0.56 mmol), dppe (0.67 g, 1.7 mmol), and *n*-Bu₄NF•3H₂O (0.47 g, 1.5 mmol) were reacted using method A given above to yield the title product. Yield 0.51 g, 91%. ³¹P NMR (CH₂Cl₂) δ 30.6. Analysis of the filtrate by ³¹P NMR spectroscopy revealed the presence of the following: [Pd(dppe)₂]²⁺, δ 58.0 (s);^{2c} Ph₂P(O)CH₂CH₂PPh₂, δ 32.4 (d, ³J_{PP} = 47.3 Hz, P(O)Ph₂), -12.4 (d, ³J_{PP} = 47.3 Hz, PPh₂);¹⁶ Ph₂PCH₂CH₂PF₂Ph₂, δ -12.4 (m, PPh₂), -40.5 (td, ¹J_{PF} = 644 Hz, ³J_{PP} = 69 Hz, PF₂Ph₂).¹⁵

Alternatively, (dppe)PdCl₂ (0.15 g, 2.6 mmol), dppe (0.21 g, 5.2 mmol), anhydrous KF (0.10 g, 1.7 mmol), and 18-crown-6 (0.100 g) were suspended in a solution of 10 mL of pyridine and 5 mL of THF. This mixture was heated at 100 °C for two hours. A ³¹P NMR spectrum of this reaction solution showed only the presence of Pd(dppe)₂, Ph₂PCH₂CH₂P(O)Ph₂, Ph₂PCH₂CH₂PF₂Ph₂, and a trace of unreacted dppe. The difluorophosphorane product accounted for approximately 65% of the total oxidation products.

Preparation of Pd(dppp)₂

PdCl₂ (0.10 g, 0.56 mmol), dppp (0.70 g, 1.7 mmol), and *n*-Bu₄NF•3H₂O (0.47 g, 1.5 mmol) were reacted using method A given above to yield 0.48 g (91%) of the yellow product. ³¹P NMR (THF) δ 4.2 (s); ¹³C NMR (CD₂Cl₂) δ 143.0 (m, Ph-*ipso*), 132.8 (m, Ph-*ortho*), 127.8 (bs, Ph-*meta*), 127.6 (s, Ph-*para*), 31.9

(m, CH₂PPh₂), 19.0 (bs, CH₂CH₂CH₂). Analysis of the filtrate by ³¹P NMR spectroscopy revealed the presence of the following: Ph₂P(O)CH₂CH₂CH₂PPh₂ δ 31.0 (s, P(O)Ph₂), -17.2 (s, PPh₂); Ph₂PCH₂CH₂CH₂PF₂Ph₂ δ -17.3 (s, PPh₂), -42.4 (t, ¹J_{PF} = 644 Hz, PF₂Ph₂).¹⁵ ¹⁹F NMR δ 125.8 (d, ¹J_{PF} = 643 Hz).

Preparation of Pd{Ph₂PCH₂C(CH₃)₂CH₂PPh₂}₂

PdCl₂ (0.10 g, 0.56 mmol), Ph₂PCH₂C(CH₃)₂CH₂PPh₂ (0.75 g, 1.7 mmol), and *n*-Bu₄NF·3H₂O (0.47 g, 1.5 mmol) were reacted using method A above to yield 0.51 g (91%) of the yellow product. An analytical sample was obtained by recrystallization from 2:1 THF:EtOH. ³¹P NMR (CH₂Cl₂) δ 1.2 (s); ¹³C NMR (CD₂Cl₂) δ 144.6 (apparent pentet, separation 6 Hz, Ph-*ipso*), 132.8 (m, Ph-*ortho*), 127.8 (s, Ph-*meta*), 127.4 (s, Ph-*para*), 41.9 (m, CH₂), 36.0 (m, CC₄), 34.6 (m, CH₃); Anal. Calcd for C₅₈H₃₀P₄Pd·2 CH₃CH₂OH: C, 68.98; H, 6.72; Pd, 9.86. Found: C, 68.95; H, 6.43; Pd, 9.65. Analysis of the filtrate by ³¹P NMR spectroscopy revealed the presence of the following: Ph₂P(O)CH₂C(CH₃)₂CH₂PPh₂ δ 26.1 (s, P(O)Ph₂), -23.3 (s, PPh₂).

Alternatively, {Ph₂PCH₂C(CH₃)₂CH₂PPh₂}PdCl₂ (0.20 g, 0.32 mmol), Ph₂PCH₂C(CH₃)₂CH₂PPh₂ (0.19 g, 0.65 mmol), anhydrous KF (0.12 g, 2.1 mmol), and 18-crown-6 (0.10 g) were suspended in 10 mL of pyridine/ 5 mL of THF and the mixture was refluxed for two hours to yield a bright yellow solution with some undissolved KF. The ³¹P NMR spectrum of this solution revealed the presence of Pd{Ph₂PCH₂C(CH₃)₂CH₂PPh₂}₂, Ph₂PCH₂C(CH₃)₂CH₂P(O)Ph₂, a trace of Ph₂P(O)CH₂C(CH₃)₂CH₂P(O)Ph₂ and unreacted dppe. A singlet at -23.6 ppm (PPh₂) and triplet at -44.4 ppm with ¹J_{PF} = 658 Hz (PF₂Ph₂) indicate the presence of the difluorophosphorane Ph₂PCH₂C(CH₃)₂CH₂PF₂Ph₂ which accounted for approximately

75% of the oxidation products. Addition of 20 mL of ethanol to this solution resulted in the precipitation of $\text{Pd}\{\text{Ph}_2\text{PCH}_2\text{C}(\text{CH}_3)_2\text{CH}_2\text{PPh}_2\}_2$ which was isolated by filtration, washed twice with 5 mL of water followed by 10 mL of ethanol, and dried *in vacuo*. Yield 0.23 g, 75%.

Preparation of $\text{Pd}(\text{dppb})_2$

PdCl_2 (0.10 g, 0.56 mmol), dppb (0.72 g, 1.7 mmol), and *n*- $\text{Bu}_4\text{NF}\cdot 3\text{H}_2\text{O}$ (0.47 g, 1.5 mmol) were reacted using method A to yield 0.35 g (65%) of the yellow product. ^{31}P NMR (CH_2Cl_2) δ 12 (broad). Analysis of the filtrate by ^{31}P NMR spectroscopy revealed the presence of the following: $\text{Ph}_2\text{P}(\text{O})(\text{CH}_2)_4\text{PPh}_2$ δ 33.7 (s, $\text{P}(\text{O})\text{Ph}_2$), -15.6 (s, PPh_2); $\text{Ph}_2\text{PF}_2(\text{CH}_2)_4\text{PPh}_2$ δ -15.6 (s, PPh_2), -40.8 (t, $^1J_{\text{PF}} = 639$ Hz, PF_2Ph_2).¹⁵

Preparation of $\text{Pd}(\text{PPh}_2\text{Me})_4$

PdCl_2 (0.10 g, 0.56 mmol), Ph_2PMe (0.57 g, 2.8 mmol), and *n*- $\text{Bu}_4\text{NF}\cdot 3\text{H}_2\text{O}$ (0.47 g, 1.5 mmol) were reacted using method A, however, no precipitate formed upon cooling. The ^{31}P NMR spectrum of this solution showed a singlet at 28.7 ppm for $\text{Ph}_2\text{P}(\text{O})\text{Me}$, unidentified resonances at 62.1 and 49.9 ppm, and a large broad resonance centered at -10.4 ppm, assigned to the presence of $\text{Pd}(\text{PPh}_2\text{Me})_x$ and free Ph_2PMe . Addition of 100 mL of methanol followed by cooling overnight yielded yellow crystals of $\text{Pd}(\text{PPh}_2\text{Me})_4$. ^{31}P NMR (THF) δ -4.2 (s).

Preparation of Pd{P(CH₂CH₂CN)₃}_x

PdCl₂ (0.10 g, 0.56 mmol), P(CH₂CH₂CN)₃ (0.55 g, 2.8 mmol), and *n*-Bu₄NF·3H₂O (0.47 g, 1.5 mmol) were reacted using the general procedure given in method A to yield a yellow solution. The ³¹P NMR spectrum of this solution showed a sharp singlet at 44.7 ppm assigned to (NCCH₂CH₂)₃P=O, and broadened singlets at 9.7 and -23.9 ppm assigned to Pd{P(CH₂CH₂CN)₃}_x and uncoordinated ligand, respectively. The palladium(0) complex was not isolated. Reaction of PdCl₂ and P(CH₂CH₂CN)₃ under these conditions without the addition of fluoride yields a product, presumably {(NCCH₂CH₂)₃P}₂PdCl₂, which exhibits a sharp singlet at 16.2 ppm. Phosphine oxide is not produced in the absence of fluoride.

Reaction of PPh₃ with PdCl₂ in DMSO

A mixture of PdCl₂ (0.10 g, 0.56 mmol), PPh₃ (0.74 g, 2.8 mmol) and water (0.50 g, 27 mmol) in 15 mL of DMSO was heated to 140 °C to give a yellow-orange solution. Upon cooling to room temperature (Ph₃P)₂PdCl₂ precipitated as a poorly soluble yellow solid. The solid was isolated by filtration, washed with diethyl ether, and dried *in vacuo*. Yield 0.35 g, 90%. A ³¹P NMR spectrum of the filtrate showed only the presence of unreacted Ph₃P.

Reaction of dppe with PdCl₂ in DMSO

A mixture of PdCl₂ (0.10 g, 0.56 mmol) and dppe (0.67 g, 1.7 mmol) in 20 mL of DMSO was heated to 140 °C to give a white mixture. This mixture was cooled to room temperature and stirred for three hours. [Pd(dppe)₂]Cl₂, 0.53 g, 96%, was isolated by filtration, washed with 15 mL of diethyl ether, and dried *in vacuo*. ³¹P NMR (CH₃CN) δ 58.1 (s).

Competition Experiment Between PPh_3 and dppe

A mixture of PdCl_2 (0.10 g, 0.56 mmol), dppe (0.67 g, 1.7 mmol), and PPh_3 (0.75 g, 2.9 mmol) in 15 mL of DMSO was heated to 130 °C. A solution of *n*- $\text{Bu}_4\text{NF}\cdot 3\text{H}_2\text{O}$ (0.47 g, 1.5 mmol) in 5 mL of DMSO was added to give a yellow solution. After cooling to room temperature, 15 mL of ethanol was added to complete the precipitation. $\text{Pd}(\text{dppe})_2$ (0.37 g, 73%) was isolated by filtration, washed with ethanol, and dried *in vacuo*. A ^{31}P NMR spectrum of the supernatant before the addition of ethanol identified the presence of $\text{Pd}(\text{dppe})_2$, $\text{Ph}_2\text{P}(\text{O})\text{CH}_2\text{CH}_2\text{PPh}_2$, $\text{Ph}_2\text{PCH}_2\text{CH}_2\text{PF}_2\text{Ph}_2$ and PPh_3 . There was no evidence for the formation of $\text{Ph}_3\text{P}=\text{O}$ or Ph_3PF_2 .

Reaction of $(\text{dppp})\text{NiBr}_2$ with *n*- $\text{Bu}_4\text{NF}\cdot 3\text{H}_2\text{O}$

A mixture of $\text{NiBr}_2\cdot\text{glyme}$ (0.15 g, 0.49 mmol) and dppp (0.60 g, 1.5 mmol) in 15 mL of acetonitrile was heated to 80 °C to give a red-violet solution containing $(\text{dppp})\text{NiBr}_2$. Addition of a solution of *n*- $\text{Bu}_4\text{NF}\cdot 3\text{H}_2\text{O}$ (0.38 g, 1.2 mmol) in 5 mL of acetonitrile resulted in the immediate formation of a yellow solution. Heat was removed and upon cooling a small quantity of yellow solid precipitated.

Preparation of $\text{Pt}(\text{dppe})_2$

A mixture of PtCl_2 (0.15 g, 0.56 mmol) and dppe (0.67 g, 1.7 mmol) in 15 mL of DMSO was heated to 130 °C to yield a milky white mixture, presumably due to the formation of $[\text{Pt}(\text{dppe})_2]\text{Cl}_2$. A solution of *n*- $\text{Bu}_4\text{NF}\cdot 3\text{H}_2\text{O}$ (0.47 g, 1.5 mmol) in 5 mL of DMSO was added to this hot mixture to form a bright yellow solution which still contained some white precipitate. The heat was removed and this mixture was stirred for two hours. A ^{31}P NMR spectrum of the supernatant exhibited resonances of

approximately equal intensity at 49.1 ppm with $^1J_{\text{Pt-P}} = 2338$ Hz and 30.3 ppm with $^1J_{\text{Pt-P}} = 3733$ Hz assigned to $[\text{Pt}(\text{dppe})_2]\text{Cl}_2$ ¹⁷ and $\text{Pt}(\text{dppe})_2$, respectively. A large quantity of unreacted dppe as well as a small quantity of $\text{Ph}_2\text{PCH}_2\text{CH}_2\text{P}(\text{O})\text{Ph}_2$ were also identified. Numerous smaller unidentified resonances were also present between 55 and 42 ppm.

Preparation of $\text{Pt}(\text{PPh}_3)_4$

PPh_3 (0.32 g, 1.2 mmol) and $(\text{Ph}_3\text{P})_2\text{PtCl}_2$ (0.48 g, 0.61 mmol) were suspended in 5 mL of THF. To this mixture was added $n\text{-Bu}_4\text{NF}\cdot 3\text{H}_2\text{O}$ (0.48 g, 1.5 mmol) in 5 mL of THF to yield a yellow solution in which some unreacted $(\text{Ph}_3\text{P})_2\text{PtCl}_2$ remained. This mixture was stirred for 30 min. The ^{31}P NMR spectrum of the supernatant showed the presence of $\text{Ph}_3\text{P}=\text{O}$ and a broad resonance at 45 ppm for $\text{Pt}(\text{PPh}_3)_x$. Two 2 mL aliquots of this supernatant were removed and reacted with methyl iodide in the first case and dppe in the second. The ^{31}P NMR spectrum of the methyl iodide reaction sample exhibited resonances at 28.3 ppm ($^1J_{\text{Pt-P}} = 3077$ Hz), 25.4 and 22.8 ppm assigned to *trans*- $(\text{Ph}_3\text{P})_2\text{Pt}(\text{Me})\text{I}$, $\text{Ph}_3\text{P}=\text{O}$ and $[\text{Ph}_3\text{PMe}]\text{I}$, respectively. The ^{31}P NMR spectrum of the dppe reaction solution exhibited resonances at 30.9 ($^1J_{\text{Pt-P}} = 3731$ Hz), 25.3, -4.8, and -12.2 ppm assigned to $\text{Pt}(\text{dppe})_2$, $\text{Ph}_3\text{P}=\text{O}$, Ph_3P , and dppe, respectively.¹⁸

Reduction of $[(\text{Ph}_3\text{P})_3\text{PdCl}]\text{BF}_4$

To a suspension of $[(\text{Ph}_3\text{P})_3\text{PdCl}]\text{BF}_4$ (0.20 g, 0.19 mmol) in 10 mL of THF was added a solution of $n\text{-Bu}_4\text{NF}\cdot 3\text{H}_2\text{O}$ (0.16 g, 0.49 mmol) in 5 mL of THF to yield a bright yellow solution within 15 seconds. The ^{31}P NMR spectrum of this solution exhibited a singlet at 24.5 ppm assigned to $\text{Ph}_3\text{P}=\text{O}$ and a broadened singlet at 22.5 ppm

assigned to $\text{Pd}(\text{PPh}_3)_2$. Three aliquots of 2 mL each were removed and treated with PPh_3 , maleic anhydride and iodobenzene, respectively. The PPh_3 reaction sample exhibited a broad resonance which shifted upfield with increasing concentration of PPh_3 as expected for the palladium(0) complex $\text{Pd}(\text{PPh}_3)_x$.¹² The ^{31}P NMR spectrum of the maleic anhydride reaction sample exhibited a sharp singlet at 27.5 ppm assigned to $(\text{Ph}_3\text{P})_2\text{Pd}(\text{C}_4\text{H}_2\text{O}_3)$ and the iodobenzene reaction sample exhibited a sharp singlet at 24.5 ppm assigned to *trans*- $(\text{Ph}_3\text{P})_2\text{Pd}(\text{Ph})\text{I}$.¹⁹

Alternatively, $[(\text{Ph}_3\text{P})_3\text{PdCl}]\text{BF}_4$ (0.285 g, 0.281 mmol) and KF (0.090 g, 1.6 mmol) were suspended in 5 mL of THF. A solution of 18-crown-6 in THF (5.5 mL, 0.20 M) was added and the mixture was stirred for one hour to give a yellow solution which contained some unreacted starting material. This mixture was heated at 60 °C for 15 min to further the reaction. The ^{31}P NMR spectrum of the resulting solution exhibited singlets at 24.2 and 21.7 ppm and a triplet at -56.2 ppm ($^1J_{\text{PF}} = 669$ Hz) assigned to $\text{Ph}_3\text{P}=\text{O}$, $\text{Pd}(\text{PPh}_3)_2$, and Ph_3PF_2 ,²⁰ respectively.

Reaction of $[(\text{Ph}_3\text{P})_3\text{PdCl}]\text{BF}_4$ with KHF_2

A mixture of $[(\text{Ph}_3\text{P})_3\text{PdCl}]\text{BF}_4$ (0.30 g, 0.29 mmol), KHF_2 (0.54 g, 0.69 mmol) and 18-crown-6 (5.5 mL, 0.20 M) in 15 mL of THF was stirred at room temperature to yield a light tan colored suspension. A ^{31}P NMR spectrum of the supernatant exhibited a singlet at 24.2 ppm and a broad resonance at 16.2 ppm assigned to $\text{Ph}_3\text{P}=\text{O}$ and $\text{Pd}(\text{PPh}_3)_x$, respectively. A small triplet assigned to Ph_3PF_2 was present at -56.0 ppm. There were additional unassigned resonances at 29.1 and 24.7 ppm. Prolonged stirring resulted in a deep brown decomposition mixture. Analogous results were obtained if dimethylaminopyridine (DMAP) was added to complex the HF present.

Synthesis of $[\text{Pd}_3\text{Cl}(\text{PPh}_2)_2(\text{PPh}_3)_3][\text{BF}_4]$

As described by Dixon et al.,⁵ $[(\text{Ph}_3\text{P})_3\text{PdCl}]\text{BF}_4$ (0.500 g, mmol) was suspended in 10 mL of THF in a thick-walled pyrex tube equipped with a small stir bar and the tube was then sealed *in vacuo*. This tube was then placed in an oil bath and heated at 125 °C for five days to yield a deep red solution which contained a yellow precipitate. After allowing the reaction mixture to cool several hours at room temperature the reaction tube was opened under nitrogen and the mixture was filtered. The pale yellow solid obtained was identified as $(\text{Ph}_3\text{P})_2\text{PdCl}_2$. A ^{31}P NMR spectrum of the filtrate exhibited resonances consistent with the presence of $[\text{Pd}_3\text{Cl}(\text{PPh}_2)_2(\text{PPh}_3)_3][\text{BF}_4]$, $[\text{Ph}_4\text{P}]^+$, and $\text{Ph}_3\text{P}=\text{O}$ as described by Dixon, as well as a broad resonance at 6 ppm. The resonance at 6 ppm was identified as $\text{Pd}(\text{PPh}_3)_x$ by the addition of iodobenzene to yield PPh_3 (-4.7 ppm) and *trans*- $(\text{Ph}_3\text{P})_2\text{Pd}(\text{Ph})\text{I}$ (25.2 ppm). No Ph_3PF_2 was observed in the filtrate. The filtrate was cooled overnight in the freezer to yield a small quantity of red-orange crystals of $[\text{Pd}_3\text{Cl}(\text{PPh}_2)_2(\text{PPh}_3)_3][\text{BF}_4]$.

Preparation of $[(\text{Ph}_3\text{P})_3\text{PdCl}][\text{OSO}_2\text{CF}_3]$

$(\text{Ph}_3\text{P})_2\text{PdCl}_2$ (0.500 g, 0.712 mmol) and $\text{AgOSO}_2\text{CF}_3$ (0.183 g, 0.712 mmol) were stirred in 50 mL of nitromethane for two hours. The AgCl which precipitated was removed by filtration through Celite. The yellow filtrate was added to diethyl ether to precipitate a pale yellow solid, presumably $[(\text{Ph}_3\text{P})_4\text{Pd}_2(\mu\text{-Cl})_2][\text{OSO}_2\text{CF}_3]_2$. A ^{31}P NMR spectrum of a CH_3NO_2 solution of this solid exhibits a singlet at 23.9 ppm as the major resonance and two much smaller, slightly broadened resonances at 35 and 34.5 ppm.

This yellow solid was redissolved in 25 mL of nitromethane and Ph_3P (0.500 g, 1.91 mmol) was added. The volume of the resulting yellow solution was reduced to 10

mL *in vacuo* and the pale yellow solid was isolated by filtration. Yield 0.54 g, 77%. ^{31}P NMR (CH_3NO_2) δ 34.2 (t, $^2J_{\text{PP}} = 16$ Hz), 30.8 (d, $^2J_{\text{PP}} = 16$ Hz).

Attempted Synthesis of $[\text{Pd}_3\text{Cl}(\text{PPh}_2)_2(\text{PPh}_3)_3][\text{OSO}_2\text{CF}_3]$

As described for the cluster synthesis above, $[(\text{Ph}_3\text{P})_3\text{PdCl}][\text{OSO}_2\text{CF}_3]$ (0.450 g, 0.418 mmol) in 10 mL of THF was sealed in a thick-walled pyrex tube and heated at 125 °C for seven days. The mixture remained yellow throughout this period and the supernatant became only lightly brown in color. The reaction mixture was filtered to yield 0.33 g (97%) of a pale yellow solid which was rinsed with 10 mL of THF and dried *in vacuo*. This solid was identified as $[(\text{Ph}_3\text{P})_4\text{Pd}(\mu\text{-Cl})_2][\text{OSO}_2\text{CF}_3]_2$ by a sharp singlet at 23.1 ppm and two smaller broadened resonances at 34.8 and 33.0 ppm in the ^{31}P NMR spectrum of a $\text{CH}_2\text{Cl}_2/\text{CH}_3\text{CN}$ solution of this compound. Addition of PPh_3 to this solution yielded a clean conversion to $[(\text{Ph}_3\text{P})_3\text{PdCl}][\text{OSO}_2\text{CF}_3]$. The ^{31}P NMR spectrum of the reaction filtrate exhibited resonances for $[(\text{Ph}_3\text{P})_3\text{PdCl}][\text{OSO}_2\text{CF}_3]$, PPh_3 , a trace of $\text{Ph}_3\text{P}=\text{O}$, and small unidentified resonances at 25.0 and 24.3 ppm.

Crystal and Molecular Structure of $\text{Pd}(\text{dppp})_2$

A yellow crystal of the title compound was mounted on a glass fiber in a random orientation. The cell constants were determined from a list of reflections found by an automated search routine. Pertinent data collection and reduction information is given in Table 1.

A total of 10317 reflections were collected in the $\pm h$, $+k$, $\pm l$ hemisphere, of which 5337 were unique and not systematically absent. The agreement factor for the averaging of 8526 observed reflections was 1.6% based on intensity and 1.2% based on F_{obs} . The intensities of three standards, checked hourly over the course of the data

collection, indicated only random variations within the errors of the measurement. Lorentz and polarization corrections were applied. An absorption correction based on a series of psi-scans was made.

The systematic absences indicated the space group to be either $C2/c$ (no. 15) or Cc (no. 9), so direct methods were used to give solutions in both choices.²¹ Only the centric group ($C2/c$) gave a reasonable solution, and this choice was verified by the final successful refinement of the structure. The position of all 30 unique non-hydrogen atoms were taken from the direct methods E-map. In the final stages of refinement, all non-hydrogen atoms were given anisotropic temperature factors, and all expected hydrogen atoms were placed in calculated positions and used for the calculation of structure factors only. The final cycle of refinement²² included 268 variable parameters and converged with unweighted and weighted agreement factors of 0.0225 and 0.0341. The standard deviation of an observation of unit weight was 1.11. The largest positive peak in the final difference Fourier had a height of $0.162 e/\text{\AA}^3$. All calculations were performed on a Digital Equipment Corp. MicroVAX II computer using the CAD4/SDP package.²³

Table 1. Crystallographic data for Pd(dppp)₂

Formula	PdP ₄ C ₅ H ₅ ₂
Formula weight	931.31
Space Group	C2/c (No. 15)
a, Å	18.396(2)
b, Å	13.290(1)
c, Å	20.186(2)
β, deg	109.383(5)
V, Å ³	4655(1)
Z	4
d _{calc} , g/cm ³	1.329
Crystal size, mm	0.35 x 0.30 x 0.48
μ(MoK _α), cm ⁻¹	5.621
Data collection instrument	Enraf-Nonius CAD4
Radiation (monochromated in incident beam)	MoK _α (λ = 0.71073 Å)
Orientation reflections, number, range (2θ)	25, 20.5-35.3
Temperature, °C	22±1

$$^a R = \sum |F_o| - |F_c| / \sum |F_o|$$

$$^b R_w = [\sum w(|F_o| - |F_c|)^2 / \sum w |F_o|^2]^{1/2}; w = 1/\sigma^2(|F_o|)$$

$$^c \text{Quality-of-fit} = [\sum w(|F_o| - |F_c|)^2 / (N_{\text{obs}} - N_{\text{parameters}})]^{1/2}$$

Table 1. Continued

Scan method	0-20
Data col. range, 2θ , deg	4-55
No. unique data, total:	5337
with $F_o^2 > 3\sigma(F_o^2)$:	4431
Number of parameters refined	268
R^a	0.0225
R_w^b	0.0341
Quality-of-fit indicator ^c	1.11
Largest shift/esd, final cycle	0.01
Largest peak, e/Å ³	0.162

RESULTS AND DISCUSSION

As stated in the introduction, we were initially interested in preparing the cation $[\text{Pd}(\text{dppp})_2]^{2+}$. Westland^{2a} previously reported that the dppe analogue $[\text{Pd}(\text{dppe})_2]\text{Cl}_2$ is conveniently prepared by reaction of $(\text{dppe})\text{PdCl}_2$ and dppe in hot DMF. Gray et al. have noted³ the formation of $[\text{Pd}(\text{dppp})_2]\text{Cl}_2$ during the photolysis of $\text{Pd}(\text{dppp})_2$ in 5% $\text{CH}_2\text{Cl}_2/\text{THF}$, but no data was reported to support this assignment. We attempted to prepare this complex by refluxing solutions of $(\text{dppp})\text{PdCl}_2$ and dppp in pyridine/acetonitrile. This route, however, does not result in chloride displacement to yield $[\text{Pd}(\text{dppp})_2]\text{Cl}_2$. The ³¹P NMR spectrum of this reaction solution exhibited resonances for the two starting materials only, although these resonances were somewhat broadened. A non-coordinating anion was thus employed. Reaction of two equivalents of dppp with $\text{Pd}(\text{BF}_4)_2 \cdot 4\text{CH}_3\text{CN}$ yields a creamy white solid which is insoluble in diethyl ether, toluene and methylene chloride, but is soluble in warm DMSO, DMF, methanol and acetonitrile. The complex is presumably $[\text{Pd}(\text{dppp})_2][\text{BF}_4]_2$.

**The Palladium Reduction Product**

The filtrate of reaction 2 deposited yellow crystals upon standing overnight. These crystals were highly soluble in THF and benzene, and its solutions exhibit a single ³¹P NMR resonance at 4.2 ppm. The presence of at least one dppp ligand was confirmed by ¹H NMR spectroscopy. To our surprise, these physical and spectroscopic characteristics matched those for the zerovalent complex $\text{Pd}(\text{dppp})_2$. This assignment was confirmed by X-ray crystallography. Selected bond distances and angles are given

in Table 2. The ORTEP drawing of the molecule is given in Figure 1. The Pd(dppp)₂ molecule is centrosymmetric and its metrics closely resemble those recently reported for the platinum analogue Pt(dppp)₂. The distortion from tetrahedral geometry around the palladium is due to the two chelating phosphine ligands. The P(1)-Pd-P(2) angle is 97.60(1)° while the other P-Pd-P angles range from 106.92(2)° to 121.54(2)°. The P-Pd distances of 2.3299(4) and 2.3314(4) Å fall in the range of 2.27-2.32 Å previously established by the molecular structures of Pd[P(C≡CPh)₃]₄,²⁴ Pd(PPh₃)₃,²⁵ Pd(PPhBu₂)₂,²⁶ and Pd(PCy₃)₂.²⁷ Longer P-Pd distances²⁸ of 2.43-2.46 Å for Pd(PPh₃)₄ presumably arise from the steric bulk of the four phosphine ligands.

The formation of Pd(dppp)₂ as a side-product in the reaction of dppp and Pd(BF₄)₂·4CH₃CN was quite puzzling since typical routes to zerovalent palladium phosphine complexes involve the reduction of Pd(II) phosphine complexes with NaBH₄,^{29,30} hydrazine,^{31,32} or KOH/phosphine.³³ No reported chemistry was found which explained our result. The only component of this system which we envisioned as

Table 2. Selected Bond Distances (Å) and Angles (deg) in Pd(dppp)₂

<u>Distances</u>			
Pd-P(1)	2.3299(4)	Pd-P(2)	2.3314(4)
<u>Angles</u>			
P(1)-Pd-P(1)'	121.54(2)	P(1)-Pd-P(2)'	116.69(1)
P(1)-Pd-P(2)	97.60(1)	P(2)-Pd-P(2)'	106.92(2)

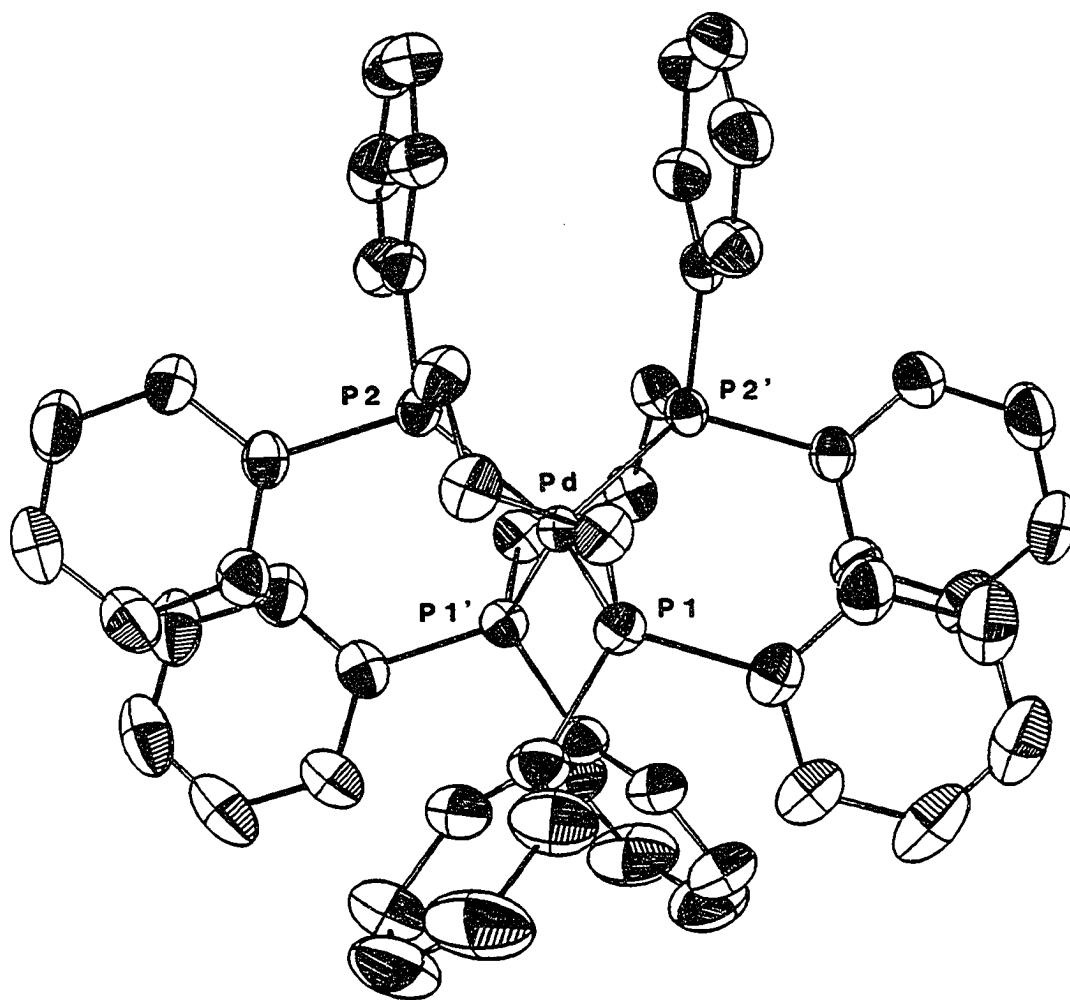
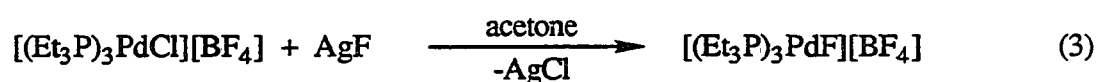


Figure 1. ORTEP drawing of Pd(dppp)₂. Thermal ellipsoids are drawn at the 50% probability level.

potentially noninnocent was tetrafluoroborate, which has previously been shown to be a suitable fluoride source for transition metal complexes.^{34,35} A survey of the literature revealed that the role fluoride might play in the chemistry of palladium(II) phosphine complexes has been scantily investigated. Only three palladium(II) phosphine complexes have been reported to contain a Pd-F bond. Of these, both $[\text{Pd}_2(\mu\text{-F})_2(\text{PPh}_3)_4]^{2+}$ and $(\text{Ph}_3\text{P})_2\text{Pd}(\text{H})(\text{F})$ were characterized by elemental analysis only.^{36,37} No spectroscopic data was offered to verify these assignments. Dixon et al. provided ^{19}F NMR spectroscopic evidence for the formation of $[(\text{Et}_3\text{P})_3\text{PdF}]\text{BF}_4$ via reaction 3, but this complex was evidently not stable enough to allow isolation.³⁸ Amazingly no further evidence has been presented to substantiate the existence of a stable Pd-F bond in palladium(II) phosphine complexes even though complexes of the type $(\text{R}_3\text{P})_2\text{PdX}_2$ have been well studied for $\text{X} = \text{Cl}, \text{Br}, \text{and I}$.

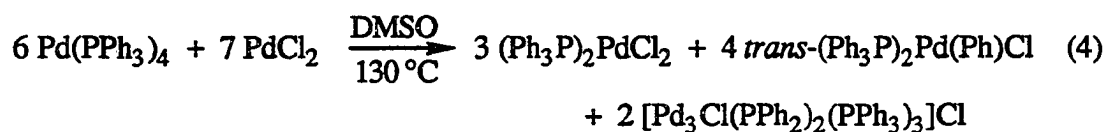


Noting this lack of a stable Pd-F bond in palladium(II) phosphine complexes, the high P-F bond strength,³⁹ and the unexpected formation of $\text{Pd}(\text{dppp})_2$ in reaction 2, we added fluoride to solutions of palladium(II) phosphine complexes anticipating that a redox reaction may occur. Addition of 2.5 equivalents of $n\text{-Bu}_4\text{NF}\cdot 3\text{H}_2\text{O}$ to a hot (130 °C) DMSO solution of PdCl_2 and five equivalents of a monodentate or three equivalents of a bidentate phosphine results in an immediate red-orange solution which rapidly turns yellow. Upon cooling, the zerovalent palladium complexes precipitate as yellow solids in yields of 70 to 90%. This method has been applied to the synthesis of the known complexes $\text{Pd}(\text{PPh}_3)_4$,³¹ $\text{Pd}(\text{PPh}_2\text{Me})_4$,⁴⁰ $\text{Pd}_2(\text{dppm})_3$,³² $\text{Pd}(\text{dppe})_2$,²⁹

$\text{Pd}(\text{dppp})_2$,^{30,33} and $\text{Pd}(\text{dppb})_2$ ⁴¹ and the new complex $\text{Pd}\{\text{Ph}_2\text{PCH}_2\text{C}(\text{CH}_3)_2\text{CH}_2\text{PPh}_2\}_2$. The conditions employed were based on those described for the synthesis of $\text{Pd}(\text{PPh}_3)_4$ with the exception that $n\text{-Bu}_4\text{NF}\cdot 3\text{H}_2\text{O}$ was substituted for hydrazine.³¹ The high temperature is required to initially dissolve the PdCl_2 and then to keep the resulting palladium(II) complex in solution. DMSO is a convenient solvent since the palladium(0) complexes generally precipitate upon cooling. When $\text{P}(\text{CH}_2\text{CH}_2\text{CN})_3$ was employed in this reaction, reduction of palladium(II) to palladium(0) was indicated by ^{31}P NMR spectroscopy which revealed the presence of phosphine oxide at 44.7 ppm and a broad resonance at 9.7 ppm consistent with a PdL_x species. Complexes of the type PdL_4 are known to exhibit broad resonances in their ^{31}P NMR spectra for monodentate ligands L because of facile ligand dissociation in solution yielding PdL_3 and PdL_4 complexes and free phosphine.⁴² The palladium(II) complex $\text{Cl}_2\text{Pd}\{\text{P}(\text{CH}_2\text{CH}_2\text{CN})_3\}_2$ exhibits a sharp resonance at 16.2 ppm in the presence of excess phosphine. This palladium(0) complex was not isolated.

Most of these reactions are remarkably clean as indicated by ^{31}P NMR spectroscopy. The reduction of PdCl_2 in the presence of PPh_3 , however, leads to the formation of a small quantity of *trans*- $(\text{Ph}_3\text{P})_2\text{Pd}(\text{Ph})\text{Cl}$. When the less soluble KF is utilized as the fluoride source for this reaction, the yield of $\text{Pd}(\text{PPh}_3)_4$ drops from 80% to 54% as the amount of *trans*- $(\text{Ph}_3\text{P})_2\text{Pd}(\text{Ph})\text{Cl}$ identified in the filtrate increases. Allowing the filtrate to stand at room temperature resulted in the crystallization of *trans*- $(\text{Ph}_3\text{P})_2\text{Pd}(\text{Ph})\text{Cl}$ which was characterized by comparison of its ^{31}P and ^1H NMR spectral data to that of an authentic sample.^{43,44} A ^{31}P NMR spectrum of the reaction filtrate also indicated the presence of $[\text{Ph}_4\text{P}]^+$ by comparison to a known sample, as well as other resonances. The decrease in yield using KF and the increasing formation of *trans*- $(\text{Ph}_3\text{P})_2\text{Pd}(\text{Ph})\text{Cl}$ is readily explained by a side reaction between the palladium(II)

starting material and the Pd(PPh₃)₄ product as shown in reaction 4. This reaction was reported by Coulson⁴⁵ to occur under conditions very similar to the ones employed here, wherein the high temperature is necessary to induce P-C bond cleavage and form the diphenylphosphido bridges of the trinuclear cluster. When the less soluble KF is utilized, the starting palladium(II) is consumed at a slower rate than with *n*-Bu₄NF•3H₂O, thus allowing this side reaction to become more important.



The Phosphorus Oxidation Product

Analysis of the filtrates of reactions x by ³¹P NMR spectroscopy yielded evidence for the formation of phosphine oxides and difluorophosphoranes in these reactions. For dppm for example, doublets at 28.8 and -27.1 ppm with ²J_{PP} = 50.5 Hz indicate the presence of Ph₂PCH₂P(O)Ph₂ by comparison to the known literature values.¹⁴ The presence of the phosphine monoxides and not the dioxides was observed in the reactions of all the bidentate ligands employed. The difluorophosphorane products were readily recognizable in the ³¹P NMR spectra of these filtrates by their large ¹J_{PF} values of 639-657 Hz. Again using dppm as an example, Ph₂PCH₂PF₂Ph₂ was identified by a doublet of triplets at -23.9 ppm with ²J_{PP} = 63.9 Hz and ³J_{PF} = 22.5 Hz and a triplet of doublets at -41.9 ppm with ¹J_{PF} = 643 Hz and ²J_{PP} = 63.9 Hz. The ¹⁹F NMR of this filtrate showed a doublet of doublet of triplets at 136.1 ppm with ¹J_{PF} = 643 Hz, ³J_{PF} = 22.5 Hz and ³J_{HF} = 15 Hz. These values are consistent with those previously reported for Ph₂PCH₂PF₂PPh₂.¹⁵ In some cases the resonances of the initially formed difluorophosphorane products were of low intensity, presumably due to

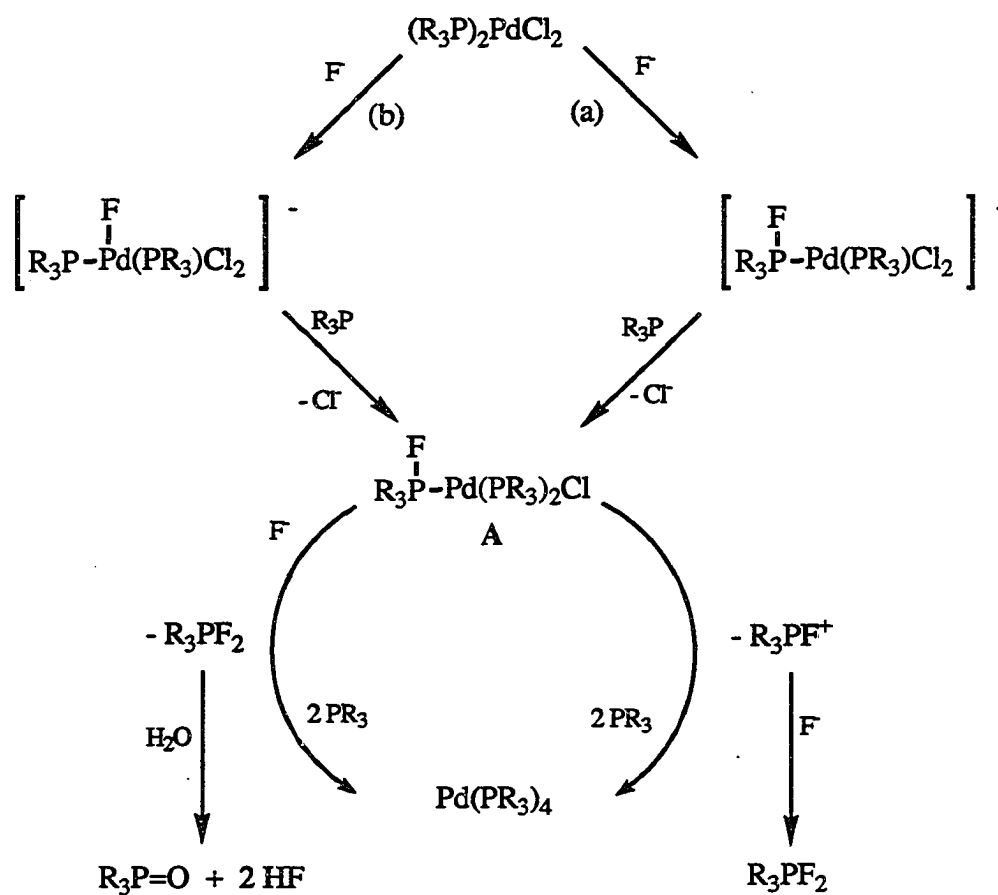
hydrolysis. Hydrolysis results from water introduced with the hydrated fluoride source yielding phosphine oxide products. If this redox reaction is carried out using an anhydrous fluoride source, the difluorophosphorane becomes the major oxidation product at the expense of the phosphine oxide product. Addition of water to such a filtrate results in hydrolysis of the difluorophosphorane to give clean conversion to the phosphine oxide. For example, using anhydrous KF as the fluoride source with 18-crown-6 to increase its solubility, the reaction of $\{\text{Ph}_2\text{PCH}_2\text{C}(\text{CH}_3)_2\text{CH}_2\text{PPh}_2\}\text{PdCl}_2$ with two equivalents of $\text{Ph}_2\text{PCH}_2\text{C}(\text{CH}_3)_2\text{CH}_2\text{PPh}_2$ in THF/pyridine at 100 °C yields a yellow solution with some undissolved KF. ^{31}P NMR spectroscopy indicated a clean reaction with only $\text{Pd}\{\text{Ph}_2\text{PCH}_2\text{C}(\text{CH}_3)_2\text{CH}_2\text{PPh}_2\}_2$, $\text{Ph}_2\text{PCH}_2\text{C}(\text{CH}_3)_2\text{CH}_2\text{PF}_2\text{Ph}_2$ and a trace of $\text{Ph}_2\text{PCH}_2\text{C}(\text{CH}_3)_2\text{CH}_2\text{P}(\text{O})\text{Ph}_2$ present. Addition of ethanol resulted in the precipitation of $\text{Pd}\{\text{Ph}_2\text{PCH}_2\text{C}(\text{CH}_3)_2\text{CH}_2\text{PPh}_2\}_2$ which was isolated in 75% yield.

Reaction Pathways for the Palladium Reduction

Plausible reaction pathways are illustrated in Scheme I. Nucleophilic attack of fluoride on a coordinated phosphine, path (a), or prior coordination of fluoride to palladium followed by a rapid migration to phosphorus, path (b), could generate an intermediate A. Although we have no direct evidence for the formation of A, Ebsworth et al. have reported⁴⁶ the synthesis and molecular structure of $(\text{Et}_3\text{P})_2\text{IrCl}_2(\text{CO})(\text{PF}_4)$ which contains a pentacoordinate phosphorus bound to iridium. This complex reacts with two equivalents of fluoride to cleave the Ir-P bond generating PF_6^- and presumably $(\text{Et}_3\text{P})_2\text{Ir}(\text{CO})\text{Cl}$. Similarly, A may react with a second equivalent of fluoride, again either by nucleophilic attack on phosphorus or by prior coordination to palladium followed by fluoride migration to phosphorus, with the transfer of two electrons from phosphorus to palladium to yield a difluorophosphorane and a palladium(0) complex.

Alternatively, A may undergo a two electron transfer to yield a fluorophosphonium cation and the palladium(0) complex. We have no evidence for the formation of a fluorophosphonium cation but the synthesis of the fluorophosphonium cation $[\text{Ph}_3\text{PF}]^+$ via fluoride abstraction from Ph_3PF_2 has been reported previously.⁴⁷ A fluorophosphonium cation produced in our system would rapidly react with fluoride or water to yield a difluorophosphorane or phosphine oxide, respectively.

Scheme I



Which paths in Scheme I are operative is uncertain, however, several conclusions concerning the mechanism of this reaction can be formulated from our results. First, reduction of palladium(II) phosphine complexes under the conditions employed here does not occur in the absence of fluoride. Reactions of PdCl_2 and PPh_3 or dppe in the presence of added water, but in the absence of fluoride, yield only $(\text{Ph}_3\text{P})_2\text{PdCl}_2$ and $[\text{Pd}(\text{dppe})_2]\text{Cl}_2$, respectively. The necessity of adventitious water has been reported for the reduction of $\text{Pd}(\text{acac})_2$ in the presence of excess PPh_3 .⁴⁸ The successful use of anhydrous fluoride sources here seems to rule out the necessity of water in our reaction system, although we always observed some phosphine oxide formation and cannot yet claim to have achieved rigorously anhydrous conditions. The necessity of fluoride has also been demonstrated by the spectroscopic identification of difluorophosphorane products. The quantity of the difluorophosphorane product observed in each reaction increases sharply at the expense of the phosphine oxide when anhydrous conditions are employed. Thus, the first oxidation product formed must be the difluorophosphorane, with formation of the phosphine oxide product resulting from hydrolysis. Second, the reducing agent in this redox reaction is a *coordinated* phosphine which provides two electrons to the palladium. The necessity of oxidizing only one coordinated phosphine per palladium explains why only one of the two phosphine groups in one equivalent of bidentate ligand becomes oxidized to give mono-difluorophosphorane and phosphine monoxide products when a slight excess of a chelating ligand is used. A competition experiment has demonstrated that the phosphine which becomes oxidized must be coordinated to the palladium. A heated solution of PdCl_2 and five equivalents of PPh_3 and three equivalents of dppe in DMSO yielded a white mixture containing $[\text{Pd}(\text{dppe})_2]\text{Cl}_2$ as expected. Addition of $n\text{-Bu}_4\text{NF}\cdot 3\text{H}_2\text{O}$ resulted in the usual redox reaction with $\text{Pd}(\text{dppe})_2$ being the isolated reduction product. Analysis of the filtrate by

^{31}P NMR spectroscopy revealed the oxidation products to be $\text{Ph}_2\text{PCH}_2\text{CH}_2\text{P}(\text{O})\text{Ph}_2$ and $\text{Ph}_2\text{PCH}_2\text{CH}_2\text{PF}_2\text{Ph}_2$ only. No $\text{Ph}_3\text{P}=\text{O}$ or Ph_3PF_2 were observed, confirming, as one might expect, that a coordinated phosphine becomes oxidized. Third, in some cases where the starting palladium complex is not soluble in the solvent employed, 2.5 equivalents of fluoride has not been sufficient to achieve complete conversion to the palladium(0) complex. For example, when a mixture of $(\text{Ph}_3\text{P})_2\text{PdCl}_2$ or $[\text{Pd}(\text{dppe})_2]\text{Cl}_2$ suspended in THF was treated with the appropriate phosphine and 2.5 equivalents of $n\text{-Bu}_4\text{NF}\cdot 3\text{H}_2\text{O}$ at room temperature, only approximately 50-75% of the starting material reacted. The reaction proceeded to completion, however, when additional fluoride was subsequently added.

According to Scheme I, fluoride could theoretically act as a catalyst for this redox reaction since, in the presence of water, the difluorophosphorane product hydrolyzes to give two equivalents of HF. However, HF is known to react with free fluoride to form HF_2^- and other stable polyhydrogen fluorides.⁴⁹ Attempts to reduce palladium(II) phosphine complexes with KHF_2 at room temperature, even in the presence of a base such as dimethylaminopyridine, yielded very little reduction and a considerable decomposition. Presumably the incomplete reduction observed in the examples mentioned above arises from the slower rates of the redox reaction due to the insolubility of the starting complex, allowing the HF produced via hydrolysis to scavenge remaining fluoride to form HF_2^- , thus shutting down the reaction.

The fluoride-induced reaction described herein has not been previously reported. The only report of a similar reaction involved the preparation of difluorophosphoranes by reacting phosphines with the strong fluorinating reagent MoF_6 .⁵⁰ The somewhat related redox reactions involving the formation of platinum(0) phosphine complexes and

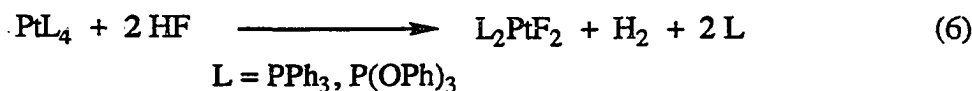
dichlorotrifluorophosphorane at high temperatures and pressures, as shown in reaction 5, have also been reported.⁵¹ The driving force in our redox reaction, in addition to



facile accessibility to both the +2 and 0 oxidation states of palladium and the proposed weak affinity of palladium for fluoride,⁵² is undoubtedly the formation of two strong P-F bonds in the difluorophosphorane product. Comparison of bond enthalpy terms for P-X bonds for the halogens X reveals a decrease down the periodic table.³⁹ For trivalent phosphorus, PX₃ bond enthalpy values of 490, 319, 264 and 184 kJ/mol have been reported for X = F, Cl, Br, and I, respectively. For pentavalent phosphorus, the bond enthalpy terms for PX₅ are approximately 465 and 257 kJ/mol for X = F and Cl, respectively. This large difference in P-X bond enthalpies for fluorine compared to the other halogens may explain why this redox reaction occurs only for fluoride. This redox reaction may also explain why so little data has been reported for a stable Pd-F bond in palladium(II) phosphine complexes.

Extension of the Redox Reaction to Platinum

In contrast to palladium(II) complexes, the coordination of fluoride to platinum(II) phosphine complexes has been well established. In 1965, McAvoy, Moss, and Sharp reported⁵³ the preparation of L₂PtF₂ (L = PPh₃, P(OPh)₃) by reaction of HF with the appropriate zerovalent platinum complex as shown in reaction 6. Both of these



complexes reportedly react with carbon monoxide to yield $L_2Pt(CO)_2F_2$. In contrast to the results of McAvoy et al., Kemmit, Peacock, and Stocks reported³⁶ that the product of reaction 6 should actually be formulated as $[(Ph_3P)_3PtF][HF_2^-]$. The results of these early works were based mainly on elemental analysis and no spectroscopic evidence was offered to verify a Pt-F bond. Since then, the complexes *trans*-(Et_3P)₂Pt(R)(F) (R = Me,⁵⁴ Ph⁵⁵), $[L_3PtF]^+$ (L = PEt_3 , PPh_3 , and $PMePh_2$),⁵⁶ and *trans*- $[(Et_3P)_2Pt(L)(F)][ClO_4]$ (L = PPh_3 , $P(OPh)_3$)⁵⁶ have been prepared as stable solids, fully characterized by ¹⁹F, ³¹P, and ¹³C NMR spectroscopies as well as elemental analyses. Additionally, the molecular structures of $[(Et_3P)_3PtF][BF_4]$ ⁵⁷ and *cis*-(Ph_3P)₂Pt{CH(CF₃)₂}(F)⁵⁸ have been determined by X-ray crystallography. The mixed halogen complexes $(Ph_3P)_2PtX(F)$ (X = Cl, Br)³⁶ and $(Et_3P)_2PtCl(F)$ ⁶¹ have also been reported.

Platinum(II) phosphine complexes also undergo this fluoride-induced redox reaction, although not as cleanly as for palladium. Addition of 2.5 equivalents of *n*-Bu₄NF·3H₂O to a suspension of $(Ph_3P)_2PtCl_2$ and PPh_3 in THF results in only partial conversion to $Pt(PPh_3)_x$ and $Ph_3P=O$. The presence of $Pt(PPh_3)_x$ was confirmed by a broad resonance at 45 ppm in the ³¹P NMR spectrum of the supernatant. Furthermore, aliquots of this supernatant were treated with methyl iodide and dppe to form *trans*-(Ph_3P)₂Pt(Me)I (28.3 ppm, ¹J_{Pt-P} = 3077 Hz) and $Pt(dppe)_2$ (30.9 ppm, ¹J_{Pt-P} = 3731 Hz), respectively.¹⁸ Similarly, reaction of $PtCl_2$ and three equivalents of dppe with 2.5 equivalents of *n*-Bu₄NF·3H₂O in DMSO yielded only partial conversion to $Pt(dppe)_2$. In addition to numerous unidentified resonances between 55 and 42 ppm, the ³¹P NMR spectrum of the supernatant revealed the presence of $[Pt(dppe)_2]Cl_2$ (49.1 ppm, ¹J_{Pt-P} = 2338 Hz),¹⁷ $Pt(dppe)_2$ (30.9 ppm, ¹J_{Pt-P} = 3733 Hz), and $Ph_2PCH_2CH_2P(O)Ph_2$.

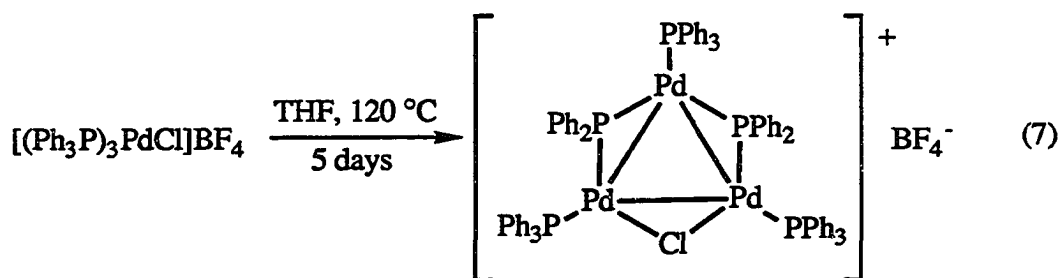
Reactions of platinum(II) and fluoride with additional phosphines have not yet been carried out.

Attempted Extension of the Redox Reaction to Nickel

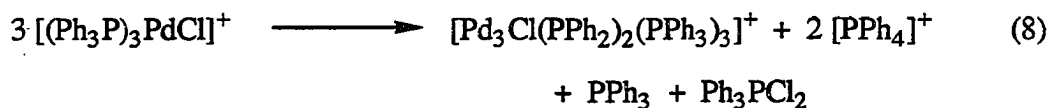
Nickel(II) phosphine complexes do not participate in this new redox reaction. Addition of 2.5 equivalents of *n*-Bu₄NF•3H₂O to a deep red solution of (dppp)NiBr₂ in acetonitrile results in the formation of a yellow solution. Cooling to room temperature results in the precipitation of a yellow solid, tentatively identified as NiF₂. This result agrees with those previously reported by McAvoy et al. who noted that the reaction of (Pr₃P)₂NiCl₂ with fluoride also yields only NiF₂.⁵³

BF₄⁻ as a Fluoride Source

The formation of Pd(dppp)₂ as a side product in the reaction of dppp with Pd(BF₄)₂•4CH₃CN suggests that BF₄⁻ may provide fluoride for the redox reaction. In support of such a proposition, Theopold has recently reported³⁴ fluoride abstraction from PF₆⁻ by [Cp*Cr(THF)₂Me]⁺ to yield [Cp*₄Cr₄(μ-F)₅Cl₂]PF₆, although no change in oxidation state accompanies this reaction. Similarly Cp₂Zr(Me)Cl reacts with AgPF₆ to give [Cp₂Zr(CH₃)(CH₃CN)]⁺ which also rapidly abstracts fluoride from PF₆⁻ to give Cp₂Zr(CH₃)F.³⁵ More interesting is the possible participation of this fluoride-induced redox reaction in the thermal decomposition of [(Ph₃P)₃PdCl][BF₄] to yield the trinuclear cluster [Pd₃Cl(PPh₂)₂(PPh₃)₃][BF₄]⁵ as outlined in reaction 7. Such a



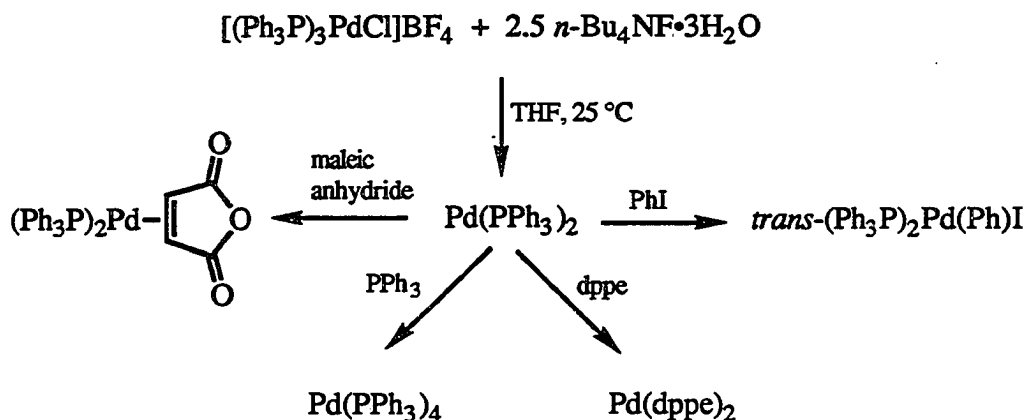
transformation requires a net two electron reduction per cluster since the average oxidation state per palladium is $+4/3$. The only oxidation product identified in this reaction was $\text{Ph}_3\text{P}=\text{O}$, formed by an unknown mechanism. A referee of the original report suggested^{5b} that cluster formation may have proceeded with the concomitant formation of $\text{Ph}_3\text{P}\text{Cl}_2$ as the oxidation product, which subsequently hydrolyzed with adventitious water to give $\text{Ph}_3\text{P}=\text{O}$. We suggest, however, that thermal decomposition



of some of the BF_4^- to yield fluoride ion occurs under the reaction conditions employed. The thermal decomposition of tetrafluoroborate salts of transition metals complexes to yield metal fluorides is well known and has been reviewed.⁶⁰ A fluoride-induced redox reaction could then ensue to form $\text{Pd}(\text{PPh}_3)_2$ and Ph_3PF_2 . From the aforementioned work by Coulson, the final step would involve reaction of $\text{Pd}(\text{PPh}_3)_2$ with a palladium(II) phosphine complex under thermal conditions to form the triangular cluster.

We have briefly reinvestigated this reaction to support our suggestion. To a suspension of $[(\text{Ph}_3\text{P})_3\text{PdCl}][\text{BF}_4]$ in THF at room temperature was added 2.5 equivalents of $n\text{-Bu}_4\text{NF}\cdot 3\text{H}_2\text{O}$ to yield an immediate yellow solution containing only $\text{Ph}_3\text{P}=\text{O}$ and $\text{Pd}(\text{PPh}_3)_2$ as indicated by ^{31}P NMR spectroscopy. Complexation of

Scheme II



$\text{Pd}(\text{PPh}_3)_2$ with additional PPh_3 or maleic anhydride and reaction with iodobenzene as shown in Scheme II confirmed this assignment.¹⁹ This observation supports our proposed route to cluster formation, provided that thermal decomposition of BF_4^- indeed occurs under Dixon's reaction conditions. Following the reported procedure,^{5b} $[(\text{Ph}_3\text{P})_3\text{PdCl}][\text{BF}_4]$ was heated at 125°C in THF for five days to yield a small quantity of the triangular cluster. Analysis of the filtrate by ^{31}P NMR spectroscopy confirmed Dixon's reported product distribution, including the presence of $\text{Ph}_3\text{P}=\text{O}$ and $\text{Pd}(\text{PPh}_3)_x$. The presence of the palladium(0) complex was confirmed by the addition of iodobenzene, maleic anhydride, and additional PPh_3 as described above. However, there was no evidence to suggest the presence of Ph_3PF_2 which may have been hydrolyzed by adventitious water. In a different approach to the problem, we removed the BF_4^- from the starting material and replaced it with the non-fluoride donating anion $-\text{OSO}_2\text{CF}_3$. Heating $[(\text{Ph}_3\text{P})_3\text{PdCl}][\text{OSO}_2\text{CF}_3]$ at 125°C for seven days resulted in no visually detectable reaction. The yellow solid, isolated in 97% yield from this reaction

mixture was identified as $[\text{Pd}_2(\mu\text{-Cl})_2(\text{PPh}_3)_4][\text{OSO}_2\text{CF}_3]$ by ^{31}P NMR spectroscopy as well as by its clean conversion to $[(\text{Ph}_3\text{P})_3\text{PdCl}][\text{OSO}_2\text{CF}_3]$ upon the addition of PPh_3 in CH_3NO_2 . A ^{31}P NMR spectrum of the reaction filtrate showed no evidence for the formation of $\text{Pd}(0)$ complexes, no evidence for P-C bond cleavage (bridging PPh_2 groups usually resonate around 200-270 ppm for palladium complexes),⁵ and no formation of $\text{Ph}_3\text{P}=\text{O}$. This result supports our contention that the thermal decomposition of BF_4^- followed by a fluoride-induced redox reaction is required for the formation of $[\text{Pd}_3\text{Cl}(\text{PPh}_2)_2(\text{PPh}_3)_3][\text{BF}_4]$ from the thermal decomposition of $[(\text{Ph}_3\text{P})_3\text{PdCl}][\text{BF}_4]$.

Conclusions

We have shown that fluoride induces a novel redox reaction among a variety of palladium(II) and several platinum(II) phosphine complexes to yield zerovalent metal phosphine complexes and difluorophosphanes. We have also presented evidence that this redox reaction contributes to the formation of $[\text{Pd}_3\text{Cl}(\text{PPh}_2)_2(\text{PPh}_3)_3][\text{BF}_4]$ from $[(\text{Ph}_3\text{P})_3\text{PdCl}][\text{BF}_4]$, with the fluoride required for the redox reaction arising from thermal decomposition of the tetrafluoroborate anion. Considering the increasing use of BF_4^- in transition metal chemistry, including its coordination via fluoride bridges to palladium(II) in $(\text{Ph}_3\text{P})_2\text{Pd}(\text{BF}_4)_2$,⁶¹ $(\text{dppf})\text{Pd}(\text{BF}_4)_2$,⁶¹ and $\{2\text{-}(6\text{-chloropyridyl})\}\text{Pd}(\text{PPh}_3)(\text{py})(\text{BF}_4)$,⁶² this fluoride-induced redox reaction may begin to take on increasing significance. The reactivity of fluoride in palladium(II) phosphine complexes, as well as the potential synthesis of compounds containing stable Pd-F bonds, merits further investigation.

ACKNOWLEDGMENTS

We thank the donors of the Petroleum Research Fund, administered by the American Chemical Society, and the Mallinckrodt Chemical Co. for support of this research. We also thank Dr. Lee M. Daniels for the crystallographic analysis of Pd(dppp)₂.

REFERENCES

1. Mason, M. R.; Duff, C. M.; Miller, L. J.; Jacobson, R. A.; Verkade, J. G. in progress.
2. See for example: (a) Westland, A. D. *J. Chem. Soc.* **1965**, 3060. (b) Engelhardt, L. M.; Patrick, J. M.; Raston, C. L.; Twiss, P.; White, A. H. *Aust. J. Chem.* **1984**, *37*, 2193. (c) Lindsay, C. H.; Benner, L. S.; Balch, A. L. *Inorg. Chem.* **1980**, *19*, 3503.
3. Harvey, P. D.; Schaefer, W. P.; Gray, H. B. *Inorg. Chem.* **1988**, *27*, 1101. See footnote 20 in this reference.
4. Mason, M. R.; Verkade, J. G. *Organometallics* **1990**, *9*, 864.
5. (a) Bushnell, G. W.; Dixon, K. R.; Moroney, P. M.; Rattray, A. D.; Wan, C. *J. Chem. Soc., Chem. Commun.* **1977**, 709. (b) Dixon, K. R.; Rattray, A. D. *Inorg. Chem.* **1978**, *17*, 1099. See footnote 16 in this reference. (c) Cartwright, S. J.; Dixon, K. R.; Rattray, A. D. *Inorg. Chem.* **1980**, *19*, 1120. (d) Berry, D. E.; Bushnell, G. W.; Dixon, K. R.; Moroney, P. M.; Wan, C. *Inorg. Chem.* **1985**, *24*, 2625.
6. Mann, F. G.; Purdie, D. *J. Chem. Soc.* **1935**, 1549.
7. Steffen, W. L.; Palenik, G. J. *Inorg. Chem.* **1976**, *15*, 2432.
8. Doyle, J. R.; Slade, P. E.; Jonassen, H. B. *Inorg. Synth.* **1960**, *6*, 216.
9. Dixon, K. R.; Hawke, D. J. *Can. J. Chem.* **1971**, *49*, 3252.
10. Kraihanzel, C. S.; Ressler, J. M.; Gray, G. M. *Inorg. Chem.* **1982**, *21*, 879.
11. Gokel, G. W.; Cram, D. J.; Liotta, C. J.; Harris, H. P.; Cook, F. L. *J. Org. Chem.* **1974**, *39*, 2445.
12. Tolman, C. A.; Seidel, W. C.; Gerlach, D. H. *J. Am. Chem. Soc.* **1972**, *94*, 2669.

13. Hunt, C. T.; Balch, A. L. *Inorg. Chem.* **1981**, *20*, 2267.
14. Grim, S. O.; Walton, E. D. *Inorg. Chem.* **1980**, *19*, 1982.
15. Ruppert, I. Z. *Naturforsch., B: Anorg. Chem., Org. Chem.* **1979**, *34B*, 662.
16. Berners-Price, S. J.; Johnson, R. K.; Mirabelli, C. K.; Faucette, L. F.; McCabe, F. L.; Sadler, P. J. *Inorg. Chem.* **1987**, *26*, 3383.
17. Anderson, G. K.; Davies, J. A.; Schoeck, D. J. *Inorg. Chem. Acta* **1983**, *76*, L251.
18. Davies, J. A.; Eagle, C. T.; Otis, D. E.; Venkataraman, U. *Organometallics* **1989**, *8*, 1080.
19. Negishi, E.; Takahashi, T.; Akiyoshi, K. *J. Chem. Soc., Chem. Commun.* **1986**, 1338.
20. Mahmood, T.; Shreeve, J. M. *Inorg. Chem.* **1985**, *24*, 1395.
21. SHELXS-86, G. M. Sheldrick, Institut für Anorganische Chemie der Universität, Göttingen, F.R.G.
22. Neutral-atom scattering factors and anomalous scattering corrections were taken from Cromer, D. T.; Waber, J. T. "International Tables for X-ray Crystallography"; The Kynoch Press: Birmingham, England, 1974; Vol. IV.
23. Enraf-Nonius Structure Determination Package; Enraf-Nonius: Delft, Holland.
24. Kuzmina, L. G.; Struchkov, Y. T.; Ukhin, L. Y.; Dolgoplova, N. A. *Koord. Khim.* **1985**, *11*, 1694.
25. Sergienko, V. S.; Porai-Koshits, M. A. *Zh. Strukt. Khim.* **1987**, *28*, 103.
26. Matsumoto, M.; Yoshioka, H.; Nakatsu, K.; Yoshida, T.; Otsuka, S. *J. Am. Chem. Soc.* **1974**, *96*, 3322.
27. Immirzi, A.; Musco, A. *J. Chem. Soc., Chem. Commun.* **1974**, 400.

28. Andrianov, V. G.; Akhrem, I. S.; Chistovalova, N. M.; Struchkov, Y. T. *Zh. Strukt. Khim.* **1976**, *17*, 135.
29. Chatt, J.; Hart, F. A.; Watson, H. R. *J. Chem. Soc.* **1962**, 2537.
30. Clark, H. C.; Kapoor, P. N.; McMahon, I. J. *J. Organomet. Chem.* **1984**, *265*, 107.
31. Coulson, D. R. *Inorg. Synth.* **1972**, *13*, 121.
32. Stern, E. W.; Maples, P. K. *J. Catal.* **1972**, *27*, 120.
33. Laing, K. R.; Robinson, S. D.; Uttley, M. F. *J. Chem. Soc., Dalton Trans.* **1974**, 1205.
34. Thomas, B. J.; Mitchell, J. F.; Theopold, K. H.; Leary, J. A. *J. Organomet. Chem.* **1988**, *348*, 333.
35. Jordan, R. F.; Dasher, W. E.; Echols, S. F. *J. Am. Chem. Soc.* **1986**, *108*, 1718.
36. Peacock, R. D.; Kemmitt, R. D. W.; Stocks, J. *J. Chem. Soc. (A)* **1971**, 846.
37. Doyle, G. *J. Organomet. Chem.* **1982**, *224*, 355.
38. Dixon, K. R.; McFarland, J. J. *J. Chem. Soc., Chem. Commun.* **1972**, 1274.
39. Emsley, J.; Hall, D. "The Chemistry of Phosphorus"; John Wiley & Sons, New York, 1976; p. 35, 51.
40. Kuran, W.; Musco, A. *Inorg. Chim. Acta* **1975**, *12*, 187.
41. Kumobayashi, H.; Mitsunashi, S.; Akutagawa, S.; Ohtsuka, S. *Chem. Lett.* **1986**, 157.
42. Musco, A.; Kuran, W.; Silvani, A.; Anker, A. W. *J. Chem. Soc., Chem. Commun.* **1973**, 939.
43. Garrou, P. E.; Heck, R. F. *J. Am. Chem. Soc.* **1976**, *98*, 4115.

44. Fitton, P.; Johnson, M. P.; McKeon, J. E. *J. Chem. Soc., Chem. Commun.* **1968**, 6.
45. Coulson, D. R. *J. Chem. Soc., Chem. Commun.* **1968**, 1530.
46. Blake, A. J.; Cockman, R. W.; Ebsworth, E. A. V.; Henderson, S. G. D.; Holloway, J. H.; Pilkington, N. J.; Rankin, D. W. H. *Phosphorus and Sulfur* **1987**, *30*, 143.
47. Seel, V. F.; Bassler, H. J. *Z. Anorg. Allg. Chem.* **1975**, *418*, 263.
48. Ratovskij, G. V.; Belych, L. B.; Burlakova, O. V.; Schmidt, F. K. *Zh. Obshch. Khim.* **1989**, *59*, 2784.
49. See for example: (a) Mootz, D.; Boenigk, D. *J. Am. Chem. Soc.* **1986**, *108*, 6634. (b) Mootz, D.; Boenigk, D. *Z. Anorg. Allg. Chem.* **1987**, *544*, 159.
50. Mathey, F.; Bensoam, J. C. *R. Acad. Sci. (Paris)* **1972**, *274c*, 1095.
51. (a) Nixon, J. F.; Sexton, M. D. *Inorg. Nucl. Chem. Lett.* **1968**, *4*, 275.
(b) Kruck, V. T.; Baur, K. *Z. Anorg. Allg. Chem.* **1969**, *364*, 192.
52. Hartley, F. R. "The Chemistry of Palladium and Platinum"; Applied Science: New York, 1973.
53. McAvoy, J.; Moss, K. C.; Sharp, D. W. A. *J. Chem. Soc.* **1965**, 1376.
54. Doherty, N. M.; Critchlow, S. C. *J. Am. Chem. Soc.* **1987**, *109*, 7906.
55. Coulson, D. R. *J. Am. Chem. Soc.* **1976**, *98*, 3111.
56. Cairns, M. A.; Dixon, K. R.; McFarland, J. J. *J. Chem. Soc., Dalton Trans.* **1975**, 1159.
57. Russell, D. R.; Mazid, M. A.; Tucker, P. A. *J. Chem. Soc., Dalton Trans.* **1980**, 1737.
58. Howard, J.; Woodward, P. *J. Chem. Soc., Dalton Trans.* **1973**, 1840.
59. Clark, H. C.; Tsang, W. S. *J. Am. Chem. Soc.* **1967**, *89*, 529.

60. Reedijk, J. *Comments Inorg. Chem.* **1982**, *1*, 379.
61. Jiang, Z.; Sen, A. *J. Am. Chem. Soc.* **1990**, *112*, 9655.
62. Isobe, K.; Nanjo, K.; Nakamura, Y. *Chem. Lett.* **1979**, 1193.

SUPPLEMENTARY MATERIAL

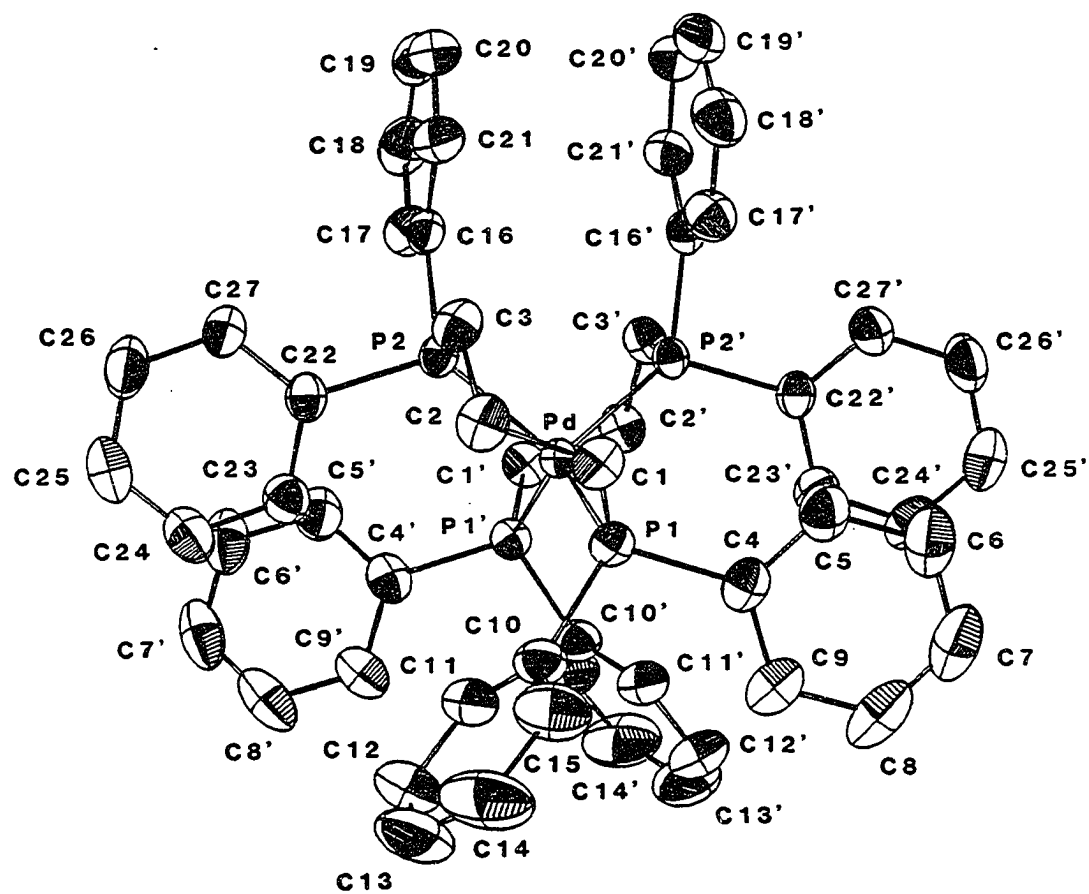


Figure 2. ORTEP diagram and complete labeling scheme for Pd(dppp)₂

Table 3. Bond distances (Å) for Pd(dppp)₂

Atom1-Atom 2	Distance	Atom1-Atom2	Distance
Pd-P(1)	2.3299(4)	C(10)-C(15)	1.402(3)
Pd-P(2)	2.3314(4)	C(11)-C(12)	1.396(3)
P(1)-C(1)	1.848(2)	C(12)-C(13)	1.369(4)
P(1)-C(4)	1.832(2)	C(13)-C(14)	1.376(4)
P(1)-C(10)	1.852(2)	C(14)-C(15)	1.391(4)
P(2)-C(3)	1.845(2)	C(16)-C(17)	1.386(2)
P(2)-C(16)	1.834(2)	C(16)-C(21)	1.392(2)
P(2)-C(22)	1.840(2)	C(17)-C(18)	1.394(3)
C(1)-C(2)	1.535(2)	C(18)-C(19)	1.370(3)
C(2)-C(3)	1.527(2)	C(19)-C(20)	1.369(3)
C(4)-C(5)	1.393(3)	C(20)-C(21)	1.394(3)
C(4)-C(9)	1.398(3)	C(22)-C(23)	1.383(3)
C(5)-C(6)	1.386(3)	C(22)-C(27)	1.389(2)
C(6)-C(7)	1.383(4)	C(23)-C(24)	1.384(3)
C(7)-C(8)	1.356(4)	C(24)-C(25)	1.366(3)
C(8)-C(9)	1.402(3)	C(25)-C(26)	1.385(3)
C(10)-C(11)	1.376(3)	C(26)-C(27)	1.390(3)

Table 4. Bond angles (deg) in Pd(dppp)₂

	Angle		Angle
P(1)-Pd-P(1)'	121.54(2)	C(4)-C(5)-C(6)	121.4(2)
P(1)-Pd-P(2)	97.60(1)	C(5)-C(6)-C(7)	120.2(2)
P(1)-Pd-P(2)'	116.69(1)	C(6)-C(7)-C(8)	119.7(2)
P(2)-Pd-P(2)'	106.92(2)	C(7)-C(8)-C(9)	120.8(2)
Pd-P(1)-C(1)	110.87(5)	C(4)-C(9)-C(8)	120.6(2)
Pd-P(1)-C(4)	121.00(5)	P(1)-C(10)-C(11)	118.5(1)
Pd-P(1)-C(10)	119.85(6)	P(1)-C(10)-C(15)	122.3(2)
C(1)-P(1)-C(4)	100.39(8)	C(11)-C(10)-C(15)	119.1(2)
C(1)-P(1)-C(10)	99.43(8)	C(10)-C(11)-C(12)	120.5(2)
C(4)-P(1)-C(10)	101.66(8)	C(11)-C(12)-C(13)	120.0(3)
Pd-P(2)-C(3)	114.23(5)	C(12)-C(13)-C(14)	120.4(2)
Pd-P(2)-C(16)	117.52(5)	C(13)-C(14)-C(15)	120.1(3)
Pd-P(2)-C(22)	119.15(5)	C(10)-C(15)-C(14)	119.8(2)
C(3)-P(2)-C(16)	102.26(8)	P(2)-C(16)-C(17)	117.0(1)
C(3)-P(2)-C(22)	100.22(7)	P(2)-C(16)-C(21)	125.0(1)
C(16)-P(2)-C(22)	100.64(7)	C(17)-C(16)-C(21)	117.9(2)
P(1)-C(1)-C(2)	113.3(1)	C(16)-C(17)-C(18)	121.2(2)
C(1)-C(2)-C(3)	114.6(1)	C(17)-C(18)-C(19)	119.9(2)

Numbers in parentheses are estimated standard deviations in the least significant digits.

Table 4. Continued

Angle		Angle	
P(2)-C(3)-C(2)	114.1(1)	C(18)-C(19)-C(20)	119.9(2)
P(1)-C(4)-C(5)	120.4(1)	C(19)-C(20)-C(21)	120.5(2)
P(1)-C(4)-C(9)	122.1(2)	C(16)-C(21)-C(20)	120.5(2)
C(5)-C(4)-C(9)	117.3(2)	P(2)-C(22)-C(23)	118.2(1)
P(2)-C(22)-C(27)	123.4(1)	C(24)-C(25)-C(26)	119.9(2)
C(23)-C(22)-C(27)	118.4(2)	C(25)-C(26)-C(27)	119.5(2)
C(22)-C(23)-C(24)	120.7(2)	C(22)-C(27)-C(26)	120.9(2)
C(23)-C(24)-C(25)	120.6(2)		

Table 5. Positional parameters for Pd(dppp)₂

Atom	x	y	z	B(Å ²)
Pd	0.000	0.00503(1)	0.250	2.097(3)
P(1)	-0.09279(2)	0.09063(3)	0.28344(2)	2.573(7)
P(2)	0.04489(2)	-0.09942(3)	0.34797(2)	2.403(7)
C(1)	-0.13019(9)	0.0108(1)	0.33981(9)	3.09(3)
C(2)	-0.06694(9)	-0.0288(2)	0.40529(8)	3.34(3)
C(3)	-0.02584(9)	-0.1231(1)	0.39300(8)	3.15(3)
C(4)	-0.18330(9)	0.1318(1)	0.21803(8)	3.24(3)
C(5)	-0.2389(1)	0.0615(2)	0.1827(1)	4.19(4)
C(6)	-0.3057(1)	0.0904(2)	0.1301(1)	5.31(5)
C(7)	-0.3177(1)	0.1903(2)	0.1102(1)	5.70(5)
C(8)	-0.2641(1)	0.2601(2)	0.1430(1)	5.49(5)
C(9)	-0.1967(1)	0.2323(2)	0.1970(1)	4.22(4)
C(10)	-0.0652(1)	0.2032(1)	0.34034(9)	3.52(4)
C(11)	0.0061(1)	0.2454(1)	0.3511(1)	4.32(5)
C(12)	0.0319(2)	0.3254(2)	0.3978(2)	6.77(7)
C(13)	-0.0139(2)	0.3622(2)	0.4337(2)	7.68(8)
C(14)	-0.0859(2)	0.3222(2)	0.4228(1)	7.48(7)

Anisotropically refined atoms are given in the form of the isotropic equivalent displacement parameter defined as: $(4/3) * [a^2*B(1,1) + b^2*B(2,2) + c^2*B(3,3) + ab(\cos \gamma)*B(1,2) + ac(\cos \beta)*B(1,3) + bc(\cos \alpha)*B(2,3)]$

Table 5. Continued

Atom	x	y	z	B(Å ²)
C(15)	-0.1126(1)	0.2434(2)	0.3756(1)	5.37(5)
C(16)	0.07473(9)	-0.2272(1)	0.33417(8)	2.78(3)
C(17)	0.1306(1)	-0.2360(2)	0.3023(1)	3.75(4)
C(18)	0.1541(1)	-0.3299(2)	0.2863(1)	4.73(5)
C(19)	0.1207(1)	-0.4155(2)	0.3008(1)	4.82(5)
C(20)	0.0653(1)	-0.4087(2)	0.3321(1)	4.86(5)
C(21)	0.0424(1)	-0.3151(2)	0.3493(1)	3.83(4)
C(22)	0.12826(8)	-0.0591(1)	0.42280(8)	2.81(3)
C(23)	0.1437(1)	0.0428(2)	0.43192(9)	3.43(4)
C(24)	0.2055(1)	0.0774(2)	0.4875(1)	4.34(4)
C(25)	0.2533(1)	0.0115(2)	0.5337(1)	4.64(5)
C(26)	0.2389(1)	-0.0909(2)	0.5260(1)	5.09(5)
C(27)	0.1763(1)	-0.1256(2)	0.4707(1)	4.22(4)

Table 6. Torsion angles (deg) in Pd(dppp)₂

Atom 1	Atom 2	Atom 3	Atom 4	Angle
P(2)	Pd	P(1)	C(1)	-28.75 (0.06)
P(2)	Pd	P(1)	C(4)	-145.77 (0.07)
P(2)	Pd	P(1)	C(10)	86.15 (0.07)
P(1)	Pd	P(2)	C(3)	25.19 (0.06)
P(1)	Pd	P(2)	C(16)	144.98 (0.06)
P(1)	Pd	P(2)	C(22)	-93.09 (0.06)
Pd	P(1)	C(1)	C(2)	56.16 (0.13)
C(4)	P(1)	C(1)	C(2)	-174.77 (0.12)
C(10)	P(1)	C(1)	C(2)	-70.95 (0.14)
Pd	P(1)	C(4)	C(5)	70.05 (0.16)
Pd	P(1)	C(4)	C(9)	-104.17 (0.15)
C(1)	P(1)	C(4)	C(5)	-52.14 (0.16)
C(1)	P(1)	C(4)	C(9)	133.64 (0.15)
C(10)	P(1)	C(4)	C(5)	-154.14 (0.15)
C(10)	P(1)	C(4)	C(9)	31.63 (0.17)
Pd	P(1)	C(10)	C(11)	12.04 (0.17)
Pd	P(1)	C(10)	C(15)	-164.44 (0.14)
C(1)	P(1)	C(10)	C(11)	132.82 (0.15)
C(1)	P(1)	C(10)	C(15)	-43.66 (0.17)

Table 6. Continued

Atom1	Atom2	Atom3	Atom4	Angle
C(4)	P(1)	C(10)	C(15)	59.11 (0.17)
Pd	P(2)	C(3)	C(2)	-46.43 (0.13)
C(16)	P(2)	C(3)	C(2)	-174.47 (0.11)
C(22)	P(2)	C(3)	C(2)	82.17 (0.12)
Pd	P(2)	C(16)	C(17)	55.75 (0.14)
Pd	P(2)	C(16)	C(21)	-120.18 (0.14)
C(3)	P(2)	C(16)	C(17)	-178.33 (0.13)
C(3)	P(2)	C(16)	C(21)	5.74 (0.16)
C(22)	P(2)	C(16)	C(17)	-75.29 (0.14)
C(22)	P(2)	C(16)	C(21)	108.77 (0.15)
Pd	P(2)	C(22)	C(23)	24.32 (0.15)
Pd	P(2)	C(22)	C(27)	-155.88 (0.14)
C(3)	P(2)	C(22)	C(23)	-100.99 (0.14)
C(3)	P(2)	C(22)	C(27)	78.81 (0.16)
C(16)	P(2)	C(22)	C(23)	154.33 (0.14)
C(16)	P(2)	C(22)	C(27)	-25.86 (0.17)
P(1)	C(1)	C(2)	C(3)	-83.22 (0.16)
C(1)	C(2)	C(3)	P(2)	76.39 (0.17)
P(1)	C(4)	C(5)	C(6)	-176.09 (0.16)

Table 6. Continued

Atom1	Atom2	Atom3	Atom4	Angle
C(9)	C(4)	C(5)	C(6)	-1.60 (0.28)
P(1)	C(4)	C(9)	C(8)	175.09 (0.16)
C(5)	C(4)	C(9)	C(8)	0.70 (0.28)
C(4)	C(5)	C(6)	C(7)	1.56 (0.32)
C(5)	C(6)	C(7)	C(8)	-0.55 (0.34)
C(6)	C(7)	C(8)	C(9)	-0.34 (0.34)
C(7)	C(8)	C(9)	C(4)	0.26 (0.31)
P(1)	C(10)	C(11)	C(12)	-174.97 (0.18)
C(15)	C(10)	C(11)	C(12)	1.63 (0.30)
P(1)	C(10)	C(15)	C(14)	173.97 (0.17)
C(11)	C(10)	C(15)	C(14)	-2.49 (0.31)
C(10)	C(11)	C(12)	C(13)	0.30 (0.37)
C(11)	C(12)	C(13)	C(14)	-1.38 (0.41)
C(12)	C(13)	C(14)	C(15)	0.49 (0.40)
C(13)	C(14)	C(15)	C(10)	1.45 (0.36)
P(2)	C(16)	C(17)	C(18)	-176.64 (0.15)
C(21)	C(16)	C(17)	C(18)	-0.41 (0.26)
P(2)	C(16)	C(21)	C(20)	175.21 (0.15)
C(17)	C(16)	C(21)	C(20)	-0.70 (0.26)

Table 6. Continued

Atom1	Atom2	Atom3	Atom4	Angle
C(16)	C(17)	C(18)	C(19)	1.32 (0.30)
C(17)	C(18)	C(19)	C(20)	-1.10 (0.33)
C(18)	C(19)	C(20)	C(21)	0.00 (0.34)
C(19)	C(20)	C(21)	C(16)	0.91 (0.32)
P(2)	C(22)	C(23)	C(24)	179.72 (0.14)
C(27)	C(22)	C(23)	C(24)	-0.09 (0.26)
P(2)	C(22)	C(27)	C(26)	179.49 (0.16)
C(23)	C(22)	C(27)	C(26)	-0.71 (0.29)
C(22)	C(23)	C(24)	C(25)	1.18 (0.31)
C(23)	C(24)	C(25)	C(26)	-1.45 (0.34)
C(24)	C(25)	C(26)	C(27)	0.64 (0.35)
C(25)	C(26)	C(27)	C(22)	0.45 (0.33)

Table 7. General displacement parameter expressions for Pd(dppp)₂

Atom	B(1,1)	B(2,2)	B(3,3)	B(1,2)	B(1,3)	B(2,3)
Pd	2.063(S)	2.343(6)	1.949(5)	0	0.753(4)	0
P(1)	2.50(1)	2.74(1)	2.69(1)	0.28(1)	1.134(9)	-0.08(1)
P(2)	2.34(1)	2.73(1)	2.11(1)	0.05(1)	0.696(9)	0.22(1)
C(1)	2.80(5)	3.65(7)	3.29(6)	0.26(5)	1.63(4)	0.26(5)
C(2)	3.50(6)	4.27(7)	2.71(5)	0.27(6)	1.66(4)	0.22(6)
C(3)	3.01(5)	3.66(7)	3.01(5)	0.16(5)	1.30(4)	0.76(5)
C(4)	2.95(5)	4.03(7)	3.02(6)	0.89(5)	1.36(4)	0.06(5)
C(5)	3.56(7)	4.77(8)	3.99(7)	0.89(6)	0.92(6)	-0.80(7)
C(6)	3.82(8)	7.3(1)	4.24(8)	1.07(8)	0.49(7)	-1.08(9)
C(7)	4.51(8)	8.2(1)	3.84(8)	2.71(8)	0.68(7)	0.10(9)
C(8)	6.03(9)	6.3(1)	4.50(8)	3.22(7)	2.27(6)	1.94(8)
C(9)	4.46(7)	4.28(8)	4.25(7)	1.27(6)	1.91(5)	1.05(7)
C(10)	4.39(7)	2.89(6)	3.32(6)	0.29(6)	1.32(5)	-0.29(5)
C(11)	4.40(8)	3.01(7)	5.20(9)	-0.13(6)	1.12(7)	-0.28(7)
C(12)	7.3(1)	3.80(9)	7.7(1)	-1.25(9)	0.6(1)	-1.4(1)
C(13)	11.2(2)	4.2(1)	6.8(1)	-0.5(1)	1.8(1)	-2.33(9)
C(14)	12.2(2)	4.7(1)	7.1(1)	0.2(1)	5.29(9)	-1.97(8)

The form of the anisotropic displacement parameter is: $\exp[-0.25\{h^2a^2B(1,1) + k^2b^2B(2,2) + 12c^2B(3,3) + 2hkabB(1,2) + 2hlacB(1,3) + 2klbcB(2,3)\}]$ where a, b, and c are reciprocal lattice constants.

Table 7. Continued

Atom	B(1,1)	B(2,2)	B(3,3)	B(1,2)	B(1,3)	B(2,3)
C(15)	7.09(9)	4.35(9)	5.78(8)	0.23(8)	3.62(6)	-1.24(7)
C(16)	2.77(5)	2.96(6)	2.27(5)	0.25(5)	0.39(4)	0.18(5)
C(17)	3.81(6)	3.87(7)	3.77(6)	0.53(6)	1.54(5)	0.01(6)
C(18)	4.74(8)	5.20(9)	4.14(8)	1.67(7)	1.29(6)	-0.41(7)
C(19)	5.26(9)	3.86(8)	4.34(9)	1.49(7)	0.27(7)	-0.54(7)
C(20)	5.14(9)	3.00(7)	5.3(1)	0.04(7)	0.24(8)	0.22(7)
C(21)	3.90(7)	3.16(7)	4.16(7)	-0.03(6)	0.99(6)	0.50(6)
C(22)	2.70(5)	3.52(6)	2.16(5)	-0.02(5)	0.73(4)	0.01(5)
C(23)	3.81(6)	3.62(7)	2.74(6)	-0.37(6)	0.92(5)	0.06(6)
C(24)	4.98(8)	4.49(8)	3.42(7)	-1.38(7)	1.23(6)	-0.46(7)
C(25)	3.65(8)	6.3(1)	3.29(8)	-0.73(7)	0.25(7)	-0.87(7)
C(26)	4.60(9)	5.6(1)	3.64(8)	1.19(8)	-0.61(7)	-0.19(8)
C(27)	4.42(8)	3.75(8)	3.37(7)	0.58(7)	-0.23(7)	0.08(7)

Table 8. General displacement parameter expressions for Pd(dppp)₂

Name	U(1,1)	U(2,2)	U(3,3)	U(1,2)	U(1,3)	U(2,3)
Pd	0.02613(6)	0.02968(7)	0.02468(6)	0	0.00954(5)	0
P(1)	0.0316(2)	0.0347(2)	0.0341(2)	0.0035(1)	0.0144(1)	-0.0011(2)
P(2)	0.0297(2)	0.0345(2)	0.0267(2)	0.0006(1)	0.0088(1)	0.0028(1)
C(1)	0.0354(6)	0.0462(9)	0.0417(7)	0.0033(6)	0.0207(5)	0.0034(6)
C(2)	0.0444(7)	0.0541(9)	0.0343(7)	0.0034(7)	0.0210(5)	0.0028(7)
C(3)	0.0382(7)	0.0464(8)	0.0381(7)	0.0020(6)	0.0165(5)	0.0097(7)
C(4)	0.0373(6)	0.0511(9)	0.0383(7)	0.0112(7)	0.0172(5)	0.0007(7)
C(5)	0.0450(8)	0.060(1)	0.0506(9)	0.0113(8)	0.0117(7)	-0.0102(9)
C(6)	0.048(1)	0.092(2)	0.054(1)	0.014(1)	0.0062(8)	-0.014(1)
C(7)	0.057(1)	0.104(2)	0.049(1)	0.034(1)	0.0086(9)	0.001(1)
C(8)	0.076(1)	0.080(1)	0.057(1)	0.0407(9)	0.0288(8)	0.025(1)
C(9)	0.0565(9)	0.054(1)	0.0538(9)	0.0160(8)	0.0241(7)	0.0132(8)
C(10)	0.0556(9)	0.0365(8)	0.0421(8)	0.0036(7)	0.0168(6)	-0.0036(7)
C(11)	0.056(1)	0.0382(9)	0.066(1)	-0.0017(8)	0.0142(9)	-0.0036(9)
C(12)	0.093(2)	0.048(1)	0.098(2)	-0.016(1)	0.007(2)	-0.017(1)
C(13)	0.142(2)	0.053(1)	0.086(2)	-0.006(2)	0.022(2)	-0.029(1)
C(14)	0.154(2)	0.060(1)	0.090(1)	0.003(1)	0.067(1)	-0.025(1)

The form of the anisotropic displacement parameter is: $\exp[-2\pi^2\{h^2a^2U(1,1) + k^2b^2U(2,2) + 12c^2U(3,3) + 2hkabU(1,2) + 2hlacU(1,3) + 2klbcU(2,3)\}]$ where a, b, and c are reciprocal lattice constants.

Table 8. Continued

Atom	U(1,1)	U(2,2)	U(3,3)	U(1,2)	U(1,3)	U(2,3)
C(15)	0.090(1)	0.055(1)	0.073(1)	0.003(1)	0.0458(8)	-0.0157(9)
C(16)	0.0350(7)	0.0375(7)	0.0288(6)	0.0032(6)	0.0049(5)	0.0023(6)
C(17)	0.0483(8)	0.0490(9)	0.0477(8)	0.0067(7)	0.0195(6)	0.0001(8)
C(18)	0.060(1)	0.066(1)	0.052(1)	0.0211(9)	0.0164(8)	-0.0052(9)
C(19)	0.067(1)	0.049(1)	0.055(1)	0.0189(9)	0.0034(9)	-0.0069(9)
C(20)	0.065(1)	0.0379(9)	0.067(1)	0.0005(9)	0.003(1)	0.0028(9)
C(21)	0.0493(9)	0.0400(9)	0.053(1)	-0.0004(7)	0.0125(7)	0.0064(8)
C(22)	0.0342(6)	0.0446(8)	0.0273(6)	-0.0003(6)	0.0092(5)	0.0001(6)
C(23)	0.0483(8)	0.0458(9)	0.0347(7)	-0.0046(8)	0.0117(6)	0.0008(7)
C(24)	0.063(1)	0.057(1)	0.0434(9)	0.0175(9)	0.0156(7)	-0.0058(9)
C(25)	0.046(1)	0.080(1)	0.042(1)	0.0093(9)	0.0032(8)	-0.0111(9)
C(26)	0.058(1)	0.071(1)	0.046(1)	0.015(1)	-0.008(1)	-0.002(1)
C(27)	0.056(1)	0.047(1)	0.0426(9)	0.0074(9)	-0.0030(8)	0.0011(8)

Table 9. Positional parameters for calculated hydrogen atoms in Pd(dppp)₂

Atom	x	y	z	B(Å ²)
H(1)	-0.1561	-0.0451	0.3129	4
H(2)	-0.1655	0.0493	0.3545	4
H(3)	-0.0898	-0.0437	0.4399	4
H(4)	-0.0295	0.0227	0.4220	4
H(5)	0.0003	-0.1529	0.4372	4
H(6)	-0.0635	-0.1685	0.3652	4
H(7)	-0.2307	-0.0075	0.1949	5
H(8)	-0.3433	0.0413	0.1075	6
H(9)	-0.3633	0.2098	0.0738	7
H(10)	-0.2723	0.3286	0.1292	7
H(11)	-0.1598	0.2821	0.2195	5
H(12)	0.0381	0.2197	0.3264	5
H(13)	0.0810	0.3543	0.4047	8
H(14)	0.0042	0.4157	0.4662	9
H(15)	-0.1174	0.3485	0.4476	9
H(16)	-0.1627	0.2168	0.3673	6
H(17)	0.1531	-0.1769	0.2911	4
H(18)	0.1932	-0.3345	0.2653	6

Table 9. Continued

Atom	x	y	z	B(Å ²)
H(19)	0.1360	-0.4795	0.2891	6
H(20)	0.0422	-0.4682	0.3420	6
H(21)	0.0043	-0.3114	0.3716	4
H(22)	0.1116	0.0894	0.3996	4
H(23)	0.2148	0.1477	0.4935	5
H(24)	0.2962	0.0358	0.5710	6
H(25)	0.2716	-0.1370	0.5582	6
H(26)	0.1661	-0.1958	0.4655	5

GENERAL SUMMARY

The research described in this dissertation shows that 2,3-bis(diphenylphosphino-methyl)-1,4-bis(diphenylphosphino)butane (**1**) coordinates to transition metals in three ways. Most importantly, **1** behaves as a bis-bidentate ligand coordinating to two transition metal fragments with the formation of six-membered chelate rings. This coordination mode has been observed for all of the transition metals employed in this study. Ligand **1** also displays a tridentate coordination mode as shown for complexes in which **1** coordinates to molybdenum tricarbonyl. This ligand does not form monometallic complexes wherein it coordinates as a tetradentate ligand. The formation of such a complex was precluded by the steric bulk of the eight phenyl substituents in this ligand as well as structural limitations which do not allow **1** to bridge two trans sites in a square planar or square pyramidal complex. Attempts to prepare such a complex for Rh(I), Ni(II), and Pd(II) led to mixtures which exhibited complex solution chemistry. For palladium, attempts to prepare a monometallic complex led to the formation of $\text{Cl}_2\text{Pd}(\text{Ph}_2\text{PCH}_2)_2\text{CHCH}(\text{CH}_2\text{P}(\text{O})\text{Ph}_2)_2$ in which **1** coordinates as a bidentate ligand to PdCl_2 and the remaining two phosphine groups have been oxidized.

It is also demonstrated that the new ditertiary phosphine ether *cis*-1,5-bis(diphenylphosphinomethyl)-3-oxa-bicyclo[3.3.0]octane (**2**) coordinates to transition metals in either a bidentate (*P, P'*) or tridentate (*P, P', O*) manner. Ligand **2** exhibits a conformational preference in its octahedral metal carbonyl complexes wherein **2** coordinates as a bidentate ligand. The coordinated ether in metal carbonyl complexes wherein **2** exhibits a tridentate coordination mode are readily substituted by pyridine, piperidine, acetonitrile and $\text{P}(\text{OCH}_2)_3\text{CCH}_3$ to yield two *fac* diastereomers in each case. For the products of the N-donor ligands, an equilibrium between free and coordinated ligand is established. Carbon monoxide also reacts stereospecifically to yield two *fac*

diastereomers as shown by the reactions of (2-*P, P', O*)M(CO)₃, M= Mo, W, with ¹³CO. This is an important observation since previous studies of the stereospecificity of ligand substitution reactions of metal carbonyl complexes have been unable to differentiate the two axial sites and thus have been unable to determine if the incoming ligand occupied the site vacated by the leaving group or the site *trans* to this position. The results presented in this thesis demonstrate that both sites become available by isomerization of diastereomeric five-coordinate intermediates.

Finally, this thesis also demonstrates the generality of a new fluoride-assisted reduction of palladium(II) and platinum(II) phosphine complexes which yields a zerovalent metal phosphine complex and a difluorophosphorane. This reaction was not, however, found to occur for phosphine complexes of nickel(II). Results described in this dissertation also suggest that this new redox reaction may participate in the formation of [Pd₃Cl(PPh₂)₂(PPh₃)₃][BF₄] from [(Ph₃P)₃PdCl][BF₄] with fluoride necessary for the redox reaction arising from the thermal decomposition of tetrafluoroborate.

ACKNOWLEDGMENTS

I would like to thank the numerous people who offered support and encouragement throughout this endeavor. In particular I would like to thank the following:

Dr. John G. Verkade for his guidance and support.

Dr. Lee M. Daniels, Dr. Victor Young, Jr., Dr. Lance Miller, Yingzhong Su, Dr. Tom Hendrixson and Dr. Robert A. Jacobson for the crystallographic results reported in this dissertation.

Dr. Vinko Rutar and Dave Scott for valuable assistance and instruction in multinuclear NMR spectroscopy.

Jan Beane for numerous mass spectral measurements.

Renie Petrie for the invaluable use of a printer and numerous formatting suggestions during the preparation of this manuscript.

A very special thanks goes to Dr. Elliott Blinn of Bowling Green State University for providing my first research opportunity, urging me to pursue a graduate degree, and for his continued support over the past eight years.

I would also like to thank the following past and present members of the Verkade group: Kevin "The Big Lamb-pass me those Pop-Tarts" Ambrisco, Dr. S. K. "Charlie" Das, Dr. Ron "The Pope" Davis, Dr. Colleen Duff, Dr. Martin Fu, Ray Garant, Dr. Dietrich Gudat, Dr. Toni Herbowski, Dr. Mary Laramay, Dr. Ceese Lensink, Dr. Wiro Menge, Dr. Ahmad Naiini, Dr. Winfried Plass, Jiri Pinkas, Dr. Fazlur Rahman, Dr. Klaus Reinhard, Dr. Harry Schmidt, Dr. Martina Schmidt, Jiansheng Tang, Yanjian Wan, Dr. Jan "Yes, I Always Play Basketball Barefoot" Woning, Dr. A. E. Wroblewski, Dr. Mao Chun Ye, and that masked wonder, the "Gentleman Cowboy".

The biggest thanks go to my parents, Marci, Lori, Mike and Mary without whom this accomplishment would have no meaning.